VIBRATION ANALYSIS USING EXPERIMENTAL DATA AND APPROXIMATE METHODS WITH CONSIDERATION OF POWER FLOW FROM MACHINERY INTO BUILT-UP STRUCTURES

by

Hugh George David Goyder

Institute of Sound and Vibration Research
Faculty of Engineering and Applied Science
University of Southampton

Thesis submitted for the Degree of

Doctor of Philosophy

April, 1978.

University of Southampton

Abstract

Faculty of Engineering and Applied Science

Doctor of Philosophy

VIBRATION ANALYSIS USING EXPERIMENTAL DATA AND APPROXIMATE METHODS WITH CONSIDERATION OF POWER FLOW FROM MACHINERY INTO BUILT-UP STRUCTURES

by Hugh George David Goyder

Typical built-up structures consist of beams, plates and beam-stiffened plates. Due to strong coupling with other parts of the structure the vibrational characteristics of these components are too complicated to be analysed exactly. However, the vibration may be approximated by the response of structures with a similar cross section and of infinite length. The wave propagation and power flow due to force and torque (moment) excitation has been studied at the driving point and in the far field for infinite beams, plates and beam stiffened plates.

An infinite, beam-stiffened plate excited by forces or torques applied to the beam behaves like an uncoupled beam at the driving point. In the far field, power transmitted by flexural waves in the beam is radiated into the plate whilst power transmitted by torsional waves in the beam is not radiated. The plate carries a cylindrical wave with a strong directivity.

The power flowing through the isolators and into the supporting foundation of a machine has been examined by approximating the driving point frequency response function of the foundation. One and two stage isolation of machines with internal force or velocity sources has been considered. Two stage isolation is superior to single stage isolation in reducing power flow, in those circumstances where the excitation spectra do not cover the two resonances of the system.

A structure with a number of resonances is difficult to analyse theoretically but may be investigated from measured data. By exciting a structure at one point and measuring the frequency response at a number of positions it is possible to construct a mathematical model of the structure. The model is valuable because it enables unmeasured frequency response functions to be predicted. Also, by modelling two separate components of a structure from measured data it is possible to obtain an estimate of the subsequent motion and power flow through the two components when coupled.

ACKNOWLEDGEMENTS

The author wishes to thank Dr. R.G. White for his guidance and encouragement. He also gratefully acknowledges the support by the Ministry of Defence (Admiralty Engineering Laboratory) of the unclassified contract under which his research was carried out.

CONTENTS

LIST OF SYMBOLS

A	Cross sectional area of beam;
	$= \frac{B_p}{GQ}$ ratio of plate bending stiffness to beam torsional stiffness (Chapters 2-4);
	Constant (Chapter 5)
B	Bending stiffness
D	Damping matrix
E	Young's modulus
F	Force or pressure
G	Shear modulus
H	Frequency response matrix
I	Second moment of area
I_1; I_2	Integrals
J	Polar mass moment of inertia per unit length
K	Stiffness matrix (Chapter 6)
	Stiffness of isolator
L	Parameter from reference [12]
M	Bending moment
	Mass of machine (Chapter 5)
	Mass matrix (Chapter 6)
P	Power
P_a	Power flow at station a
P_s	Power supplied by source
P_u	Power associated with shear
P_m	power associated with bending
Q	Torsion constant
Q_f	Power flow transmission spectrum for a force source
Q_v	Power flow transmission spectrum for a velocity source
T	Torque
T_p	Total power flow
a	Radius of disc over which torque applied to plate acts
e	2.718 ... Base of natural logarithm
f	(subscript) flexural wave motion
i	Imaginary operator ($\sqrt{-1}$);
	(subscript) instantaneous value

k	Wavenumber
ℓ	(subscript) longitudinal wave motion
n	number of resonance frequencies
p	Pole position
r, ϕ	Polar coordinates
s	Ratio of beam to plate wave numbers ($= \frac{k_b}{k_p}$) (Chapter 4)
	Exponent of frequency dependence (Chapter 5)
	Number of response stations (Chapter 6)
t	Time
	(subscript) torsional wave motion
u	shear force
v	Velocity
x, y, z	Coordinates in Cartesian space

α	Coordinate in wavenumber space
β	Mobility of subsystem
γ, δ	Normalised real and imaginary parts of mobility
Γ	Integration path
δ_o	Dirac delta function
η	Loss factor
θ	Angular displacement
ν	Poisson's ratio
ξ	Displacement
ζ	Imaginary component of flexural wavenumber $K(1 + i\zeta)$
π	3.1415...
ρ	Density
ϕ	Phase angle
ψ	Eigenvector
ω	Angular frequency

CHAPTER 1

INTRODUCTION

1.1 Introduction

Typical built-up structures such as buildings or ships are an assembly of many different components all of which interact strongly when set into vibration. Certain components such as beams or plates are relatively easy to analyse individually when there is no coupling with other elements. However, when built into a structure the vibration of a component is strongly dependent on the other elements to which it is attached and the calculation of the motion becomes very complicated or even impossible. In order to obtain some widely applicable formulae, methods of vibration analysis based on approximate or measurement methods are developed in this thesis.

In a built-up structure a common source of vibration is a machinery installation which, due to some internal excitation, injects vibrational energy into its supporting foundations. This energy is carried by wave motion within the foundation until some boundary or discontinuity is encountered. Here some of the energy in the wave will be reflected back into the foundation the remainder being transmitted through the boundaries to other parts of the structure. If a significant amount of energy is reflected to and fro within the foundation then resonances will occur at those frequencies for which the wave motion interferes constructively. The power which is transmitted through the boundaries of the foundation is available for radiation or as unwanted vibration in the remaining portion of the structure and this is a significant problem. A direct approach for controlling the unwanted power is to minimise the net vibratory power flow into the foundation at the source. The use of power flow in calculations is very valuable because it combines both forces and velocities in a single concept. An attempt to decrease the radiation or vibration in a structure by reducing only the force or velocity may not necessarily be successful. However, an improvement may be ensured by decreasing the net vibrational power applied to a structure.

The foundation of a machine is a crucial component since it is responsible for the conversion of the machinery excitation into propagating wave motion. Therefore the first part of this thesis is a study of wave motion and power flow in a range of common foundations such as beams, plates and beam-stiffened plates. The existence of damping and of a large number of resonances enables foundations to be approximated by components of infinite extent. This is equivalent to assuming that at the boundaries of the foundation there are no reflections and all power is propagated away. This approach greatly assists the analysis and, in particular, enables the power flow into the structure due to different types of excitation to be derived. Having established the behaviour of the foundation the reduction in power flow resulting from the isolation of machinery may be estimated. When there are significant reflections from boundaries and individual resonances are apparent, the theoretical approach described above becomes less accurate. Consequently the second part of this thesis is concerned with those frequency ranges where there is resonant behaviour of the structure. Starting with measured data computer based procedures are formulated which enable mathematical models of the structure to be formed. The models may be used to predict unmeasured responses thus greatly reducing the experimental testing time required. Other applications of the mathematical model are also considered. In particular, the possibility of modelling two components and then predicting their behaviour when joined is examined critically.

1.2 The Principal Methods of Vibration Analysis

An exact solution for the vibration of a structure may be obtained by forming the differential equations for the motion and solving them for the appropriate boundary conditions. It is useful to obtain the harmonic response since, if the structure is linear, then the response due to transient or periodic excitation may then be determined exactly by means of a Fourier transform. The calculations involved in a vibration analysis may be simplified by reducing the complete solution to an infinite series in which each term corresponds to one resonance of the

structure; this procedure is usually described as modal analysis.

The complexity of a practical structure unfortunately prevents this type of detailed analysis because it is not possible to formulate and solve all the differential equations. Even relatively simple components are difficult to analyse if they are built into a structure in such a manner that the boundary conditions cannot be determined. However when a structure has several components the response of the entire structure may be calculated from the response of the individual components. If many components are involved, procedures of this type (often known as mobility or receptance methods) become unwieldy. Consequently only relatively simple structures may be analysed exactly to obtain the response of a prescribed excitation.

Various approximate methods, each appropriate to different circumstances, enable a wide range of vibration problems to be solved. If the effect of the boundaries is considered to be unimportant then the structure may be approximated by considering it to be of infinite length. This type of analysis is usually formulated in terms of wave motion. If a structure has well defined mass and stiffness elements then an approximate mathematical model can be formulated and solved in which there are pure mass elements and pure stiffness elements. Both these types of approximate analysis are used in Part One of this thesis.

An approximate method which is capable of great accuracy in the finite element method. In this procedure the structure is divided into a number of elements each element having a certain deformation pattern. By considering the strain and kinetic energies of the structure the resonance frequencies and modes of vibration may be calculated. The deformation is built-up out of the deformation of the individual elements; consequently the emphasis in the analysis is centred on determining the deformation of elements rather than the deformation of the entire structure. A finite element analysis may only be applied to particular problems and will only produce numerical results. Because of the complexity of a practical built-up structure detailed representation of individual components is not generally possible but an overall response may be determined.

Because of the detailed description that would be required the

finite element method is not suitable for high frequencies when there are many resonances. In this regime statistical energy analysis is more appropriate. This is an approximate method used for analysing the interaction between two components. When there are many resonances present in the components of a system then averaged properties may be used to predict an averaged response of the coupled system. The average modal energies of each system must be known together with the nature of the coupling. This type of analysis is generally only appropriate when both the components being considered have a high modal density and the coupling can be calculated or estimated.

By combining measured data with theoretical data it is possible to obtain information about a complicated structure. This type of analysis is considered in Part Two of this thesis.

1.3 Objectives of This Work

The aim of this study is to formulate and evaluate methods for the vibration analysis of complicated practical built-up structures. To this end a theoretical study of commonly occurring components of structures is commenced with the aim of determining simple widely applicable general formulae which indicate trends of behaviour and give approximate solutions. In particular this approach is to be applied to the problem of machinery isolation where it is considered that the use of power flow should provide a unifying concept.

A further intention is to establish procedures by which the fundamental nature of an existing structure may be determined from measured data.

1.4 Conventions and Definitions

There are two conventions for describing a harmonic wave propagating in the positive x-direction. These conventions are either

$$e^{i(kx - \omega t)} \tag{1.1}$$

or

$$e^{i(\omega t - kx)} \tag{1.2}$$

The first convention (1.1) gives a positive wave number for motion in the positive x-direction but negative frequency dependence. This convention will be used when considering the spatial response of a structure. The second convention (1.2) gives a positive frequency dependence with negative wave numbers and is more suitable for describing the frequency response of a structure. Care will be taken to state which convention is being employed in any problem and in particular all tables will use the second convention. To convert from one convention to the other it is merely necessary to replace every i $(= \sqrt{-1})$ in an equation by $-i$.

Power is the rate at which work is done and is given by the relationship

$$P_i = F_i V_i \tag{1.3}$$

where F_i and V_i are the instantaneous values of force and velocity at a point. (Instantaneous values will be indicated by the subscript i.) When power flows through an area it is necessary to consider it as an intensity and therefore with the force F_i determined as a stress. With a vibrating structure the net flow of power is more important than the instantaneous value and when force and velocity are harmonic this is given by

$$P = \frac{\omega}{2\pi} \int_0^{2\pi/\omega} F_i V_i \, dt \tag{1.4}$$

where ω is the frequency of vibration. If the force and velocity are written as:-

$$F_i = Fe^{i\omega t} \qquad V_i = Ve^{i\omega t}$$

where F and V are complex and may thus include a relative phase angle, then:-

$$P = \tfrac{1}{2}|V||F| \cos\phi$$

or
$$P = \tfrac{1}{2}\mathrm{Re}\{FV^*\} = \tfrac{1}{2}\mathrm{Re}\{F^*V\} \qquad (1.5)$$
$$= \tfrac{1}{2}\left[\mathrm{Re}\{F\}\mathrm{Re}\{V\} + \mathrm{Im}\{F\}\mathrm{Im}\{V\}\right]$$

where ϕ is the phase angle and * denotes the complex conjugate. The ratio of the complex harmonic velocity to the complex harmonic force is the mobility and this quantity is a property of the structure alone. One may substitute therefore for either the force or the velocity to give:-

$$P = \tfrac{1}{2}|F|^2\mathrm{Re}\{\beta\} = \tfrac{1}{2}|V|^2\frac{\mathrm{Re}\{\beta\}}{|\beta|^2} \qquad (1.6)$$

where
$$\beta = \frac{V}{F}\ .$$

These formulae hold for both conventions of $e^{-i\omega t}$ and $e^{+i\omega t}$.

It is convenient to represent damping in a structure by means of a complex Young's modulus [1]. The relationship between stress and strain may be written as:-

$$\frac{\text{Stress}}{\text{Strain}} = \begin{cases} E(1 + i\eta) & \text{for } e^{i\omega t} \text{ frequency dependence} \\ E(1 - i\eta) & \text{for } e^{-i\omega t} \text{ frequency dependence} \end{cases}$$

where E is the Young's modulus and η is the loss factor for the material.

This representation of damping leads to a complex resonance frequency and a complex wave number. If a structure has an undamped resonance at ω_o then the introduction of damping leads to a resonance frequency of:-

$$\omega_o\left(1 + \frac{i\eta}{2}\right) \quad \text{for } e^{i\omega t} \text{ frequency dependence} \qquad (1.7)$$

$$\omega_o\left(1 - \frac{i\eta}{2}\right) \quad \text{for } e^{-i\omega t} \text{ frequency dependence} \qquad (1.8)$$

where, because η is small, only first order terms have been included.

For longitudinal and torsional waves the wave number is proportional to $(\frac{1}{E})^{\frac{1}{2}}$; therefore the complex wave number is given by:-

$k(1 - \frac{i\eta}{2})$ for $e^{i\omega t}$ frequency dependence (1.9)

$k(1 + \frac{i\eta}{2})$ for $e^{-i\omega t}$ frequency dependence (1.10)

Similarly for flexural waves, the wavenumber is proportional to $(\frac{1}{E})^{\frac{1}{4}}$; therefore it may be written as:-

$k(1 - \frac{i\eta}{4})$ for $e^{i\omega t}$ frequency dependence (1.11)

$k(1 + \frac{i\eta}{4})$ for $e^{-i\omega t}$ frequency dependence. (1.12)

PART ONE

CHAPTER 2

WAVE PROPAGATION AND POWER FLOW IN BEAMS AND PLATES

2.1 Introduction

Problems in vibration isolation may be considerably simplified by considering the vibrational power flow in a structure. A typical problem is idealized by figure 2.1. Power is injected into a structure such as a building or ship by a machine with an internal vibration source, which is mounted on an isolator. Due to the isolator foundation being flexible, power is transmitted through the structure to the sink where it appears as unwanted vibration or radiation.

The aim of vibration isolation procedures is to reduce the velocity amplitudes at the sink by making appropriate modifications to the isolator and isolator foundation. A direct approach would therefore be to calculate the response at the sink due to an excitation at the source and to design the isolator, foundation and structure to minimise the unwanted vibration. Because of the variety of possible structures and because of their often complicated nature, direct calculations of this type are extremely difficult. In addition, an exact description of the unwanted vibration cannot always be formulated, especially in the case of radiation for which the velocity distribution over the surface of the structure must be established.

Standard methods of vibration isolation (for example [1,2,3,4]) therefore simplify the problem by only analysing the reduction of force or velocity at the foundation.

An approach to vibration isolation may be formulated by considering the power flowing into the structure at the mounting point of the isolator. If the isolator and foundation are designed to minimise this power flow then all unwanted vibration will be minimised.

The power that enters a structure is a function of the characteristics of the source, isolator and foundation. The isolator and source are easily modelled but the foundations are often difficult to describe. In the following chapters the characteristics of the foundations have been

simplified according to the method developed by Skudrzyk [5]. This method allows a finite damped structure to be approximated by an equivalent structure of infinite extent with no reflecting devices. Thus it is assumed that waves propagating away from the source are attenuated by damping or radiation and are not reflected back to the source to form standing waves. Alternatively, this is equivalent to assuming that there are many modes of vibration contributing to the motion at any one frequency without one mode being dominant.

A number of typical foundations such as beams, plates and beam-stiffened plates have therefore been analysed as if they were of infinite extent. Wave propagation in these types of structure has been studied previously by many authors; however, except for Heckl [6], Cremer, Heckl and Ungar [7], Noiseux [8] and Pavic [9] there has been little detailed consideration of power flow. In the following chapters the power flowing into each infinite foundation due to a point source and the subsequent flow of power throughout the structure are given. As foundations may be excited by forces or torques, both these types of source have been considered. The results are summarised for the simpler foundations in Table I.

A unified approach has been adopted for analysing the various infinite structures. In each case a wave equation has been derived in a right handed coordinate system with a source applied as a spatial delta function (written δ_o). Harmonic time dependence of the form $e^{-i\omega t}$ is assumed giving a linear differential equation in one or two dimensions. By applying a spatial Fourier transform the differential equation is transformed into an algebraic equation in wavenumber space. The solution is obtained by taking the inverse Fourier transform, the integral being evaluated by contour integration. These procedures are described in references [10,11]. The definition of the Fourier transform used is:-

$$\tilde{\xi}(\alpha) = \int_{-\infty}^{\infty} \xi(y) e^{-i\alpha y} dy \qquad (2.1)$$

and the inversion integral is:-

$$\xi(y) = \frac{1}{2\pi} \int_{-\infty}^{\infty} \tilde{\xi}(\alpha) e^{i\alpha y} d\alpha \qquad (2.2)$$

A $\tilde{}$ over a function represents the transform of that function and the coordinate in wavenumber space will be denoted by α. In the two-dimensional case the Fourier transform will be written as:-

$$\tilde{\tilde{\xi}}(\alpha_x, \alpha_y) = \int_{-\infty}^{\infty}\int_{-\infty}^{\infty}\xi(x, y)e^{-i\alpha_x x}e^{-i\alpha_y y}\,dxdy \tag{2.3}$$

and the inversion integral as:-

$$\xi(x, y) = \frac{1}{4\pi^2}\int_{-\infty}^{\infty}\int_{-\infty}^{\infty}\tilde{\tilde{\xi}}(\alpha_x, \alpha_y)e^{i\alpha_x x}e^{i\alpha_y y}\,d\alpha_x d\alpha_y \tag{2.4}$$

2.2 Torsional and Longitudinal Wave Motion in Beams

Since torsional and longitudinal waves both obey the same second order differential equation, results obtained by examining torsional waves are also applicable to longitudinal waves. Torsional waves will be considered here because of the two this type of wave motion is generally more important.

Figure 2.2 shows an infinite beam with shear modulus G, torsion constant Q and mass moment of inertia per unit length J. The beam lies along the y axis with a torque of amplitude $Te^{-i\omega t}\delta_o$ applied at y = 0. The angular displacement at any point is given by $\theta(y)$. The equation of motion is derived in Appendix I and is:-

$$J\frac{\partial^2\theta_i}{\partial t^2} = GQ\frac{\partial^2\theta_i}{\partial y^2} + Te^{-i\omega t}\delta_o \tag{2.5}$$

This equation assumes that the torsional wavelengths are greater than the cross section dimensions of the beam.

Assuming harmonic time dependence of the form $e^{-i\omega t}$ this equation may be written as:-

$$\frac{\partial^2\theta}{\partial y^2} + k_t^2\theta = -\frac{T}{GQ}\delta_o \tag{2.6}$$

where $k_t^2 = \frac{\omega^2 J}{GQ}$ and θ now refers to the complex amplitude of the

angular displacement. The equivalent equation for longitudinal waves is:-

$$\frac{\partial^2 \xi}{\partial y^2} + k_\ell^2 \xi = -\frac{F}{AE}\delta_o \qquad (2.7)$$

where $k_\ell^2 = \frac{\omega^2 \rho}{E}$ and $\xi(y)$ is the displacement, A the cross sectional area, E the Young's modulus and F the applied force. Only torsional waves will be considered below but to convert the results for longitudinal waves the equivalent terms in equations (2.7) and (2.6) may be interchanged.

The Fourier transform (equation (2.1)) in the y-direction gives:-

$$\overset{\sim}{\theta}(\alpha) = \frac{-T}{GQ}\frac{1}{k_t^2 - \alpha^2} \qquad (2.8)$$

The solution is given by the inverse Fourier transform of equation (2.8) and is:-

$$\theta(y) = \frac{-T}{2\pi GQ}\int_{-\infty}^{\infty} \frac{e^{i\alpha y}}{k_t^2 - \alpha^2}\, d\alpha. \qquad (2.9)$$

This integral has two poles at $\alpha = \pm k_t$ which are shown together with the integration contour in figure 2.3. The contour is deformed to pass beneath the pole at $\alpha = +k_t$ since with the inclusion of damping this pole would lie above the real axis. The pole at $\alpha = -k_t$ is not included in the contour since this pole with damping would lie beneath the real axis.

The residue of the integral is $\frac{e^{ik_t y}}{-2k_t}$ and the solution is therefore:-

$$\theta(y) = \frac{iT}{GQ}\frac{e^{ik_t y}}{2k_t} \qquad (2.10)$$

or in terms of mobility with $e^{-i\omega t}$ frequency dependence:-

$$\frac{-i\omega\theta}{T} = \frac{\omega e^{ik_t y}}{2GQk_t} = \frac{e^{ik_t y}}{2\sqrt{GQJ}} \qquad (2.11)$$

The mobility at the driving point (y = 0) is therefore a real constant independent of frequency.

2.3 Power Flow in Torsional Wave Motion

Using equation (1.6) for the power supplied to a structure gives:-

$$P_s = \frac{|T|^2}{4\sqrt{GQJ'}} \tag{2.12}$$

where P_s denotes the power supplied by a source.

The power flow at any station along the beam is given by equation (1.5). The angular velocity is

$$\dot{\theta}_i = \frac{T}{2\sqrt{GQJ'}} e^{i(k_t y - \omega t)}$$

and the internal twisting moment is given by:-

$$M_i = -GQ \frac{\partial \theta_i}{\partial y} = \frac{T}{2} e^{i(k_t y - \omega t)}$$

denoting the power at any station by P_a gives:-

$$P_a = \frac{|T|^2}{8\sqrt{GQJ'}} \tag{2.13}$$

P_a is half the power supplied by the source, the remaining power going in the negative y-direction. If damping is included then both k_t and G become complex and so therefore do $\dot{\theta}_i$ and M_i. Writing G as $G(1 - i\eta)$, k_t as $k_t(1 + \frac{i\eta}{2})$ and only including terms in η to first order gives:-

$$P_a = \frac{|T|^2}{8\sqrt{GQJ'}} e^{-k_t \eta y}. \tag{2.14}$$

The power is therefore seen to decay exponentially with distance from the source.

2.4 Flexural Wave Motion in Beams

Unlike other wave types, flexural waves cause two internal forces to act in a beam. As will be shown these two forces (one associated with bending, the other with shear) are both important since they carry equal amounts of power in the far field. In the near field, in addition to propagating waves, non propagating waves couple the two forces according to the particular boundary conditions imposed. In addition, flexural waves are dispersive being represented by a fourth order differential equation in which the wave speed is proportional to the square root of frequency. The differential equation for a beam including sources due to force and torque excitation is given in Appendix II.

In deriving the equation of motion no account has been taken of the effects of rotary inertia and shear deformation. It is assumed that the wavelengths of the propagating flexural waves are always greater than the cross-sectional dimensions of the beam in the frequency range of interest.

2.5 Force Excitation of a Uniform Beam

Figure 2.4 shows an infinite uniform beam of density ρ, cross-sectional area A, second moment of area I and Young's modulus E, laying along the y-axis. A harmonic force of amplitude $Fe^{-i\omega t}\delta_o$ is applied at the origin $y = 0$. The differential equation representing the motion is derived in Appendix II and for harmonic time dependence of the form $e^{-i\omega t}$ is:-

$$\frac{\partial^4 \xi}{\partial y^4} - k^4 \xi = \frac{F}{EI}\delta_o \tag{2.15}$$

where $k^4 = \frac{\omega^2 \rho A}{EI}$ and $\xi(y)$ is the displacement in the z-direction.

Taking the spatial Fourier transform in the y-direction gives:-

$$\tilde{\xi}(\alpha) = \frac{F}{EI}\frac{1}{\alpha^4 - k^4} \tag{2.16}$$

where α is the coordinate in wavenumber space. The solution is given by the inverse Fourier transform of equation (2.16), namely:-

$$\xi(y) = \frac{F}{2\pi EI} \int_{-\infty}^{\infty} \frac{e^{i\alpha y}}{\alpha^4 - k^4} \, d\alpha \qquad (2.17)$$

This equation has four poles ($\alpha = \pm k$ and $\alpha = \pm ik$) which are shown on figure 2.5 together with the contour of integration. The contour has once again been indented to include only those poles which correspond to sources. The residue due to the pole at $\alpha = +k$ is $e^{iky}/4k^3$ and the residue at $\alpha = +ik$ is $e^{-ky}/-4ik^3$. The solution for $x \geq 0$ is therefore:-

$$\xi(y) = \frac{iF}{4EIk^3} \left[e^{iky} + ie^{-ky}\right] \qquad (2.18)$$

The instantaneous values of the transverse velocity and angular velocity for frequency dependence of the form $e^{-i\omega t}$ are:-

$$\dot{\xi}_i(y) = \frac{F\omega}{4EIk^3} \left[e^{iky} + ie^{-ky}\right] e^{-i\omega t} \qquad (2.19)$$

and

$$\dot{\theta}_i(y) = \frac{iF\omega}{4EIk^2} \left[e^{iky} - e^{-ky}\right] e^{-i\omega t} \qquad (2.20)$$

where $\dot{\theta}_i$ is the instantaneous angular velocity. The point mobility at the origin between the driving force and the transverse velocity is therefore:-

$$\beta = \frac{\omega}{4EIk^3}(1 + i) = \frac{(1 + i)}{4\rho A\sqrt{\omega}} \left(\frac{\rho A}{EI}\right)^{\frac{1}{4}} \qquad (2.21)$$

This mobility decreases with increasing frequency and behaves at any frequency like a dashpot and mass in parallel.

The transfer mobility between the driving force and angular velocity may be found from equation (2.20). This mobility is clearly zero at the origin as would be expected from symmetry.

Equations (2.19) and (2.20) include a term of the form e^{-ky} which represents the near field. This term has the same magnitude as the propagating wave at $y = 0$ but rapidly decays with distance from the origin. By writing this near field term as $e^{-2\pi(y/\lambda)}$ where λ is the

wavelength it may be seen that at a distance of one wavelength from the source it has decreased to less than 0.2% of its value at the origin. Therefore for large values of $k\,y$ the real exponential terms may be ignored in equations (2.19) and (2.20) leaving only the complex exponentials.

2.6 Power Flow in a Uniform Beam with Force Excitation

The power supplied by the source is given by the time average of the transverse velocity and the driving force. Using equation (1.6) gives:-

$$P_s = \frac{|F|^2}{8\rho A\sqrt{\omega}} \left(\frac{\rho A}{EI}\right)^{\frac{1}{4}} = \frac{|F|^2}{8EIk^3} \tag{2.22}$$

The power supplied by a driving force normal to a beam therefore decreases with increasing frequency.

At any point along the beam there is an internal shear force and an internal bending moment. Both of these forces transmit power. The instantaneous value of the shear force is given by:-

$$u_i = EI\,\frac{\partial^3 \xi}{\partial y^3} = \frac{F}{4}\left[e^{iky} + e^{-ky}\right]e^{-i\omega t} \tag{2.23}$$

and the instantaneous value of the bending moment by

$$M_i = -EI\,\frac{\partial^2 \xi}{\partial y^2} = \frac{F}{4k}\left[ie^{iky} + e^{-ky}\right]e^{-i\omega t} \tag{2.24}$$

The power flow associated with shear may be found from equation (1.5) by substituting the values for the shear force and transverse velocity from equations (2.23) and (2.19) to give:-

$$\begin{aligned} P_u &= \tfrac{1}{2}\mathrm{Re}\{ui\omega\xi^*\} \\ &= \frac{|F|^2\omega}{32EIk^3}\left[1 + e^{-ky}(\sin ky + \cos ky)\right] \end{aligned} \tag{2.25}$$

Similarly, the power associated with bending may be found by

substituting the values of bending moment (equation (2.24)) and angular velocity (equation (2.20)) into equation (1.5) to give:-

$$P_m = \tfrac{1}{2}\mathrm{Re}\{Mi\omega\theta^*\}$$

$$= \frac{|F|^2\omega}{32EIk^3}\left[1 - e^{-k_f y}(\cos ky + \sin ky)\right] \qquad (2.26)$$

The total power flowing at any station is the sum of these two powers and is:-

$$P_a = P_u + P_m = \frac{|F|^2\omega}{16EIk^3}\,. \qquad (2.27)$$

The total power flowing in the positive y-direction is therefore independent of distance and equal to half the power supplied by the source.

Both the power associated with the shear force (P_u) and the power associated with bending (P_m) have real exponential terms which are important in the near field. In the far field the exponential term may be ignored (at distances greater than one wavelength $e^{-k_f y}$ is less than 0.002 and P_u and P_m are seen to be equal. In the near field the power is influenced by the nature of the source. At the origin all the power of the transverse driving force is transferred to the shear component P_u. As the distance from the source increases P_u decreases and the power is transferred to the moment component P_m. This transference of power proceeds with increasing distance from the source until both P_u and P_m are equal. The near field is therefore seen to couple the two components of the power flow enabling work to be done by one component on the other.

The effect of internal damping may be analysed by allowing the Young's modulus and wavenumber to have an imaginary part. Substituting $E(1 - i\eta)$ for the Young's modulus and $k(1 + i\zeta)$ for the wavenumber, where it may be seen from equation (1.12) that $4\zeta = \eta$, enables the transverse velocity and angular velocity to be written as:-

$$\dot{\xi}_i = \frac{F\omega(1 + i\zeta)}{4EIk^3}\left[\, e^{-yk\zeta}e^{iyk} + ie^{-yk}e^{-iyk\zeta}\,\right] \qquad (2.28)$$

$$\dot{\theta}_i = \frac{F\omega(1 + 2i\zeta)}{4EIk^2} \left[e^{-yk\zeta} e^{iyk} - ie^{-yk} e^{-iyk\zeta}\right] \qquad (2.29)$$

Both velocities therefore decrease exponentially with distance from the source. Substitution of the complex values of the Young's modulus and wavenumber into equations (2.23) and (2.24) give the shear force and bending moment for damped vibrations. By using equation (1.5) the power flow associated with each component may again be found. After some algebra it may be shown that the power flow associated with shear is:-

$$P_u = \frac{|F|^2\omega}{32EIk^3} \left[e^{-2yk\zeta} - \zeta e^{-2yk} + e^{-yk(1+\zeta)} \left[\sin(yk(1+\zeta)) + \cos(yk(1+\zeta))\right](1 - \zeta)\right] \qquad (2.30)$$

and the power associated with bending is:-

$$P_m = \frac{|F|^2\omega}{32EIk^3} \left[e^{-2yk\zeta} + 3\zeta e^{-2yk} - e^{-yk(1+\zeta)} \left[\cos(ky(1+\zeta) + \sin(ky(1+\zeta))\right](1 + 3\zeta)\right] \qquad (2.31)$$

while the total power flow is:-

$$P_a = P_u + P_m$$

$$= \frac{|F|^2\omega}{16EIk^3} \left[e^{-2ky\zeta} + \zeta e^{-2ky} - 2\zeta e^{-ky(1+\zeta)} \left[\cos(ky(1+\zeta)) + \sin(ky(1+\zeta))\right]\right] \qquad (2.32)$$

The power supplied by the source (2Pa evaluated at y = 0) is less than that in the undamped case because of the additional phase difference between the driving force and transverse velocity at the origin. For light damping the second and third terms in equation (2.32) may be ignored in the far field and the power flow is seen to decay exponentially with distance from the source.

2.7 Torque Excitation of a Uniform Beam

A simple means of applying a torque to a beam is to use a lever and apply an harmonic force parallel to the beam at the end of the lever-arm. This arrangement is commonly seen where a machine is supported by a cantilever attached to a vertical wall, or more generally where a floor slab is attached to its vertical supports.

The power supplied to a beam by a torque source is proportional to the square root of frequency. A torque source, unlike a force source, will therefore be important at high frequencies. Within the beam the two components of power flow are, once again, equal in the far field, but in the near field the power is initially associated with the bending moment alone.

Consider a uniform infinite beam laying along the y axis of cross-sectional area A, second moment of area I, Young's modulus E and density ρ. Let a torque of the form $Te^{-i\omega t}\delta_o$ per unit length be applied at the origin in which δ_o is a spatial delta function. The differential equation for harmonic frequency dependence of the form $e^{-i\omega t}$ is:-

$$\frac{\partial^4 \xi}{\partial y^4} - \frac{\omega^2 \rho A}{EI}\xi = -\frac{1}{EI}\frac{\partial}{\partial x}(T\delta_o) \tag{2.34}$$

Taking the Fourier transform in the y direction gives:-

$$\alpha^4 \tilde{\xi} - k^4 \tilde{\xi} = -\frac{i\alpha}{EI} T \tag{2.35}$$

where $$k^4 = \frac{\omega^2 \rho A}{EI} .$$

The solution is given by the inverse Fourier transform of equation (2.35) which may be written as:-

$$\xi(y) = \frac{-T}{2\pi EI} \int_{-\infty}^{\infty} \frac{i\alpha}{\alpha^4 - k^4} e^{i\alpha y} d\alpha \tag{2.36}$$

This equation has poles in the same position as in the case of a beam with force excitation and the same contour (fig. 2.5) may be used for integration. The displacement is therefore given by:-

$$\xi(y) = \frac{T}{4EIk^2}\left[e^{iky} - e^{-ky}\right] \tag{2.37}$$

The solution consists of a propagating wave and a non propagating near field.

At the origin, the near field is out of phase with the propagating wave and, as would be expected from symmetry, there is no transverse motion.

The instantaneous values of the transverse velocity and angular velocity for frequency dependence of the form $e^{-i\omega t}$ are:-

$$\dot{\xi}_i(y) = \frac{-i\omega T}{4EIk^2}\left[e^{iky} - e^{-ky}\right]e^{-i\omega t} \tag{2.38}$$

and

$$\dot{\theta}_i(y) = \frac{\omega T}{4EIk}\left[e^{iky} - ie^{-ky}\right]e^{-i\omega t} \tag{2.39}$$

The point mobility at the origin between the driving torque and the angular velocity may be found by substituting $y = 0$ in equation (2.39) to give:-

$$\beta = \frac{\omega(1 - i)}{4EIk} = \frac{(1 - i)\sqrt{\omega}}{4EI}\left(\frac{EI}{\rho A}\right)^{\frac{1}{4}} \tag{2.40}$$

This mobility increases with frequency, behaving at any frequency like that of a damper and spring in parallel.

2.8 Power Flow in a Uniform Beam with Torque Excitation

The power supplied by a torque source may be found by substituting the point mobility into equation (1.6) to give:-

$$P_s = \frac{|T|^2\sqrt{\omega}}{8EI}\left(\frac{EI}{\rho A}\right)^{\frac{1}{4}} . \tag{2.41}$$

The power flow into the beam therefore increases with frequency, making a torque source particularly significant at high frequencies.

The two components of power flow within the beam may be calculated in the same manner as that used for a force source. The power associated with the shear force is calculated by substituting the values of transverse velocity and shear force into equation (1.5) to give:-

$$P_u = \frac{|T|^2\omega}{32EIk}\left[1 - e^{-ky}[\cos ky - \sin ky]\right] \qquad (2.42)$$

Similarly, the power associated with the bending moment is:-

$$P_m = \frac{|T|^2\omega}{32EIk}\left[1 + e^{-ky}[\cos ky - \sin ky]\right] \qquad (2.43)$$

and the total power flowing is given by the sum of these two components and is:-

$$P_a = P_u + P_m = \frac{|T|^2\omega}{16EIk}. \qquad (2.44)$$

The power supplied by the torque source is therefore initially ($y = 0$) associated with P_m, the bending moment contribution, while there is no power flow in the shear component. The bending moment contribution decays in the near field transferring power to the shear component P_u. In the far field both P_m and P_u carry equal amounts of power in a similar manner to that found in a beam with a force source. The effect of damping on the power flow may once again be found by introducing a complex Young's modulus and a complex wavenumber. By writing the wavenumber as $k(1 + i\zeta)$ where, to first order, $4\zeta = \eta$, the displacement of the beam may be written as:-

$$\xi(y) = \frac{T(1 + 2i\zeta)}{4EIk^2}\left[e^{-ky\zeta}e^{iky} - e^{-ky}e^{-iky\zeta}\right] \qquad (2.45)$$

The motion of the beam therefore decays exponentially with distance from the torque source. Calculating the two components of the power flow for the damped case gives, after some algebra:-

$$P_u = \frac{|T|^2\omega}{32EIk}\left[e^{-2ky\zeta} - \zeta e^{-2ky} - e^{-ky(1+\zeta)}\left[\cos(ky(1+\zeta)) - \sin(ky(1+\zeta))\right](1-\zeta)\right] \quad (2.46)$$

for the component associated with shear, and

$$P_m = \frac{|T|^2\omega}{32EIk}\left[e^{-2ky\zeta} + 3\zeta e^{-2kx} + e^{-xk(1+\zeta)}\left[\cos(ky(1+\zeta)) - \sin(ky(1+\zeta))\right](1+3\zeta)\right] \quad (2.47)$$

for the component associated with bending.

The total power flow is thus:-

$$P_a = P_u + P_m$$

$$= \frac{|T|^2\omega}{16EIk}\left[e^{-2ky\zeta} + \zeta e^{-2ky} + 2\zeta e^{-ky(1+\zeta)}\left[\cos(ky(1+\zeta)) - \sin(ky(1+\zeta))\right]\right]. \quad (2.48)$$

The power supplied by the torque ($2P_a$ evaluated at $y = 0$) is thus greater when there is damping compared to the undamped case. If the damping is small then only the first term in equation (2.48) is important and this is an exponential decay with distance from the source.

CHAPTER 3

FLEXURAL WAVE PROPAGATION AND POWER FLOW IN PLATES

3.1 Introduction

There are three components of power flow within a plate carrying flexural waves. As in a beam, any element of the plate is acted upon by a shear force and a bending moment both of which transmit power. However, in a plate there is an additional bending moment, due to twisting, which may also transmit power. The shear force and bending moments must be considered as stresses, because of the two dimensional nature of a plate and therefore the power expressed as an intensity.

A transverse force source or a torque source acting on an infinite plate create a cylindrical propagating wave, which carries energy, and a nonpropagating near field. These two types of sources, the power they supply and the power propagated will be considered in the following sections. Exact solutions for an infinite plate excited by a transverse force are available in terms of Hankel functions [7]. However, these solutions will not be used but instead approximate solutions will be employed. These approximate solutions are more easily manipulated and will be directly comparable to the more complex structures studied later. A particular problem is encountered with torque sources where it is found that the classical plate equation is not applicable; an approximate solution is however given.

For the case of force excitation of a plate the wave propagation and power flow are given in reference [7]. The calculations will be repeated here using different methods and in a manner that enables general equations for wave propagation and power flow to be developed. These general equations will then be used extensively in the following chapter.

3.2 Flexural Vibrations of an Infinite Uniform Plate Driven by a Transverse Driving Force

The wave equation for a plate acted on by forces and torques is given in Appendix III. For a transverse point force applied at the origin and for harmonic time dependence of the form $e^{-i\omega t}$ the plate equation may be written:-

$$\nabla^4 \xi(x, y) - \omega^2 \frac{\rho h}{B} \xi(x, y) = \frac{F}{B} \delta_o \tag{3.1}$$

where ∇^4 is the Laplace operator squared, h the plate thickness, ρ the volume density and B the bending stiffness which is given by

$$B = \frac{h^3 E}{12(1 - \nu^2)} \tag{3.2}$$

where ν is Poisson's ratio. The force is of magnitude F and δ_o is the two dimensional Dirac delta function.

It has been assumed that the plate is thin and therefore that shear and rotation within the plate can be neglected.

The Laplace operator in equation (3.1) may be written in either Cartesian or polar coordinates. Using Cartesian coordinates and taking a two dimensional Fourier transform (defined in equation (2.3)) of the plate equation gives:-

$$\left[\alpha_x^4 + 2\alpha_x^2\alpha_y^2 + \alpha_y^4\right]\tilde{\tilde{\xi}} - \frac{\omega^2\rho h}{B}\tilde{\tilde{\xi}} = \frac{F}{B} \tag{3.3}$$

for an infinite plate where α_x and α_y are the two coordinates in wavenumber space. This may be rewritten as

$$\tilde{\tilde{\xi}} = \frac{F}{2Bk^2}\left[\frac{1}{\alpha_x^2 + \alpha_y^2 - k^2} - \frac{1}{\alpha_x^2 + \alpha_y^2 + k^2}\right] \tag{3.4}$$

where k is the free plate wavenumber defined as:-

$$k^4 = \frac{\omega^2\rho h}{B} . \tag{3.5}$$

The inversion integral (equation (2.4)) is a double integral; integration with respect to α_x will be considered first. This integral has poles at $\sqrt{k^2 - \alpha_y^2}$ and $i\sqrt{k^2 + \alpha_y^2}$ and therefore a contour integration may be performed directly to give:-

$$\xi(x,y) = \frac{Fi}{4Bk^2\pi} \int_{-\infty}^{\infty} \frac{e^{i\alpha_y y} e^{ix\sqrt{k^2-\alpha_y^2}}}{2\sqrt{k^2 - \alpha_y^2}} - \frac{e^{i\alpha_y y} e^{-x\sqrt{k^2+\alpha_y^2}}}{2i\sqrt{k^2 + \alpha_y^2}} \, d\alpha_y \qquad (3.6)$$

Integration with respect to α_y is difficult due to the multivalued nature of $\sqrt{k^2 \pm \alpha_y^2}$. A contour integration could be performed but the contour would have to be indented to exclude the branch points at k and ik and therefore does not lead to a simple method for solving the integral. Two special solutions of the integral will be considered - the response at the driving point and the response in the far field.

3.3 The Response at the Driving Point of a Plate with Force Excitation

For this case $x = y = 0$ in equation (3.6) and the inversion integral simplifies to:-

$$\xi(0, 0) = \frac{Fi}{8Bk^2\pi} \int_{-\infty}^{\infty} \frac{1}{\sqrt{k^2 - \alpha_y^2}} - \frac{1}{i\sqrt{k^2 + \alpha_y^2}} \, d\alpha_y \qquad (3.7)$$

In order to perform this integration it is necessary to give meaning to the square root function $\sqrt{k^2 - \alpha_y^2}$. This may be done by enforcing the condition that an outgoing wave decays towards infinity giving the square root function the values:-

$$\sqrt{k^2 - \alpha_y^2} = |\sqrt{k^2 - \alpha_y^2}| \qquad \text{for} \qquad \alpha_y^2 < k^2$$

$$\sqrt{k^2 - \alpha_y^2} = i|\sqrt{k^2 - \alpha_y^2}| \qquad \text{for} \qquad \alpha_y^2 > k^2.$$

The value of the integral for $\alpha_y^2 = k^2$ may be found by defining a Cauchy principal value at this point.

The response at the driving point is eventually given by:-

$$\xi(0, 0) = \frac{Fi}{8Bk^2} \tag{3.8}$$

The mobility at the driving point is therefore:-

$$\beta = \frac{\omega}{8Bk^2} = \frac{1}{8\sqrt{B\rho h}} \tag{3.9}$$

This mobility is purely real and is independent of frequency. The point response of an infinite plate excited by a transverse force therefore behaves like that of a viscous damper at all frequencies. From symmetry it is immediately seen that there is no rotation at the driving point.

3.4 The Response in the Far Field of a Plate with Force Excitation

Away from the source for large values of x and y the exponential terms in equation (3.6) dominate. An approximate solution based on the method of steepest descent [10, 11] is therefore highly applicable. Considering the two terms of equation (3.6) separately and by making the substitutions:-

$$\begin{aligned} x &= r \cos \phi \\ y &= r \sin \phi \\ \alpha_y &= k \sin q \end{aligned} \tag{3.10}$$

to convert to polar coordinates r and ϕ the first term in equation (3.6) may be written as:-

$$I_1 = \int_{-\frac{\pi}{2} + i\infty}^{\frac{\pi}{2} - i\infty} e^{ikr \cos(q - \phi)} dq \tag{3.11}$$

The path of integration to this substitution is shown in the complex q plane in fig. 3.1.

A saddle point of the exponent occurs at $q = \phi$; deforming the path of integration to pass through this point according to the method of steepest descent enables a first order solution to be obtained. The new path is:-

$$\cos(\mathrm{Re}\{q\} - \phi)\cosh(\mathrm{Im}\{q\}) = 1 \tag{3.12}$$

which is sketched on fig. 3.1. The approximate solution to equation (3.10) is therefore:-

$$I_1 = e^{i(rk - \frac{\pi}{4})} \sqrt{\frac{2\pi}{rk}} \tag{3.13}$$

The second term in equation (3.6) is solved in a similar manner. Making the substitution

$$\begin{aligned} x &= r\cos\phi \\ y &= r\sin\phi \\ \alpha_y &= k\sinh q \end{aligned} \tag{3.14}$$

enables the second term to be written as:-

$$I_2 = \int_{-\infty}^{\infty} e^{rk_e - \cos(iq + \phi)}\, dq \tag{3.15}$$

The saddle point for this integral is at $q = 0 + i\phi$; the path of integration deformed to pass through this point is shown in figure 3.2. The approximate solution of this integral is thus:-

$$I_2 = e^{-rk} \sqrt{\frac{2\pi}{rk}} \tag{3.16}$$

The complete solution in the far field in polar coordinates may now be written as:-

$$\xi(r, \phi) = \frac{Fi}{8Bk^2} \sqrt{\frac{2}{rk\pi}} \left[e^{i(rk - \frac{\pi}{4})} + ie^{-rk} \right] \tag{3.17}$$

The second term decays with distance from the origin and will not be important in the far field. The first term is that of a propagating

cylindrical wave. The amplitude of the cylindrical wave decreases with distance being inversely proportional to the square root of the distance from the driving force.

3.5 Power Flow Intensity Due to Cylindrical Waves in a Plate

As will be shown, point sources on plates or beam stiffened plates create cylindrical wavefields. Since these types of structures are considered later general equations for the power flow associated with a cylindrical wave will now be derived. Consider a polar coordinate system coordinates r, ϕ with a source at $r = 0$. A cylindrical wave in the far field of an infinite plate may be represented to first order by:-

$$\xi(r, \phi) = \frac{e^{i(rk - \frac{\pi}{4})}}{\sqrt{rk}} f(\phi) \qquad (3.18)$$

where $f(\phi)$ is a function representing the angular distribution amplitude of the wave around the source. If $f(\phi)$ is a constant then the cylindrical wave will have the same amplitude for all points of equal radius from the source. If the source has directional properties the variation of amplitude for different angles is given by $f(\phi)$. A section of the plate normal to the radial or circumferential direction has a shear force, a bending moment and a twisting moment acting on it.

The twisting moment is a bending moment which does not occur in beams but occurs in plates because of the Poisson effect. The two bending moments act at right angles to each other, the complete set of forces on a plate element being shown in figure A.3. Since only plates of uniform thickness are considered here the shear force and the two bending moments may be expressed as force or moment per unit length. The power flow intensity is therefore also derived as a power per unit length.

There are thus six components of power flow intensity at a point in a plate (three in the radial direction and three in the circumferential direction) each given by the time average of force (or moment) with velocity (or angular velocity) according to equation (1.5).

The equations for the shear force and bending moments in the radial and circumferential direction are given in Appendix III. In developing equations for the power flow intensity only first order terms in kr have been retained. The subscripts u, m and T will be used to indicate power flow intensity components associated with shear bending and twisting and an additional subscript r or ϕ will be used to indicate the radial or circumferential directions.

The components of the power flow intensity in the radial direction are:-

$$P_{ur} = \tfrac{1}{2}\mathrm{Re}\{U_{rz}\dot{\xi}^*\} \tag{3.19}$$

$$P_{mr} = \tfrac{1}{2}\mathrm{Re}\{M_{r\phi}(-\frac{\partial\dot{\xi}}{\partial r})^*\} \tag{3.20}$$

$$P_{Tr} = \tfrac{1}{2}\mathrm{Re}\{M_{rr}(\frac{1}{r}\frac{\partial\dot{\xi}}{\partial r})^*\} \tag{3.21}$$

The asterisk denotes the complex conjugate. The shear force U_{rz} and the bending moments $M_{r\phi}$ and M_{rr} (each per unit length) may be found in terms of the displacement of the plate by employing relations (A.16)-(A.21). The components of the radial power flow intensity are thus found to be:-

$$P_{ur} = \frac{B|f(\phi)|^2}{2}\frac{\omega k^2}{rk} \tag{3.22}$$

$$P_{mr} = \frac{B|f(\phi)|^2}{2}\frac{\omega k^3}{rk} \tag{3.23}$$

$$P_{rr} = \frac{B(1-\nu)}{2}\left|\frac{\partial f(\phi)}{(rk)^3}\right|^2\frac{\omega k^3}{(rk)^3} \tag{3.24}$$

where only terms of first order in rk have been retained. As in a beam the shear component P_{ur} and the bending component P_{mr} are equal. The power flow intensity associated with each component decreases with increasing distance from the source. The twisting component P_{Tr} decreases particularly quickly because of the term in $(rk)^3$ in the denominator. For this reason the twisting component of power flow will

be of no importance in the far field unless the value of $\left|\frac{\partial f(\phi)}{\partial \phi}\right|^2$ is particularly large (as, for example, at a discontinuity).

The power flow intensity in the circumferential direction is calculated in a similar manner. The components of power flow per unit length are thus:-

$$P_{u\phi} = \tfrac{1}{2}\mathrm{Re}\{U_{\phi z}\dot{\xi}^*\} \tag{3.25}$$

$$P_{m\phi} = \tfrac{1}{2}\mathrm{Re}\{M_{\phi r}(\frac{1}{r}\frac{\partial \dot{\xi}}{\partial \phi})^*\} \tag{3.26}$$

$$P_{T\phi} = \tfrac{1}{2}\mathrm{Re}\{M_{\phi\phi}(-\frac{\partial \dot{\xi}}{\partial r})^*\} \tag{3.27}$$

Assuming the cylindrical wave form of equation (3.18) the internal shear forces and bending moments may once again be calculated by using relations (A.16)-(A.21). The components of power flow intensity are therefore:-

$$P_{u\phi} = \frac{B}{2}\,\mathrm{Re}\{(\frac{-k^3}{rk\sqrt{rk}}\,\frac{\partial f}{\partial \phi} + \frac{k^3}{(rk)^3\sqrt{rk}}\,\frac{\partial^3 f}{\partial \phi^3})(\frac{i\omega}{\sqrt{rk}}f^*)\} \tag{3.28}$$

$$P_{m\phi} = \frac{B}{2}\,\mathrm{Re}\{(\frac{i\omega k^3}{r(rk)^*}(f - 2\,\frac{\partial^2 f}{\partial \phi^2}) + \frac{(1-\vartheta)\omega k^3 f}{(rk)^3} + \frac{i\omega\mu k^3 f}{(rk)^2})(\frac{\partial f}{\partial \phi})^*\} \tag{3.29}$$

$$P_{T\phi} = \frac{B(1-\vartheta)}{2}\,\mathrm{Re}\{(\frac{-2\omega k^3}{(rk)^3} - \frac{i\omega k^3}{(rk)^2})\,\frac{\partial f}{\partial \phi}\,f^*\} \tag{3.30}$$

These three equations are strongly dependent upon $f(\phi)$ - the amplitude distribution of the wave around the source. For waves whose amplitude is independent of ϕ these three components of power flow intensity are zero.

3.6 Power Flow in a Plate with Force Excitation

The power flowing into the plate at the driving point may be calculated by substituting the mobility into equation (1.6) to give:-

$$P_s = \frac{|F|^2}{16\sqrt{B\rho h}} \tag{3.31}$$

The total power supplied by the force source is independent of frequency and inversely proportional to the square of the plate thickness.

Using the results developed in the last section, an equation for the power flowing in a plate driven by a transverse driving force is readily obtained. In this case the cylindrical wave propagates equally in all directions away from the source and $f(\phi)$ (equation (3.18)) is independent of angle. From equations (3.17) and (3.18) $f(\phi)$ is given by:-

$$f(\phi) = \frac{iF\sqrt{2}}{Bk^2\sqrt{\pi}} \tag{3.32}$$

Because the wave has no angular dependence, power is only carried by the shear and bending components in the radial direction. The radial twisting components and the three components in the circumferential direction are all zero. The power flow per unit length transmitted by the shear component in the radial direction may be calculated from equation (3.22) and is

$$P_{ur} = \frac{|F|^2\omega}{64\pi Brk^2} = \frac{|F|^2}{64\pi\sqrt{\rho hB}} \cdot \frac{1}{r} \tag{3.33}$$

This formula is based on the assumption that far field conditions are being considered and for this case the moment component of power flow intensity, P_{mr}, will equal the shear component. The total power flow intensity in the radial direction is given by the sum of the two components and may be written as:-

$$P_{ar} = P_{ur} + P_{mr} = \frac{|F|^2}{32\pi\sqrt{\rho hB}} \frac{1}{r} \tag{3.34}$$

The power flow intensity in a plate with a transverse driving force is thus inversely proportional to the distance from the source.

3.7 Flexural Vibrations of an Infinite Uniform Plate due to Torque Excitation

The classical plate equation is inadequate when dealing with the response of a plate in the near field of a torque source. A solution of the particular problem has been obtained by Dyer [12] based on the more general equation developed by Mindlin. Except for this one problem the classical plate equation may be used to calculate the power flow supplied by the source and to calculate the response and the power flow in the far field of the plate. For completeness, the solution in the near field from reference [12] will be given but all other calculations will proceed from the classical plate equation derived in Appendix III.

For a torque source applied at the origin about the x axis and for harmonic time dependence of the form $e^{-i\omega t}$ the plate equation may be written as:-

$$\nabla^4 \xi(x, y) - k^4 \xi(x, y) = -\frac{1}{B} \frac{\partial}{\partial y} \left[T_{xx} \delta_x \delta_y \right] \qquad (3.35)$$

k is the free plate wavenumber and B the bending stiffness. Employing Cartesian coordinates and taking the two dimensional Fourier transform gives:

$$\tilde{\xi}(\alpha_x, \alpha_y) = -\frac{T_{xx}}{2Bk^2} \left[\frac{i\alpha_y}{\alpha_x^2 + \alpha_y^2 - k^2} - \frac{i\alpha_y}{\alpha_x^2 + \alpha_y^2 + k^2} \right] \qquad (3.36)$$

where α_x and α_y are the two coordinates in wavenumber space. The solution is given by the inverse Fourier transform of this equation.

For the solution at the driving point the angular displacement rather than the transverse displacement is required. Writing θ for the angular displacement and making the small angle approximation gives:-

$$\theta = \frac{\partial \xi}{\partial y} \quad \text{and therefore} \quad \tilde{\theta} = i\alpha_y \tilde{\xi}$$

The angular displacement at the driving point may now be written as:-

$$\theta = \frac{T}{8\pi^2 Bk^2} \int_{-\infty}^{\infty}\int \left[\frac{i\alpha_y^2}{\alpha_x^2 + \alpha_y^2 - k^2} - \frac{i\alpha_y^2}{\alpha_x^2 + \alpha_y^2 + k^2}\right] d\alpha_x d\alpha_y \tag{3.37}$$

As in the case of a plate excited by a transverse driving force, integration with respect to α_x will be considered first. This integration process has two poles at $\sqrt{k^2 - \alpha_y^2}$ and at $i\sqrt{k^2 + \alpha_y^2}$ and again may be performed by means of a contour integration.

The result of this first integration for the response at the driving point may be written as:-

$$\theta(0, 0) = \frac{T}{8\pi Bk^2} \int_{-\infty}^{\infty} \left[\frac{i\alpha_y}{\sqrt{k^2 - \alpha_y^2}} - \frac{\alpha_y^2}{\sqrt{k^2 + \alpha_y^2}}\right] d\alpha_y \tag{3.38}$$

The final integral is straightforward except for the singularities which may be approached, as in the case of a transverse driving force, by defining Cauchy principal values. The mobility at the driving point is thus:-

$$\beta = \frac{\omega}{16B}\left[1 - \frac{i4}{\pi} \operatorname*{Lt}_{b\to\infty} (b)\right] \tag{3.39}$$

The limit arrives as a consequence of the Cauchy principal value and implies that an infinite imaginary component of velocity will result from a torque source. This unsatisfactory result arises from the assumption in classical plate theory that there is no transverse shear deformation. The solution to this problem derived by Dyer [12] using a more general plate equation gives

$$\beta = \frac{\omega}{8B(1 + L)}\left[1 + \frac{i4}{\pi} \ln ka - \frac{i8L}{\pi(1 - \nu)} \left(\frac{h}{\pi a}\right)^2\right] \tag{3.40}$$

for the point mobility. In this equation the moment is considered to act over a disc of radius a which is small ($(ka)^2 << 1$). The parameter L is an expression in terms of Bessel functions which approaches unity when the disc radius a is greater than the plate thickness h.

Reference [12] gives values of h for a wide range of a/h. For cases of practical interest the real parts of equation (3.39) and (3.40) are essentially equal.

Thus the point mobility of a plate due to torque excitation appears at any frequency to be like that of a dashpot and spring in parallel.

3.8 The Responses in the Far Field of a Plate with Torque Excitation

The solution to this problem is the inverse Fourier transform of equation (3.36) which may be written as:-

$$\xi(x, y) = \frac{-Ti}{8Bk^2\pi^2} \int_{-\infty}^{\infty}\int \left[\frac{\alpha_y e^{i\alpha_y y} e^{i\alpha_x x}}{\alpha_x^2 + \alpha_y^2 - k^2} - \frac{\alpha_y e^{i\alpha_y y} e^{i\alpha_x x}}{\alpha_x^2 + \alpha_y^2 + k^2}\right] d\alpha_x d\alpha_y \tag{3.41}$$

Performing a contour integration with respect to α_x results in the following expression:-

$$\xi(x, y) = \frac{T}{8Bk^2\pi} \int_{-\infty}^{\infty}\left[\frac{e^{i\alpha_y y} e^{i\sqrt{k^2 - \alpha_y^2}\, x}\, \alpha_y}{\sqrt{k^2 - \alpha_y^2}}\right.$$

$$\left. - \frac{e^{i\alpha_y y} e^{-\sqrt{k^2 + \alpha_y^2}\, x}\, \alpha_y}{i\sqrt{k^2 + \alpha_y^2}}\right] d\alpha_y \tag{3.42}$$

where the residues are due to poles at $\sqrt{k^2 - \alpha_y^2}$ and $i\sqrt{k^2 + \alpha_y^2}$.

The remaining integral may not be solved exactly but an approximate solution valid in the far field may be found by the method of steepest descent. The solution may be obtained in a manner similar to that obtained for a plate excited by a transverse driving force. By considering the integration of the two terms in equation (3.42) separately and by making the following substitutions:-

$$x = r \cos \phi$$
$$y = r \sin \phi$$
$$\alpha_y = k \sin q$$

the integral of the first term may be written as:-

$$I_1 = \int_{-\frac{\pi}{2}+i}^{\frac{\pi}{2}-i} e^{ikr \cos(q-\phi)} \, k \sin q \, dq \qquad (3.43)$$

Except for the term $k \sin q$ this expression is the same as the equivalent expression for force excitation of a plate. The same integration path (figure 3.1) may therefore be used and the approximate solution to the first integral is:-

$$I_1 = k\sqrt{\frac{2\pi}{rk}} \, e^{i(rk - \frac{\pi}{4})} \sin \phi \qquad (3.44)$$

The integral of the second term of equation (3.42) may be written as:-

$$I_2 = \int_{-\infty}^{\infty} e^{rk} \, e^{-\cos(iq+\phi)} k \sinh q \, dq \qquad (3.45)$$

after making the substitutions:-

$$x = r \cos \phi$$
$$y = r \sin \phi$$
$$\alpha_y = k \sinh q.$$

The integration path for the equivalent integral for force excitation of a plate (figure 3.2) may once again be used and the approximate solution of equation (3.45) is:-

$$I_2 = ik\sqrt{\frac{2\pi}{rk}} \, e^{-rk} \sin \phi. \qquad (3.46)$$

This term decays exponentially with distance from the origin and will thus be of no importance in the far field.

The displacement in the far field of a plate due to a torque excitation may now be written as:-

$$\xi = \frac{T}{8Bk}\sqrt{\frac{2}{rk\pi}}\, e^{i(rk - \frac{\pi}{4})} \sin\phi \qquad (3.47)$$

The disturbance thus travels out from the source as a cylindrical wave with a strong angular directivity.

3.9 Power Flow in an Infinite Plate with Torque Excitation

The power flowing into a plate from a torque source may be found by substituting the real part of the driving point mobility into equation (1.6). For practical structures the classical point mobility (equation (3.39)) and the exact point mobility (equation (3.40)) give the same result:-

$$P_s = \frac{\omega|T|^2}{32B} \qquad (3.48)$$

The power flow supplied by the source is proportional to ω and will therefore be very important at high frequencies.

The power flow intensity in the far field of a plate with a torque source is strongly dependent on the direction in which the torque is applied. If the x and y axes of a rectangular coordinate system lie in the plane of a plate and a torque is applied about the x axis then the principal direction of power flow will be along the y axis.

The general equations developed in section 3.5 may be used to calculate the six components of power flow intensity. In this case the directivity function of the cylindrical wave $f(\phi)$ is given by:-

$$f(\phi) = \frac{T}{8Bk}\sqrt{\frac{2}{\pi}} \sin\phi \qquad (3.49)$$

In the radial direction the power flow intensities associated with shear and bending are equal and are given by:-

$$P_{ur} = P_{mr} = \frac{|T|^2 \omega k \sin^2\phi}{64\pi B r k} \tag{3.50}$$

The twisting component of power flow in the radial direction is:-

$$P_{Tr} = \frac{|T|^2 (1 - \vartheta)\omega k \cos^2\phi}{64\pi B r^3 k^3} \tag{3.51}$$

The shear and bending components are inversely proportional to r the distance from the source with the twisting component decreasing more rapidly being inversely proportional to r^3. The radial twisting component is therefore relatively unimportant as a power transmission mechanism. The dependence of the power flow on $\sin^2\phi$ results in a strongly directional far field. The maximum power flow intensity occurs when ϕ equals 90^o which is at right angles to the applied torque.

The circumferential power flow intensities may be calculated from equations (3.28), (3.29) and (3.30). The shear component $P_{u\phi}$ is zero; the other two components, bending $P_{m\phi}$ and twisting $P_{r\phi}$, are

$$P_{m\phi} = \frac{|T|^2 (1 - \vartheta)\omega k \sin\phi \cos\phi}{64\pi B r^3 k^3} \tag{3.52}$$

$$P_{T\phi} = \frac{-|T|^2 (1 - \vartheta)\omega k \sin\phi \cos\phi}{32\pi B r^3 k^3} \tag{3.53}$$

Both of these components are small compared to the radial power flow being inversely proportional to r^3.

3.10 A Comparison between Finite and Infinite Structures

Due to reflections from discontinuities any finite structure will exhibit resonances which would not be apparent in the response of an infinite structure. The magnitude of the vibration amplitudes at resonances are controlled by the damping of the structure and generally the largest response will occur at the first resonance. Thus when a finite structure is being represented by an equivalent infinite structure the largest error that will occur will be at a resonance frequency. The mobility at the driving point of any finite structure (for $e^{-i\omega t}$ fre-

quency dependence) may be written as:-

$$\frac{V}{F} = -i\omega \sum_{N} \frac{[\psi^{(n)}]^2}{\omega_n^2(1 - i\eta) - \omega^2} \tag{3.54}$$

where ω_n is the real resonance frequency, η the hysteretic loss factor and $\psi^{(n)}{}_n$ is the amplitude of the mode shape at the driving point (see section 6.2). At a low frequency resonance, for light damping, the contribution of off-resonant terms is negligible compared to the magnitude of the term at resonance. Thus the driving point mobility of a finite structure at resonance may be written as:-

$$\frac{V}{F} = \frac{[\psi^{(n)}]^2}{\omega_n \eta} \tag{3.55}$$

if there is a wide frequency spacing between resonances. It may be seen that the mobility value is largest for the lowest value of resonance frequency assuming $\psi^{(n)}$ does not vary significantly for different resonances.

The largest peaks in the mobility spectra of finite beams and plates have been calculated. These peak mobility values represent a worst case if a finite structure is modelled as being infinite. Table I contains a list of the peak mobilities and also a list of the ratios of the peak point mobility of the finite structure to the point mobility of the infinite structure. The ratio is written in modulus form rather than as a complex quantity.

For torsional and longitudinal waves the response was calculated at the mid-point of a beam with clamped ends. For flexural waves a beam with simply supported ends and excitation at the midpoint was considered. In the case of torque excitation the second resonance frequency was used because a torque excitation at the midpoint of a beam will not produce any motion at the first resonance frequency. When considering a finite plate it was assumed that the plate was rectangular and simply supported at the boundaries with excitation applied in the middle. Once again it was necessary to use the second resonance frequency when considering torque excitation. The ratio of the mobility of the finite structure at

resonance to the mobility of the infinite case takes a particularly simple form, in most cases being inversely proportional to the loss factor.

CHAPTER 4

WAVE PROPAGATION AND POWER FLOW IN BEAM-STIFFENED PLATES

4.1 Introduction

Beam-stiffened plates are frequently used components in all common structures and are therefore a most important type of foundation. In this chapter an analysis is made of an infinite plate to which a single infinite beam is attached. Three types of excitation each applied to the beam are individually examined.

Consider an infinite plate laying in the x-y plane of a rectangular coordinate system with an infinite beam laying along the y-axis (see figure 4.1). The first excitation considered is a force normal to the plate, the second a torque applied about the x axis and the third a torque applied about the y axis.

The general conclusion from these calculations is that the power flowing into the system is controlled by the beam while the subsequent flow of power throughout the structure is governed by the plate.

The response of a beam stiffened plate due to force excitation has been analysed in the near field by Lamb [13] and in the far field by Kovinskaya and Nikiforov [14] and Fahy and Lindqvist [15]. The response due to torque excitation and the power flow in the beam and plate are not considered in these papers. It is assumed in these references and in the following analysis that there is pure flexural wave motion in the plate and that the beam may carry flexural or torsional waves.

The response of the structure is obtained by a novel method in the analysis which follows below. The method used in references [13, 14, 15] modelled the plate by cutting it along the y axis and making two semi-infinite plates on the boundaries of which forces and torques are applied. The motion of the beam laying along the y axis was then deduced from the exciting force and the reaction of the two semi-infinite plates. The analysis used here makes use of the more general plate and beam equations derived in Appendices I, II and III. The beam and plate are considered

separately and the response of each due to a general line excitation determined. The combined motion of the beam and plate are then found by satisfying compatibility relationships. In this manner the responses are calculated in much the same way as when joining components using mobility methods.

It is assumed that the beam and plate respond in simple bending or torsion and that there is no additional internal wave motion (for example, relative motion of web and flange in an I-beam stiffener). This assumption and the effect of a non coincident neutral axis in the beam and plate have been considered by Nilsson [16] and shown to be valid for low frequencies. The onset of internal wave motion marks the upper frequency limit of applicability of the following analysis.

4.2 Formulation of the Equations for the Response of an Infinite Plate Stiffened by an Infinite Beam

The response of an infinite, beam-stiffened plate to three types of excitation is considered in this section. The excitation in each case is harmonic with a wave propagating in the positive x direction written as $e^{i(kx - \omega t)}$. The beam and plate with the forces acting on them are shown in figure 4.2. The plate laying in the x, y plane has a line excitation of forces and torques along the y axis due to the presence of the beam. The equation of motion of the plate may thus be written as:-

$$\nabla^4 \xi_p(x,y) - k_p{}^4 \xi_p(x,y) = \frac{1}{B_p}\left[F_p(y)\delta_x + \frac{\partial}{\partial x}(T_{yp}(y)\delta_x) - \frac{\partial}{\partial y}(T_{xp}(y)\delta_x)\right] \tag{4.1}$$

The subscript p is used to denote the properties of the plate, the subscript b being used for the beam. $F_p(y)$ is the normal force per unit length applied to the plate, $T_{yp}(y)$ is the torque per unit length parallel to the y axis and $T_{xp}(y)$ the torque per unit length parallel to the x axis. All these forces and torques are applied along the y-axis, the delta function δ_x giving them the correct dimension of force or torque per unit area. k_p is the free plate wavenumber and B_p the plate bending stiffness.

In general, the beam may carry both flexural and torsional waves. It is assumed that these two types of wave motion are uncoupled, which is valid if the beam has a symmetrical cross-section. The equation of motion for beam flexure is given by:-

$$\frac{\partial^4 \xi_b(y)}{\partial y^4} - k_b{}^4 \xi_b(y) = \frac{1}{B_b}\left[F_b(y) - \frac{\partial}{\partial y}\left(T_{xb}(y)\right)\right] \qquad (4.2)$$

$F_b(y)$ is the force per unit length applied to the beam, $T_{xb}(y)$ the torque per unit length (see figure 4.2), k_b the beam wavenumber and B_b (= EI) the beam bending stiffness.

The torsional motion of the beam is given by:-

$$\frac{\partial^2 \theta(y)}{\partial y^2} + k_t{}^2 \theta(y) = \frac{1}{GQ}\left[-T_{yb}(y)\right] \qquad (4.3)$$

where $\theta(y)$ is the angle of rotation of the beam about the y axis, T_{yb} the applied torque per unit length, GQ the torsional stiffness for the beam and k_t the torsional wave number.

The equations for equilibrium of forces and torques are:-

$$F_o \delta_y = F_b(y) + F_p(y) \qquad (4.4)$$

$$T_{xo} \delta_y = T_{xb}(y) + T_{xp}(y) \qquad (4.5)$$

$$T_{yo} \delta_y = T_{yb}(y) + T_{yp}(y) \qquad (4.6)$$

where F_o, T_{xo} and T_{yo} are the force and the torques applied at the origin which excite the structure. The spatial delta function δ_y enables each point excitation to be expressed as a force per unit length or a torque per unit length. Continuity of displacement and slope is enforced by the relations:-

$$\xi_b(y) = \xi_p(x, y)\big|_{x=0} \qquad (4.7)$$

$$\theta(y) = -\frac{\partial \xi_p(x,y)}{\partial x}\Big|_{x=0} \qquad (4.8)$$

The above set of equations may be solved by evaluating the Fourier transform in the y direction and substituting for the various unknowns. To obtain the Fourier transform of the plate motion in the y direction it is first necessary to take the two dimensional plate Fourier transform and then inverse transform for the x coordinate. The two dimensional plate Fourier transform may be written as:-

$$\tilde{\tilde{\xi}}_p(\alpha_x, \alpha_y) = \frac{1}{B_p} \frac{\tilde{F}_p + i\alpha_x \tilde{T}_{yp} - i\alpha_y \tilde{T}_{xp}}{(\alpha_x^2 + \alpha_y^2 - k_p^2)(\alpha_x^2 + \alpha_y^2 - k_p^2)} \tag{4.9}$$

Because $\tilde{F}_p$, $\tilde{T}_{yp}$ and $\tilde{T}_{xp}$ are independent of α_x the inverse transformation for this coordinate may be performed without difficulty. After contour integration, the plate Fourier transform in the y direction is:-

$$\tilde{\tilde{\xi}}_p(x, \alpha_y) = \frac{i}{4B_p k_p^2} \left[\frac{(\tilde{F}_p + i\sqrt{k_p^2 - \alpha_y^2}\,\tilde{T}_{yp} - i\alpha_y \tilde{T}_{xp}) e^{i\sqrt{k_p^2 - \alpha_y^2}\,x}}{\sqrt{k_p^2 - \alpha_y^2}} \right.$$

$$\left. + \frac{i(\tilde{F}_p - \sqrt{k_p^2 + \alpha_y^2}\,\tilde{T}_{yp} - i\alpha_y \tilde{T}_{xp}) e^{-\sqrt{k_p^2 + \alpha_y^2}\,x}}{\sqrt{k_p^2 + \alpha_y^2}} \right] \tag{4.10}$$

The remaining equations (4.2, 4.3) are only dependent on y and may be transformed to produce a set of linear simultaneous equations. After much algebra, the unknowns in equation (4.10) may be eliminated to give:-

$$\tilde{\tilde{\xi}}_p(x, \alpha_y) = (F_o - i\alpha_y T_{xo}) e^{i\sqrt{k_p^2 - \alpha_y^2}\,x} D_1 + T_{yo} e^{i\sqrt{k_p^2 - \alpha_y^2}\,x} D_2$$

$$+ (F_o - i\alpha_y T_{xo}) e^{-\sqrt{k_p^2 + \alpha_y^2}\,x} D_3 + T_{yo} e^{-\sqrt{k_p^2 + \alpha_y^2}\,x} D_4 \tag{4.11}$$

where D_1, D_2, D_3 and D_4 are all functions of α_y and may be written as:-

$$D_1 = \frac{1}{B_b(\sqrt{k_p^2 + \alpha_y^2} + i\sqrt{k_p^2 - \alpha_y^2})} \times \frac{\sqrt{k_p^2 + \alpha_y^2}}{\alpha_y^4 - k_b^4 - i2\frac{B_p}{B_b}(k_p^4 - \alpha_y^4)\{\frac{1}{\sqrt{k_p^2 - \alpha_y^2}} - \frac{i}{\sqrt{k_p^2 + \alpha_y^2}}\}} \quad (4.12)$$

$$D_2 = \frac{-1}{GQ(\sqrt{k_p^2 + \alpha_y^2} + i\sqrt{k_p^2 - \alpha_y^2})(\alpha_y^2 - k_t^2 + 2\frac{B_p}{GQ}\{\sqrt{k_p^2 + \alpha_y^2} - i\sqrt{k_p^2 - \alpha_y^2}\})} \quad (4.13)$$

$$D_3 = \frac{1}{B_b(\sqrt{k_p^2 + \alpha_y^2} + i\sqrt{k_p^2 - \alpha_y^2})} \times \frac{i\sqrt{k_p^2 - \alpha_y^2}}{\alpha_y^4 - k_b^4 - i2\frac{B_p}{B_b}(k_p^4 - \alpha_y^4)\{\frac{1}{\sqrt{k_p^2 - \alpha_y^2}} - \frac{i}{\sqrt{k_p^2 + \alpha_y^2}}\}} \quad (4.14)$$

$$D_4 = -D_2 \quad (4.15)$$

The solution of this problem, the displacement of the beam and plate, is given by the inverse Fourier transform of equation (4.11). The overall response of the structure is a linear superposition of the response to each excitation. In the following sections the response of the structure to each separate excitation will therefore be considered. It is not possible to obtain an exact solution for any of the inverse Fourier transforms; thus approximate solutions for the point response and the response in the far field will be considered.

4.3 Force Excitation of an Infinite, Beam-stiffened Plate

Setting $T_{xo} = T_{yo} = 0$ in equation (4.11) and considering the inverse Fourier transform with $x = y = 0$ gives the equation for the point response of the system. This may be written as:-

$$\xi_p(0,\,0) = \frac{F_o}{2\pi B_b}\int_{-\infty}^{\infty} \frac{1}{\alpha_y^4 - k_b^4 - i2\frac{B_p}{B_b}(k_p^4 - \alpha_y^4)\left\{\frac{1}{\sqrt{k_p^2 - \alpha_y^2}} - \frac{i}{\sqrt{k_p^2 - \alpha_y^2}}\right\}}\, d\alpha_y \tag{4.16}$$

This equation is the same as that deduced by Lamb [13] who also obtained an approximate solution by means of contour integration. The contour used is shown in figure 4.3; it includes the two poles of the integral and is deformed along two branch cuts to exclude the branch points (at $\alpha = k_p$ and $\alpha = ik_p$), where the square root functions are not analytic. The integral is given by the sum of the residues minus the extra contribution where the integral has been deformed along the branch cuts. On examining the terms of the integral, Lamb found that $B_p/(B_b k_b)$ was small compared to unity and proceeded to evaluate the integral to first order in this coupling parameter. The position of the poles was found by Newton's method, the first estimate of their position being k_b and ik_b. The branch cut integrals may be evaluated after having been simplified to first order terms. The complete result given by Lamb for the driving point mobility is:-

$$\beta = \frac{\omega}{4B_b k_b^3}\left(1 + i - \frac{i4B_p}{\pi B_b k_b}\left\{1 + \frac{3 - s^2}{2s^2\sqrt{1 - s^2}}\cos^{-1}s\right.\right.$$

$$\left.\left. + \frac{3 + s^2}{2s^3\sqrt{1 + s^2}}\sinh^{-1}s\right\}\right) \tag{4.17}$$

where $s = k_b/k_p$. This result is very similar to the point mobility of a beam the difference being in an additional imaginary term. At high frequencies the coupling term $B_p/(B_b k_b)$ is very small and thus the mobility will deviate from that of a free infinite beam only at low frequencies.

The response in the far field is best determined by considering equation (4.11) with $T_{xo} = T_{yo} = 0$; the equation then reduces to:-

$$\xi_p(x,y) = \frac{F_o}{2\pi}\int_{-\infty}^{\infty} D_1 e^{i\sqrt{k_p^2 - \alpha_y^2}\,x}\, e^{i\alpha_y y} + D_3 e^{-\sqrt{k_p^2 + \alpha_y^2}\,x}\, e^{i\alpha_y y}\, d\alpha_y \tag{4.18}$$

An approximate solution to this integral has been obtained by Kovinskaya and Nikiforov [14] using the method of steepest descent. The solution obtained is only concerned with the wave field excited in the plate, the motion of the beam being ignored. For the purposes of this study it is important to discover whether the beam or plate is the important element in power flow. The far field of the beam-plate system has therefore been analysed in a manner similar to that in reference [14] but in more detail.

Equation (4.18) is similar to equation (3.6) - the response of a plate to force excitation - and the method of steepest descent is applicable. However, care must be taken with the terms D_1 and D_3 because these contain poles and are therefore not always slowly varying compared with the exponential term. The standard coordinate transformation may be made:-

$$\begin{aligned} \alpha_y &= k_p \sin q \\ x &= r \cos \phi \\ y &= r \sin \phi \end{aligned}$$

The first term of the integral of equation (4.18) thus reduces to:-

$$k_p \int_{-\frac{\pi}{2} + i\infty}^{\frac{\pi}{2} - i\infty} D_1 e^{ik_p r \cos(q - \phi)} \cos q \, dq \qquad (4.19)$$

The path of steepest descent is the same as that found for a point excited plate and is shown on figure 4.4 together with the poles of D_1 and the undeformed contour. It may be seen from the figure that according to the value of ϕ the poles may lie either to the right or left of the steepest descent path. If the path of integration has to be swept over a pole to reach the steepest descent path then a contribution from the pole must be included in the solution for the integral [11].

The y axis along which the beam is laying corresponds to $\phi = 90^o$ and for this angle it can be seen that contributions from the poles must be included. This extra term in the solution of the integral thus corresponds to a narrow zone of the structure containing the beam along which an extra wave propagates. As in the case of an infinite plate with

force excitation, the solution of the integral along the path of steepest descent is a cylindrical wave of the form:-

$$w(r, \phi) = \frac{e^{i(rk_p - \frac{\pi}{4})}}{rk_p} f(\phi) \qquad (4.20)$$

where in this case

$$f(\phi) = \frac{F_o}{B_b\sqrt{2\pi}(\sqrt{1 + \sin^2\phi} + i\cos\phi)} \times \frac{ik_p \cos\phi \sqrt{1 + \sin^2\phi}}{k_p^4 \sin^4\phi - k_b^4 - 2i\frac{B_p}{B_b} k_p^3 (1 + \sin^2\phi)\cos^2\phi\{\frac{1}{\cos\phi} - \frac{i}{\sqrt{1 + \sin^2\phi}}\}} \qquad (4.21)$$

This is the solution found by Kovingskaya and Nikiforov. The additional term due to the contribution of the pole will be given later.

The second term of equation (4.18) may also be evaluated by the method of steepest descent.

The transformation to polar coordinates may be achieved by means of the equations:-

$$x = r\cos\phi$$
$$y = r\sin\phi$$
$$\alpha_y = k_p \sinh q$$

The complex q plane showing the path of steepest descent and the position of the poles of D_3 is shown in figure 4.5. Once again it may be seen that in order to move the path of integration to the steepest descent path it may be necessary to pass over a pole. The contribution of the pole must then be added to the solution. The result of the integration along the path of steepest descent in this case results in an exponentially decaying wave which will be of no importance in the far field.

The contribution of the poles will now be considered. The position of the two poles of D_1 and D_3 has been calculated by Lamb [13] in conjunction with the point excitation of a beam-stiffened plate. In the α_y plane their position is:-

$$p_1 = k_b\left[1 + \frac{iB_p\sqrt{1 - s^4}}{2B_b k_b s^3}\{\sqrt{1 + s^2} - i\sqrt{1 - s^2}\}\right] \tag{4.22}$$

$$p_2 = ik_b\left[1 + \frac{iB_p\sqrt{1 - s^4}}{2B_b k_b s^3}\{\sqrt{1 - s^2} - i\sqrt{1 + s^2}\}\right] \tag{4.23}$$

These pole positions have been calculated to first order in the small coupling parameter $B_p/(B_b k_b)$. Both poles have an imaginary part, the imaginary part of p_1 being particularly small. The existence of the imaginary part of the pole means that the contribution to the far field response will decay with distance and these terms may not be important at very large distances from the source. However, the criterion for the far field of the plate is that $k_p r \gg 1$ while the criterion for the beam is $k_b y \gg 1$. Since k_p is generally much larger than k_b, exponentially decaying terms for the beam will still be important in the plate far field.

There are four contributions to the response in the far field arising from the two poles in each of D_1 and D_3. The pole p_2 has a large imaginary part which will produce a rapidly decaying field and will therefore not be considered. The pole p_1 produces a slowly decaying propagating wave in a narrow sector which includes the beam. Only the response of the beam will be considered here, this being the most interesting part of the additional contribution. The motion of the beam is best calculated from equation (4.18) and by working in α_y space rather than q space. With $x = 0$ the problem reduces to solving for the residue of the integral

$$\xi_p(0, y) = \frac{F_o}{2\pi} \times \int_{-\infty}^{\infty} \frac{e^{i\alpha_y y}}{B_b\left[\alpha_y^4 - k_b^4 - \frac{i2B_p}{B_b}(k_p^4 - \alpha_y^4)\left\{\frac{1}{\sqrt{k_p^2 - \alpha_y^2}^3} - \frac{i}{\sqrt{k_p^2 + \alpha_y^2}^3}\right\}\right]} d\alpha_y \tag{4.24}$$

at the pole p_1. Recalling that the coupling parameter $B_p/(B_b k_b)$ is small, a first order approximation may be found which results in:-

$$\xi_p(0, y) = \frac{F_o i}{4B_b k_b^3}\left\{1 + \frac{iB_p}{2B_b k_b s^3}\left[\frac{s^2 - 3}{(1 - s^2)^{\frac{1}{2}}} + i\,\frac{s^2 + 3}{(1 + s^2)^{\frac{1}{2}}}\right]\right\}$$

$$\times \quad e^{ik_b\left(1 + \frac{iB_p(1 - s^4)^{\frac{1}{2}}}{2B_b k_b s^3}\left[(1 + s^2)^{\frac{1}{2}} - i(1 - s^2)^{\frac{1}{2}}\right]\right)y} \qquad (4.25)$$

The general nature of the wave field in a beam stiffened plate may now be discussed. In the plate there is a cylindrical wave given by equation (4.20). In addition, in a narrow sector on either side of the beam there is an additional contribution which must be added to the cylindrical wave. A sketch of the wave field is given in figure 4.6. An analysis of the shape of the cylindrical wave field shows that at $\phi = 90^o$ (along the beam) there is no motion. The direction in which the cylindrical wave field is a maximum is given by [14] and occurs for that value of ϕ for which:-

$$\sin \phi = \frac{k_b}{k_p} . \qquad (4.26)$$

This condition corresponds to wave trace matching between the beam and the plate. The cylindrical wave does not contribute to the motion of the beam, the response here being given by equation (4.25). This equation indicates that along the beam a wave propagates with a wave speed slightly less than the free beam wave speed and an amplitude which decays with distance according to the relation:-

$$\text{attenuation} = -8.69\left[\frac{B_p(1 - s^4)^{\frac{1}{2}}(1 + s^2)^{\frac{1}{2}}}{2B_b s^3}\right] \quad \text{dB/metre} \qquad (4.27)$$

By setting $B_p = 0$ (no plate stiffness) in equation (4.25) the relation correctly degenerates to the response of a free infinite beam as given by equation (2.18). The attenuation of the wave in the beam is due to radiation into the plate and from equation (4.27) it is seen that this is independent of frequency. A case study made by Fahy and Lindqvist [15] of an infinite beam stiffened plate includes a calculation of the attenuation

along the beam. The calculation was performed by employing a computer to solve the equations of motion for a particular structure at various frequencies. The results given in reference [15] for a structure of shiplike dimensions demonstrated that the attenuation was essentially independent of frequency with a value of approximately 2 dB/metre. Equation (4.27) gives an attenuation of 1.4 dB/metre for the shiplike structure. The dimensions of the beam and plate are shown in figure 4.7.

4.4 Power Flow in Beam-stiffened Plate with Force Excitation

The power supplied by the source may readily be found by substituting the point mobility, equation (4.17), into equation (1.6). The power supplied by a point force is thus:-

$$P_s = \frac{|F|^2}{8\rho A\sqrt{\omega}} \left(\frac{\rho A}{EI}\right)^{\frac{1}{4}} = \frac{|F|^2 \omega}{8EIk_b^3} \tag{4.28}$$

The characteristics of the plate do not enter into this equation, the power being the same as for an uncoupled beam. The power supplied decreases with increasing frequency being inversely proportional to the square root of frequency.

In the far field, the power carried by the beam may be calculated from the internal shear force and bending moment in the beam. The power associated with each of the components is the same, the total power, the sum of both components, being:-

$$P_{ab} = \frac{|F|^2 \omega}{16B_b k_b^3} \left[1 - \frac{B_p(3 + 3s^4 + 2s^2)}{2B_b k_b s^3\sqrt{1 + s^2}}\right] e^{-\frac{B_p\sqrt{1 - s^4}\sqrt{1 + s^2}\, y}{B_b s^3}} \tag{4.29}$$

where only first order terms in $\frac{B_p}{B_b k_b}$ have been retained. The power in the beam thus decays with distance, power being radiated into the plate. The amplitude of the power is dependent on frequency; for high frequencies the coupling parameter $B_p/(B_b k_b)$ is very small and the amplitude approaches that of an uncoupled beam. Thus it may be seen that the majority of the power is initially associated with the beam and that the power is radiated into the plate as propagation along the beam occurs.

At very large distances from the source the power in the beam will be negligible compared with the power in the plate. In order to establish which of the beam or plate is more important as a transmission path it is possible to find a position along the beam at which half the power supplied by the source is transmitted by the beam. For positions further from the source than the half power distance the beam will be less significant than the plate as a power transmission path. By equating the power transmitted in the positive y direction along the beam (equation (4.29)) to one quarter of the power supplied by the source (equation (4.28)) the half power positions are found to be at:-

$$y_{\frac{1}{2}} = \mp \frac{B_b s^3}{B_p (1 - s^4)^{\frac{1}{2}} (1 + s^2)^{\frac{1}{2}}} \log_e \left[\frac{1}{1 - \frac{B_p (3 + 2s^2 + 3s^4)^{\frac{1}{2}}}{2 B_b k_b s^3 (1 + s^2)^{\frac{1}{2}}}} \right] \quad (4.30)$$

This distance is frequency dependent because of the term in k_b; $y_{\frac{1}{2}}$ increases with increasing frequency becoming asymptotically independent as the coupling term $B_p/(B_b k_b)$ becomes small. For the structure analysed by Fahy and Lindqvist [15] (figure 4.7) the half power distance is at 0.4m at 250 Hz and 1m at 500 Hz.

The distribution of power flow intensity in the plate is difficult to compute exactly because of the complexity of the angular dependence of the cylindrical wave. In the radial direction in the far field the shear and bending components will carry equal amounts of power. Assuming the twisting component to be small, which will be valid for large distances, the radial power flow intensity may be found by substituting equation (4.21) into equations (3.22) and (3.23) to give:-

$$P_{ar} = \frac{|F|^2 B_p s^4 \omega}{4\pi r B_b^2 k_b^4} \quad \frac{\cos^2 (1 + \sin^2 \phi)}{\left[\sin^4 \phi - s^4 - \frac{2B_p}{B_b k_b} s \sqrt{1 + \sin^2 \phi \cos^2 \phi} \right]^2} \quad (4.31)$$

where only first order terms in $\frac{B_p}{B_b k_b}$ have been retained. This function is strongly dependent on ϕ the direction of maximum power flow being given approximately by

$$\sin \phi = \frac{k_b}{k_p} \quad (4.32)$$

4.5 Torque Excitation of an Infinite Beam Stiffened Plate - Symmetrical Motion

This section contains an analysis of the response of an infinite plate laying in the x-y plane with a beam stiffener attached along the y axis to which a torque excitation about the x axis is applied (figure 4.1). The resulting motion is symmetrical because the motion is identical for both positive and negative x values and the beam carries no torsional waves. The analysis is similar to the previously examined problem of force excitation of a beam-stiffened plate but since this problem has not been considered at all in the literature all relevant details will be given. The response at the driving point is given first, the response in the far field being given later. The response of the structure to a torque of harmonic dependence $e^{-i\omega t}$ applied about the x axis is given by equation (4.11) with $F_o = 0$ and $T_{yo} = 0$:-

$$\xi_p(x, y) = \frac{T_{xo}}{2} \int_{-\infty}^{\infty} -i\alpha_y e^{i\sqrt{k_p^2 - \alpha_y^2}\, x} e^{i\alpha_y y} D_1 - i\alpha_y e^{-\sqrt{k_p^2 + \alpha_y^2}\, x} e^{i\alpha_y y} D_3 d\alpha_y \tag{4.33}$$

To calculate the point response the angular displacement at the driving point is required. Taking the derivative in the y direction and setting $x = y = 0$ reduces equation (4.33) to:-

$$\left.\frac{\partial \xi_p}{\partial y}\right|_{x=y=0} = \frac{T_{xo}}{2\pi B_b} \int_{-\infty}^{\infty} \frac{\alpha_y^2}{\alpha_y^4 - k_b^4 - \frac{2iB_p}{B_b}(k_p^4 - \alpha_y^4)\left\{\frac{1}{\sqrt{k_p^2 - \alpha_y^2}} - \frac{i}{\sqrt{k_p^2 + \alpha_y^2}}\right\}} d\alpha_y \tag{4.34}$$

An approximate solution may be obtained for this integral by using contour integration and by expanding in terms of the small coupling parameter $B_p/(B_b k_b)$. (Only an outline of the procedure is given below; however, in order to provide examples of the methods used the details of the integration are given in Appendix IV.) For simplicity the integral may be written as:-

$$I = \int_{-\infty}^{\infty} \frac{\alpha_y^2}{g(\alpha)} d\alpha_y \tag{4.35}$$

where

$$g(\alpha_y) = \alpha_y^4 - k_b^4 - \frac{2iB_p}{B_b}(k_p^4 - \alpha_y^4)\left[\frac{1}{\sqrt{k_p^2 - \alpha_y^2}} - \frac{i}{\sqrt{k_p^2 + \alpha_y^2}}\right] \tag{4.36}$$

The contour of integration on the α_y plane is shown in figure 4.3. The contour is deformed to exclude the branch points of $g(\alpha_y)$ at k_p and ik_p but includes the two poles p_1, p_2 of the integral in the upper half plane. The solution of the integral may be written as:-

$$I = 2\pi i\left[\text{Res}(p_1) + \text{Res}(p_2)\right] - \int_{\Gamma_1} - \int_{\Gamma_2} \tag{4.37}$$

where Γ_1 and Γ_2 are the two paths around the branch lines. The position of the poles is the same as in the previous problem of force excitation and may be found by using Newton's method and using k_b and ik_b as first approximations.

The two pole positions p_1 and p_2 are given by equations (4.22) and (4.23).

The value of the residues are found from:-

$$\text{Res}(p_1;\ p_2) = \frac{\alpha_y^2}{\frac{\partial}{\partial\alpha_y}(g)}\Bigg|_{\alpha = p_1;p_2} \tag{4.38}$$

After much algebra the residues, to first order in the coupling parameter, are found to be:-

$$\text{Res}(p_1) = \frac{1}{4k_b}\left[1 - \frac{iB_p}{2B_b k_b s^3}\left[\frac{2s^4 - s^2 + 1}{(1 - s^2)^{\frac{1}{2}}} - i\,\frac{2s^4 + s^2 + 1}{(1 + s^2)^{\frac{1}{2}}}\right]\right] \tag{4.39}$$

$$\text{Res}(p_2) = \frac{-i}{4k_b}\left[1 - \frac{iB_p}{2B_b k_b s^3}\left[\frac{2s^4 + s^2 + 1}{(1 + s^2)^{\frac{1}{2}}} - i\,\frac{2s^4 - s^2 + 1}{(1 - s^2)^{\frac{1}{2}}}\right]\right] \tag{4.40}$$

It is necessary to evaluate the integral along the branch cuts Γ_1 and Γ_2 from infinity to infinity. Along the branch cuts α_y is always greater than k_p and this enables the integral to be written to first order as:-

$$\int_{\Gamma_1;\Gamma_2} \frac{\alpha_y^2}{g(\alpha_y)}\, d\alpha_y = \int_{\Gamma_1;\Gamma_2} \left[\frac{\alpha_y^2}{\alpha^4(1 - \frac{k_b^4}{\alpha_y^4})} + \frac{2iB_p\,(\frac{k_p^4}{\alpha_y^4} - 1)}{B_b\alpha_y^4(1 - \frac{k_b^4}{\alpha_y^4})(\frac{k_p^2}{\alpha^2} - 1)^{\frac{1}{2}}} \right.$$

$$\left. + \frac{2\alpha_y(\frac{k_p^4}{\alpha_y^4} - 1)B_p}{B_b\alpha_y^4(1 - \frac{k_b^4}{\alpha_y^4})^2(\frac{k_p^2}{\alpha_y^2} + 1)^{\frac{1}{2}}} \right] d\alpha_y \qquad (4.41)$$

The first and third terms of the integral around the branch cut Γ_1 do not contribute since they have the same value on both sides of the cut. Making the substitution $\alpha_y = k_p q$ the first branch cut integral may be written as:-

$$\int_{\Gamma_1} = \frac{4B_p}{B_b k_p^2} \int_1^\infty \frac{(q^4 - 1)q^2}{(q^4 - s^4)^2(q^2 - 1)^{\frac{1}{2}}}\, dq \qquad (4.42)$$

When considering the second branch cut at Γ_2 only the third term of equation (4.41) contributes and after making the substitution $\alpha_y = ik_p q$ the integral reduces to:-

$$\int_{\Gamma_2} = \frac{-4B_p}{B_b k_p^2} \int_1^\infty \frac{(q^4 - 1)q^2}{(q^4 - s^4)^2(q^2 - 1)^{\frac{1}{2}}}\, dq \qquad (4.43)$$

The two branch cut integrals have equal value and opposite sign and therefore add to zero. The complete solution for the integral I is therefore given by the sum of the residues. The driving point mobility for $e^{-i\omega t}$ dependence is thus given by:-

$$\beta = \frac{\sqrt{\omega}}{4B_b}\left(\frac{B_b}{A}\right)^{\frac{1}{4}}\left[1 - i - \frac{B_p(2s^4 + s^2 + 1)}{B_b k_b s^3 (1 + s^2)^{\frac{1}{2}}}\right] \qquad (4.44)$$

This result is similar to the driving point mobility of a beam with torque excitation. The real part of the mobility includes additional term which will only be important at low frequencies.

The response in the far field of a beam-stiffened plate with torque excitation will now be considered. A torque applied about the x axis to the beam causes a far field response that is similar in character to the far field response due to force excitation. Comparison of the equations for force and torque excitation, equations (4.18) and (4.33), shows that the torque excitation problem differs only by the inclusion of an additional $i\alpha_y$ term. The nature of the far field is once again a cylindrical wave in the plate and a decaying wave confined to a narrow sector on either side of the beam. The details of the calculations are very similar to those used when examining the far field of a force excited beam-stiffened plate and it is thus unnecessary to repeat the calculations here. The cylindrical wave is determined by transforming to polar coordinates and using the method of steepest descent. The poles of D_1 and D_3 are in the same position as with force excitation and once again determine the wave motion along the beam. The non decaying solution of the cylindrical wave has the form

$$\xi_p(r, \phi) = \frac{e^{i(rk - \frac{\pi}{4})}}{\sqrt{rk_p}} f(\phi) \qquad (4.45)$$

where in this case:-

$$f(\phi) = \frac{1}{B_b\sqrt{2\pi}\{\sqrt{1 + \sin^2\phi} + i\cos\phi\}} \times \frac{-iT_{xo}k_p^2 \sin\phi\cos\phi\sqrt{1 + \sin^2\phi}}{k_p^4\sin^4\phi - k_b^4 - 2i\frac{B_p}{B_b}k_p^3(1 + \sin^2\phi)\cos^2\phi\{\frac{1}{\cos\phi} - \frac{i}{\sqrt{1 + \sin^2\phi}}\}} \qquad (4.46)$$

Along the beam the motion is controlled by the pole with the small imaginary part, the wave motion being given by the residue of:-

$$\xi_p(0, y) = \frac{T_{xo}}{2\pi B_b} \times \int_{-\infty}^{\infty} \frac{-i\alpha_y e^{i\alpha_y y}}{\alpha_y^4 - k_b^4 - 2i\frac{B_p}{B_b}(k_p^4 - \alpha_y^4)\left[\frac{1}{\sqrt{k_p^2 - \alpha_y^2}} - \frac{i}{\sqrt{k_p^2 + \alpha_y^2}}\right]} d\alpha_y \quad (4.47)$$

This equation is obtained from equation (4.33) by setting x = 0. The resulting motion of the beam takes the form:

$$\xi_p(0, y) = \frac{T_{xo}}{4B_b k_b^2}\left[1 + \frac{iB_p}{2B_b k_b s^3}\left[\frac{s^2 - s^4 - 2}{(1 - s^2)^{\frac{1}{2}}} + i\frac{s^2 + s^4 + 2}{(1 + s^2)^{\frac{1}{2}}}\right]\right] \times e^{ik_b}\left[1 + \frac{i(1 - s^4)^{\frac{1}{2}}B_p}{2B_b k_b s^3}\left[(1 + s^2)^{\frac{1}{2}} - i(1 - s^2)^{\frac{1}{2}}\right]\right]y \quad (4.48)$$

The general nature of the response of the structure is thus very similar to the response due to force excitation. The cylindrical wave in the plate does not contribute to the motion of the beam and in this case there is no motion along the x axis. The maximum response on the plate occurs when there is wave tracing between the beam and plate, the approximate angle being given by equation (4.26). The wave along the beam has the same decay rate (equation (4.27)) as in the case of force excitation.

4.6 Power Flow in Beam-stiffened Plate with Symmetrical Torque Excitation

The power supplied by the driving torque is given by:-

$$P_s = \frac{|T_{xo}|^2 \omega}{8B_b k_b}\left[1 - \frac{B_p(2s^4 + s^2 + 1)}{2B_b s^3(1 + s^2)^{\frac{1}{2}} k_b}\right] \quad (4.49)$$

When the coupling factor $B_p/B_b k_b$ is small (i.e., at high frequencies) the power supplied is similar to that of a torque excited beam. At low frequencies the power entering the system is reduced as the coupling term becomes more important.

The power carried by the beam in the far field may once again be found by calculating the internal shear force and bending moment. The power flows associated with each of these components are equal; the total power flowing in the positive y direction being:

$$P_{ab} = \frac{|T_{xo}|^2 \omega}{16 B_b k_b} \left[1 - \frac{B_p(2s^2 + 5s^4 + 1)}{2B_b k_b s^3 (1 + s^2)^{\frac{1}{2}}}\right] e^{-\frac{B_p(1 - s^4)^{\frac{1}{2}}(1 + s^2)^{\frac{1}{2}}}{B_b s^3} y} \tag{4.50}$$

once again only first terms in the coupling parameter have been retained.

The half power positions occurring at that distance from the source where there is an equal amount of power in the beam and plate may be written as:-

$$y_{\frac{1}{2}} = \mp \frac{B_b s^3}{B_p (1 - s^4)^{\frac{1}{2}} (1 + s^2)^{\frac{1}{2}}} \log_e \left[\frac{\frac{1}{2}}{1 - \frac{B_p(1 + 3s^2)}{2B_b k_b s (1 + s^2)^{\frac{1}{2}}}} \right] \tag{4.51}$$

This expression is similar to that obtained for force excitation and applying it to the structure examined by Fahy and Lindquist [15] the half power distance is found to be at 2.14 m at 250 Hz and to be relatively independent of frequency for high frequencies.

The power flow intensity in the plate in the radial direction may be calculated after assuming that the power transmitted by twisting is negligible. The power flow intensities for the bending and shear components are equal, the total power being given by:-

$$P_{ar} = \frac{|T_{xo}|^2 \omega B_p}{4\pi B_b^2 r k_p^2} \frac{\sin^2\theta \cos^2\theta (1 + \sin^2\theta)}{\left[\sin^4\theta - s^4 - \frac{2B_p}{B_b k_b}(1 + \sin^2\theta)^{\frac{1}{2}} \cos^2\theta\right]^2} \quad ; \tag{4.52}$$

the direction of maximum power flow intensity is again given approximately by equation (4.32).

4.7 Torque Excitation of an Infinite Beam Stiffened Plate - Asymmetrical Motion

The structure considered in this section consists of an infinite plate laying in the x-y plane with a beam stiffener laying along the y-axis.

Excitation is due to a point harmonic torque applied to the beam, the torque being in the x-z plane with its axis coincident with the y axis (figure 4.1). This type of excitation can create torsional waves in the beam and will cause the plate to have asymmetrical motion where displacements for negative values of x will be 180^{o} out of phase with positive x values. Along the y axis there will be no displacement of the plate or beam but rotation will occur.

In order to understand how energy is transmitted in this type of system it is useful to consider the beam and plate individually and the subsequent effect each has on the other when they are joined. Torsional waves in an uncoupled infinite free beam travel at a speed independent of frequency. Flexural waves in an infinite free plate travel at a speed which is proportional to the square root of frequency. At low frequencies, the torsional wave speed in the free beam is greater than that of flexural waves in the free plate and thus when they are coupled the beam will radiate into the plate. At high frequencies the wave speed in the free beam is less than that in the free plate and when coupled no energy will be radiated. In the previous two problems of force excitation and symmetrical torque, excitation of a beam-stiffened plate, both the beam and plate carried flexural waves. Flexural waves in a free beam are faster than flexural waves in a plate at all frequencies and thus, when coupled, the beam always radiates into the plate.

At low and high frequencies, asymmetrical motion of the beam-stiffened plate tends to be similar to the particular cases treated earlier. At low frequencies or when the beam torsional stiffness and inertia are relatively small, the structure behaves like a plate. At high frequencies or when the plate bending stiffness is relatively small, the system behaves like a beam under torsional wave motion. For the structure of ship-like dimensions studied by Fahy and Lindquist [15], the critical frequency at which the beam and plate wave speeds were identical occurred at 125 Hz. Thus it can be seen that the frequency range of interest spans all types of behaviour.

The low frequency behaviour, as in the case of torque excitation of a plate, is difficult to analyse and no detailed calculations have been made for the near field response. An approximate solution has been obtained for the response above the coincidence frequency and this is given below. Because of the complicated nature of the response, the structure considered by Fahy and Lindquist is used to illustrate the problem.

Setting $F_o = 0$ and $T_{xo} = 0$ in equation (4.11) gives the displacement of the beam and plate which may be written as:-

$$\xi_p(x, y) = \frac{T_{yo}}{2\pi} \int_{-\infty}^{\infty} \left[D_2 e^{i\sqrt{k_p^2 - \alpha_y^2}\, x} + D_4 e^{-\sqrt{k_p^2 + \alpha_y^2}\, x} \right] e^{i\alpha_y y} \, d\alpha_y \tag{4.53}$$

To calculate the response at the driving point the angular displacement rather than the transverse displacement is required. Writing θ for the angular displacement, using the relation

$$\theta = -\frac{\partial w}{\partial x}$$

and setting $x = y = 0$ enables the point response to be written as:-

$$\theta(0, 0) = \frac{T_{yo}}{2\pi GQ} \int_{-\infty}^{\infty} \frac{1}{\alpha_y^2 - k_t^2 + \frac{2B_p}{GQ} \{\sqrt{k_p^2 + \alpha_y^2} - i\sqrt{k_p^2 - \alpha_y^2}\}} \, d\alpha_y \tag{4.54}$$

By setting GQ and k_t (beam torsional stiffness and wave number) equal to zero the equation degenerates to give the response of a plate. Similarly by setting B_p (plate bending stiffness) equal to zero the equation gives the torsional response of a beam.

To solve equation (4.54) by contour integration it is necessary to locate the poles of the integrand and to define a contour which excludes the branch points at k_p and ik_p. The pole positions are given by the zeros of the denominator of the integrand. At high frequencies the denominator is dominated by k_t^2 and the poles will tend towards this value. In order to examine the behaviour of the denominator a numerical analysis was performed using the structure examined by Fahy and Lindquist [15]. The denominator may be multiplied out to remove the square roots and produce a polynomial. This procedure introduces additional zeros because all the alternative definitions of the square roots become admissible. The polynomial produced is quartic in α^2 and the four roots may be calculated for a range of frequencies using standard computer programs. In order to determine which roots are introduced by the multiplying out procedure the roots may be substituted

back into the original expression for the denominator with the correct square root definitions to check that this expression becomes zero. This test establishes which roots are acceptable and which must be rejected. The results of this analysis are shown in figure 4.8 for the frequency range 0-1500 Hz.

The value of k_t and k_p are also included. It was found that for frequencies less than the coincidence frequency (where $k_t = k_p$) the denominator has no zeros. For frequencies slighly greater than the coincidence frequency there is one zero corresponding to a real value of α at each frequency. Thus there is no torsional wave motion beneath the coincidence frequency and one unattenuated wave at all frequencies slightly greater than the coincidence frequency. This result is consistent with the low frequency behaviour being similar to a plate response and the high frequency behaviour being similar to a beam response.

The second stage in solving the integral of equation (4.54) is to define branch lines along which the contour may be indented so that branch points may be excluded. The branch lines must be chosen so that the subsequent integration around the branch line is solvable. No branch line has been found which enables the integration to be performed for frequencies less than the coincidence frequency. For frequencies greater than the coincidence frequency an appropriate branch line has been found which enables an approximate solution of the branch line integrals to be obtained.

A solution to first order for the point response of a beam stiffened plate with symmetrical torque excitation for frequencies greater than the coincidence frequency may thus be formulated. The integral of equation (5.54) may be evaluated along the contour of figure 4.9, the value of the integral being given by:-

$$\frac{\theta 2\pi GQ}{T_{yo}} = I = 2\pi i \left[\text{Res}(p)\right] - \int_{\Gamma} \qquad (4.56)$$

where $\text{Res}(p)$ is the residue of the real pole and Γ is the path of integration around the branch lines. In this case the branch lines have been drawn so that one branch line integral excludes both branch points. An approximate value of the pole position may be obtained by

expanding the expression for the denominator of the integrand in terms of k_p/α. The pole is always greater than k_p and by expanding the square root functions the denominator may be written:-

$$\alpha_y^2 - k_t^2 + 2A\alpha_y \left[1 + \tfrac{1}{2}\frac{k_p^2}{\alpha_y^2} - \tfrac{1}{8}\frac{k_p^4}{\alpha_y^4} \ldots + 1 - \tfrac{1}{2}\frac{k_p^2}{\alpha_y^2} - \tfrac{1}{8}\frac{k_p^4}{\alpha_y^4} \ldots .\right]$$

$$\fallingdotseq \alpha_y^2 + 4A\alpha_y - k_t^2 \qquad (4.57)$$

where $A = \frac{B_p}{QG}$ and terms of k_p/α of fourth order and above compared with unity have been ignored. This gives an approximate pole position of:-

$$p = -2A + \sqrt{4A^2 + k_t^2} \qquad (4.58)$$

which may be seen to approach k_t at high frequencies. The residue of the pole is found from the expression:-

$$\text{Res}(p) = \left.\frac{1}{\frac{\partial g(\alpha)}{d\alpha_y}}\right|_{\alpha=p} \qquad (4.59)$$

where $g(\alpha)$ is the expression on the denominator of the integrand. Evaluating the residue to the same order of approximation in k_p/α_y gives:-

$$\text{Res}(p) = \frac{1}{2\sqrt{4A^2 + k_t^2}} \qquad (4.60)$$

The branch line integral may be divided into six different integrals, each corresponding to a different definition of the square root functions, as follows:-

$$\int_\Gamma = \int_{+0+i\infty}^{+0+ik_p} + \int_{+0+ik_p}^{+0+i0} + \int_{0+i0}^{k_p+i0} + \int_{k_p-i0}^{-0-i0} + \int_{-0-i0}^{-0+ik_p} + \int_{-0+ik_p}^{-0+i\infty}$$

$$= I_1 + I_2 + I_3 + I_4 + I_5 + I_6$$

By combining integrals with the same range, this may be reduced to three integrals:

$$I_1 + I_6 = \int_{k_p}^{\infty} \frac{-4A\left[\sqrt{\gamma^2 - k_p^2} + \sqrt{\gamma^2 + k_p^2}\right] d\gamma}{(\gamma^2 + k_t^2)^2 + 8A^2\left[\gamma^2 + \sqrt{\gamma^4 - k_p^4}\right]} \tag{4.61}$$

$$I_2 + I_5 = \int_0^{k_p} \frac{-4A\sqrt{k_p^2 + \gamma^2}}{(\gamma^2 + k_t^2)^2 - 4A(\gamma^2 + k_t^2)\sqrt{k_p^2 - \gamma^2} + 8A^2 k_p^2} d\gamma \tag{4.62}$$

$$I_3 + I_4 = \int_0^{k_p} \frac{-4Ai\sqrt{k_p^2 - \alpha^2}}{(\alpha_y^2 - k_t^2)^2 + 4A(\alpha_y^2 - k_t^2)\sqrt{k_p^2 + \alpha_y^2} + 8A^2 k_p^2} d\alpha_y \tag{4.63}$$

where the substitution $\alpha_y = i\gamma$ has been made on those portions of the branch line that lie along the imaginary axis. To permit integration of these expressions the integrands may be expanded in terms of k_p/k_t and A/k_t. Both of these coupling terms decrease with increasing frequency and are less than unity for typical structures in the frequency range being considered here. The accuracy of the branch line integrals will depend on the degree of approximation involved in the expansion of the integrals and the number of terms of the expansion included. In the following derivation, terms in k_p^4/k_t^4 and A^4/k_t^4 and higher will be ignored in comparison to unity.

In the integral $I_1 + I_6$ the term $\frac{8A^2\gamma^2}{(\gamma^2 + k_t^2)^2}$ has a maximum value at $\gamma = k_t$ of $\frac{2A^2}{k_t^2}$; by expanding in terms of this coupling parameter the integral may be written as:

$$I_1 + I_6 = -4A \int_{k_p}^{\infty} \frac{\sqrt{\gamma^2 - k_p^2}}{(\gamma^2 + k_t^2)^2} + \frac{\sqrt{\gamma^2 + k_p^2}}{(\gamma^2 + k_t^2)^2} - \frac{8A^2(2\gamma^2 + k_p^2)\sqrt{\gamma^2 - k_p^2}}{(\gamma^2 + k_t^2)^4}$$

$$- \frac{8A^2(2\gamma^2 - k_p^2)\sqrt{\gamma^2 + k_p^2}}{(\gamma^2 + k_t^2)^4} d\gamma \tag{4.64}$$

This integral may be solved exactly by means of a partial fraction expansion. The first two terms may be rewritten as eight terms and the third and fourth terms as sixteen terms. Integrals $I_2 + I_5$ and $I_3 + I_4$ may

be expanded in terms of k_p/k_t and A/k_t to the order of approximation given above to result in

$$I_2 + I_5 = -\frac{4A}{k_t^4}\int_o^{k_p} \sqrt{k_p^2 + \gamma^2} - \frac{2\gamma^2}{k_t^2}\sqrt{k_p^2 + \gamma^2} + \frac{4A}{k_t^2}\sqrt{k_p^4 - \gamma^4}\; d\gamma \tag{4.65}$$

and

$$I_3 + I_4 = -\frac{4Ai}{k_t^4}\int_o^{k_p} \sqrt{k_p^2 - \alpha^2} + \frac{2\alpha^2}{k_t^2}\sqrt{k_p^2 - \alpha^2} + \frac{4A}{k_t^2}\sqrt{k_p^4 - \alpha^4}\; d\alpha \tag{4.66}$$

The first two terms in each integral may be solved exactly and the last term may be rewritten as:-

$$\int_o^{k_p} \sqrt{k_p^4 - \gamma^4}\; d\gamma = k_p^3 \int_o^1 \sqrt{1 - x^4}\; dx \tag{4.67}$$

The value of this last integral is small compared with other terms and may be ignored.

After expanding all the terms in the complete solution and ignoring those which are fourth order or higher and hence are small in magnitude compared with unity, the branch line integral may be written as:-

$$\int_\Gamma = -\frac{4A}{k_t^2} - \frac{i\pi A k_p^2}{k_t^4} - \frac{4Ak_p^2}{k_t^4}\log_e(1 + \sqrt{2}) - \frac{Ak_p^2}{k_t^4}\log\left[\frac{i\sqrt{2} - i + \frac{k_p}{k_t}}{i\sqrt{2} + i + \frac{k_p}{k_t}}\right] + \frac{8}{3}\frac{A^3}{k_t^4} \tag{4.68}$$

The rotation at the driving point may be found from equation (4.56) by subtracting the branch line integral from the pole solution. The driving point mobility β is given by:-

$$\beta = \frac{-i\omega\theta}{T} \tag{4.69}$$

which may be written as:-

$$\beta = \frac{\omega}{GQ}\left[\frac{1}{2k_t} - \frac{A^2}{k_t^3} - \frac{2iA}{\pi k_t^2} + \frac{Ak_p^2}{2k_t^4} - \frac{2Aik_p^2}{\pi k_t^4}\log_e(1+\sqrt{2})\right.$$

$$\left. - \frac{iAk_p^2}{2\pi k_t^4}\log_e\left[\frac{i\sqrt{2} - i + \frac{k_p}{k_t}}{i\sqrt{2} + i + \frac{k_p}{k_t}}\right] + \frac{4iA^3}{3\pi k_t^4}\right] \tag{4.70}$$

where the pole solution has also been expanded in terms of A/k_p. It may be seen that for high frequencies this mobility approaches that of a beam with torsional excitation.

4.8 The Response in the Far-field of a Beam-stiffened Plate with Asymmetrical Torque Excitation

The existence of a real pole indicates a non-attenuating torsional wave propagating along the beam. The beam in the far field does not therefore radiate into the plate. However, in the near field at the driving point, the wave in the beam is discontinuous and energy is radiated into the plate from this point. At low frequencies, when there is no pole, all the energy goes directly into the plate from the driving point.

The displacement in the far field may be found from equation (4.11) with $F_o = 0$ and $T_{xo} = 0$. The solution, the inverse Fourier Transform, may be written:-

$$\xi_p(x, y) = \frac{T_{yo}}{2\pi GQ}\int_{-\infty}^{\infty} \frac{1}{\sqrt{k_p^2 + \alpha_y^2} + i\sqrt{k_p^2 - \alpha_y^2}}$$

$$\frac{\left[e^{-\sqrt{k_p^2+\alpha_y^2}\,x} - e^{i\sqrt{k_p^2-\alpha_y^2}\,x}\right]e^{i\alpha_y y}}{\alpha_y^2 - k_t^2 + 2A\left[\sqrt{k_p^2 + \alpha_y^2} - i\sqrt{k_p^2 - \alpha_y^2}\right]}\, d\alpha_y$$

This integral may be solved by the method of steepest descent as in the

case of the response of a plate to force or torque excitation. By writing the equation as the difference of two integrals (each integral containing one of the exponentials in x) and making the same substitutions as given in the previous problems, the response in the far field is given by:-

$$\xi_p(r, \phi) = \frac{e^{i(rk_p - \frac{\pi}{4})}}{\sqrt{rk_p}} \, f(\phi) \tag{4.72}$$

where, in this case:-

$$f(\phi) = \frac{-T_{yo} \cos \phi}{GQ\sqrt{2\pi}(\sqrt{1 + \sin^2\theta} + i \cos \phi)} \times \frac{1}{k_p^2 \sin^2\phi - k_t^2 + 2A(k_p \sqrt{1 + \sin^2\phi} - ik_p \cos \phi)} \tag{4.73}$$

An exponentially decaying near field wave is also radiated but may be ignored in the far field.

A cylindrical wave therefore radiates from the driving point with approximately cosine dependence. (See figure 4.2). As may be seen by letting $\phi = \pi/2$ there is no displacement, due to the cylindrical wave, along the beam.

As in the case of force excitation of a beam-stiffened plate for values of ϕ approaching $\pi/2$ and for frequencies greater than the coincidence frequency, the path of steepest descent crosses a pole and an additional contribution must be added to the solution. On either side of the beam there is a small sector of the plate which has an additional response due to the rotation of the beam. The response in this sector decays with distance having the form of a near field and therefore not radiating into the plate. The rotation of the beam in the far field may be found by calculating the residue of equation (4.71) due to the pole and taking the derivative in the x-direction. Using the value of the pole estimated in the previous section the rotation of the beam is given by:-

$$\theta(0, y) = \frac{iT_{yo}}{GQ} \frac{e^{i(-2A + \sqrt{4A^2 + k_t^2})y}}{2\sqrt{4A^2 + k_t^2}} \tag{4.74}$$

Thus at frequencies below coincidence there is no wave in the beam and only a cylindrical wave in the plate with approximate cosine dependence. At frequencies above coincidence there is a torsional wave in the beam which does not radiate into the plate, the plate response being given by a cylindrical wave deriving its energy from the driving point.

4.9 Power Flow in Beam-stiffened Plate with Asymmetrical Torque Excitation

At frequencies less than the coincidence frequency no power is carried by the beam, all the power being radiated into the plate. No formulae have been found for the driving point mobility at frequencies less than coincidence and therefore the nature of the power supplied by the source is unknown.

At frequencies greater than the coincidence frequency the beam carries a torsional wave along which power is propagated without attenuation. Some power is also transmitted by the plate, the power being radiated from the driving point.

Using the approximate value for the point mobility for frequencies above coincidence, derived in section 4.7, enables the power supplied by the source, in this case the torque, to be written as:-

$$P_s = \frac{|T|^2}{2\sqrt{GQJ}} \left[\frac{1}{2} - \frac{A^2}{k_t^2} + \frac{Ak_p^2}{2k_t^3} \right] \qquad (4.75)$$

This power is the same as for that of a beam alone except for additional coupling terms due to the plate.

In the far field the power carried by the cylindrical wave may be calculated using equations (3.19)-(3.24). The power flow intensity in the radial direction associated with shear and bending may be written as:-

$$P_{ur} = P_{mr} = |T_{yo}|^2 \frac{B_p \omega k_p^2}{8\pi r (GQ)^2} \times \frac{\cos^2\theta}{\left[(k_p^2 \sin^2\theta - k_t^2)^2 + 4Ak_p \sqrt{1 + \sin^2\theta}\,(k_p^2 \sin^2\theta - k_t^2) + 8A^2 k_p^2 \right]} \qquad (4.76)$$

This formula is valid for all frequencies above and below coincidence. As in the case of torque excitation of a plate the power flow intensity has approximately cosine dependence.

At frequencies above the coincidence frequency the power flowing in torsional waves in the beam may be calculated from the angular velocity and the internal twisting moments. Using the approximate value for the pole and calculating this power to the same order of accuracy as used previously gives the following value for the power flowing in the beam:-

$$P_a = \frac{|T|^2}{8\sqrt{GQJ}} \left[1 - \frac{2A}{k_t} - \frac{2A^2}{k_t^2} + \frac{8A^3}{k_t^3} \right] \qquad (4.77)$$

It is necessary to determine whether the plate or the beam transmits more power. By subtracting the power carried in the positive and negative y directions along the beam from the power supplied by the source it is possible to calculate the total power radiated into the plate. Writing P_p for the power radiated into the plate gives:

$$P_p = P_s - 2P_a = \frac{|T|^2}{2\sqrt{GQJ}} \left[\frac{A}{k_t} + \frac{Ak_p^2}{2k_t^3} - \frac{4A^3}{k_t^3} \right] \qquad (4.78)$$

Thus for high frequencies when $\frac{A}{k_t}$ is small it may be seen that the power in the beam is greater than the power in the plate.

CHAPTER 5

POWER FLOW THROUGH ISOLATORS

5.1 Introduction

The vibratory power flowing from a machine through an isolator and into a flexible foundation is available for radiation from or vibration in the structure on which the machine is mounted. Previous chapters have examined the nature of typical flexible foundations and given simple formulae which approximate their behaviour. In this section, simple models for the machine and isolator are proposed that enable the amount of vibrational power flowing into the structure to be evaluated.

Two extremes are used to model the excitation within a machine - a force source and a velocity source. Each of these sources is assumed to be constant and independent of the motion of the foundation and isolator. These extremes are used because the excitation which a machine creates and the extent to which this is modified by the motion of the machine is difficult to predict and has not received much investigation in the literature.

Both one and two stage isolation systems are considered, the elements of the machine and isolator being modelled as masses or springs. The flexible foundation is treated as having a mobility with a straight line, frequency dependence when plotted on log-log scales. In practice, a machine is supported by a number of isolators; however the above simplifications enable the general characteristics of the power flow into the structure to be evaluated in terms of the principal components of a machinery installation.

Mass-spring models of machines on flexible foundations have been considered previously [2, 3, 4] but no attempt has been made to examine how the design of foundations and isolators controls the power flow from the machine. The aim of isolation is to minimise the power flowing into the structure by optimising the isolator design with respect to source and receiver characteristics so that the power available for subsequent radiation and vibration is a minimum. Traditional vibration isolation concentrates on minimising the velocity and force at the foundation by

optimising only the isolator; this will not necessarily reduce radiation or vibration in any part of the structure on which the machine is mounted.

The formulae for power flow are presented in a manner which facilitates the design of isolation systems. In order to minimise power flow it is first necessary to design an appropriate foundation. The effectiveness of various types of foundation is considered in this investigation so that a suitable strategy may be adopted. For example, the analysis indicates that special foundations must be built for some machines or alternatively that some parts of a structure are unsuitable while other parts more suitable for the mounting of machinery. Once a foundation has been chosen, the power flow may be further reduced by adjusting the properties of the isolator. Thus this analysis treats the foundation and the isolator as two separate elements, both of which must be carefully chosen so that there is minimum power flow into the structure.

The results of this investigation are summarised in tables II and III.

5.2 Power Flow into the Structure

The aim of this analysis is to provide formulae for the power flowing into a foundation as a function of frequency. If the source contains only a single frequency then the time averaged power flow from the foundation at the driving frequency may be calculated in terms of the vibration amplitude of the source and the mobilities of the machine, isolator and foundation. If the excitation at the source contains a broad band of frequencies and is described via a spectral density function then the power flow spectral density may be derived, expressing the average power flowing per unit bandwidth into the foundation.

Clearly the power flow is strongly dependent on the magnitude and phase of the foundation mobility. In the cases studied in the previous chapters the mobility spectra were approximately dependent on the frequency to a real power. In general, straight line approximations may often be made to the modulus of a measured mobility spectrum when plotted on a log-log scale. Thus the modulus of the foundation mobility may be represented, to a good approximation, by a law of the form:-

$$|\beta| = A\omega^{s} \qquad (5.1)$$

where β is the foundation mobility and A is a positive constant. The exponent s is a real constant which may be estimated experimentally from the slope of a log-log plot of a mobility spectrum or by calculation. A complicated mobility spectrum may be represented adequately by a number of lines, each of the form of equation (5.1). When considering power flow it is necessary to know both the modulus and the phase or alternatively the real and imaginary parts of the mobility rather than the modulus alone. By means of Hilbert transforms [10] it has been shown by Bode [17] that phase characteristics may be deduced from modulus spectra. A mobility spectrum of the form of equation (5.1) will have a phase given by:-

$$\phi(\omega) = s\,\frac{\pi}{2}\,. \tag{5.2}$$

If equation (5.1) only represents the mobility modulus over a finite frequency interval and outside of this interval the modulus is different then the phase will only vary significantly from the above value at the ends of the interval. The point mobility of a foundation which has a straight line characteristic when plotted on log-log scales may thus be written as:-

$$\beta = Ae^{is\frac{\pi}{2}}\omega^s = A\omega^s(\cos\tfrac{s\pi}{2} + i\sin\tfrac{s\pi}{2}) \tag{5.3}$$

As has been shown in section 1.2, the power flowing into a structure due to a harmonic force is dependent upon the real part of the mobility and in this case the formula for the power flow is:-

$$P = \tfrac{1}{2}\,\mathrm{Re}\{\beta\}|F|^2 = \tfrac{1}{2}A\omega^s|F|^2\cos\tfrac{s\pi}{2} \tag{5.4}$$

where F is the amplitude of the force applied to the foundation. Since the foundation is passive, no power may flow out of the structure at the driving point and thus P may never be negative. This implies that the phase angle is restricted to lie between $+\frac{\pi}{2}$ and $-\frac{\pi}{2}$ and thus s must lie in the range:-

$$-1 < s < 1. \tag{5.5}$$

When $s = \pm 1$ the mobility corresponds to a stiffness or mass line which represents the extreme cases between which all point mobilities of this form must lie. Thus if a straight line approximation is made to the mobility modulus plotted on a log-log scale the phase angle is automatically determined and must be in the range $-\frac{\pi}{2}$ to $+\frac{\pi}{2}$.

It should be noted that in its detailed behaviour the slope of a log-log mobility spectrum may be outside the range of relation (5.5), as for example near a resonance. It has been assumed above, however, that an average line has been drawn through resonances so that the overall nature of the mobility is represented.

5.3 Single Stage Isolation of a Rigid Machine with a Force Source

Figure 5.1 gives a simple representation of a single stage isolator. A rigid machine of mass M is supported by a simple massless spring isolator of stiffness K which isolates the machine from a flexible foundation of point mobility β. A force of amplitude F and frequency dependence $e^{i\omega t}$ represents the internal force within the machine. The force is assumed to be stationary and its spectrum to be independent of the motion of the machine. The power flowing into the structure may be written:-

$$P = \tfrac{1}{2}\mathrm{Re}\{\beta\}|T_F|^2|F|^2 \qquad (5.6)$$

where T_F is the force transmissibility defined as the complex ratio of the harmonic force at the foundation to a harmonic driving force and P is the time averaged power flow into the structure. Force transmissibility is widely used in vibration isolation theory [2, 18] to represent the performance of an isolator. However, since the transmissibility is also a function of the foundation mobility β it is not a suitable concept for the analysis of power flow. Rewriting equation (5.6) as:-

$$P(\omega) = Q_f(\omega)|F(\omega)|^2 \qquad (5.7)$$

enables a power flow transmission spectrum for a force source Q_f to be defined. Q_f is purely real and only dependent on the properties of

the machine, isolator and foundation. If the excitation takes the form of a single harmonic then P in equation (5.7) is the total power flow, alternatively if the excitation is defined via a spectral density function then P is the power flow spectral density.

Writing the power flow in full gives:-

$$P = \frac{\mathrm{Re}\{\beta\}}{2\left|1 - \frac{\omega^2}{\omega_o^2} + i\omega M\beta\right|^2} |F|^2 \qquad (5.8)$$

where $\omega_o^2 = \frac{K}{M}$ is the resonance frequency of the system with the flexible foundation clamped. It may be seen that if β in the denominator of this expression is relatively small then the power flow transmission spectrum will have a significant peak at $\omega = \omega_o$; alternatively if β is large then there will be no significant peak. Since β can never have an average frequency dependence of power greater than or equal to unity, the term in ω^2 will always dominate at high frequencies and the power flow transmission spectra will decrease at approximately ω^{-4}.

Substituting the value of β corresponding to a simple power law (equation (5.3)) into the equation for the power flow enables the power flow transmission spectra to be written as:-

$$Q_f = \frac{\gamma\left(\frac{\omega}{\omega_o}\right)^s}{2M\omega_o\left|1 - \frac{\omega^2}{\omega_o^2} + i(\gamma + i\delta)\left(\frac{\omega}{\omega_o}\right)^{s+1}\right|^2} \qquad (5.9)$$

where $\gamma = M\omega_o^{s+1} A \cos\frac{s\pi}{2}$

$$\delta = M\omega_o^{s+1} A \sin\frac{s\pi}{2} .$$

It is not possible to find a method for normalising this equation in any general manner; the procedure adopted here has been to normalise in terms of the properties of the isolator and machine so that the effects of various foundation mobilities can be seen. γ and δ are the normalised real and imaginary parts of β ($\beta = A\cos\frac{s\pi}{2} + i A \sin\frac{s\pi}{2}$); a large value of γ and δ corresponding to a very mobile foundation while a small value indicates a rigid foundation.

Table II gives the essential behaviour of equation (5.9). The power flow transmission spectra may be approximated on a log-log scale by straight lines at high ($\frac{\omega}{\omega_o} > 1$) and low ($\frac{\omega}{\omega_o} < 1$) frequencies. If $\delta^2 + \gamma^2$ is small there will be a peak at $\frac{\omega}{\omega_o} = 1$ where the two lines intersect. Alternatively if $\delta^2 + \gamma^2$ is large a third straight line may be drawn, the three lines having break points at frequencies above and below $\frac{\omega}{\omega_o} = 1$. The criteria for small or large $(\delta^2 + \gamma^2)$, the height of the peak, the behaviour of the three lines and the position of the break points are given in table II. The criterion for small or large $(\delta^2 + \gamma^2)$ is obtained by establishing whether the peak at $\frac{\omega}{\omega_o} = 1$ is greater or less than the value of the power flow spectrum at the intersection of the two lines for high and low frequency dependence. Figure 5.2 gives a sketch of a power flow transmission spectrum for $s = -\frac{1}{2}$ (corresponding to a beam-like foundation) for small and large values of $(\delta^2 + \gamma^2)$. Exact spectra are shown in figure 5.3 for the same values of s and $(\delta^2 + \gamma^2)$.

In general, equations (5.8) and (5.9) show that the overall levels of the power flow transmission spectra are controlled by the foundation mobility while the spectrum shape is governed by the stiffness and mass of the isolator and machine. Since the foundation mobility always appears in the numerator of the power flow equations it is necessary to choose a small value of A (equation (5.3)) in order to minimise the power flow. When determining the shape of the power flow spectrum there are two alternative extremes. Either $\gamma^2 + \delta^2$ is chosen to be small so that there is a peak in the spectrum or alternatively $\gamma^2 + \delta^2$ is large and there is no peak but the levels are increased at high frequencies. This choice will be governed by the nature of the force spectrum in which there may, for example, be specific harmonics which must be avoided.

The motion of the machine is important since too large a velocity may be unacceptable. The source velocity is given by:-

$$V = \frac{iF}{M} \frac{\left[\frac{\omega^2}{\omega_o^2} - i(\gamma + i\delta)(\frac{\omega}{\omega_o})^{s+1}\right]}{\left[1 - \frac{\omega^2}{\omega_o^2} + i(\gamma + i\delta)(\frac{\omega}{\omega_o})^{s+1}\right]} \qquad (5.10)$$

The low and high frequency dependences are given in table III where it may be seen that the velocity may be approximated on a log log scale by a straight line for all values of $\gamma^2 + \delta^2$ for frequencies greater than the resonance frequency. Examples of velocity spectra given by equation (5.10) for two values of $(\delta^2 + \gamma^2)$ are given in figure 5.4.

5.4 Two Stage Isolation of a Rigid Machine with a Force Source by Means of a Blocking Mass

This type of isolation involves an additional mass which is placed between two springs to form a force attenuating element. Figure 5.5 shows an idealised configuration with a machine of mass M_1, two springs K_1 and K_2 and the additional mass M_2. With a force source of $Fe^{i\omega t}$ the time averaged power flow into the foundation may be written:-

$$P = \frac{Re\{\beta\}|F|^2}{2} \quad \frac{1}{\left|(1 - \frac{\omega^2}{\omega_1^2})(1 - \frac{\omega^2}{\omega_2^2}) + i\omega\beta \frac{M_1 M_2}{K_1}(\frac{\omega_1^2}{\omega^2} + \frac{\omega_2^2}{\omega^2} - \frac{\omega_o^2}{\omega^2} - 1)\right|^2} \tag{5.11}$$

where $\omega_o^2 = \frac{K_2}{M_2}$.

The two resonance frequencies of the system with the foundation clamped are ω_1 and ω_2 and $\omega_1 > \omega_o > \omega_2$. The power flow transmission spectrum exhibits two peaks corresponding to the resonance frequencies of the system, which if β is not large will occur at approximately ω_1 and ω_2. The modulus of the denominator of this equation is dominated at high and low frequencies by the term:-

$$(1 - \frac{\omega^2}{\omega_1^2})(1 - \frac{\omega^2}{\omega_2^2})$$

which only contains parameters concerned with the isolator and masses. Thus, again, the overall level of power flow is controlled by the foundation while the particular shape is governed by the isolation system characteristics. The straight line mobility characteristic of equation (5.3) enables the power flow transmission spectrum to be written as:-

$$Q_f = \frac{K_1}{2M_1M_2\omega_o^3} \frac{\gamma\left(\frac{\omega}{\omega_o}\right)^2}{\left|\left(1-\frac{\omega^2}{\omega_1^2}\right)\left(1-\frac{\omega^2}{\omega_2^2}\right) + i(\gamma+i\delta)\left(\frac{\omega}{\omega_o}\right)^{s+3}\left[\frac{\omega_1^2}{\omega^2}+\frac{\omega_2^2}{\omega^2}-\frac{\omega_o^2}{\omega^2}-1\right]\right|^2} \tag{5.12}$$

where

$$\gamma = \frac{AM_1M_2}{K_1}\,\omega_o^{s+3}\,\cos\frac{s\pi}{2}$$

$$\delta = \frac{AM_1M_2}{K_1}\,\omega_o^{s+3}\,\sin\frac{s\pi}{2}$$

Table II gives approximate formulae for the low and high frequency dependences and the level of the peaks. Figure 5.6 shows power flow spectra for s = 0 (a plate-like foundation) for three values of foundation mobility.

At high frequencies, the two stage isolator gives significantly better power flow isolation (decreasing at $1/\omega^{8-s}$) compared with the single stage isolator (decreasing at $1/\omega^{4-s}$). However, the two stage isolator does have two peaks in the power flow spectrum which must be carefully positioned in order to avoid significant harmonics in the excitation.

The velocity of the machine and of M_2 may readily be determined and are given by:-

$$V_1 = \frac{F\{i\omega K_2\left[\left(1-\frac{\omega^2}{\omega_1^2}\right)\left(1-\frac{\omega^2}{\omega_2^2}\right) + i\omega^3\beta\frac{M_1M_2}{K_1}\left(\frac{\omega_1^2}{\omega^2}+\frac{\omega_2^2}{\omega^2}-\frac{\omega_o^2}{\omega^2}-1\right)\right] + K_1(\beta K_2 + i\omega)\}}{K_2(K_1-\omega^2M_1)\left[\left(1-\frac{\omega^2}{\omega_1^2}\right)\left(1-\frac{\omega^2}{\omega_2^2}\right) + i\omega^3\beta\frac{M_1M_2}{K_1}\left(\frac{\omega_1^2}{\omega^2}+\frac{\omega_2^2}{\omega^2}-\frac{\omega_o^2}{\omega^2}-1\right)\right]} \tag{5.13}$$

$$V_2 = \frac{F(\beta K_2 + i\omega)}{K_2\left[\left(1-\frac{\omega^2}{\omega_1^2}\right)\left(1-\frac{\omega^2}{\omega_2^2}\right) + i\omega^3\beta\frac{M_1M_2}{K_1}\left(\frac{\omega_1^2}{\omega^2}+\frac{\omega_2^2}{\omega^2}-\frac{\omega_o^2}{\omega^2}-1\right)\right]} \tag{5.14}$$

For a foundation with a simple mobility of the form of equation (5.3) there are two resonance frequencies of the structure, the magnitude of the resonances being controlled by the foundation mobility. Table III

gives the high and low frequency dependence of the velocity of the masses and the height of the peaks for small values of $(\delta^2 + \gamma^2)$. Figure 5.7 gives the modulus of the velocity of the machine and figure 5.8 gives the modulus of the velocity of the isolator blocking mass (M_2) for a plate-like foundation.

5.5 Single Stage Isolaton of a Machine with a Velocity Source

An excitation which causes a machine to have the same velocity irrespective of the supporting isolator and substructure may be modelled as a velocity source. In these circumstances the resulting power flow is proportional to the square of the velocity of the machine and by writing:-

$$P = Q_v |V|^2 \tag{5.15}$$

the power flow transmission spectrum Q_v for a velocity source may be defined. As in the case of a force source, the power P will be a spectral density function if the velocity is described as a spectral density and a specific value if the velocity is a single harmonic. For a velocity source of the form $Ve^{i\omega t}$ applied to a machine on an isolator of stiffness K, the power flow into the flexible foundation is:-

$$P = \frac{K^2 Re\{\beta\}}{2|i\omega + \beta K|^2} |V|^2 \tag{5.16}$$

Substituting the value of β given by equation (5.3) into equation (5.16) enables the power transmission spectrum to be written as:-

$$Q_v = \frac{K\gamma\omega^s}{2|i\omega + \omega^s(\gamma + \delta)|^2} \tag{5.17}$$

where $\gamma = AK \cos \frac{s\pi}{2}$

$\delta = AK \sin \frac{s\pi}{2}$

For a velocity source, the mass of the machine is irrelevant and since this simple system does not contain any resonant elements there will be no peaks in the spectra. The low and high frequency dependence and the break point between these two types of behaviour is given in table II. At frequencies

greater than the break point the power flow transmission spectrum always decreases with increasing frequency. However at low frequencies the spectrum may either increase or decrease depending on whether s is negative or positive. Figure 5.9 gives power flow transmission spectra for a number of values of γ and for $s = -\frac{1}{2}$. In this case with a negative value of s it is seen that the break point is a maximum in the power flow transmission spectra.

5.6 Two Stage Isolation of a Machine with a Velocity Source

Figure 5.10 represents a two stage isolator on a flexible foundation with a velocity source. The power flowing into the foundation due to the harmonic velocity source $Ve^{i\omega t}$ is:-

$$P = \frac{Re\{\beta\}|V|^2}{2\omega_o^2} \; \frac{\frac{\omega_o^4}{\omega_1^4}\left(\frac{\omega_1^2}{\omega_o^2} - 1\right)}{\frac{\omega^2}{\omega_o^2}} \; \frac{1}{\left|\left(1 - \frac{\omega^2}{\omega_1^2}\right) - \frac{i\beta K_2}{\omega}\left(1 - \frac{\omega^2}{\omega_1^2} - \frac{\omega_o^2}{\omega_1^2}\right)\right|^2} \tag{5.18}$$

where

$$\omega_o^2 = \frac{K_2}{M_2}$$

$$\omega_1^2 = \frac{K_1}{M_2} + \omega_o^2$$

ω_1^2 is the resonance frequency of the system with the foundation clamped and a kinematic excitation applied to the upper isolator. The parameter ω_o^2 is always less than ω_1^2. M_2 is the blocking mass which separates the two isolator springs K_1 and K_2. Employing the form of foundation mobility given by equation (5.3) enables the power flow transmission spectrum to be written as:-

$$Q_v = \left(\frac{\omega_o}{\omega_1}\right)^4 \left(\frac{\omega_1^2}{\omega_o^2} - 1\right) \; \frac{\gamma\left(\frac{\omega_o}{\omega}\right)^{2-s}}{2\omega_o K_2\left|1 - \frac{\omega^2}{\omega_1^2} - i(\gamma + i\delta)\left(\frac{\omega_o}{\omega}\right)^{1-s}\left(1 - \frac{\omega^2}{\omega_1^2} - \frac{\omega_o^2}{\omega_1^2}\right)\right|^2} \tag{5.19}$$

where $$\gamma = \frac{AK_2}{\omega_o^{1-s}} \cos\frac{s\pi}{2}$$

$$\delta = \frac{AK_2}{\omega_o^{1-s}} \sin\frac{s\pi}{2}$$

This spectrum will have a peak at approximately $\omega = \omega_1$ the resonance frequency of the system. Table II gives the low and high frequency dependence and the value of power flow at $\omega = \omega_1$. At intermediate frequencies approaching ω_1, the behaviour depends on whether $(\gamma^2 + \delta^2)$ is large or small and is complicated due to the number of terms on the denominator of Q_v. Figure 5.11 shows power flow transmission spectra for three values of $(\gamma^2 + \delta^2)$ which encompasses the range of behaviour found. Once again it is seen that the overall level of the power flow transmission spectrum is determined by the magnitude of the foundation mobility while the general shape is controlled by the isolator mass and stiffnesses. The velocity of the blocking mass (M_2) in the isolator is given by:-

$$V_2 = \frac{V(\omega_1^2 - \omega_o^2)\left[1 - i(\gamma + i\delta)\left(\frac{\omega_o}{\omega}\right)^{1-s}\right]}{\omega_1^2\left[1 - \frac{\omega^2}{\omega_1^2} - i(\gamma + i\delta)\left(\frac{\omega_o}{\omega}\right)^{1-s}\left(1 - \frac{\omega_o^2}{\omega_1^2} - \frac{\omega^2}{\omega_1^2}\right)\right]} \qquad (5.20)$$

This velocity has one peak at approximately $\omega = \omega_1$. Table III gives the low and high frequency dependence and figure 5.12 shows the velocity for a foundation mobility with $s = -\frac{1}{2}$. By considering small and large values of ω the magnitude of the velocity at frequencies away from the resonance is seen to be independent of the foundation mobility.

5.7 Power Flow Due to a Band Limited Excitation Spectrum

If the force or velocity spectral density of the excitation is constant between two frequencies ω_A and ω_B and zero outside this interval, then the total power flow, T_p, into the structure is given by:-

$$T_p = F^2 \int_{\omega_A}^{\omega_B} Q_f \, d\omega \qquad (5.21)$$

or
$$T_p = V^2 \int_{\omega_A}^{\omega_B} Q_v \, d\omega \tag{5.22}$$

for force or velocity sources, respectively. F^2 and V^2 are the magnitudes of the spectral density functions between ω_A and ω_B. If the power flow transmission spectrum does not contain a peak in the interval $[\omega_A; \omega_B]$ then this integral may readily be evaluated using the high or low frequency approximations of table II.

When the excitation interval does contain a peak of the power flow transmission spectrum then the integral may still be performed by making suitable approximations. For the case of force excitation with a single stage isolator the total power is given by:-

$$T_p = \frac{F^2}{2M\omega_o} \int_{\omega_A}^{\omega_B} \frac{\gamma(\frac{\omega}{\omega_o})^s}{(1 - \frac{\omega^2}{\omega_o^2})^2 - 2(1 - \frac{\omega^2}{\omega_o^2})\delta(\frac{\omega}{\omega_o})^{s+1} + (\gamma^2 + \delta^2)(\frac{\omega}{\omega_o})^{2+2s}} d\omega \tag{5.23}$$

If the foundation mobility is not too large so that there is a peak at ω_1 which lies within the interval $[\omega_A; \omega_B]$ then the approximation:-

$$\omega_o^2 - \omega^2 = (\omega_o - \omega)(\omega_o + \omega) \simeq 2\omega_o(\omega_o - \omega) \tag{5.24}$$

may be made which enables the total power to be written as:-

$$T_p = \frac{F^2}{2M\omega_o} \int_{\omega_A}^{\omega_B} \frac{\gamma\omega_o^2}{4(\omega_o^2 - \omega^2)^2 - 4\omega_o(\omega_o - \omega) + \omega_o^2(\gamma^2 + \delta^2)} d\omega \tag{5.25}$$

This integral may be evaluated to give:-

$$T_p = \frac{F^2}{4M} \left[\tan^{-1}\left(\frac{2\frac{\omega_B}{\omega_o} - 2 + \delta}{\gamma}\right) - \tan^{-1}\left(\frac{2\frac{\omega_A}{\omega_o} - 2 + \delta}{\gamma}\right)\right] \tag{5.26}$$

The two inverse tangents approach $\pm \frac{\pi}{2}$ as the frequency bandwidth between ω_A and ω_B, centered about the peak, is increased. The approximate value of the integral is thus:-

$$T_p = \frac{F^2\pi}{4M} \tag{5.27}$$

In particular, the total power flow is independent of the nature of the foundation and the stiffness of the isolator. Figure 5.13 gives the exact running integral of equation (5.23) for two values of foundation mobility with $s = \frac{1}{2}$. It may be seen from this figure that equation (5.27) continues to apply even for values of $(\gamma^2 + \delta^2) > 1$. This is because s is positive, giving the power flow transmi-sion spectrum a maximum at the first break point which may also be approximated by equation (5.24). The step-like running integral demonstrates that the contribution of the peak of the power flow transmission spectrum to the total power flow occurs over a narrow frequency interval. Thus an excitation spectrum which does not vary extensively within the range of the peak will not change the form of the integral significantly and an average value of F^2 may be used in equation (5.27).

Since the peak contributes by far the largest amount of power to the total power flow it is important that the frequency at which the peak occurs (approximately ω_o) should be chosen to lie outside the significant ranges of the excitation spectrum. If, however, the excitation spectrum does include the peak, then the isolator is irrelevant and the power flow may only be minimised by increasing the mass of the machine.

Calculations similar to the one above may be performed for a two stage isolator with a force source and for velocity sources. The total power flow for a machine with a two stage isolator excited by a band limited force source may be written:-

$$T_p = \frac{F^2K_1}{2M_1M_2\omega_o^3} \int_{\omega_A}^{\omega_B} \frac{\gamma(\frac{\omega}{\omega_o})^s}{\left[(1 - \frac{\omega^2}{\omega_1^2})(1 - \frac{\omega^2}{\omega_2^2}) - i(\gamma + i\delta)(\frac{\omega}{\omega_o})^{s+3}(\frac{\omega_1^2 + \omega_2^2 - \omega_o^2}{\omega^2} - 1)\right]} d\omega \tag{5.28}$$

The most significant contributions to the total power flow are due to the peaks at the resonance frequencies of the system. When the resonance frequency at ω_1 lies in the band ω_A to ω_B an approximation similar to the one used above may be employed to evaluate the integral. The solution once again leads to a step-like function of inverse tangents which tend to $\pm \frac{\pi}{2}$ as the excitation interval is expanded on either side of the peak in the power flow transmission spectrum. The power flow associated with the

peak at ω_1 is thus approximately:-

$$T_{p1} = \frac{F^2 K_1 \pi}{4M_1 M_2 (\omega_2^2 - \omega_o^2)} \tag{5.29}$$

and similarly the power associated with the peak at ω_2 is:-

$$T_{p2} = \frac{F^2 K_1 \pi \omega_1^2}{4M_1 M_2 (\omega_o^2 - \omega_1^2)\omega_2^2} \tag{5.30}$$

Both these expressions are independent of the foundation mobility and only include parameters concerned with the machine mass, isolator stiffness and isolator mass. By carefully choosing ω_1^2, ω_2^2 and ω_o^2 the amount of power associated with each resonance may be carefully controlled; clearly by selecting ω_o^2 to be close to either ω_1^2 or ω_2^2 will cause very large amounts of power to flow.

The power flow transmission spectrum for a machine on a single stage isolator with a velocity source does not have any peaks. If s is positive then the spectrum always decreases and the largest contributions to the total power flow are due to low frequencies in the excitation spectral density. If s is negative then there is a maximum in the power flow transmission spectrum at the break point between the high and low frequency dependences. If the excitation spectrum is flat and of magnitude V^2 and band limited between frequencies ω_A and ω_B then the total power is given by:-

$$T_p = \frac{V^2 K}{2} \int_{\omega_A}^{\omega_B} \frac{\gamma \omega^s}{|i\omega + \omega^s(\gamma + i\delta)|^2} d\omega \tag{5.31}$$

This equation may be solved exactly to give:-

$$T_p = \frac{V^2 K}{2(1 - s)} \left[\tan^{-1}\left(\frac{\omega^{1-s} + \gamma}{\gamma}\right)\right]_{\omega_A}^{\omega_B} \tag{5.32}$$

If s is negative and the break point occurs between ω_A and ω_B, then the inverse tangents tend to $\frac{\pi}{2}$ and $\frac{s\pi}{2}$, resulting in a total power flow of:-

$$T_p = \frac{V^2 K \pi}{4} \tag{5.33}$$

The total power flow is thus independent of foundation mobility and is proportional to the isolator stiffness.

For a machine with a velocity source and a two stage isolator the total power flow is given by:-

$$T_p = \frac{V^2}{2\omega_o K_o} \left(\frac{\omega_o}{\omega_1}\right)^4 \left(\frac{\omega_1^2}{\omega_o^2} - 1\right)$$

$$\times \int_{\omega_A}^{\omega_B} \frac{\gamma \left(\frac{\omega}{\omega_o}\right)^s \frac{\omega_o^2}{\omega^2}}{\left|1 - \frac{\omega^2}{\omega_1^2} - i(\gamma + i\delta)\left(\frac{\omega_o}{\omega}\right)^{1-s}\left(1 - \frac{\omega^2}{\omega_1^2} - \frac{\omega_o^2}{\omega_1^2}\right)\right|^2} d\omega \tag{5.34}$$

where as before it has been assumed that the excitation spectrum is flat and of magnitude V^2 between ω_A and ω_B and zero outside this interval. If the peak in the power flow transmission spectrum occurs within the interval ω_A to ω_B then the approximation (5.24) may be used in order to solve the integral. The solution is once again an inverse tangent and the approximate value of the total power flow is:-

$$T_p = \frac{V^2}{M_2}\left(1 - \frac{\omega_o^2}{\omega_1^2}\right)\frac{\pi}{4} \tag{5.35}$$

As before, the total power flow is independent of the foundation mobility.

5.8 Selection of Foundations and Isolators

Torque excitation as well as force excitation of foundations has been an important consideration in this analysis. This is because the method in which a machine is mounted often results in torques being the mechanism by which the foundation is excited. For example, torques occur when there is rocking of a machine on a horizontal foundation or alternatively when a machine is mounted as in figure 5.14, where the support acts as a lever,

creating flexural wave motion in the vertical member. When a lever of length ℓ is the cause of flexural wave motion, the relationship between the force and velocity at the tip of the lever and the torque and angular velocity at the root of the lever (see figure 5.14) may be written:-

$$\frac{V}{F} = \beta_f = \ell^2 \frac{\dot{\theta}}{T} = \ell^2 \beta_T \tag{5.36}$$

where β_f and β_T are the point mobilities for a driving force at the end of the lever and for a torque applied to the member at the root of the lever, respectively. Equation (5.36) assumes that the angle through which the lever rotates remains small.

Figure 5.16 gives a comparison between typical beam and plate-like foundations excited by torques or forces. The power flow into a foundation is given by:-

$$P = \tfrac{1}{2} \mathrm{Re}\{\beta_f\} |F|^2 \tag{5.37}$$

or

$$P = \frac{\ell^2}{2} \mathrm{Re}\{\beta_T\} |F|^2 \tag{5.38}$$

where in this case F is the force applied either to the foundation or to the end of a lever of length ℓ. Figure 5.16 gives power flow transmission spectra for an infinite beam and plate of the dimensions shown in figure 5.15 and with a lever of length 1.0m. Clearly in this case a plate-like foundation is inferior to a beam, the best foundation being one in which the force is applied to a beam in a perpendicular direction. From equation (5.38) it may be seen that the length of the lever is important, a long lever being particularly poor.

The introduction of isolators between the machine and foundation always results in a reduction in power flow as long as the excitation spectrum does not include those frequencies which are the resonance frequencies of the system. The use of a two stage isolator will always produce a significantly greater reduction in power flow than a single stage isolator; however, the introduction of a second peak in the power flow transmission spectra may result in this form of isolation only being appropriate for high frequency excitations. If the excitation spectrum does extend over the resonance frequencies then the relatively large amount of power flow

resulting is independent of the foundation characteristics and the use of an isolator may not be beneficial.

The importance of the nature of the source of excitation within a machine has been repeatedly demonstrated in this chapter. Clearly it is important to establish whether excitation by a particular machine has the nature of a force or velocity source and is independent of the isolation system or whether a source mobility should be included when designing isolators. In addition, the spectral distribution of the excitation must also be known before an effective isolation system can be designed which will reduce power flow.

Other factors which affect the power flow into a structure require study. Specifically no attempt has been made here to evaluate the result of resonances (wave effects) within isolators or the levers by which machines are supported. Also due to the size of most machines, a multi-point isolation and support system is necessary which will introduce additional complications when studying power flow.

PART TWO

CHAPTER 6

STRUCTURAL MODELLING BY THE CURVE FITTING OF MEASURED FREQUENCY RESPONSE DATA

6.1 Introduction

The complexity of a typical built-up structure often prevents its detailed vibrational characteristics being predicted theoretically. Previous chapters have analysed the sources of vibrational energy in terms of the approximate behaviour of typical foundations. As an alternative approach it is possible to analyse an existing structure employing only measured data and making no assumptions about the form of possible governing differential equations.

The first part of this chapter is concerned with creating a mathematical model of a structure by employing only measured frequency response data. The advantage of this approach is that large amounts of measured data can be reduced to simple numerical parameters which give an immediate insight into the vibration mechanisms of a structure. Once constructed, the model may be used in further analyses to investigate the effects of connecting subsystems or of making modifications to the structure. For example, where there is a problem of excessive vibration the model may be used to test and evaluate various vibration control measures.

A subsequent section will consider methods of mathematical modelling when some of the properties of the structure are known.

The mathematical model is constructed by employing a digital computer to curve fit general algebraic equations for the frequency response of a structure to measured frequency response data. It is convenient to obtain the data by a method of transient testing [19, 20] since this measurement method enables detailed information from complicated structures to be obtained in a short time. However, any method is suitable as long as it results in a digitised frequency response curve within a computer.

A curve fitting procedure may be applied to one frequency response curve or simultaneously to a set of responses. In the latter case, the fitted model may subsequently be used to predict other responses which have not

been measured. In general, sufficient data for the model may be obtained by employing only one excitation point and measuring the transfer functions to all the stations of interest. From the model fitted to this measured data it is possible to construct a frequency response curve giving the relationship between any possible forcing and response stations.

Since only one excitation station need be used, the problems of data measurement are simplified. The excitation station can be chosen to be the most convenient and the responses of the structure to types of excitation which are physically difficult to apply, for example, torques, are readily obtainable.

In this chapter, algebraic equations for the frequency response of a structure are initially derived. Next, the ways in which measurements may be taken are discussed and different methods for curve fitting reviewed. A technique for curve fitting is then presented and the success of the method illustrated with practical data. Methods of modelling when some information concerning the structure is known are considered in the final section.

6.2 Formulation of the Equations for the Frequency Response of a Structure

It is necessary to develop the general frequency response equations for the steady state, harmonic response of a structure in a suitable form for employing in the curve fitting of measured data. To do this, use is made of the "damped normal modes" derived by Mead [21]. The procedure is outlined here and the theory is given in full in Appendix IV.

The following assumptions are made, first that the structure is linear and secondly, that the damping is hysteretic (proportional to the displacement). Damping is included because energy absorption within structures is of interest and hysteretic damping is employed since this is accepted as being the best model for built-up structures [1]. Finally, it is assumed that the dynamic behaviour of the structure may be represented by the familiar matrix equation:-

$$-\omega^2[M]\{\xi\} + [K + {}^{i}D]\{\xi\} = \{f\} \qquad (6.1)$$

where M, K and D are the inertia, stiffness and damping matrices, respectively and ξ and f are the displacements and forces at each station. This equation is based upon a discrete mass-spring model and when using it for continuous systems it is assumed that any desired accuracy may be achieved by including as many elements as necessary in the column matrix ξ. For a discrete system the number of resonance frequencies is equal to the number of stations. However, to represent the motion of a continuous, vibrating surface to a high degree of spatial accuracy it is necessary to use a large number of stations and if equation (6.1) is employed this will imply an equally large number of resonance frequencies. Alternatively, to represent n resonances to a desired accuracy in the frequency domain at least n response stations have to be considered.

When taking measurements, equation (6.1) is unsatisfactory because of the strict equality between the number of stations and modes. Consider, for example, the case in which one force excites the structure and the response is measured at one station. In these circumstances f is known completely since all the elements are zero except the one corresponding to the applied force and of the column matrix ξ the only element known is at the response station. Clearly (if the response contains more than one resonance) there are more unknowns than equations.

The constraint of always employing an equal number of resonance frequencies and measuring stations may be relaxed by finding the eigenvalues and eigenvectors of equation (6.1) and performing a coordinate transformation. (Appendix IV) Equation (6.1) may then be written in the form:

$$\{\xi\} = [R] \left[\frac{1}{\omega_n^2 - \omega^2}\right] [R^T]\{f\} \qquad (6.2)$$

Here R is a square matrix independent of frequency with columns equal to the complex mode shapes (eigenvectors) of the structure. The frequency dependent terms of the equation are restricted to the diagonal matrix where ω_n are complex resonance frequencies (eigenvalues).

Returning to the conditions of experimental measurement, to find the response due to a force at station j, only the j^{th} column of the matrix R^T need be considered. If we are only interested in one response station, for example, station k, then only row k of the matrix R need be considered. The response may then be written as:

$$\xi_k = \sum_n \frac{\psi_k^{(n)} \psi_j^{(n)}}{\omega_n^2 - \omega^2} f_j \qquad (6.3)$$

or

$$\alpha_{kj} = \sum_n \frac{\psi_k^{(n)} \psi_j^{(n)}}{\omega_n^2 - \omega^2} \qquad (6.4)$$

where α_{kj} is the receptance between station k and j and $\psi_k^{(n)}$ is the eigenvector element for station k, mode n. Each term in the receptance series contains essentially two complex constants - $(R_{kn} \times R_{nj})$ and ω_n^2. These constants may be found by means of nonlinear least squares curve fitting to measured receptance data.

Equation (6.2) expresses the same relationship between forces and displacements as equation (6.1) but only as many rows of the matrix R as is convenient need be included when employing this equation.

It is usual when making frequency response measurements to have one forcing station and several response measurement stations. Let there be s response stations, one forcing station (j) and n resonance frequencies. Equation (6.2) may then be written as:-

$$\underset{s \times 1}{\{\xi\}} = \underset{s \times n}{[Q]} \begin{bmatrix} \frac{1}{\omega_n^2 - \omega^2} \end{bmatrix} \underset{n \times n}{} \begin{bmatrix} P \end{bmatrix} \underset{n \times 1}{} f_j \qquad (6.5)$$

where P is the j^{th} column of R^T, and Q is a rectangular matrix composed of s rows of R. Mobility frequency response data is often convenient to use and the equation may then be written as:-

$$\{\dot{\alpha}\} = [Q] \begin{bmatrix} \frac{i\omega}{\omega_n^2 - \omega^2} \end{bmatrix} \begin{bmatrix} P \end{bmatrix} \qquad (6.6)$$

This equation is employed in the curve fitting process given in section 6.5. When only one response station and one forcing station are employed, a series form for (6.6) may be used.

$$\alpha_{kj} = \sum_{n} \frac{i\omega \, \psi_k^{(n)} \psi_j^{(n)}}{\omega_n^2 - \omega^2} \qquad (6.7)$$

This equation is employed when curve fitting to one response curve only.

6.3 The Measurement of a Complete Frequency Response Matrix

The complete frequency response matrix relates the steady state harmonic response at any station to the set of steady harmonic forces applied to the structure. The relation may be written as:-

$$\{\xi\} e^{i\omega t} = [H(i\omega)] \{f\} e^{i\omega t} \qquad (6.8)$$

where the elements of ξ and f are the response and force, respectively at a particular station. The frequency response matrix H is square with complex, frequency dependent elements. H is called a receptance, mobility or inertance matrix depending on whether the response is displacement velocity or acceleration, respectively. The column matrix f can include torques as well as forces and similarly the column of responses ξ can include rotations. The frequency response matrix H generally has fewer rows that the number of degrees of freedom of the structure since it includes only those stations which are of interest.

A direct method of obtaining the matrix H is to apply a single force to the structure and to measure the response at each station through a given frequency range. In this way, a column of H may be measured. The force may then be applied to another station and a second column measured.

There are practical difficulties in measuring the matrix in this manner and further problems are found when handling the data. Problems associated with the direct measurement method will now be discussed and the way in which these problems are overcome by modelling the structure will then be given. Practical difficulties arise when the response due to torque excitation has to be measured or the force has to be applied at an inconvenient station. If a method of transient testing is employed then positioning the exciter is the most time consuming part of the procedure.

The frequency response matrix H grows rapidly as the number of stations to be considered increases. If a fine resolution is required

then the complete matrix has to be measured and stored for each frequency value. When further calculations are made employing measured data then the size and resolution of the matrix imposes severe constraints. In addition, since the dynamic range of a frequency response matrix is often large, noise in the measured data can create an ill-conditioned calculation.

By curve fitting the measured data to extract those parameters which characterise the structure, it is possible to alleviate many of the above problems. The most immediate result is that only one forcing station need be used to measure the entire frequency response matrix. Clearly by fitting equation (6.6) employing data from only one forcing station, the matrix Q may be found. Each row of Q is associated with a particular station and the column P is the transpose of that row of Q corresponding to the forcing station. Therefore to obtain the response due to any particular forcing station an appropriate column P is selected from the matrix Q and equation (6.6) evaluated.

In series form this ability to use only one forcing station may be demonstrated by considering a structure with two stations. Let the stations be termed 1 and 2 and consider the three frequency responses of interest:-

$$H_{11}(i\omega) = i\omega \sum_n \frac{\psi_1^{(n)} \psi_1^{(n)}}{\omega_n^2 - \omega^2} \tag{6.9}$$

$$H_{12}(i\omega) = i\omega \sum_n \frac{\psi_1^{(n)} \psi_2^{(n)}}{\omega_n^2 - \omega^2} \tag{6.10}$$

$$H_{22}(i\omega) = i\omega \sum_n \frac{\psi_2^{(n)} \psi_2^{(n)}}{\omega_n^2 - \omega^2} \tag{6.11}$$

H_{11} and H_{12} may be measured by forcing at station 1 for example, and thus $\psi_1^{(n)}$, $\psi_2^{(n)}$ can be found for each mode. H_{22} can then be written down immediately since it contains no additional parameters.

After curve fitting measured data the analysis of a structure is simplified. The storage problems associated with measured frequency response matrices are no longer of concern, the relatively large number of

measured data points being replaced by a comparatively small matrix of modal parameters Q and a column of resonance frequencies. The parameters obtained from the curve fitting process are themselves of immediate interest. The resonance frequencies and loss factors are best estimates for the structure and the columns of Q are the mode shapes.

If frequency response spectra are required then they may be plotted employing equation (6.6). The plots may be drawn with any resolution and are noise free so that their use in further calculations is much facilitated.

Instead of using frequency response spectra it is possible to work with equation (6.6) directly. When a large number of stations has to be considered, as for example when two structures are being connected and the modified response is required, then an algebraic equation for each structure may be obtained via measurement and curve fitting. The response may then be calculated in the same way as if the equations had been obtained by solving the differential equations for the structure.

6.4 Methods of Mathematical Modelling

In order to obtain a mathematical model of a frequency response curve it is necessary to find the value of $\psi_k^{(n)} \psi_j^{(n)}$ and ω_n^2 in each term of the series of equation (6.6). References 22-28 give various methods for obtaining these unknowns. Each method has some advantage and is generally suited to some specific problem. In particular, three of the five methods given in the references have been developed for aircraft resonance testing where detailed mode shapes and damping ratios are important with relatively few resonance frequencies requiring examination.

Klosterman [22, 23] gives four procedures for determining the parameters of the series of equation (6.6) based largely on graphical methods applied to frequency response curves plotted on the Argand diagram. These methods are suitable when the frequency spacing between resonances is large and have the advantage of being a very direct procedure since each term in the series is determined individually. Klosterman also proposed a method for close resonance frequencies but this method requires the use of many measurement stations.

Dat and Meurzec [24] and also 't Mannetje [25] base their curve fitting methods on the least squares principle. In this case the series of equation (6.7) is multiplied out to produce a rational fraction of two polynomials. By applying a suitable weighting function, the curve fitting may be formulated as a linear least squares procedure and the coefficients of the polynomial found. An iterative procedure enables the method to converge to best values for the coefficients which may then be rewritten in terms of the original parameters of the series. This method is suitable when there are only a small number of resonances to be considered but becomes unwieldy with a large number of resonances because of the high degree of the polynomials. It is also unsuitable if a number of different frequency responses for the same structure must be modelled simultaneously.

In order to avoid the use of high degree polynomials, Flannelly, Berman and Giansante [26, 27] employed the unknown parameters in equation (6.7) directly. In this case the curve fitting procedure was developed for the case when there are many measurement stations and relatively few resonance frequencies. After performing sufficient iterations the method enables the mode shapes to be obtained immediately but because of the difficulty of dealing with many stations the resonance frequencies are obtained after some further calculations which establish a best value in the least-squares sense.

The method developed by Gaukroyer, Skingle and Heron [28] is widely applicable since it may be used for curve fitting a large number of close resonances. The model is formulated in a form similar to equation (6.7) but for viscous damping. The procedure given is suitable for the case where there is only one response and excitation station. The method follows a linearised iterative least squares procedure and determines the unknowns in the series directly.

In general, the most difficult case to model is one where there are frequency response curves from many stations and close resonance frequencies in the frequency range of interest. None of the above methods cover this degree of complexity, although using the method due to Gaukroyer, Skingle and Heron on each frequency response curve separately and then averaging the results for each resonance frequency could suffice.

However, if this procedure were adopted a best model is not obtained and it is possible that the model would not be consistent within itself. The method proposed in the following section enables simultaneous curve fitting of many frequency response curves for the case where the excitation is applied at one station only.

A disadvantage of the computer based methods reviewed above is that all the unknowns are solved for simultaneously and if the procedure collapses it is not possible to determine which mode is at fault. A method which determines the parameters for each mode independently is therefore desirable so that a constant evaluation of the progress in curve fitting may be made.

6.5 Curve Fitting to Measured Frequency Response Data

To demonstrate the principles the simple case of curve fitting to one frequency response curve only will be considered here, the general case being reserved for appendix V.

The aim is to obtain the best estimates for the parameters of equation (6.7) from measured data. The procedure developed for this application of curve fitting is based on the "least squares" principle which may be formulated as follows. Let the measured values be $H(i\omega)$ and the algebraic function which is to be fitted be $F(i\omega)$. If the parameters of the function F, which have to be chosen to give a best fit, are $a_1, a_2, \ldots$ then for each frequency ω_k we may write:

$$E_k = F(i\omega_k, a_1, a_2, \ldots) - H(i\omega_k) \tag{6.12}$$

where E_k is the error. The error may be expressed as a scalar by multiplying by its complex conjugate.

$$e_k^2 = \bar{E}_k E_k = \left[\overline{F(i\omega_k, a_1, a_2, \ldots)} - \overline{H(i\omega_k)}\right]\left[F(i\omega_k, a_1, \ldots) - H(i\omega_k)\right] \tag{6.13}$$

A total error may now be formed by summing all the errors over the frequency interval to give

$$\sum_k w_k^2 e_k^2 = \sum_k w_k^2 \left[\overline{F(i\omega_k;\ a_1;a_2\ \ldots)} - \overline{H(i\omega_k)} \right] \left[F(i\omega_k;a_1;a_2\ \ldots) - H(i\omega_k) \right] \tag{6.14}$$

w_k is a weighting function applied to each point.

It is now necessary to find suitable values for the parameters a_1, a_2,... which make $\sum_k w_k^2 e_k^2$ a minimum. This may be done by taking the derivative of equation (6.14) with respect to each parameter a_j and equating to zero. In this manner as many equations as unknowns may be found and if the function F is a linear function of a_j then these equations will be linear and may be solved to find the best estimates for a_1; a_2; a_3; .... The unknown parameters in the algebraic function $F(i\omega_k;\ a_1;\ a_2;\ \ldots)$ are then known and the function is a best approximation to the data $H(i\omega)$.

In the particular case considered here the algebraic function is $\sum_n \frac{i\omega \psi_1^{(n)} \psi_2^{(n)}}{\omega_n^2 - \omega^2}$ and it is necessary to express this function in a suitable linear form. Clearly the product $\psi_1^{(n)} \psi_2^{(n)}$ is not separable and the substitution $\psi_1^{(n)} \psi_2^{(n)} = X_n$ may be made.

The function may now be written as:

$$\sum_n \frac{i\omega\ X_n}{\omega_n^2 - \omega^2} \tag{6.15}$$

where each term in the series has two complex unknowns X_n and ω_n^2 (which correspond to four real unknowns) which have to be obtained by the curve fitting procedure.

If a large number of modes is to be considered term by term fitting of series (6.15) is preferable. It is readily seen that the information contained in a frequency interval around ω_n is most pertinent to the n^{th} term and that information distant from ω_n is of little value. If it is desired to fit only one term at a time the error equations (6.12) may be written as:

$$E_k = \left[\frac{i\omega_k X_j}{\omega_j^2 - \omega_k^2} + \sum_{\substack{n \\ n \neq j}} \frac{i\omega_k X_n}{\omega_n^2 - \omega_k^2} - H(i\omega_k) \right] \tag{6.16}$$

Essentially, the term $\sum_{\substack{n \\ n\neq j}} \frac{i\omega X_n}{\omega_n^2 - \omega^2}$ represents the contribution of off-resonance terms in an interval containing the term $\frac{i\omega X_j}{\omega_n^2 - \omega^2}$. If the contribution of the off-resonance terms are subtracted from the measured frequency response data then the corrected data will be that of a single degree of freedom system.

Therefore the substitution

$$\sum_{n\neq j} \frac{i\omega_k X_n}{\omega_n^2 - \omega^2} - H(i\omega_k) = A(i\omega_k) \tag{6.17}$$

is employed to give

$$E_k = \left[\frac{i\omega_n X_j}{\omega_j^2 - \omega_k^2} + A(i\omega_k)\right] \tag{6.18}$$

where $A(i\omega)$ are the new 'measured values'. Application of equation (6.16) implies that the terms in the series are already known. In practice, an iterative technique may be used and only estimates of the contributions are required.

Equation (6.18) is still nonlinear. The application of a Taylor series expansion would be usual in most nonlinear least squares fitting procedures but in this case the expansion would have poor convergence since ω_j^2 is close to ω^2. Instead, equation (6.18) is rewritten as:

$$E_k = \frac{1}{\omega_j^2 - \omega_k^2}\left[i\omega_k X_j + (\omega_j^2 - \omega_k^2)A(i\omega)\right] \tag{6.19}$$

If $\frac{1}{\omega_j^2 - \omega_k^2}$ is assumed to be known approximately from a previous estimate then equation (6.19) is a linear error function weighted by $\frac{1}{\omega_j^2 - \omega_k^2}$. The modulus squared error is given by:

$$e_k^2 = \bar{E}_k E_k = |w_k|^2\left[-i\omega_k \bar{X}_j + (\bar{\omega}_j^2 - \omega_k^2)\bar{A}(i\omega_k)\right]\left[i\omega_k X_j + (\omega_j^2 - \omega_k^2)A(i\omega_k)\right] \tag{6.20}$$

where w is the weighting function $\frac{1}{\omega_j^2 - \omega_k^2}$ and the sum of errors

is given by:

$$\sum_k e_k^2 = \sum |w_k|^2 \left[\omega_k^2 |X_j|^2 - i\omega_k \bar{X}_j (\omega_j^2 - \omega^2) A(i\omega) + i\omega_k (\bar{\omega}_j^2 - \omega^2) \bar{A}(i\omega) X_j \right.$$

$$\left. + |(\omega_j^2 - \omega^2) A(i\omega)|^2 \right] \qquad (6.21)$$

The sum of errors being taken over an interval centred on the resonance frequency ω_j.

By equating real and imaginary parts the two complex unknowns X_j and ω_j^2 may be written as the four real unknowns X_j^R; X_j^I; $(\omega_j^2)^R$ and $(\omega_j^2)^I$. By taking the derivative of equation (6.22) with respect to each of these unknowns and equating to zero, the following four equations are obtained:

$$0 = 2X_j^R \sum |w_k|^2 \omega^2 - \sum |w|^2 \, i\omega(\omega_j^2 - \omega^2) A_k + \sum |w_k|^2 \, i\omega(\bar{\omega}_j^2 - \omega^2) \bar{A}_k$$

$$0 = 2X_j^I \sum |w_k|^2 \omega^2 - \sum |w^2| \omega(\omega_j^2 - \omega^2) A_k - \sum |w_k|^2 (\bar{\omega}_j^2 - \omega^2) \bar{A}_k$$

$$0 = -i\bar{X}_j \sum |w_k|^2 \omega A + iX_j \sum |w_k|^2 \, \omega \bar{A} + 2\sum |w_k|^2 \, (\omega_j^{2R} - \omega_k^2) |A_k|^2$$

$$0 = \bar{X}_j \sum |w_k|^2 \omega A + X_j \sum |w_k|^2 \, \omega \bar{A} + 2(\omega_j^2)^I \sum |w_k|^2 |A_k|^2$$

The four equations may be written as two equations in two complex unknowns X_j; ω_j^2.

$$0 = X_j \sum |w_k|^2 \omega^2 - i\omega_j^2 \sum |w_k|^2 \omega A_k + i\sum |w|^2 \omega_k^3 A_k \qquad (6.22)$$

$$0 = iX_j \sum |w_k|^2 \omega \bar{A}_k + \omega_j^2 \sum |w_k|^2 |A_k|^2 - \sum |w_k|^2 \omega_k^2 |A|^2 \qquad (6.23)$$

These equations may be solved to give X_j and ω_j^2. In this manner the best estimate for the parameters of a single term in the series are found.

The following procedure may now be adopted to find each term of the series. First the frequency response curve is divided into intervals (which may overlap) each containing one resonance frequency and therefore corresponding to one term in the series. Initial approximations to all the terms are obtained and for each interval, best estimates for X_j and

ω_j^2 are calculated employing equations (6.22) and (6.23).

This completes the first iteration. A second iteration may now be performed for which more accurate estimates of the off-resonant contributions and the weighting functions are available. Further iterations can be made until the convergence is sufficient.

The use of a digital computer is thus necessary to perform the calculation with sufficient speed. This curve fitting procedure will thus evaluate as many terms of series (6.15) as there are resonance frequencies in the measured data.

One improvement to the method is worth including. The series (6.15) has been evaluated for a finite number of terms but naturally for a continuous structure an infinite number of terms should be included. This may be expressed by writing:-

$$\sum_{n=1}^{\infty} \frac{i\omega X_n}{\omega_n^2 - \omega^2} = R_m(i\omega) + \sum_{j=1}^{k} \frac{i\omega X_j}{\omega_j^2 - \omega^2} + R_s(i\omega) \qquad (6.24)$$

where R_m and R_s are remainders and $\sum_{j=1}^{k} \frac{i\omega X_j}{\omega_j^2 - \omega^2}$ is the sum of terms for resonance frequencies within the measurement interval. R_m is the remainder expressing the contribution of terms associated with resonance frequencies lower than those in the measurement interval and R_s is associated with resonance frequencies greater than those in the measurement interval. R_m and R_s are terms which have to be evaluated away from their resonance frequencies and therefore a Taylor series may be used. The frequency dependence of R_m and R_s may be written as:

$$R_m = \frac{-iX_m}{\omega} \qquad (6.25)$$

$$R_s = i\omega X_s \qquad (6.26)$$

where only the first term of the Taylor series has been included. It can be seen that R_m is a mass contribution and R_s a stiffness contribution. X_m and X_s may be also evaluated by the least squares method. The procedure used is to subtract the effects of resonances within the measurement

interval from the measured data so that only the contributions from outside the measurement interval remain. Since equations (6.25) and (6.26) are linear, their calculation follows the standard least squares method.

The effects of the remainders may be included in the main curve fitting procedures in equation (6.18). The contributions of the remainders may be subtracted from the measured data to leave only the response due to those resonances within the measurement interval.

A flow chart giving the essence of the computer program is given in Appendix VI.

6.6 Examples of Curve Fitting

A simple structure was employed to obtain measured data to test the curve fitting procedure. The structure consisted of a simply supported beam 35 mm x 65 mm x 2 m. Data were obtained in all cases by means of transient excitation employing a rapid frequency sweep. The frequency response curves were calculated by dividing the Fourier transform of the response by the Fourier transform of the excitation as described in [19]. As acceleration transducers were used to obtain the responses, a further division by $i\omega$ was made to obtain mobility frequency response data. Eleven response stations were employed in total, stations 1 and 2 being used in addition as forcing stations. The distribution of stations is shown in figure 6.1.

Station 1 was first employed as a forcing station and the response there and at every other station obtained. This gave a complete set of mobility curves which were then curve fitted simultaneously to give a model of the structure. On examination, the measured data were seen to contain more resonances in the frequency range examined than would be expected for a simply supported beam. This was presumably due to poor end fixings, motion of the supporting structure and motion of the beam in other than a single plane. The number of resonances actually used was 14 instead of 5 as expected. This merely provided a better test of the curve fitting procedure.

Figure 6.2 shows the modulus and phase of the measured point response which may be compared to figure 6.3 which is the fitted data. Fitted data

was obtained by plotting out the response of the model due to a particular excitation. Figure 6.4 shows the Argand diagram ("vector plot") of the point response and the fitted response (with a very fine resolution) is shown in figure 6.5. The same sequence of frequency response curves is shown in figures 6.6-6.9 for a transfer response. Figures 6.6 and 6.8 being measured data and figures 6.7 and 6.9 being fitted curves.

Two, three dimensional plots of the measured data are shown in figure 6.10 giving both the linear and the log modulus. The corresponding fitted responses are shown in figure 6.12. Phase information would, of course, have also been presented but is omitted from these plots for clarity. In addition to modelling considerations, this type of presentation facilitates a visual appraisal of the data as well as greatly reducing the number of diagrams that have to be presented when reporting on a series of experiments. Curve fitting produces two sets of parameters, the complex resonance frequencies and the complex mode shapes. The loss factors are given in figure 6.13 plotted against the corresponding resonance frequencies. The complex mode shapes, plotted for stations at equal increments along the beam, are given in figures 6.14.1 and 6.14.2.

The following procedure was employed to test the ability of the model to predict responses which had not been measured. The model obtained by forcing at station 1 was used to predict the response to an excitation applied at station 2. Excitation was then actually applied at station 2 and a series of frequency responses obtained; thus the predicted data could be compared with measured data. Figure 6.15 gives a predicted transfer response (station 7 forcing at 2) and the measured response is given in figure 6.16. Similarly, figures 6.17 and 6.18 also give predicted and measured transfer responses (station 1 forcing at 2) respectively. A set of predicted responses for stations at equal increments along the beam is given in figure 6.19 which may be compared with the set obtained by measurement in figure 6.20.

No absolute criterion for the accuracy of the model obtained by curve fitting has been presented. However, the tests on the beam show the general success of the procedure and the areas for concern.

The main inaccuracies in the fitted data are associated with anti-resonances. This is to be expected since they are associated with numerical values in the frequency response data which are small compared with those

at resonances and thus they have little influence on the curve fitting. In addition, contributions from resonances outside the curve fitting interval will be of greater relative importance at antiresonances where all contributions are small as opposed to resonances where one mode dominates. The modelling is arranged to give a minimum error to the fitted Argand diagram, this could be changed to improve accuracy for the antiresonances by adding a weighting function which biases the curve fitting towards small values.

The set of complex mode shapes appear satisfactory. The imaginary part of each mode shape (except the ninth mode) is small compared to its real part. This is to be expected since, with the assumption of hysteretic damping in the modelling process, the modes of a uniform structure should have a zero imaginary part. This is largely satisfied by each mode except the ninth mode. The large imaginary part was due to an error in the measurement system. There is a 180^{o} phase shift in the point mobility response at the resonance frequency of this mode (see figure 6.2). It is not physically possible for a passive system to exhibit a 180^{o} phase shift between the velocity and the force of a point response. This measurement error has resulted in the model constructing a mode which is 180^{o} out of phase with respect to the other modes.

The prediction of unmeasured responses from one set of modelled data is satisfactory. The largest errors occurred with the fifth mode at 182 Hz. This error was due to station 2 being situated almost on the node of this mode. A station situated on the node of a vibrational mode receives no information concerning that mode and if predictions are made employing this station as an excitation station the errors may be large. To overcome this difficulty two excitation stations could be employed which complement each other. This would however require a more advanced computer program.

The stiffness remainder of equation (6.24) (R_s) was included when curve fitting the measured data. The contribution of this stiffness parameter to the point response of figure 6.2 is shown in figure 6.21. The contribution to the transfer response of figure 6.6 is shown in figure 6.22.

The stiffness remainder of the point response is significant particularly at antiresonances and at high frequencies. In contrast, the contribution to the transfer response is small (notice different scales

between figures 6.22 and 6.6). This difference is presumably due to variations in phase between the resonances outside the measurement range. The modal responses in a point characteristic are all in phase and will therefore reinforce each other to make a significant stiffness remainder. A transfer response has modal contributions which may be in phase or out of phase. Thus the contributions of each resonance to the stiffness remainder may be positive or negative and will tend to sum to zero mean value.

6.7 Methods of Modelling when Some of the Properties of the Structure are Known

In the previous section no assumptions (other than of hysteretic damping) were made about the nature of the structure being modelled. However, if some information is known it should be included in the modelling process and may lead to valuable simplifications.

If the damping within a structure is small then a simple method for modelling a structure requiring measurements of mobility at only a few frequencies is possible. This method, given by Ewins [29] is capable of great accuracy especially when applied to point frequency responses.

In many circumstances the differential equation for an element of a structure is known but its interaction with the remainder of the structure unknown. For example, a beam built into a structure will satisfy the differential equation for a beam but in general it is not possible to predict the behaviour of the beam since the boundary conditions are unknown. However by using a maximum of four measurement stations the response of any part of the beam may be obtained. The theory behind this method when applied to a beam and an illustrative example is given below.

By using standard Bernoulli-Euler beam theory the steady state harmonic response of a damped beam for $e^{i\omega t}$ frequency dependence may be written [1]:

$$\xi(y) = Ae^{iky} + Be^{-iky} + Ce^{ky} + De^{-ky} \qquad (6.27)$$

where ξ is the displacement of the beam and k the complex wavenumber. The four terms A, B, C, D are independent of y (position along the beam) but dependent on frequency and boundary conditions. For simplicity it may be assumed that the beam is excited at one boundary. The wavenumber k is complex and may be written as:-

$$k = k'(1 - \frac{i\eta}{4}) \tag{6.28}$$

(Derived in section 1.2) where k' is the undamped wavenumber for a beam given by:-

$$k' = \sqrt{\omega} \left(\frac{\rho A_s}{B_b}\right)^{\frac{1}{4}}$$

for which ρ is the volume density, A_s the cross section area and B_b the bending stiffness of the beam. Thus k' can readily be calculated from the properties of the cross section and the material of the beam. The loss factor for the beam may be obtained by means of a standard method [29] and thus the complex wavenumber in equation (6.27) found. By exciting the beam at one station and measuring transfer frequency responses to four different stations, four simultaneous equations for the four unknowns A, B, C, D may be obtained for each frequency. By solving for the four unknowns equation (6.27) is completely determined and the frequency response for any station may be predicted.

If the beam is in motion due to some given harmonic excitation (for example where the beam is set into vibration by a remote machine) then once again the motion at four stations may be measured and the four unknowns deduced. The four unknowns A, B, C, D when used in equation (6.27) will now predict the vibration anywhere along the beam for the conditions of excitation found during measurement. When the excitation is broad band in nature then spectral density and cross-spectral density measurements of the motion at the four stations may be made. The predicted motion of a point on the beam in this case will also be in the form of a spectral density function.

If that part of the beam where predictions are to be made is away from boundaries the third and fourth terms in equation (6.27) will be small and may be neglected. In these circumstances only two measurement stations are necessary.

The procedure given above was tested on a cantilevered aluminium beam of dimensions 930 mm x 100 mm x 1.62 mm. The excitation and measurement stations are shown in figure 6.23. The response of the beam at a station away from discontinuities was chosen for prediction (station 3) and thus only two measurement stations (1 and 2) were needed. Figures 6.24

and 6.25 give the transfer frequency response (inertance) of the two measurement stations obtained by the method of reference [19]. Figure 6.26 gives a predicted transfer response for station 3 based on the two measured responses which may be compared with figure 6.27 which is the actual response measured subsequently.

The correspondence between the predicted and measured responses is good, particularly at high frequencies. At low frequencies the errors may be due to neglecting the near field terms of equation (6.27) which are more important at low frequencies.

No analysis has been made of the effect of errors on the procedure given above. In addition, no method for calculating unmeasured point responses from measured data has been investigated. Clearly, both of these areas require further work. The possibility of extending the principles of this form of modelling to other types of structure should also be considered.

CHAPTER 7

APPLICATIONS OF MATHEMATICAL MODELLING

7.1 Introduction

Once a mathematical model of a structure has been obtained a variety of further analyses becomes possible. One important application which has already been described in the previous chapter is the prediction of unmeasured frequency responses. This ability much reduces the amount of data that must be measured and enables the response to physically difficult forms of excitation, for example, torques, to be predicted.

Two other possible applications will be discussed in the following section. The first is the determination of the characteristics of the structure from the mathematical model and secondly the prediction of the response of two systems that have been modelled independently and are then connected.

7.2 The Distribution of Mass Stiffness and Damping Within a Structure

The mathematical model obtained by curve fitting measured frequency response data according to the method of section 6.5 is in the form of complex resonance frequencies and mode shapes. The possibility exists of inverting this form of representation and returning to the mass, stiffness and damping matrices of a structure. These matrices would provide valuable information since the role of one part of a structure could be clearly identified. In particular, the damping matrix would indicate which areas of a structure are important for absorbing energy and which areas are acting as transmission paths.

The principal difficulty in formulating a procedure for the inversion lies in the fact that the model is based on relatively few measurement stations and only represents a finite number of resonance frequencies. A practical structure has an infinite number of coordinates and resonance frequencies and thus its behaviour can only be estimated from the model formulated in section 6.5. Thus any model of a structure based on finite

mass stiffness and damping matrices will introduce two sources of error; one error being due to a finite spatial representation and a second error being due to the use of a finite number of resonance frequencies. It will be shown that the second source of error results in significant difficulties.

Berman and Flannelly [30] have formulated a procedure for obtaining mass and stiffness matrices for the case in which there are many measurement stations and relatively few resonance frequencies. They show how modifications to the mass and stiffness matrices lead to new resonance frequencies and mode shapes. Consideration is given below to the alternative case where there are few measurement stations and many resonance frequencies. The fundamental assumption is that if a practical structure is modelled with a large number of degrees of freedom and the frequency response of every coordinate of the model closely agrees with the response of an equivalent point of the structure, then the mass stiffness and damping matrices of the model represent the distribution of mass stiffness and damping in the structure. Clearly the model can only represent the structure over a limited frequency interval and thus the mass stiffness and damping matrices will not be correct for frequencies outside the measured frequency range. The orthogonality relationships for such a model may be written:-

$$R^T M R = I \tag{7.1}$$

$$R^T K R = \begin{bmatrix} \omega_n^2 \end{bmatrix} \tag{7.2}$$

where M and K are the mass and complex stiffness matrices and the columns of the square matrix R are the complex mode shapes. The mode shapes have been normalised so that the right hand side of (7.1) is the unit matrix. The right hand side of (7.2) is a diagonal matrix of complex resonance frequencies. The two orthogonality conditions may be combined to give:-

$$K = MR \begin{bmatrix} \omega_n^2 \end{bmatrix} R^T M \tag{7.3}$$

For uniform structures the mass matrix will be diagonal and the equation may be rewritten:-

$$\begin{bmatrix} K_{11} & K_{12} \\ K_{21} & K_{22} \end{bmatrix} = \begin{bmatrix} M_1 & 0 \\ 0 & M_2 \end{bmatrix} \begin{bmatrix} R_1 \\ R_2 \end{bmatrix} \begin{bmatrix} \omega_n^2 \end{bmatrix} \begin{bmatrix} R_1^T & R_2^T \end{bmatrix} \begin{bmatrix} M_1 & 0 \\ 0 & M_2 \end{bmatrix} \tag{7.4}$$

This equation has been partitioned into stations at which measurements are taken (subscript 1) and stations which responses are unmeasured (subscript 2). As a result, the measured portion of the stiffness matrix may be written:-

$$K_{11} = M_1 R_1 \left[\omega_n^2\right] R_1^T M_1 \tag{7.5}$$

and a single element of the stiffness matrix will be:-

$$k_{rs} = m_r m_s \sum_{n=1}^{N} \omega_n^2 \psi_r^{(n)} \psi_s^{(n)} = K'_{rs}(1 + i\eta_{rs}) \tag{7.6}$$

where m_r and m_s are the masses at stations r and s and $\psi_r^{(n)}$ and $\psi_s^{(n)}$ are the magnitudes of the n^{th} mode shape at stations r and s. η_{rs} is the loss factor associated with the stiffness between the two stations. From this equation it is seen that the stiffness is strongly dependent on the higher resonance frequencies, which usually contain the greatest errors due to the influence of resonant modes of vibration outside the frequency range modelled. In order to examine this formulation a beam with a non uniform distribution of damping was modelled and the complex stiffness obtained in areas of different damping. The experiment failed to produce meaningful results presumably due to the sensitivity of equation (7.6) to small errors. A procedure for calculating the mass, stiffness and damping matrices based on equation (7.6) is therefore not tenable.

7.4 The Response of a Structure Predicted From its Constituent Components

When the frequency responses of two separate components of a structure have been measured or calculated then a prediction may be made of the response of the two components when joined. This type of procedure is particularly valuable when a modification must be made to an existing structure and the new response obtained.

Done and Hughes [31, 32] have analysed the effect of adding mass or stiffness to an existing structure and have established methods for obtaining the bounds within which the response will lie. The analysis in this case only requires knowledge of the frequency response at the points on the structure where the modifications are to be made.

The more general case where there are two components to be joined, has been considered by Klosterman [22], Ewins and Sainsbury [33] and by Ewins and Gleeson [34]. The procedure here is to obtain frequency responses for both components at the points at which the connections are to be made and to calculate the new responses using impedance coupling techniques.

In both these types of analysis physically awkward frequency response measurements may have to be made. For example, torques are very difficult to apply to a structure but are often the mechanism by which components are connected. This difficulty may be overcome by obtaining a mathematical model of the component (using a convenient method of excitation) and predicting the responses due to torques from the model. An additional advantage of using a model is that measured data are replaced by smoothed data and therefore errors due to noise will not be so prominent.

By obtaining the frequency response of the separated components of a structure it becomes possible to estimate the power flow in the joined system. To calculate the power flow at a connecting point it is necessary to know both the forces and the velocities. The velocities may be obtained directly by measurements and the forces deduced from the inverse of the mobility.

In the next section an error analysis is given for the response of a structure predicted from component responses and in the following section the power flow between connected components is considered.

7.4 Errors in System Coupling Methods

This method of calculating the response of a structure consists of combining the mobilities of the components frequency by frequency to calculate a new frequency response curve. The simplest case is where the two components are joined at one coordinate and the mobility of the combined structure is required at the connection point. This case is given by

Bishop and Johnson [35] and in their notation the mobility α of the combined system is:-

$$\alpha = \frac{\beta\gamma}{\beta + \gamma} \tag{7.7}$$

where β and γ are the point mobilities of the two components when separate. For undamped structures the real part of the mobilities is zero and the resonance frequencies of the combined structure are given by the zeros of the denominator which condition may be written

$$\beta + \gamma = 0 \tag{7.8}$$

For structures with damping, the above equation is satisfied by complex frequencies which correspond to the complex resonance frequencies and thus includes a loss factor. When β and γ are expressed as frequency response functions then the new resonance frequencies of the combined system may be found by forming the sum $\beta + \gamma$ and searching for minima (anti-resonances) of the modulus. It is readily seen that for the condition of equation (7.8) to be approached β and γ must approximately be in anti-phase. From equation (7.7) it may be seen that if either of β or γ is relatively small then the combined mobility will be approximately equal to the smaller of the component mobilities.

By expanding equation (7.7) to first order in a Taylor series an error equation may be written:-

$$\frac{\Delta\alpha}{\alpha} = \frac{\gamma}{\beta + \gamma} \frac{\Delta\beta}{\beta} + \frac{\beta}{\beta + \gamma} \frac{\Delta\gamma}{\gamma} \tag{7.9}$$

where $\frac{\Delta\alpha}{\alpha}$ is the relative error in the predicted mobility due to relative errors $\frac{\Delta\beta}{\beta}$ and $\frac{\Delta\gamma}{\gamma}$ in the component mobilities. From this equation it may be seen that the most significant error occurs at the resonance frequencies of the combined system. Away from the resonance frequencies the error in the combined mobility is of the same order as for the constituent mobilities.

It may therefore be concluded that the best method for finding resonance frequencies is to use equation (7.8) instead of searching the predicted frequency response for maxima. Since the frequency response of the

combined structure can only be relatively accurate away from resonances the predicted response is best treated as a guide to the average response of the structure rather than as a detailed prediction.

The same error analysis may be extended to components which are connected at a number of coordinates and yields the same conclusions.

The structure shown in figure 7.1 was used to examine the previous considerations experimentally. The structure has two principal components which may be joined at stations 5 and 6 which are a force and torque connection, respectively. The response of the combined structure to a harmonic force at station one was required, this configuration being similar to that of a machine on a flexible foundation. System β consisted of an aluminium beam 200 mm x 35 mm x 1 mm with a rod 50 mm long and terminated by a washer at one end (to which the connection was made) with the other end clamped. System γ (which represented the foundation) was an aluminium beam of dimensions 888 mm x 100 mm x 1.62 mm clamped at both ends. In order to measure the frequency response of the two components, a force excitation was applied to station 1 for system β and station 5 for system γ. The rotation at the coupling point was measured by means of two accelerometers, the signals from which were differenced to obtain an angular acceleration. Both components were modelled according to the method of section 6.5 so that those necessary unmeasured frequency responses could be obtained. The mobilities at four stations of the joined system were then predicted and are shown in figures 7.2-7.5. The structure was then physically joined and the mobilities at the four stations measured; these are also shown in figures 7.2-7.5 for comparison. The frequency response spectra are plotted with a resolution of 0.244 Hz; the curves are shown again in figures 7.6-7.9 where the spectra have been averaged to give a new resolution of 24.4 Hz. It may be seen that the averaged responses for the measured and predicted data are similar while the detailed responses have significant differences.

7.5 Measurement of Power Flow Between Connected Components

The connection points between two components of a structure act as paths for power flow. The power flow at such a junction is given by the time average of the force and velocity. The velocity may be measured directly and thus presents no difficulty but the force must be obtained by indirect means. If the mobility of the component of the structure has been

obtained then it may be inverted to obtain the force in terms of the velocity. In the simple case of a component with a point mobility of β and only one force applied to it, the power flow may be written:-

$$P = \tfrac{1}{2} \frac{\mathrm{Re}\{\beta\}}{|\beta|^2} |V|^2 \tag{7.10}$$

The disadvantage of this formulation for the power flow is that at the anti-resonances of the component, $|\beta|$ is very small and this will introduce significant errors at these frequencies. This result continues to be valid if the analysis is extended to components with a number of connection points. Once again, therefore, measurements performed in this manner should not be regarded as detailed results but treated as an indication of the general level of power flow.

The power flow between the two components of the structure described in the previous section was obtained by the above method. In this case the internal force (F) and torque (T) applied to component γ at stations 5 and 6 are given by:-

$$\begin{bmatrix} F_5 \\ T_6 \end{bmatrix} = \begin{bmatrix} \gamma_{55} & \gamma_{56} \\ \gamma_{65} & \gamma_{66} \end{bmatrix}^{-1} \begin{bmatrix} V_5 \\ \dot{\theta}_6 \end{bmatrix} \tag{7.11}$$

where V_5 and $\dot{\theta}_6$ are the velocity and angular velocity at the connection point. Thus two point and one transfer mobility is required. The power flow associated with the force and with the torque at the connecting point were obtained for unit force applied at station 1. The power flowing into the structure and the power flowing at the connection points is shown in figures 7.10-7.13. (It should be noted that negative power flows are possible at the connection points where a circulation of net power flow is possible.) The mobilities of the connection points were all measured directly, no modelling being used. As can be seen, there is a significant discrepancy between the amount of power flowing into the component γ compared to the power flowing into the whole structure. Clearly the effects of antiresonances can be severe and a method for reducing the errors associated with these frequencies is required.

PART THREE

CHAPTER 8

CONCLUSIONS

It has been possible to make a theoretical examination of several types of machinery foundation by making the assumption that they are of infinite extent. This assumption is applicable in those circumstances where there are no significant reflections from discontinuities or boundaries within the foundation.

A beam, when used as a foundation, can be excited by forces or torques and may carry flexural or torsional waves. In these circumstances the beam acts as a wave-guide carrying all the power away from the source; if the beam is damped, the propagating waves will be attenuated exponentially with distance. The moduli of driving point mobilities of these foundations may be represented by straight lines when plotted against frequency on log-log scales.

The power flowing in an infinite uniform plate is carried by cylindrical waves. When the excitation is a force the cylindrical waves are symmetrical around the source but when a torque is applied the resulting wave field is strongly directional. The power supplied to a plate by a constant harmonic force is independent of frequency whilst the power supplied by a torque is proportional to frequency and therefore relatively large at high frequencies. These results are summarised in table I.

In a foundation consisting of a beam-stiffened plate with the excitation applied to the beam the motion at the driving point is largely controlled by the beam. If the beam is excited by a force or torque so that it carries flexural waves then the power transmitted by these waves will initially be associated with the beam. As the waves move away from the source they radiate into the plate so that in the far field more power is transmitted by the plate than by the beam. A strongly directional cylindrical wave is also carried by the plate. If torsional waves are excited in the beam then no power associated with these waves will be radiated into the plate. For this type of excitation the beam and plate

are strongly coupled, with the beam being dominant at high frequencies and the plate being more significant at low frequencies.

In order to reduce the power flowing into a structure an isolator may be introduced between a vibrating machine and its supporting foundation. By making the assumption that the modulus of the driving point mobility of the foundation has a straight line frequency response on a log-log plot it has been possible to analyse the effect of various isolation systems. The power flowing into a foundation from a machine with a harmonic force source will always be reduced by the introduction of an isolator if the resonance frequency of the mass of the machine on the stiffness of the isolator is less than the excitation frequency. A two stage isolation system consisting of a mass element between two springs gives an increased reduction in power flow, compared with a single stage isolation system, as long as the additional resonance frequency is avoided. These results are also valid for a machine with a harmonic velocity source. When a force or velocity source has broad band frequency content which includes the resonance frequency of the isolation system, then the isolator will not be effective.

It has been shown that a structure which exhibits resonances may be modelled purely from measured data. The model is valuable because it not only smooths the original frequency response measurements but enables the complete frequency response matrix to be obtained from a limited amount of data.

The computer program, developed to construct a model, curve fitted measured data to produce the complex resonance frequencies and mode shapes. The model adequately represented the original data and successfully predicted frequency responses which had not been measured. The principal inaccuracies in the modelling procedure were found to be associated with small frequency response values, in particular with antiresonances. When predicting frequency response data from a model, the situation of a measurement station near a node gave rise to some errors.

A second method of modelling applicable to beams was formulated and successfully applied. This method enables the motion at any point on a beam to be predicted from response measurements at a maximum of four stations.

A procedure for deriving the distribution of mass stiffness and damping within a structure from the mathematical model obtained through curve fitting was unsuccessful. This method failed because of the sensitivity of the mathematical model to resonances outside the frequency range in which measurements were taken.

The prediction of the response of a structure from measurements and the derivation of models of the components can only be carried out with limited accuracy. An analysis demonstrated that significant errors occur in the predicted frequency response near the resonance frequencies of the combined structure due to small errors in the measured frequency response of the components. However, the average level of the frequency response of the combined structure can be predicted satisfactorily. Similarly, deducing the time averaged power flow into a component of a built-up structure from frequency response measurements of the separated components introduces large errors due to small errors in the frequency response of the component.

The first part of this thesis has shown that relatively simple formulae may be derived for the response of structures such as beams, plates and beam-stiffened plates. Future work should seek to extend this type of analysis to more general cases such as plates with parallel beam-stiffeners and with excitation applied as a force or torque to either plate or beam. Also the effect of internal wave motion within the stiffeners should be examined, since this will be important for stiffeners of large dimensions at high frequencies.

The principal uncertainties when calculating the power flow through a machinery isolator and into the foundation is the nature of the source and the mobility of the machine. A method for determining these two unknowns must be devised so that a more realistic analysis may be made. An analysis of power flow should also be made which includes the effect of there being several isolators on practical machines.

When modelling a structure from measured data it would be useful if a degree of accuracy for the model could be determined. This would enable an assessment to be made of the use of the model in further analysis. An additional improvement to the computer program would be the inclusion of a procedure which enabled the curve fitting of data obtained from a

set of frequency response measurements with several forcing stations.

Clearly, considerable simplifications are possible when modelling a well known structure such as a beam. An attempt should be made to extend this type of modelling to plates and other commonly occurring structural elements.

When combining systems and obtaining the overall response and power flow from measured data an improvement in accuracy can be obtained by averaging in the frequency domain. This improvement should be quantified so that it is possible to obtain some measure of accuracy of an averaged predicted response for the coupled system.

REFERENCES

1. Snowdon, J.C. "Vibration and shock in damped mechanical systems". John Wiley and Sons, Inc., 1968.

2. Sykes, A.O. "Isolation of vibration when machinery and foundation are resilient and when wave effects occur in the mount". Noise Control 6, 1960, 23.

3. Soliman, J.I. and Hallam, M.G. "Vibration isolation between non-rigid machines and non-rigid foundations". J. Sound Vib. 8(2), 1968, 329.

4. Munjal, M.L. "A rational synthesis of vibration isolators". J. Sound Vib. 39(2), 1975, 247.

5. Skudrzyk "Vibrations of a system with a finite or an infinite number of resonances". J. Acoust. Soc. Am. 30, 1958, 1140.

6. Heckl, M.A. "Compendium of impedance formulas". B.B.N. Report No. 774, 1961.

7. Cremer, L., Heckl, M.A., Ungar, E.E. "Structure-borne sound". Springer-Verlag, 1973.

8. Noiseux, D.U. "Measurement of power flow in uniform beams and plates". J. Acoust. Soc. Am. 47, 1970, 238.

9. Pavic, G. "Measurement of structure borne wave intensity. Part I: Formulation of the methods". J. Sound Vib. 49, 1976, 221.

10. Skudrzyk "The foundations of acoustics". Springer-Verlag, 1971.

11. Felsen, L.B. and Marcuvitz, N. "Radiation and scattering of Waves". Prentice-Hall, Inc., 1973.

12. Dyer, I. "Moment impedance of plates". J. Acoust. Soc. Am. 32, 10, 1960, 1290.

13. Lamb, G.L. "Input impedance of a beam coupled to a plate". J. Acoust. Soc. Am. 33, 5, 1961, 628.

14. Kovinskaya, S.I. and Nikiforov, A.S. "Flexural wave fields in infinite beam-reinforced plates under point excitation". Soviet Physics-Acoustics 19, 1, 1973, 32.

15. Fahy, F.J. and Lindqvist, E. "Wave propagation in damped stiffened structures characteristic of ship construction". J. Sound Vib. 45(1), 1976, 115.

16. Nilsson, A.C. "Wave propagation in simple hull-frame structures of ships". J. Sound Vib. 44(3), 1976, 393.

17. Bode, H.W. "Network analysis and feedback amplifier design". D. van Nostrand Company, Inc. 1945.

18. Harris, C.M. and Crede, C.E. "Shock and Vibration Handbook". McGraw-Hill, 1961.

19. White, R.G. "Evaluation of the dynamic characteristics of structures by transient testing". J. Sound Vib. 15(2), 1971, 147.

20. Holmes, P.J. and White, R.G. "Data analysis criteria and instrumentation requirements for the transient measurement of mechanical impedance". J. Sound Vib. 25(2), 1972, 217.

21. Mead, D.J. "The existence of normal modes of linear systems with arbitrary damping". Symposium on Structural Dynamics, Loughborough University, Paper No. C5, Vol. I, 1970.

22. Klosterman, A.L. "On the experimental determination and use of modal representations of dynamic characteristics". Ph.D. dissertation, University of Cincinnati, 1971.

23. Klosterman, A.L. and Lemon, J.R. "Dynamic design analysis via the building block approach". Shock and Vibration Bulletin 40(4).

24. Dat, R. and Meurzec, J.L. "Exploitation by mathematical smoothing of admittance measurements of a linear system". Recherche Aerospatiale 4, 1972, 209.

25. Mannetje, J.J't. "Transfer-function identification using a complex curve-fitting technique". J. Mech. Eng. Sci. 15 No. 5, 1973, 339.

26. Flannelly, W.G., Giansante, N and Berman, A. "System identification with excitation of one degree of freedom". Kaman Aerospace Corporation, Research Note 71-1, 1971.

27. Flannelly, W.G., Berman, A., Barnsby, R.M. "Theory of structural dynamic testing using impedance techniques" (Two Vols.), Kaman Aerospace Corporation, Report No. R-823, 1970.

28. Gaukroger, D.R., Skingle, C.W. and Heron, K.H. "Numerical Analysis of Vector Response Loci". J. Sound Vib. 29(3), 341, 1973.

29. Ewins, D.J. "Measurement and application of mechanical impedance data". J. Soc.E.E.- (three parts), June 1976.

30. Berman, A. and Flannelly, W.G. "Theory of incomplete models of dynamic structures". A.I.A.A. Journal 9(8), 1971, 1481.

31. Done, G.T.S. and Hughes, A.D. "The response of a vibrating structure as a function of structural parameters". J. Sound Vib. 38(2), 1975, 253.

32. Done, G.T.S., Hughes, A.D. and Webby "The response of a vibrating structure as a function of structural parameters - application and experiment". J. Sound Vib. 49(2), 1976, 149.

33. Ewins, D.J. and Sainsbury, M.G. "Mobility measurements for the vibration analysis of connected structures". Shock and Vibration Bulletin 42(1), 1972, 105.

34. Ewins, D.J. and Gleeson, P.T. "Experimental determination of multi-directional mobility data for beams". Shock and Vibration Bulletin 45, 1975.

35. Bishop, R.E.D. and Johnson, D.C. "The mechanics of vibration". Cambridge University Press, 1960.

36. Timoshenko, S. "Theory of Plates and Shells".

TABLE I. Properties of infinite system.

Symbols used in Table I.

ξ = Amplitude of harmonic displacement

θ = Amplitude of harmonic angular displacement

A = Cross sectional area of beam

E = Young's modulus

ρ = Volume density

GQ = Torsional stiffness

J = Polar moment of inertia per unit length

I = Second moment of area of beam

B_p = Bending stiffness of plate = $Eh^3/12(1-\nu)$

ν = Poisson's ratio

h = plate thickness

a = Radius of disc over which torque is applied to plate

L = Parameter from [12] which tends to unity for large a/h

ℓ = Length of finite beam

ℓ_1; ℓ_2 Length of sides of finite rectangular plate

η = Loss factor

r; ϕ Polar coordinates for plate

ω = Frequency in radians

Notes:

* Torque applied about axis parallel to ℓ_2

Time dependence of form $e^{i\omega t}$ assumed

System		Driving Point Mobility	Power Flow into system (P_s) Force or Torque Source	Power Flow into System; Velocity or Angular Velocity Source	Onset of Infinite Behaviour	Largest Point Mobility of Finite System	Ratio of Finite System Maximum to Infinite System	Wavenumber (k)	Displacement of Structure
Beam longitudinal wave motion; force excitation	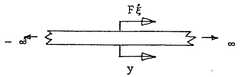	$\frac{\dot{\xi}}{F} = \frac{1}{2A\sqrt{E\rho}}$	$P_s = \frac{\lvert F\rvert^2}{4A\sqrt{E\rho}}$	$P_s = 4\lvert\dot{\xi}\rvert^2 A\sqrt{E\rho}$	$\omega > \frac{\pi}{\eta\ell}\sqrt{\left(\frac{E}{\rho}\right)}$	$\beta_\ell = \frac{2}{\pi A\eta\sqrt{E\rho}}$	$\frlvert\beta_\ell\frrvert / \frlvert\beta_\infty\frrvert = \frac{4}{\pi\eta}$	$k = \omega\sqrt{\left(\frac{\rho}{E}\right)}$	$\xi(y) = \frac{-iFe^{-iky}}{2\omega A\sqrt{E\rho}}$
Beam torsional wave motion; torque excitation	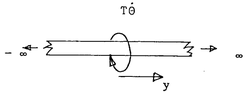	$\frac{\dot{\theta}}{T} = \frac{1}{2\sqrt{GQJ}}$	$P_s = \frac{\lvert T\rvert^2}{4\sqrt{GQJ}}$	$P_s = 4\lvert\dot{\theta}\rvert^2\sqrt{GQJ}$	$\omega > \frac{\pi}{\eta\ell}\sqrt{\left(\frac{GQ}{J}\right)}$	$\beta_\ell = \frac{2}{\pi\eta\sqrt{GQJ}}$	$\frlvert\beta_\ell\frrvert / \frlvert\beta_\infty\frrvert = \frac{4}{\pi\eta}$	$k = \omega\sqrt{\left(\frac{J}{GQ}\right)}$	$\theta(y) = \frac{-iTe^{-iky}}{2\omega\sqrt{GQJ}}$
Beam flexural wave motion; force excitation	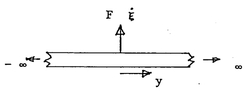	$\frac{\dot{\xi}}{F} = \frac{(1-i)}{4A\rho\sqrt{\omega}}\left(\frac{A\rho}{EI}\right)^{\frac{1}{4}}$	$P_s = \frac{\lvert F\rvert^2}{8A\rho\sqrt{\omega}}\left(\frac{A\rho}{EI}\right)^{\frac{1}{4}}$	$P_s = \lvert\dot{\xi}\rvert^2 A\rho\sqrt{\omega}\left(\frac{EI}{\rho A}\right)^{\frac{1}{4}}$	$\sqrt{\omega} > \frac{4\pi}{\eta\ell}\left(\frac{EI}{\rho A}\right)^{\frac{1}{4}}$	$\beta_\ell = \frac{2\ell}{\pi^2\eta\sqrt{\rho AEI}}$	$\frlvert\beta_\ell\frrvert / \frlvert\beta_\infty\frrvert = \frac{4\sqrt{2}}{\pi\eta}$	$k = \sqrt{\omega}\left(\frac{\rho A}{EI}\right)^{\frac{1}{4}}$	$\xi(y) = \frac{-iF}{4EIk^3}\left[e^{-iky} - ie^{-ky}\right]$
Beam flexural wave motion; torque excitation	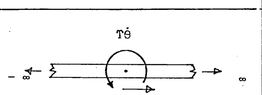	$\frac{\dot{\theta}}{T} = \frac{(1+i)\sqrt{\omega}}{4EI}\left(\frac{EI}{\rho A}\right)^{\frac{1}{4}}$	$P_s = \frac{\lvert T\rvert^2\sqrt{\omega}}{8EI}\left(\frac{EI}{\rho A}\right)^{\frac{1}{4}}$	$P_s = \frac{\lvert\dot{\theta}\rvert^2 EI}{\sqrt{\omega}}\left(\frac{\rho A}{EI}\right)^{\frac{1}{4}}$	$\sqrt{\omega} > \frac{4\pi}{\eta\ell}\left(\frac{EI}{\rho A}\right)^{\frac{1}{4}}$	$\beta_\ell = \frac{2}{\ell\eta\sqrt{\rho AEI}}$	$\frlvert\beta_\ell\frrvert / \frlvert\beta_\infty\frrvert = \frac{2\sqrt{2}}{\pi\eta}$	$k = \sqrt{\omega}\left(\frac{\rho A}{EI}\right)^{\frac{1}{4}}$	$\xi(y) = \frac{T}{4EIk^2}\left[e^{-iky} - e^{-ky}\right]$
Plate flexural wave motion; force excitation	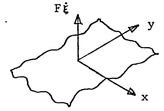	$\frac{\dot{\xi}}{F} = \frac{1}{8\sqrt{B_p\rho h}}$	$P_s = \frac{\lvert F\rvert^2}{16\sqrt{B_p\rho h}}$	$P_s = 4\lvert\dot{\xi}\rvert^2\sqrt{B_p\rho h}$	$\omega > \frac{8}{A\ell_1\ell_2}\sqrt{\left(\frac{B_p}{\rho A}\right)}$	$\beta_\ell = \frac{4\ell_1\ell_2}{\pi^2\eta\sqrt{hB_p}(\ell_1^2+\ell_2^2)}$	$\frlvert\beta_\ell\frrvert / \frlvert\beta_\infty\frrvert = \frac{32\ell_1\ell_2}{\pi^2\eta(\ell_1^2+\ell_2^2)}$	$k = \sqrt{\omega}\left(\frac{\rho h}{B_p}\right)^{\frac{1}{4}}$	Valid in far-field only $\xi(r,\phi) = \frac{-iF}{8B_pk^2}\sqrt{\left(\frac{2}{\pi kr}\right)}e^{-i(kr-\frac{\pi}{4})}$
Plate flexural wave motion; torque excitation	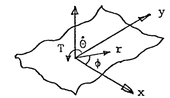	$\frac{\dot{\theta}}{T} = \frac{\omega}{8B_p(1+L)}\left[1 - \frac{i4}{\pi}\ell n\,ka + \frac{i8L}{\pi(1-\nu)}\left(\frac{h}{\pi a}\right)^2\right]$	$P_s = \frac{\omega\lvert T\rvert^2}{16B_p(1+L)}$	$P_s = \frac{4\lvert\dot{\theta}\rvert^2 B_p(1+L)}{\omega\{1+\left[\frac{4}{\pi}\ell nka - \frac{8L}{\pi(1-\nu)}\left(\frac{h}{\pi a}\right)^2\right]^2\}}$	$\omega > \frac{8}{\ell_1\ell_2\eta}\sqrt{\left(\frac{B_p}{\rho A}\right)}$	$\beta_\ell = \frac{16\ell_2}{\eta\sqrt{\rho hB_p}\,\ell_1(2\ell_2^2+\ell_1^2)}$ *		$k = \sqrt{\omega}\left(\frac{\rho h}{B_p}\right)^{\frac{1}{4}}$	Valid in far-field only $(r,\phi) = \frac{T}{8B_pk}\sqrt{\left(\frac{2}{\pi kr}\right)}e^{-(rk-\frac{\pi}{4})}\sin\phi$

TABLE II Power flow into foundations from machinery sources on isolators.

Force Source Single Stage Isolator	Power Flow into Foundation $\omega_o = \sqrt{(\frac{K}{M})}$ Foundation Mobility $= \frac{\gamma + i\delta}{M\omega_o} (\frac{\omega}{\omega_o})^s$	Approximate Power Flow $\frac{\omega}{\omega_o} << 1$		Approximate Power Flow $\frac{\omega}{\omega_o} >> 1$	Power Flow at $\omega = \omega_o$ (Peak if $\gamma^2 + \delta^2 < 1$)	Power Flow at Intermediate Frequencies $\gamma^2 + \delta^2 > 1$	Low Frequency Break Point $\gamma^2 + \delta^2 > 1$	High Frequency Break Point $\gamma^2 + \delta^2 > 1$
	$P = \frac{\lvert F\rvert^2}{2M\omega_o} \frac{\gamma(\frac{\omega}{\omega_o})^s}{\lvert 1 - \frac{\omega^2}{\omega_o^2} + i(\gamma + i\delta)(\frac{\omega}{\omega_o})^{s+1}\rvert^2}$	$P = \frac{\lvert F\rvert^2}{2M\omega_o} (\frac{\omega}{\omega_o})^s$		$P = \frac{\lvert F\rvert^2}{2M\omega_o} (\frac{\omega_o}{\omega})^{4-s}$	$P = \frac{\lvert F\rvert^2}{2M\omega_o} \frac{\gamma}{\gamma^2 + \delta^2}$	$P = \frac{\lvert F\rvert^2}{2M\omega_o} \frac{\gamma}{\gamma^2 + \delta^2} (\frac{\omega_o}{\omega})^{2+s}$	$(\frac{\omega}{\omega_o})^{2s+2} = \frac{1}{\gamma^2 + \delta^2}$	$(\frac{\omega}{\omega_o})^{2-2s} = \gamma^2 + \delta^2$
Force Source Two Stage Isolator	Power Flow into Foundation $\omega_o = \sqrt{(\frac{K_2}{M_2})}$ ω_1; ω_2 resonance frequencies with base clamped. Foundation Mobility $= \frac{(\gamma + i\delta) K_1}{M_1 M_2 \omega_o^3} (\frac{\omega}{\omega_o})^s$	Approximate Power Flow $\frac{\omega}{\omega_1} << 1$		Approximate Power Flow $\frac{\omega}{\omega_2} >> 1$	Power Flow at $\omega = \omega_1$	Power flow at $\omega = \omega_2$		
	$P = \frac{\lvert F\rvert^2 K_1}{2M_1M_2\omega_o^3} \frac{\gamma(\frac{\omega}{\omega_o})^s}{\lvert(1 - \frac{\omega^2}{\omega_1^2})(1 - \frac{\omega^2}{\omega_2^2}) + i(\gamma + i\delta)(\frac{\omega}{\omega_o})^{s+3}(\frac{\omega_1^2 + \omega_2^2 - \omega_o^2}{\omega^2} - 1)\rvert^2}$	$P = \frac{\lvert F\rvert^2 K_1 \gamma}{2M_1M_2\omega_o^3} (\frac{\omega}{\omega_o})^s$		$P = \frac{\lvert F\rvert^2 K_1 \gamma}{2M_1M_2\omega_o^2} (\frac{\omega_1^2\omega_2^2}{\omega^4}) (\frac{\omega}{\omega_o})^s$	$P = \frac{\lvert F\rvert^2 K_1 \gamma}{2M_1M_2\omega_o^3(\gamma^2 + \delta^2)} (\frac{\omega_o}{\omega_1})^{6+s} (\frac{\omega_1^2}{\omega_2^2 - \omega_o^2})^2$	$P = \frac{\lvert F\rvert^2 K_1 \gamma}{2M_1M_2\omega_o^3(\gamma^2 + \delta^2)} (\frac{\omega_o}{\omega_2})^{6+s} (\frac{\omega_2^2}{\omega_1^2 - \omega_o^2})^2$		
Velocity Source Single Stage Isolator	Power Flow into Foundation Foundation Mobility $= \frac{(\gamma + i\delta)\omega^s}{K}$	Approximate Power Flow $\omega^{2-2s} << \gamma^2 + \delta^2$		Approximate Power Flow $\omega^{2-2s} >> \gamma^2 + \delta^2$	Break Point Between Low and High Frequency Behaviour			
	$P = \frac{\lvert V\rvert^2 K}{2} \frac{\gamma\omega^s}{\lvert i\omega + \omega^s(\gamma + i\delta)\rvert^2}$	$P = \frac{\lvert V\rvert^2 K\gamma}{2(\gamma^2 + \delta^2)\omega^s}$		$P = \frac{\lvert V\rvert^2 K\gamma}{2\omega^{2-s}}$	$\omega^{2-2s} = \gamma^2 + \delta^2$			
Velocity Source Two Stage Isolator	Power Flow into Foundation $\omega_o = \sqrt{(\frac{K_2}{M_2})}$ ω_1 Resonance frequency with base clamped. Foundation Mobility $= \frac{\omega_o(\gamma + i\delta)}{K_2} (\frac{\omega}{\omega_o})^s$	Approximate Power Flow $\frac{\omega}{\omega_1} << 1$		Approximate Power Flow $\frac{\omega}{\omega_1} >> 1$	Power Flow at $\omega = \omega_1$			
	$P = \frac{\lvert V\rvert^2}{2\omega_o K_2} (\frac{\omega_o}{\omega_1})^4 (\frac{\omega_1^2}{\omega_o^2} - 1) \frac{\gamma(\frac{\omega}{\omega_o})^s \frac{\omega_o^2}{\omega^2}}{\lvert 1 - \frac{\omega^2}{\omega_1^2} - i(\gamma + i\delta)(\frac{\omega_o}{\omega})^{1-s}(1 - \frac{\omega^2}{\omega_1^2} - \frac{\omega_o^2}{\omega_1^2})\rvert^2}$	$P = \frac{\lvert V\rvert^2 \gamma \omega_o^2}{2K_2\omega_o(\gamma^2 + \delta^2)(\omega_1^2 - \omega_o^2)} (\frac{\omega}{\omega})^s$		$P = \frac{\lvert V\rvert^2(\omega_1^2 - \omega_o^2)\gamma}{2K_2\omega_o^3} (\frac{\omega_o}{\omega})^{6-s}$	$P = \frac{\lvert V\rvert^2(\omega_1^2 - \omega_o^2)\gamma}{2K_2\omega_o^3(\gamma^2 + \delta^2)} (\frac{\omega_o}{\omega_1})^s$			

TABLE III. Velocities of components of isolation systems.

Force Source Single Stage Isolator	Exact Velocity $\omega_o = \sqrt{\left(\frac{K}{M}\right)}$ Foundation Mobility $= \frac{\gamma + i\delta}{M\omega_o}\left(\frac{\omega}{\omega_o}\right)^s$		Approximate Velocity $\frac{\omega}{\omega_o} \ll 1$	Approximate Velocity $\frac{\omega}{\omega_o} \gg 1$
Machine	$V = \frac{iF\left[\frac{\omega^2}{\omega_o^2} - i(\gamma + i\delta)\left(\frac{\omega}{\omega_o}\right)^{s+1}\right]}{M\omega\left[1 - \frac{\omega^2}{\omega_o^2} + i(\gamma + i\delta)\left(\frac{\omega}{\omega_o}\right)^{s+1}\right]}$		$V = \frac{F(\gamma + i\delta)}{M\omega_o}\left(\frac{\omega}{\omega_o}\right)^s$	$V = \frac{-iF}{M\omega}$
Force Source Two Stage Isolator	Exact Velocity $\omega_o = \sqrt{\left(\frac{K_2}{M_2}\right)}$ ω_1; ω_2 Resonance frequencies with base clamped Foundation Mobility $= \frac{(\gamma + i\delta)}{M_1 M_2 \omega_o^3} K_1 \left(\frac{\omega}{\omega_o}\right)^s$		Approximate Velocity $\frac{\omega}{\omega_1} \ll 1$	Approximate Velocity $\frac{\omega}{\omega_2} \gg 1$
Machine	$V_1 = \frac{F\omega\{i(1 - \frac{\omega^2}{\omega_1^2})(1 - \frac{\omega^2}{\omega_2^2}) + i(\gamma+i\delta)(\frac{\omega}{\omega_o})^{3+s}(\frac{\omega_1^2}{\omega^2} + \frac{\omega_2^2}{\omega^2} - \frac{\omega_o^2}{\omega^2} - 1) + \frac{\omega_1^2\omega_2^2}{\omega^4}((\gamma+i\delta)(\frac{\omega}{\omega_o})^{3+s} + \frac{i\omega^4}{\omega_1^2\omega_2^2})(\frac{\omega_1^2}{\omega_o^2} + \frac{\omega_2^2}{\omega_o^2} - 1 - \frac{\omega_1^2\omega_2^2}{\omega_o^4})\}}{K_1\left[1 - \frac{\omega^2\omega_o^2}{\omega_1^2\omega_2^2}\right]\left[(1 - \frac{\omega^2}{\omega_1^2})(1 - \frac{\omega^2}{\omega_2^2}) + i(\gamma + i\delta)(\frac{\omega}{\omega_o})^{s+3}(\frac{\omega_1^2}{\omega^2} + \frac{\omega_2^2}{\omega^2} - \frac{\omega_o^2}{\omega^2} - 1)\right]}$		$V_1 = \frac{F\omega_1^2\omega_2^2(\gamma + i\delta)}{K_1\omega_o^3}\left(\frac{\omega}{\omega_o}\right)^s\left[\frac{\omega_1^2}{\omega_o^2} + \frac{\omega_2^2}{\omega_o^2} - 1 - \frac{\omega_1^2\omega_2^2}{\omega_o^4}\right]$	$V_1 = \frac{-iF\omega_1^2\omega_2^2}{K_1\omega_o^2\omega}$
Isolator Mass	$V_2 = \frac{F\omega_1^2\omega_2^2\left[(\gamma + i\delta)\left(\frac{\omega}{\omega_o}\right)^{s+3} + \frac{i\omega^4}{\omega_1^2\omega_2^2}\right]}{K_2\omega^3\left[(1 - \frac{\omega^2}{\omega_1^2})(1 - \frac{\omega^2}{\omega_2^2}) + i(\gamma + i\delta)\left(\frac{\omega}{\omega_o}\right)^{s+3}(\frac{\omega_1^2}{\omega^2} + \frac{\omega_2^2}{\omega^2} - \frac{\omega_o^2}{\omega^2} - 1)\right]}$		$V_2 = \frac{F\omega_1^2\omega_2^2(\gamma + i\delta)}{K_2\omega_o^3}\left(\frac{\omega}{\omega_o}\right)^s$	$V_2 = \frac{iF\omega_1^2\omega_2^2}{K_2\omega^3}$
Velocity Source Two Stage Isolator	Exact Velocity $\omega_o = \sqrt{\left(\frac{K_2}{M_2}\right)}$ ω_1 Resonance frequency with base clamped Foundation Mobility $= \frac{\omega_o(\gamma + i\delta)}{K_2}\left(\frac{\omega}{\omega_o}\right)^s$		Approximate Velocity $\frac{\omega}{\omega_1} \ll 1$	Approximate Velocity $\frac{\omega}{\omega_1} \gg 1$
Isolator Mass	$V_2 = \frac{V_1(\omega_1^2 - \omega_o^2)\left[1 - i(\gamma + i\delta)\left(\frac{\omega_o}{\omega}\right)^{1-s}\right]}{\omega_1^2\left[(1 - \frac{\omega^2}{\omega_1^2}) + i(\gamma + i\delta)\left(\frac{\omega_o}{\omega}\right)^{1-s}(1 - \frac{\omega_o^2}{\omega_1^2} - \frac{\omega^2}{\omega_1^2})\right]}$		$V_2 = V_1$	$V_2 = \frac{-V_1(\omega_1^2 - \omega_o^2)}{\omega^2}$

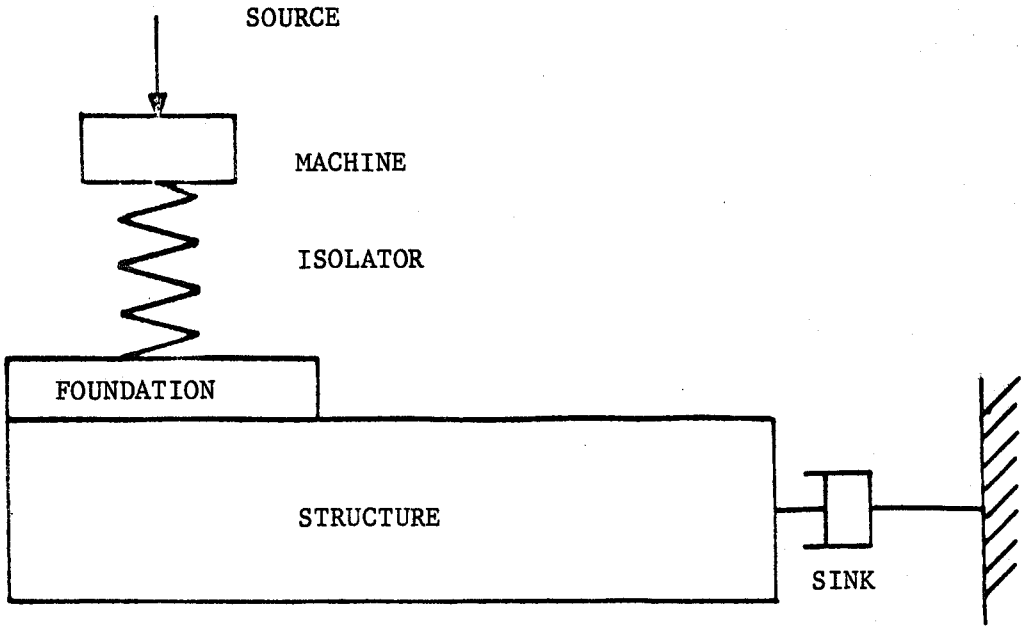

Fig. 2.1 A typical configuration in problems of vibrating isolation

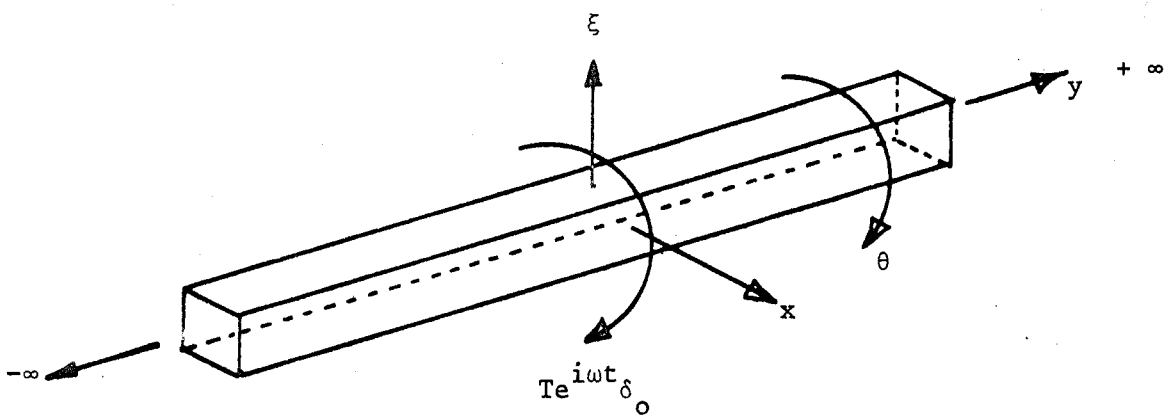

Fig. 2.2 An infinite beam with torsional excitation.

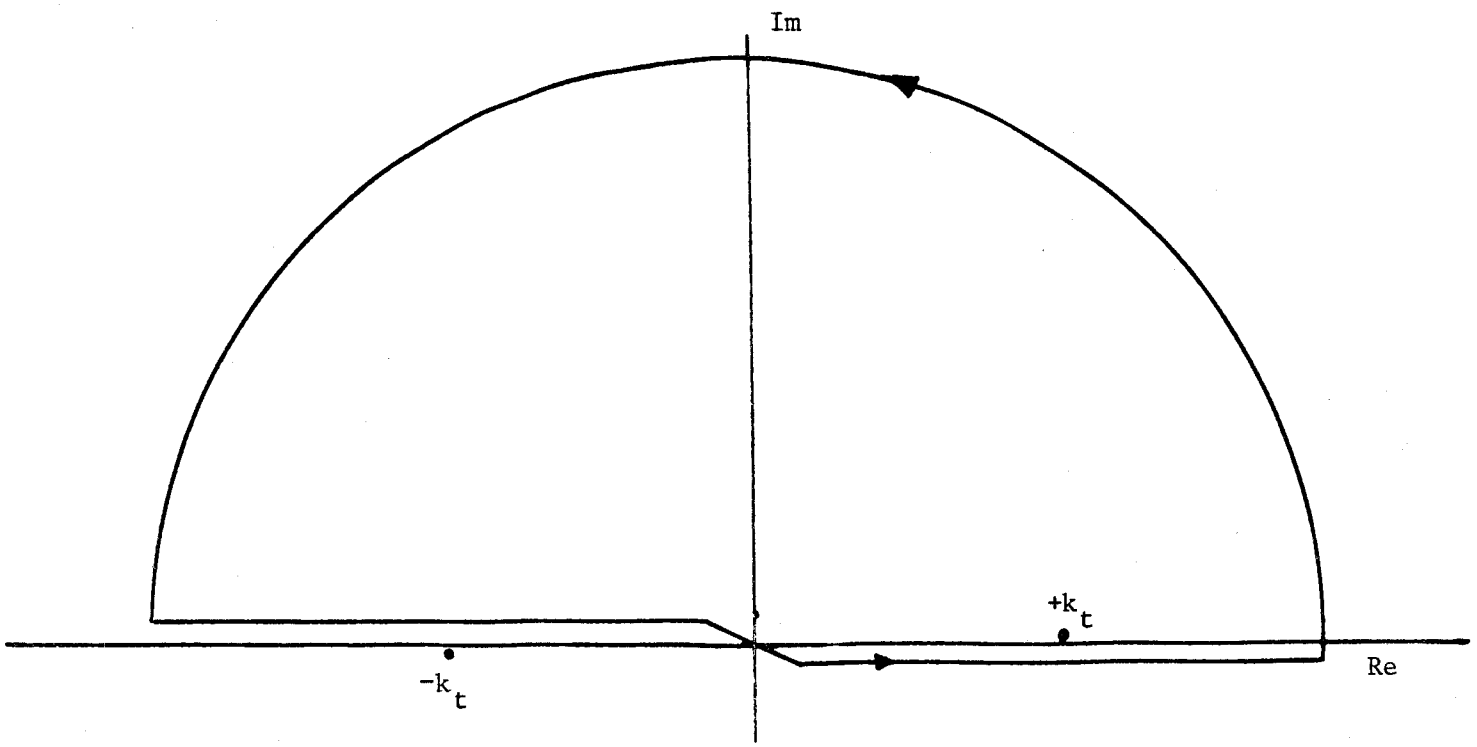

Figure 2.3 Contour of integration for equation 2.9.

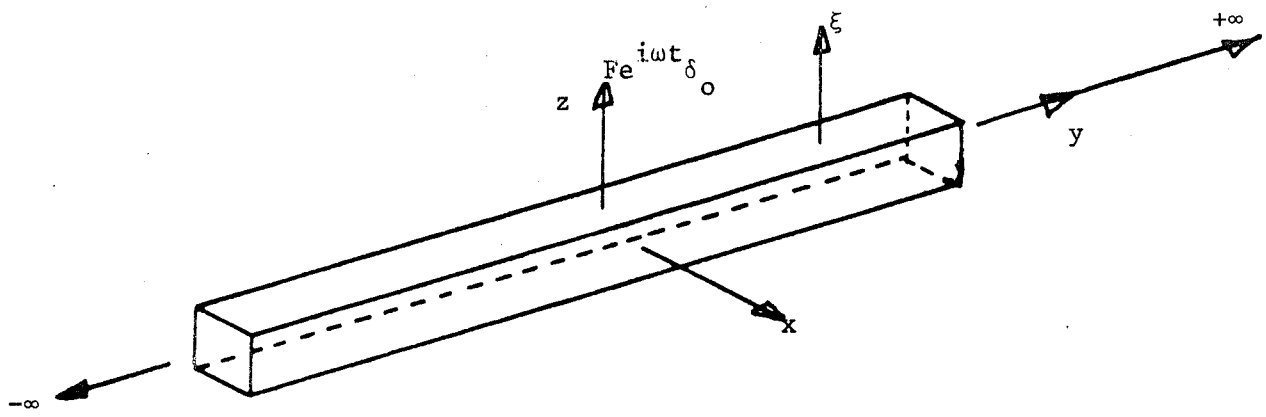

Figure 2.4 An infinite beam with force excitation.

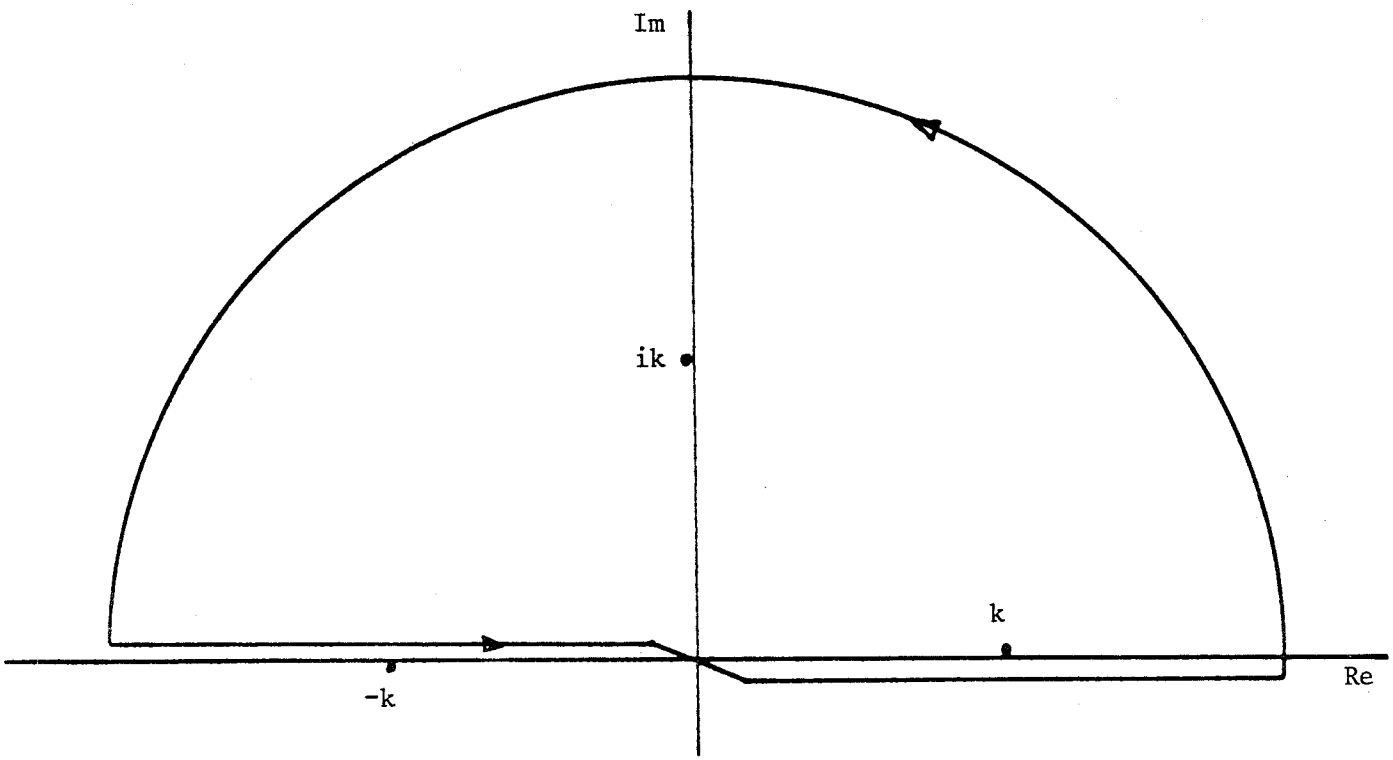

Figure 2.5 Contour of integration for equation 2.17 and 2.36.

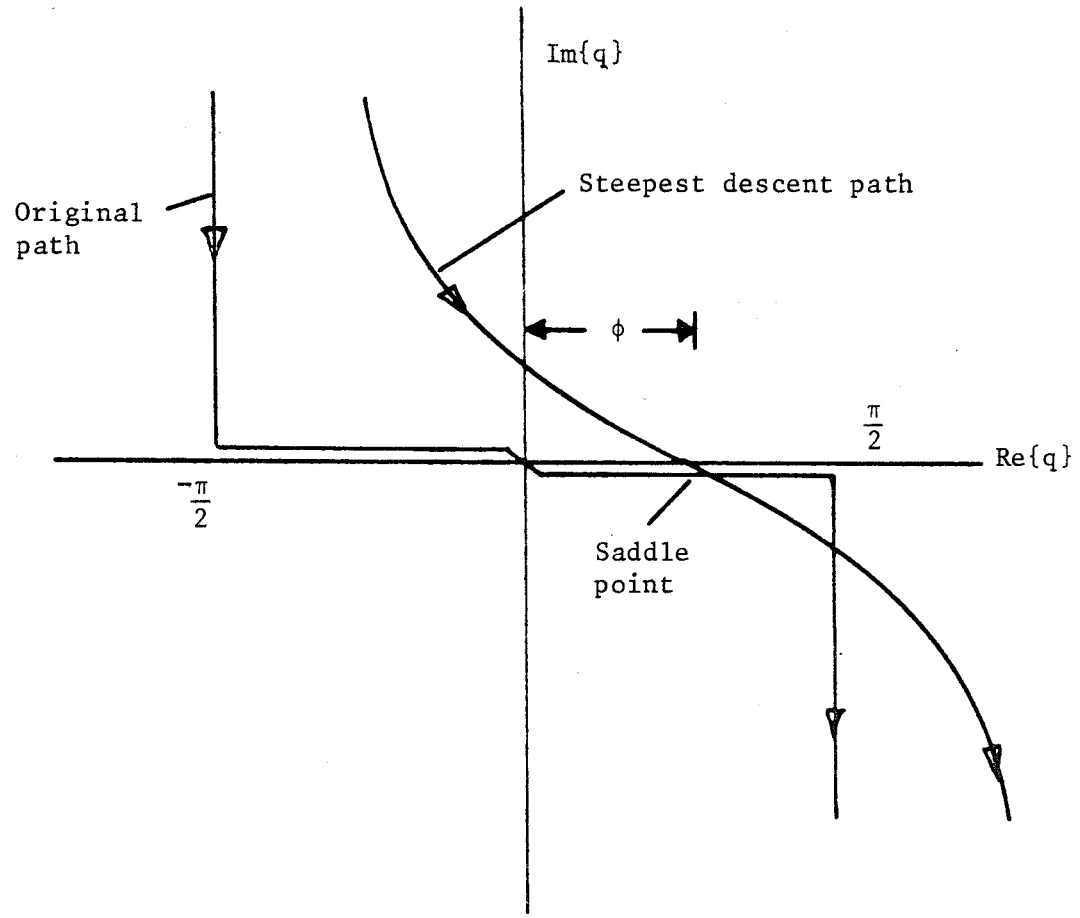

Figure 3.1 Path of steepest descent for integral 3.10.

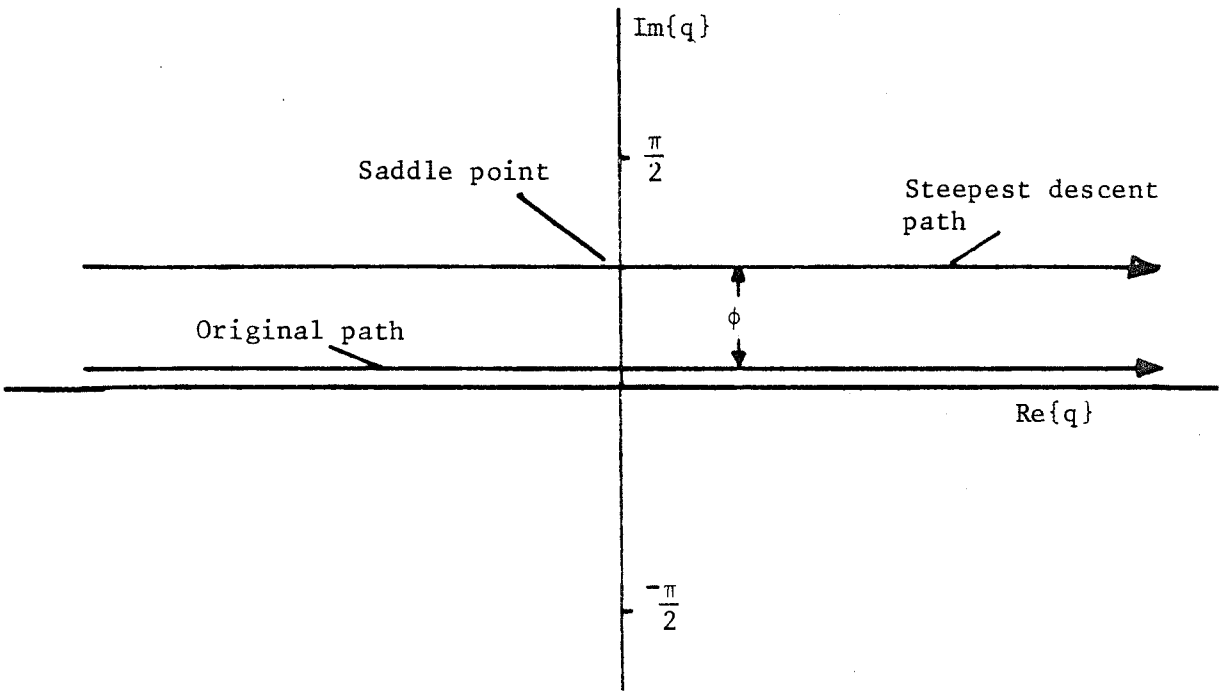

Figure 3.2 Path of steepest descent for integral 3.14.

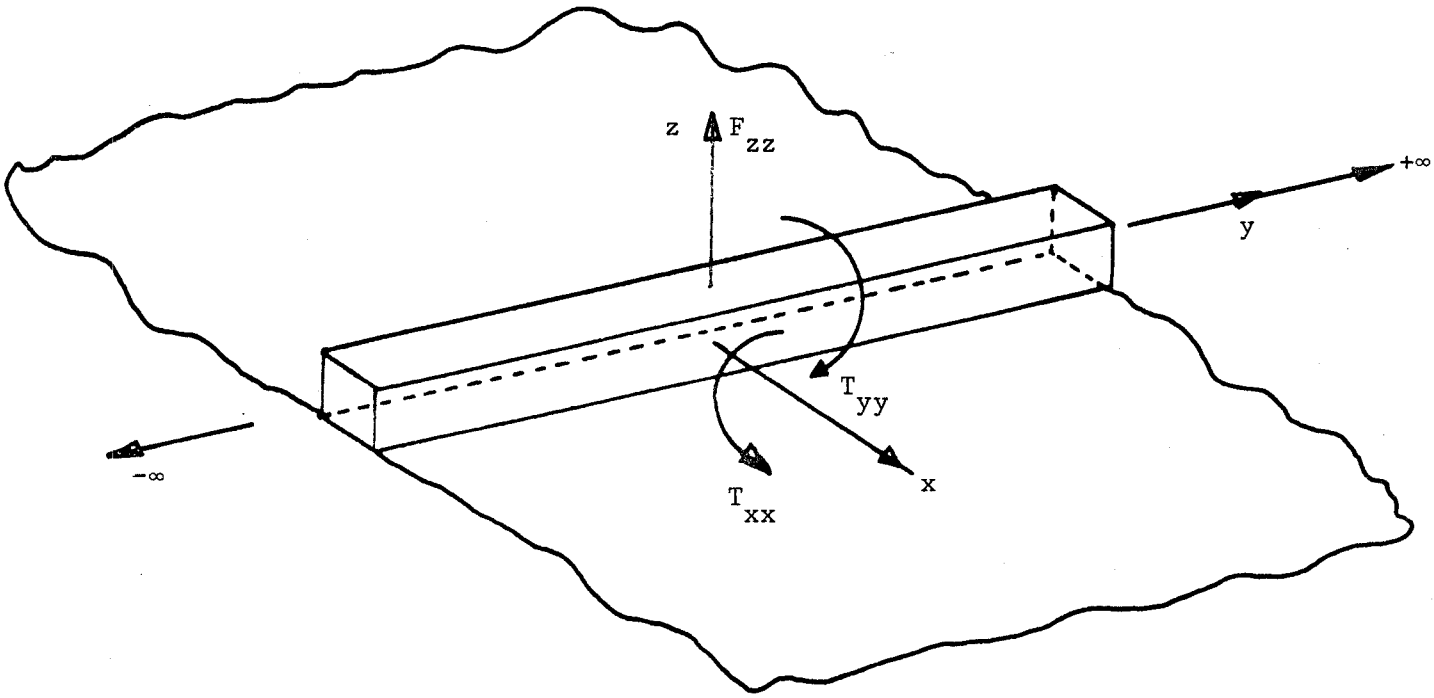

Figure 4.1 An infinite beam-stiffened plate with three types of excitation.

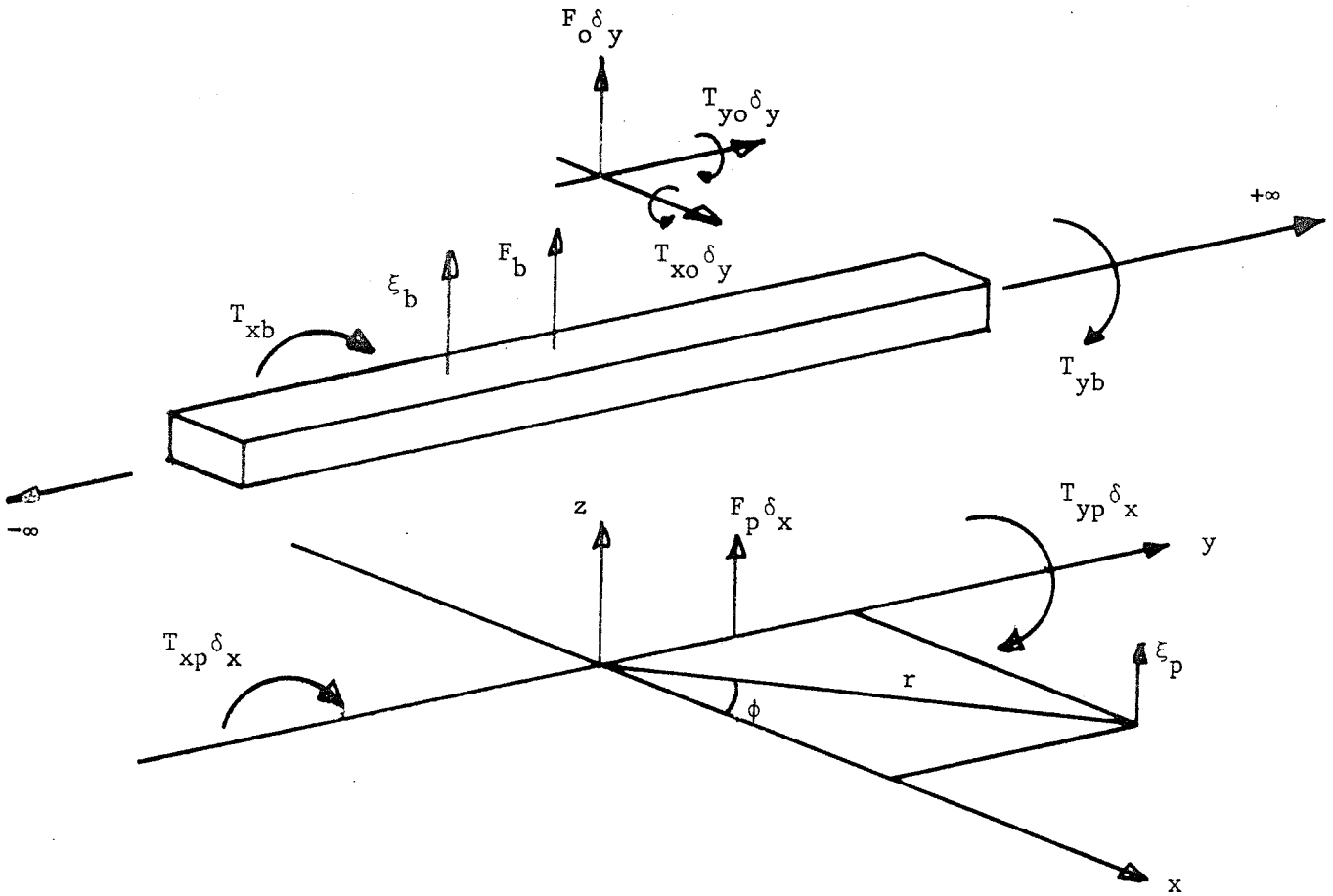

Figure 4.2 Line force and torques acting between plate and beam and externally applied excitation.

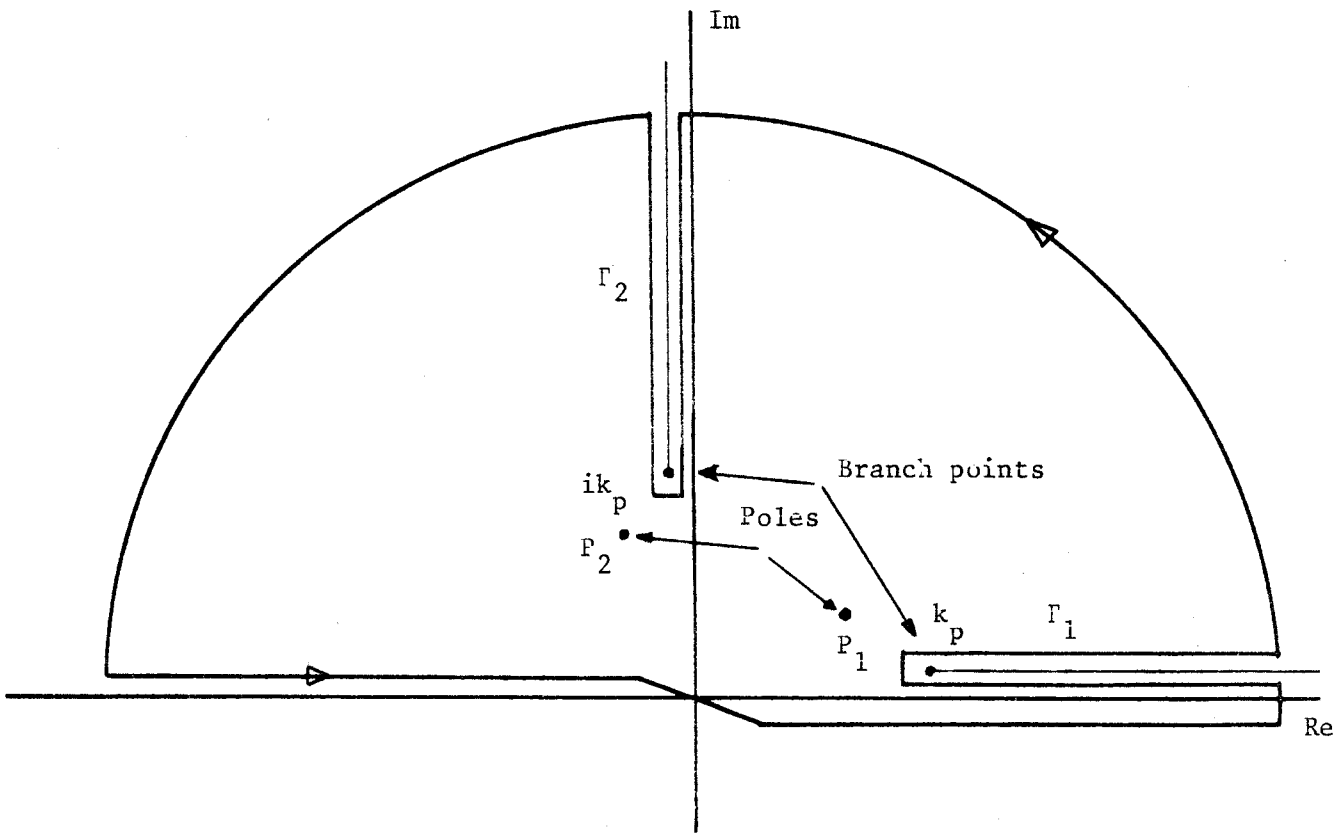

Figure 4.3 Contour of integration for equation 4.16.

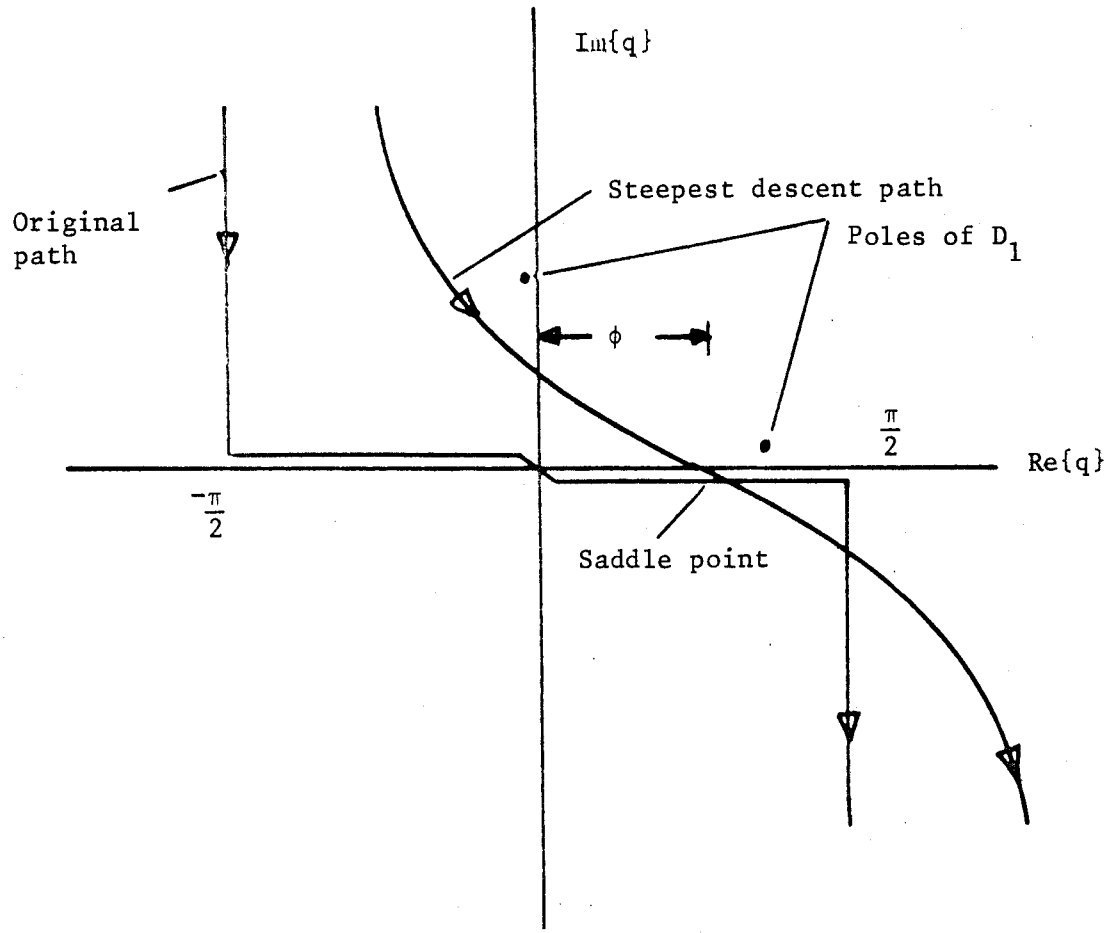

Figure 4.4 Path of steepest descent for integral 4.18.

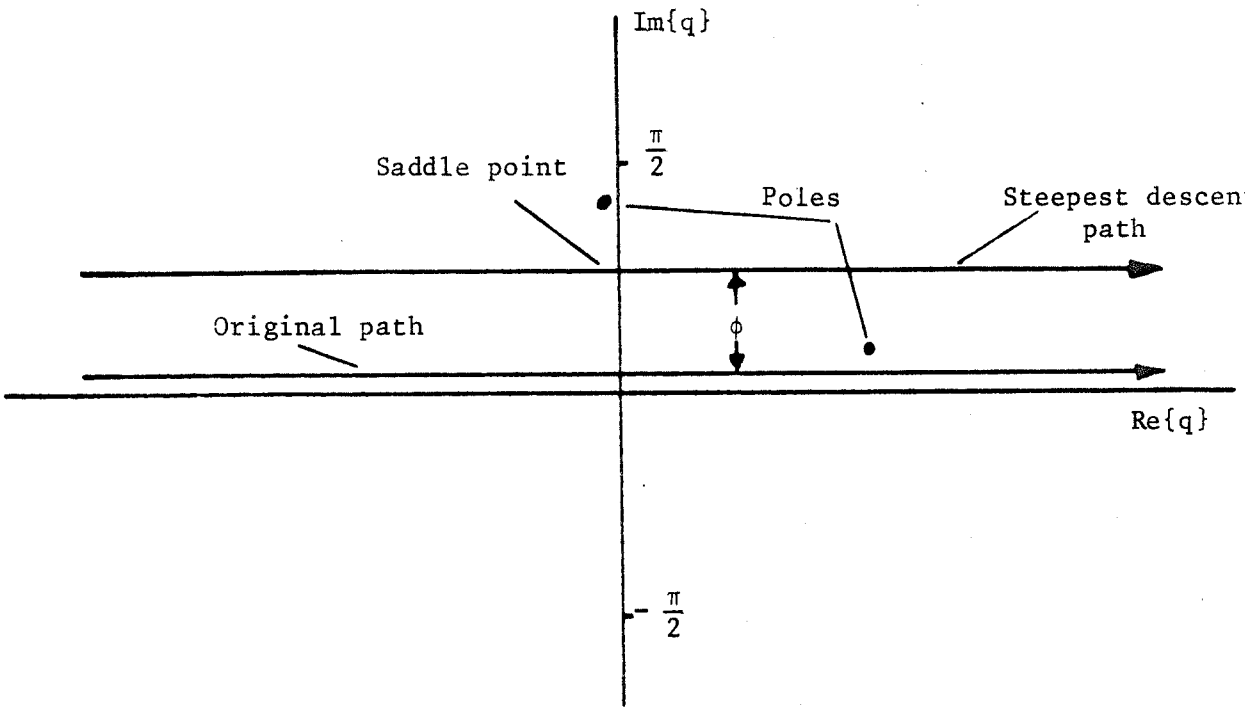

Figure 4.5 Path of steepest descent for integral 4.18.

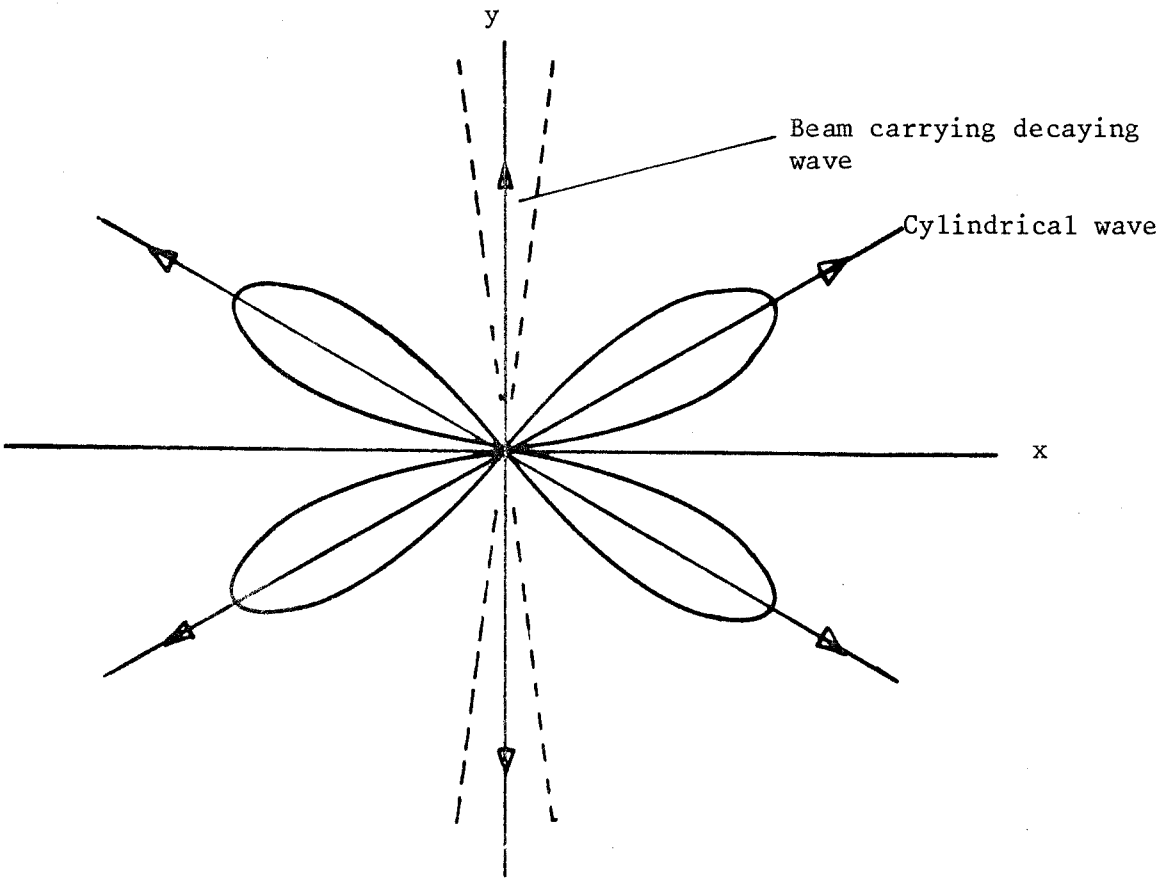

Figure 4.6 Wave field on beam stiffened plate due to force excitation or torque excitation about x-axis.

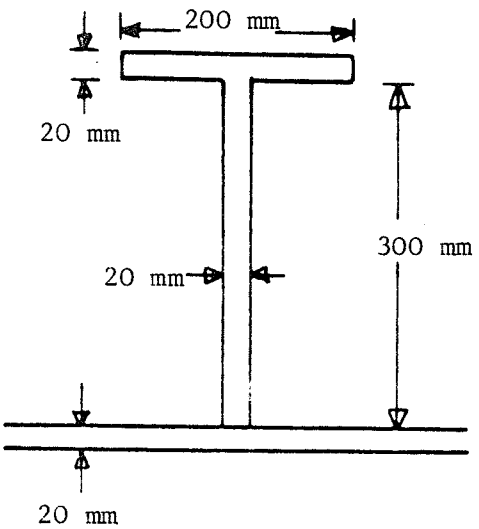

Figure 4.7 Cross section of beam and plate of ship-like dimensions. Steel $E = 19.5\ 10^{10}\ Nm^{-2}$; $\rho = 7700\ kg\ m^{-3}$.

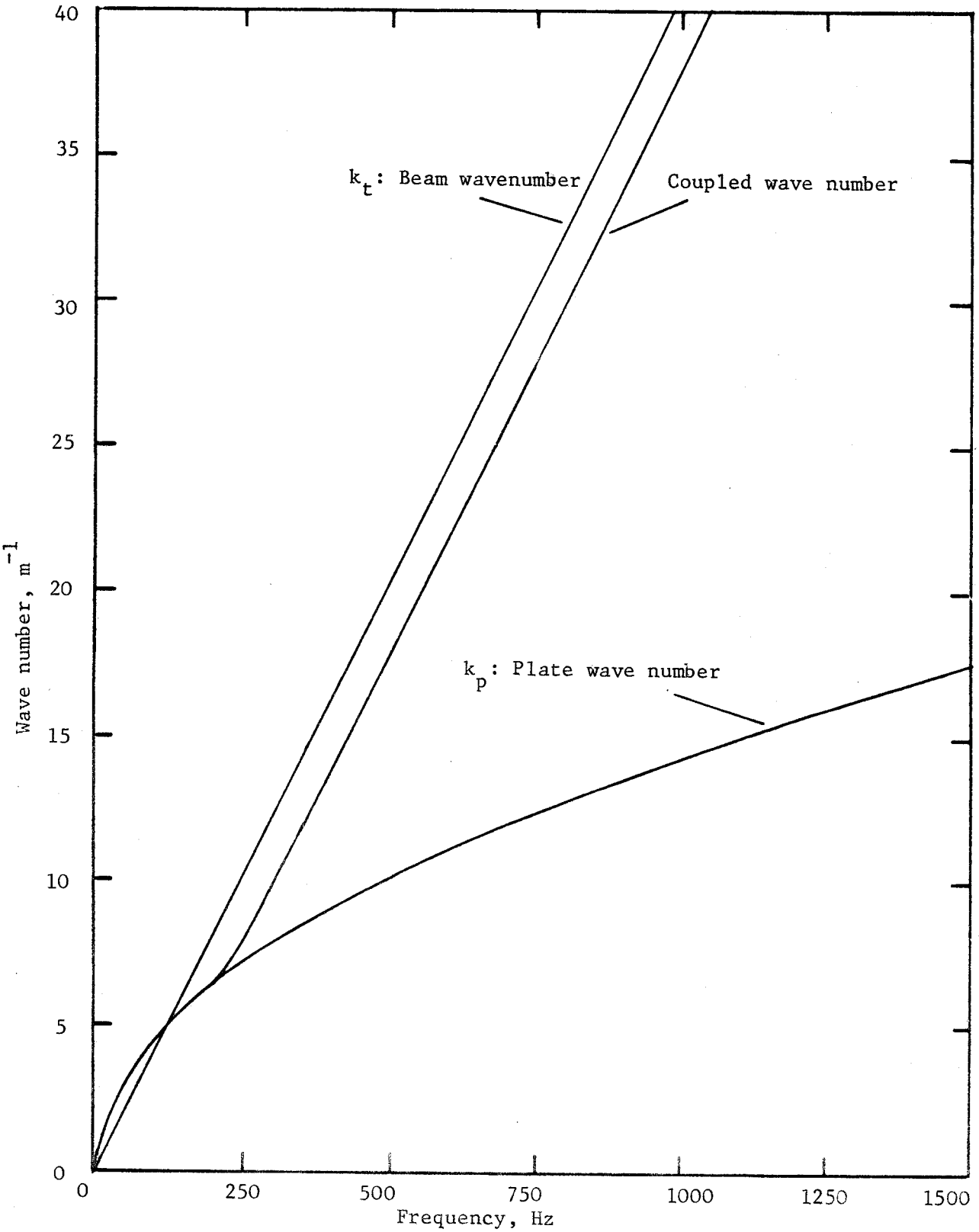

Figure 4.8 Position of pole (coupled beam plate torsional wave number) of equation 4.54.

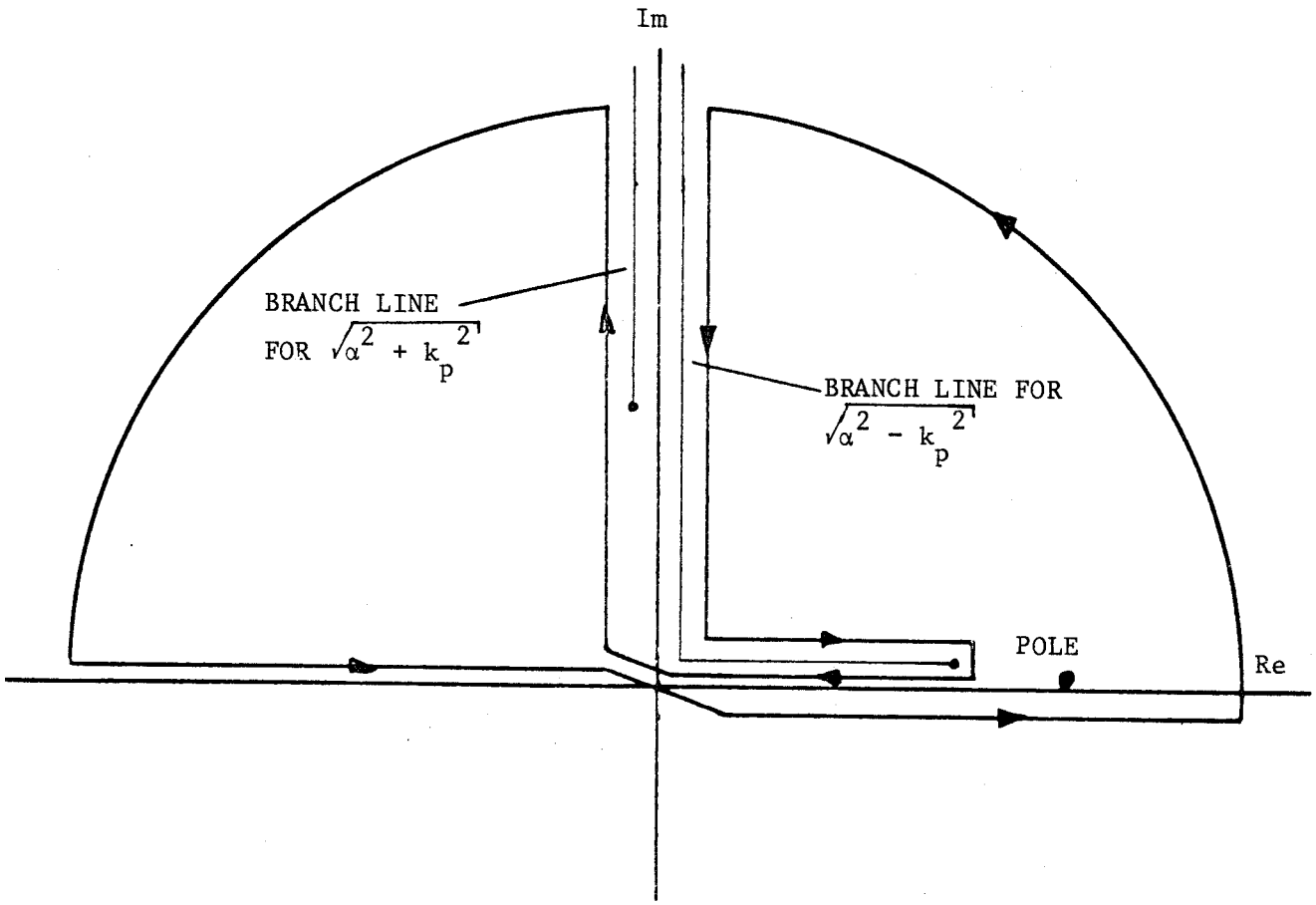

Figure 4.9 Contour for integration of equation 5.54.

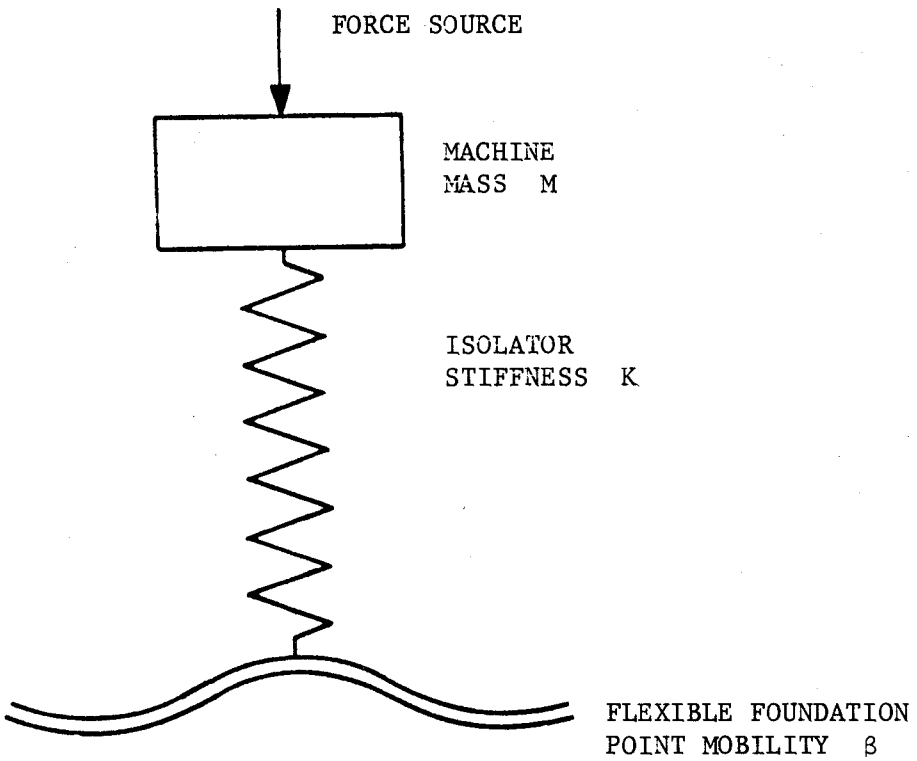

Figure 5.1 Single stage isolator with force source.

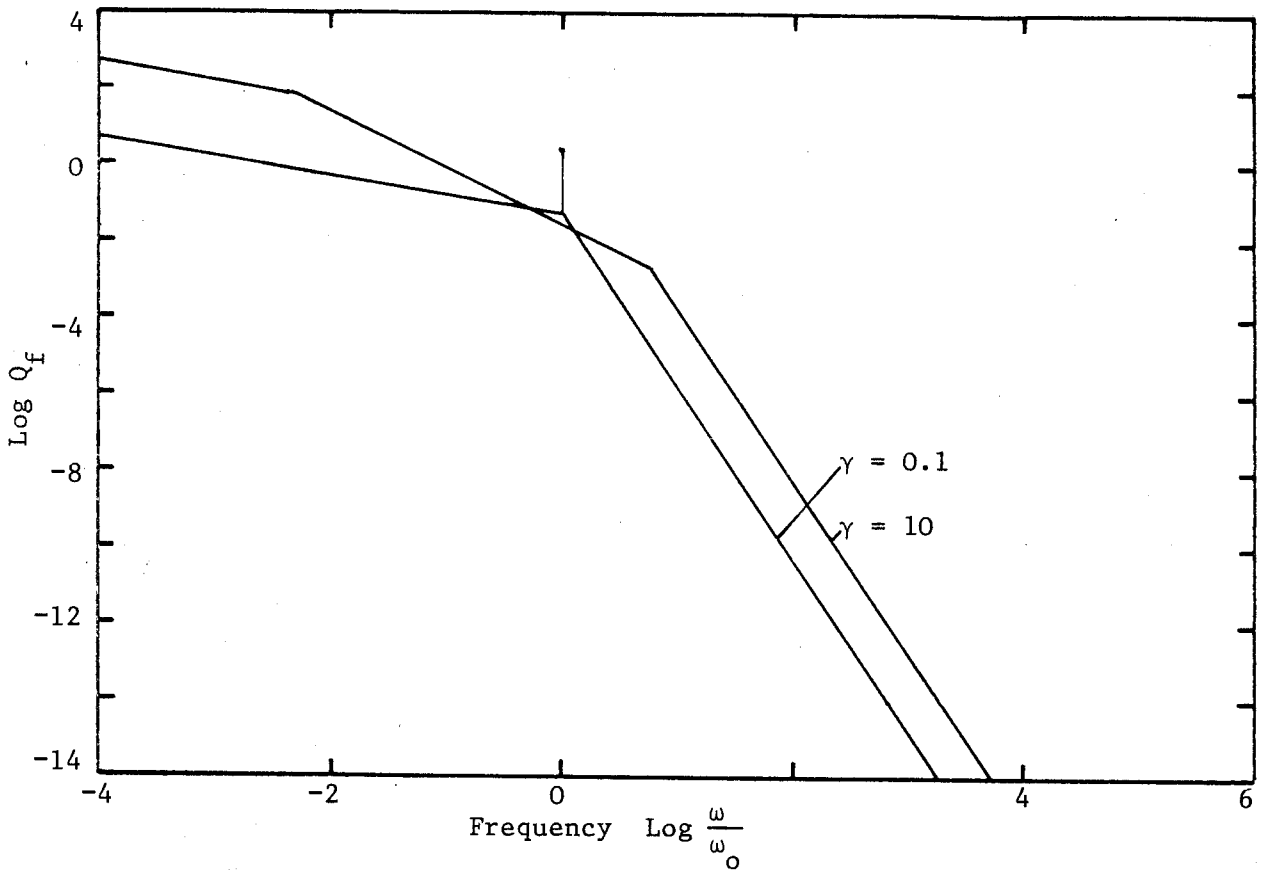

Figure 5.2 Power flow transmission spectra for single stage isolator with force source and beam-like foundation ($s = -\frac{1}{2}$; $M\omega_o = 1$): approximate values based on table II.

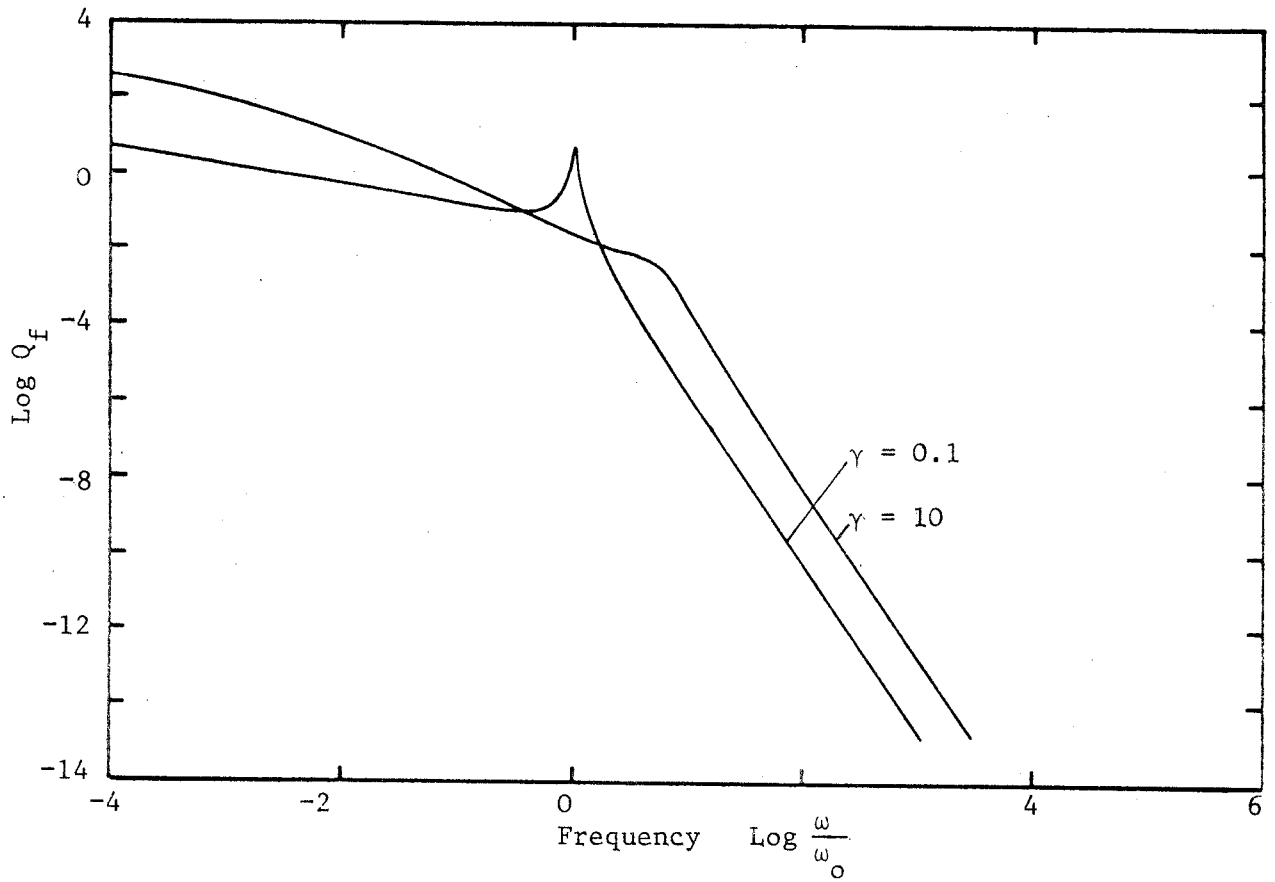

Figure 5.3 Power flow transmission spectra for single stage isolator with force source and beam-like foundation ($s = -\frac{1}{2}$; $M\omega_o = 1$).

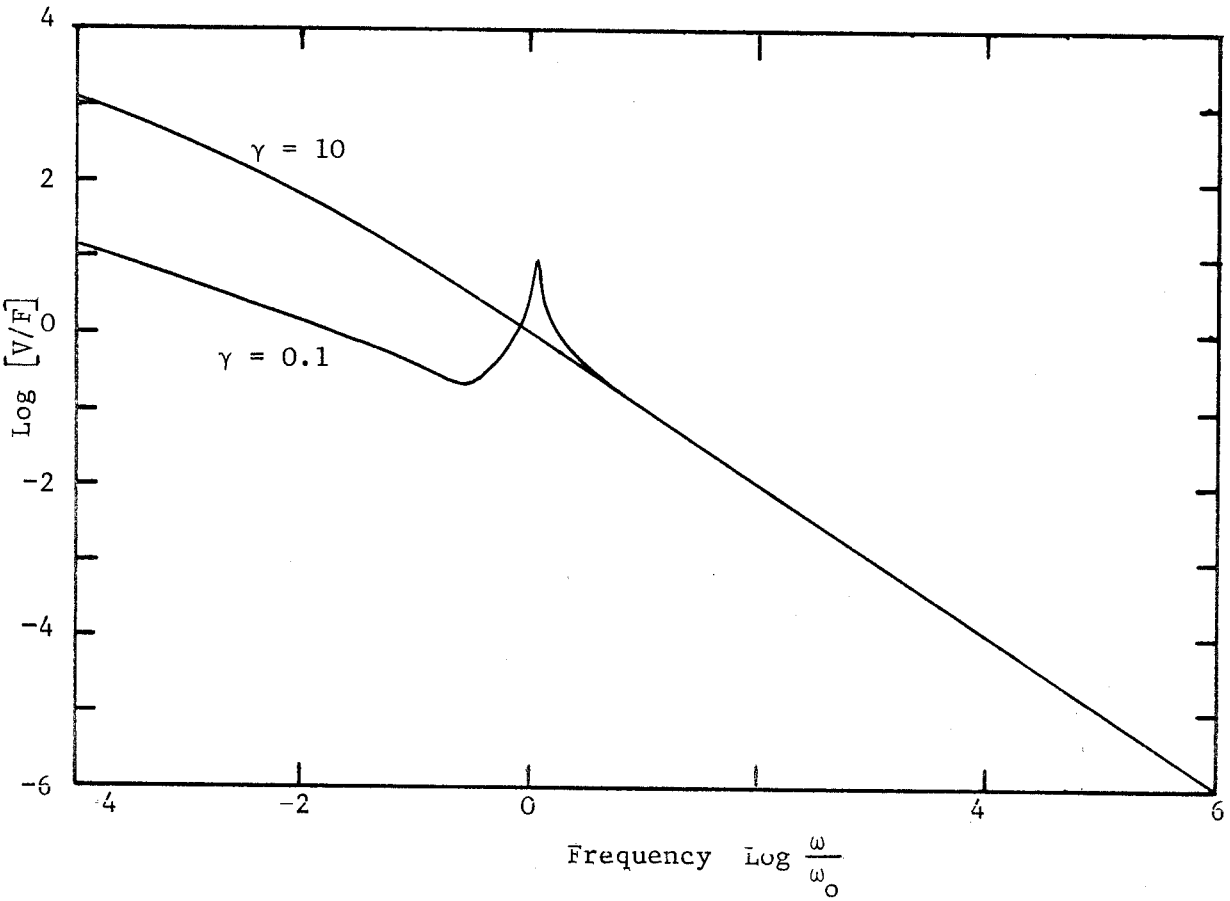

Figure 5.4 Velocity of machine on single stage isolator with beam-like foundation and force source.

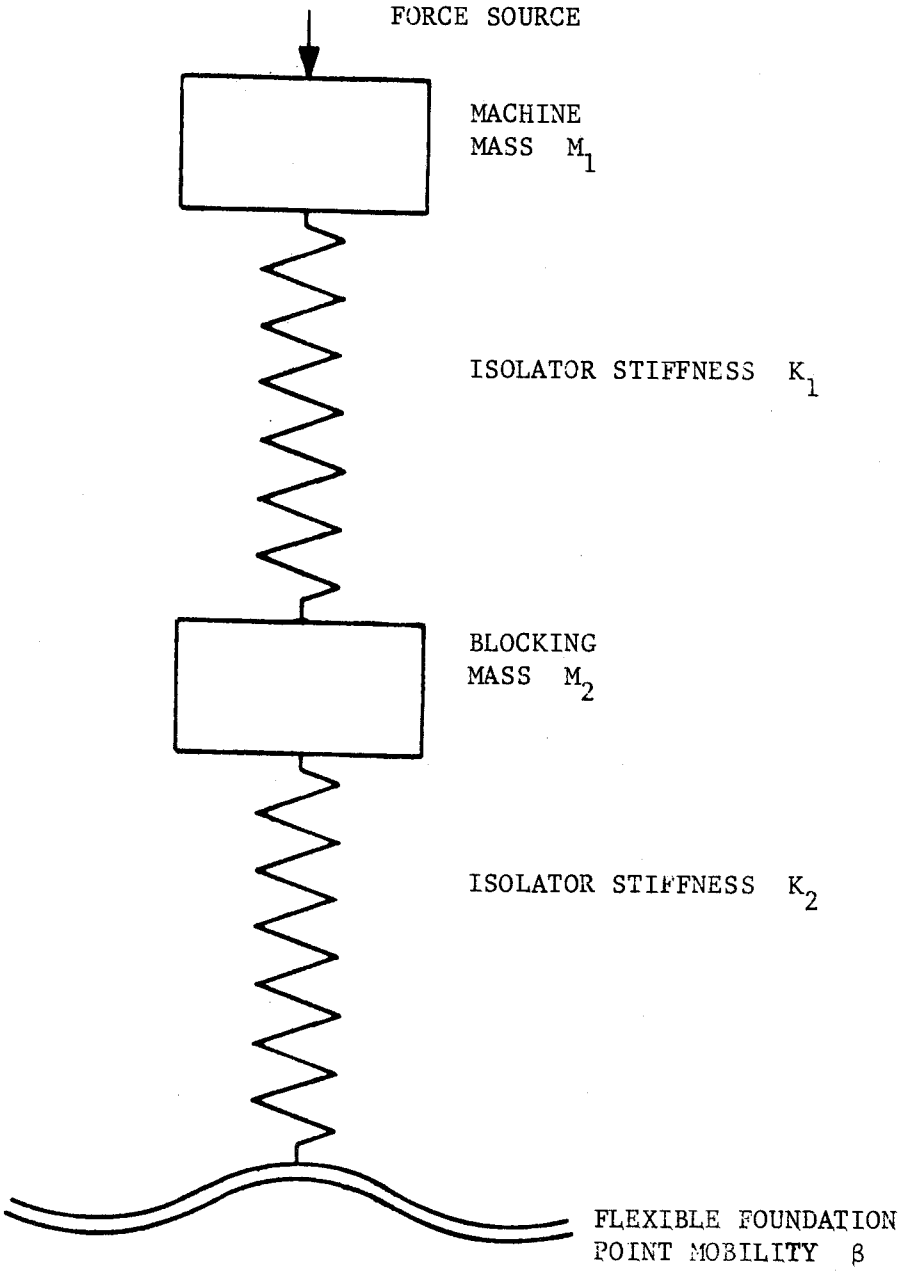

Figure 5.5 Two stage isolation system with force source.

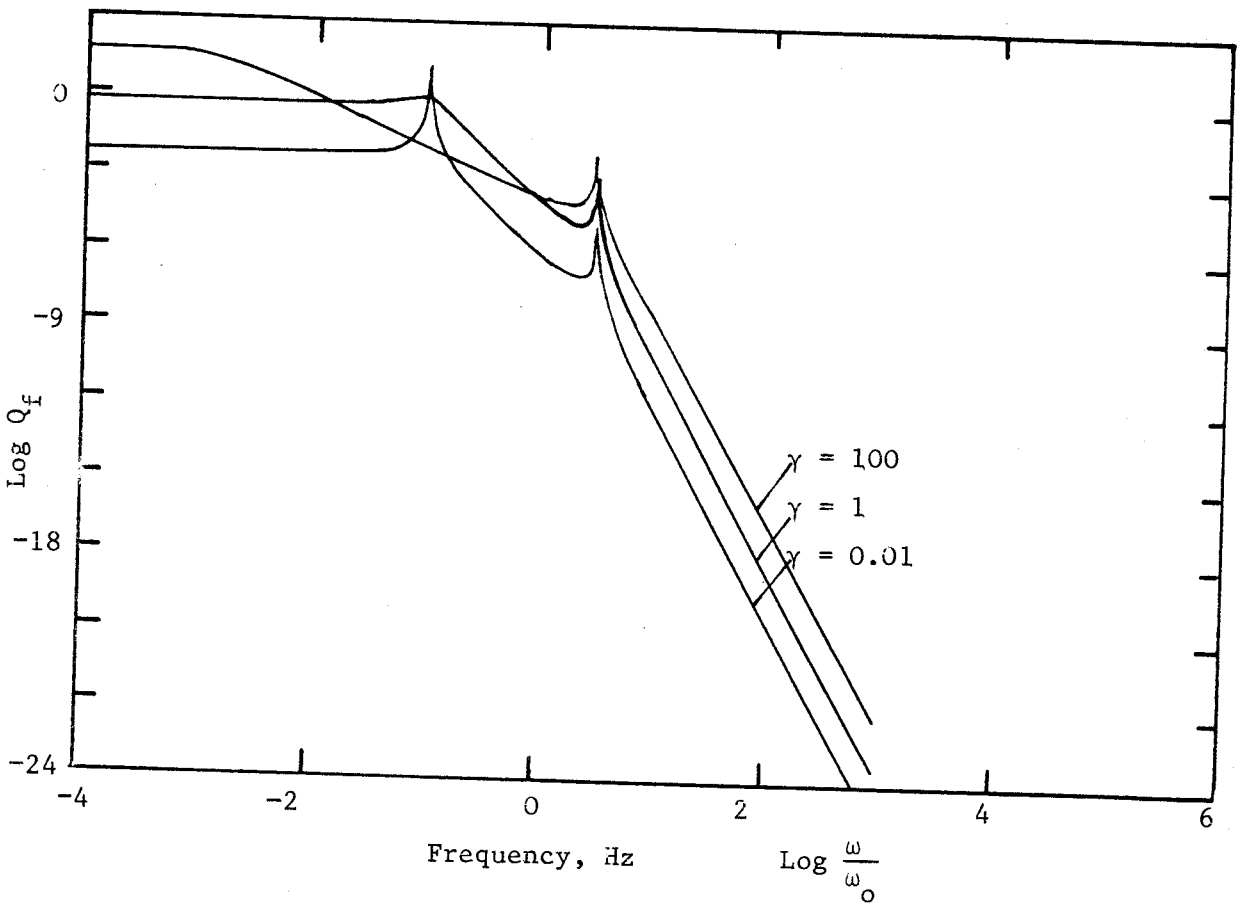

Figure 5.6 Power flow transmission spectra for two stage isolator with force source (s = 0; $K_1/(M_1 M_2 \omega_o^3 = 1)$; $\omega_1 = 0.1$; $\omega_2 = 3.0$; $\omega_o = 1$).

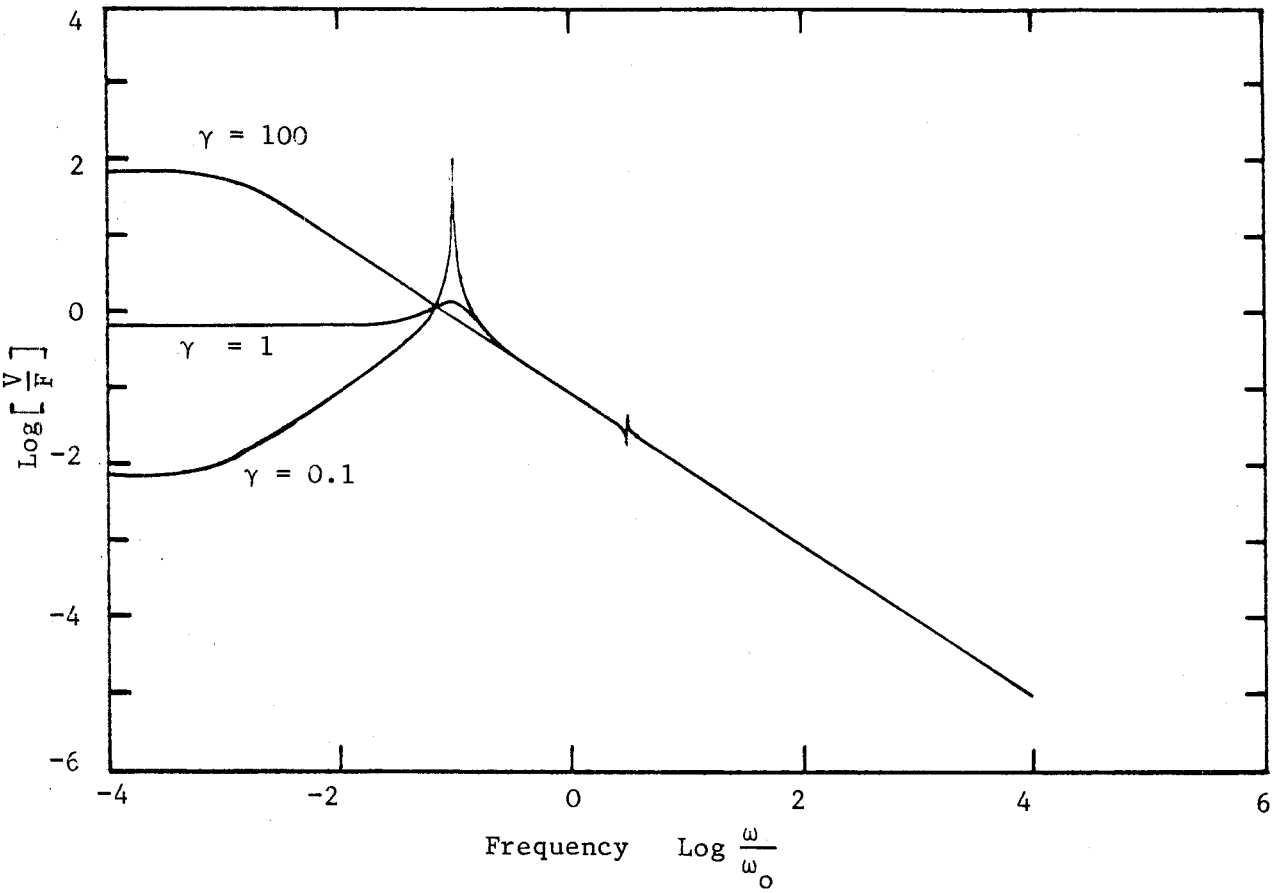

Figure 5.7 Velocity of machine on two stage isolator with force source and plate-like foundation (s = 0; $\frac{\omega_o}{K_1}$ = 1.0; ω_1 = 0.1; ω_2 = 3.0. ω_o = 1.0).

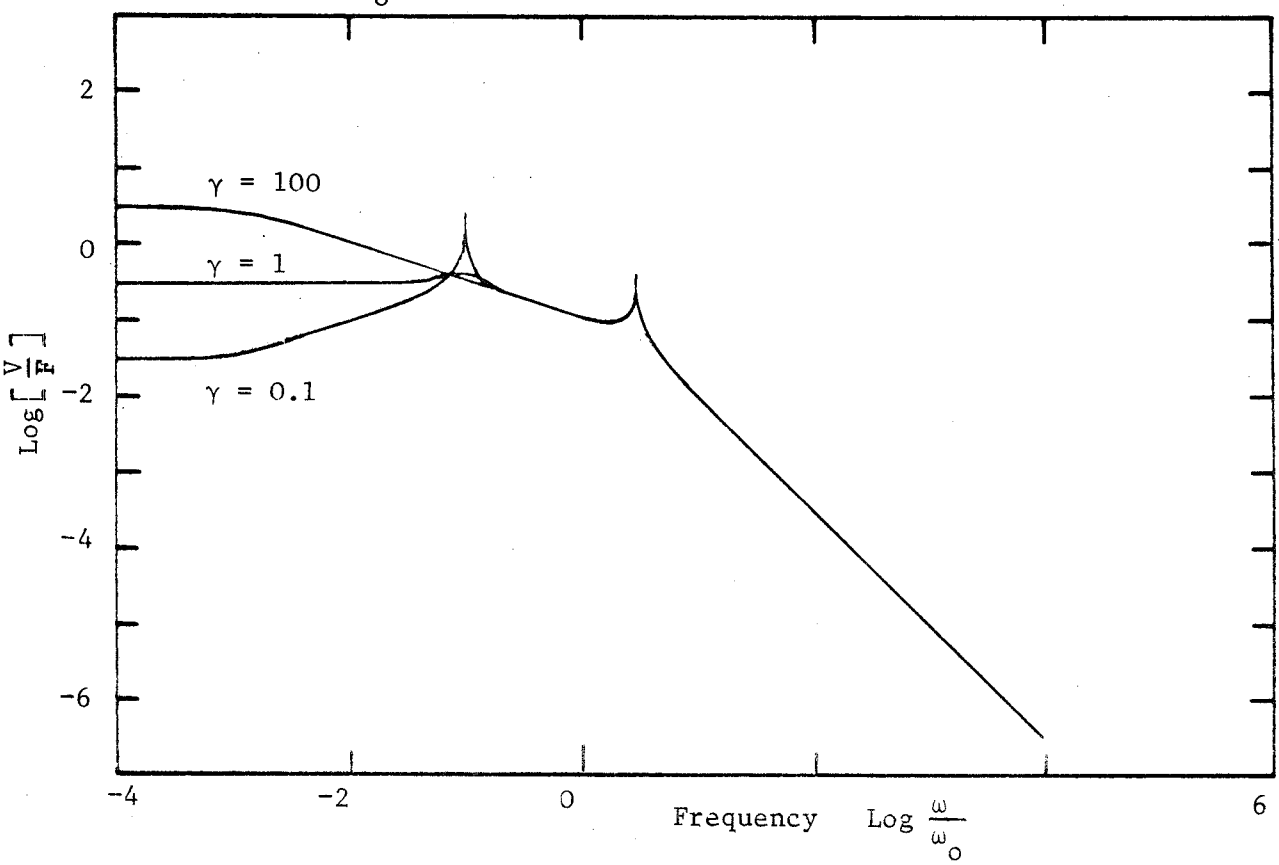

Figure 5.8 Velocity of blocking mass of two stage isolator with force source and plate-like foundation (s = 0; ω_o/K_1 = 1.0; ω_1 = 0.1. ω_1 = 1.0; ω_2 = 3.0; ω_o = 1.0

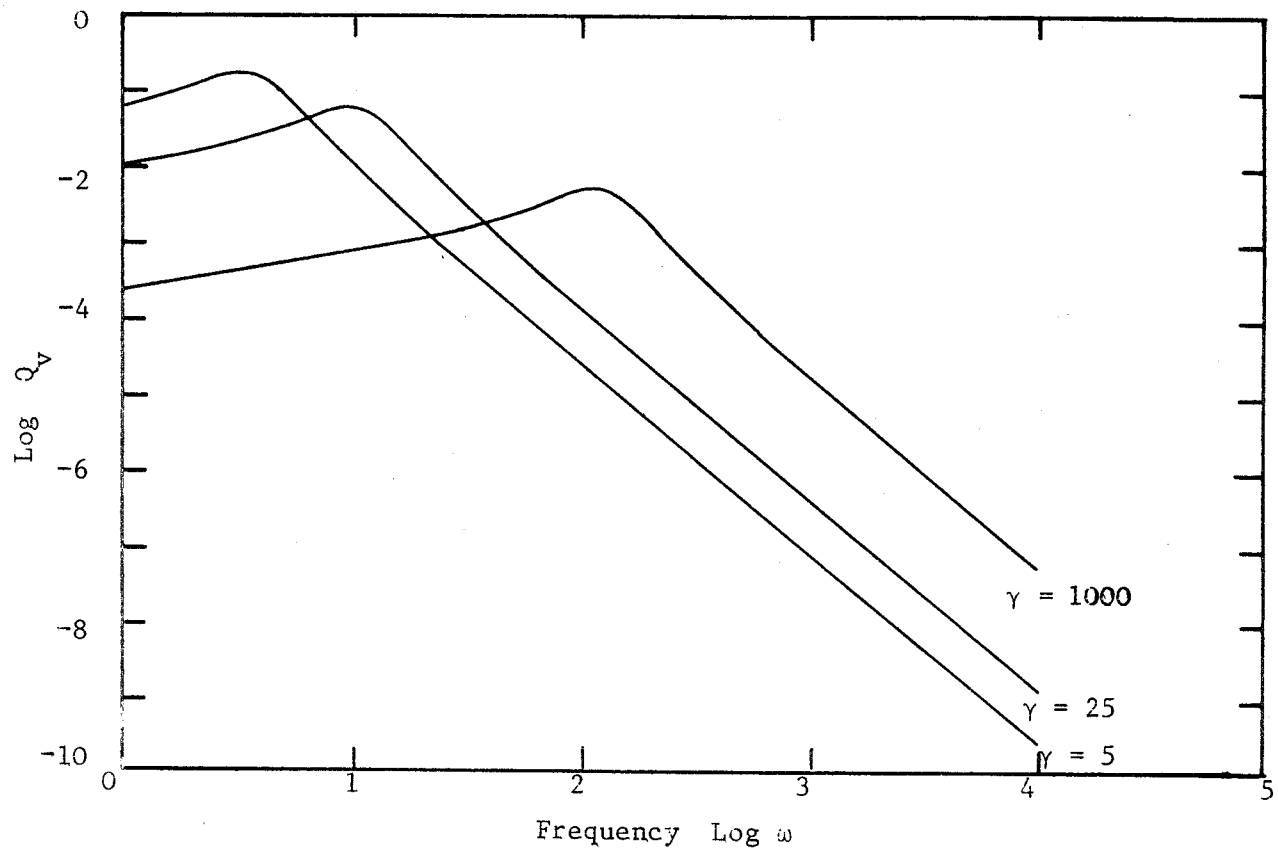

Figure 5.9 Power flow transmission spectra for velocity source and single stage isolator with beam-like foundation ($s = -\frac{1}{2}$; $K = 1.0$).

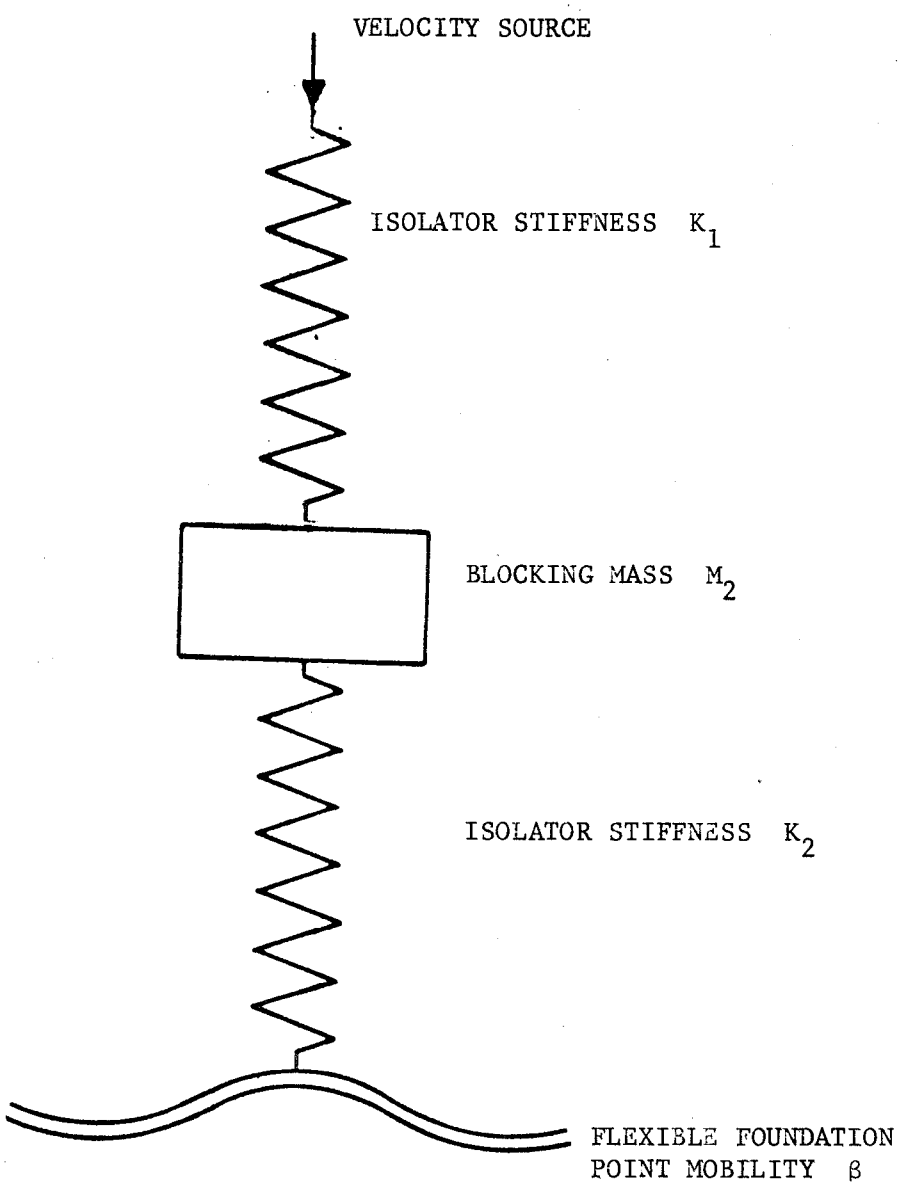

Figure 5.10 Two stage isolation system with velocity source.

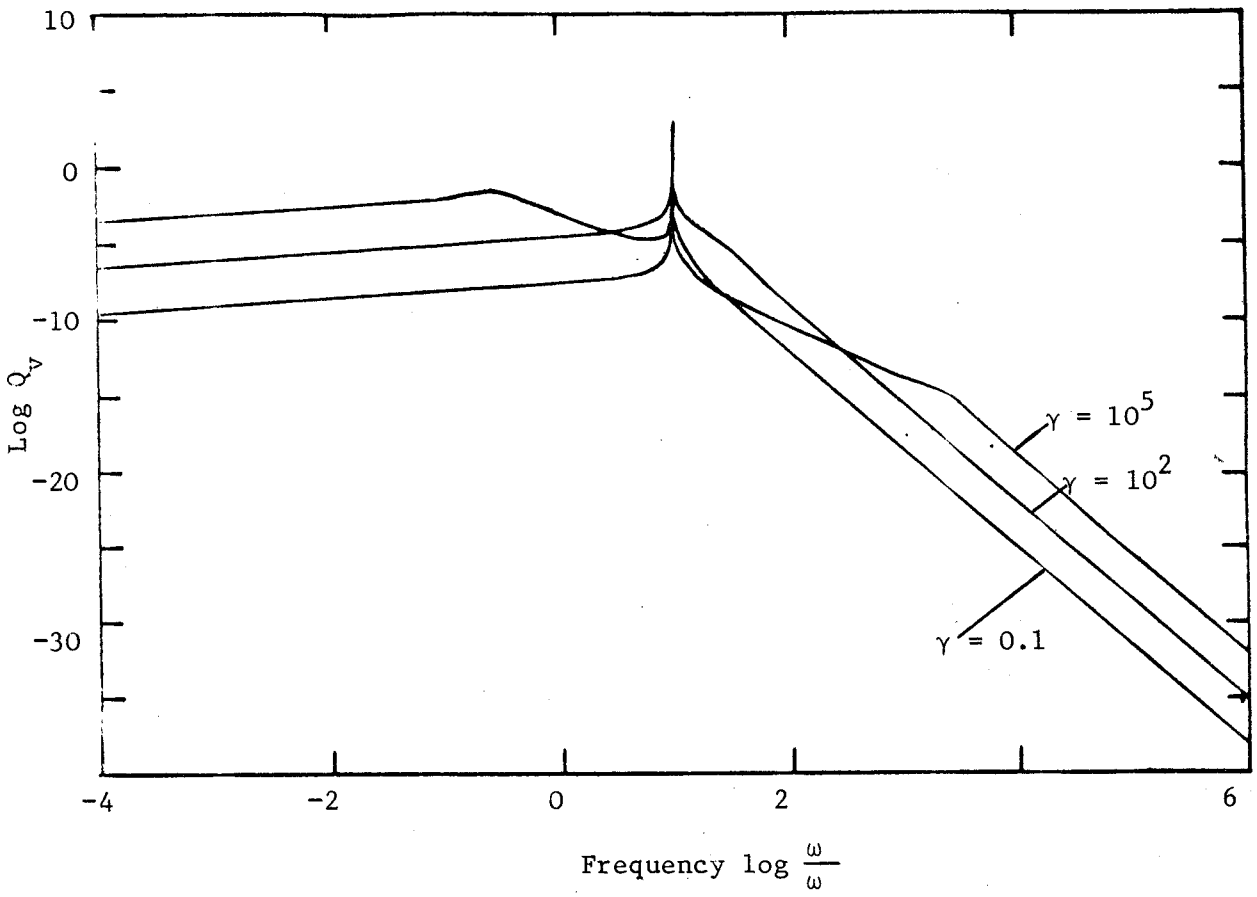

Figure 5.11 Power flow transmission spectra for two stage isolator and beam-like foundation ($s = -\frac{1}{2}$; $\omega_o K_2 = 1.0$; $\omega_o = 1.0$; $\omega_1 = 10$)

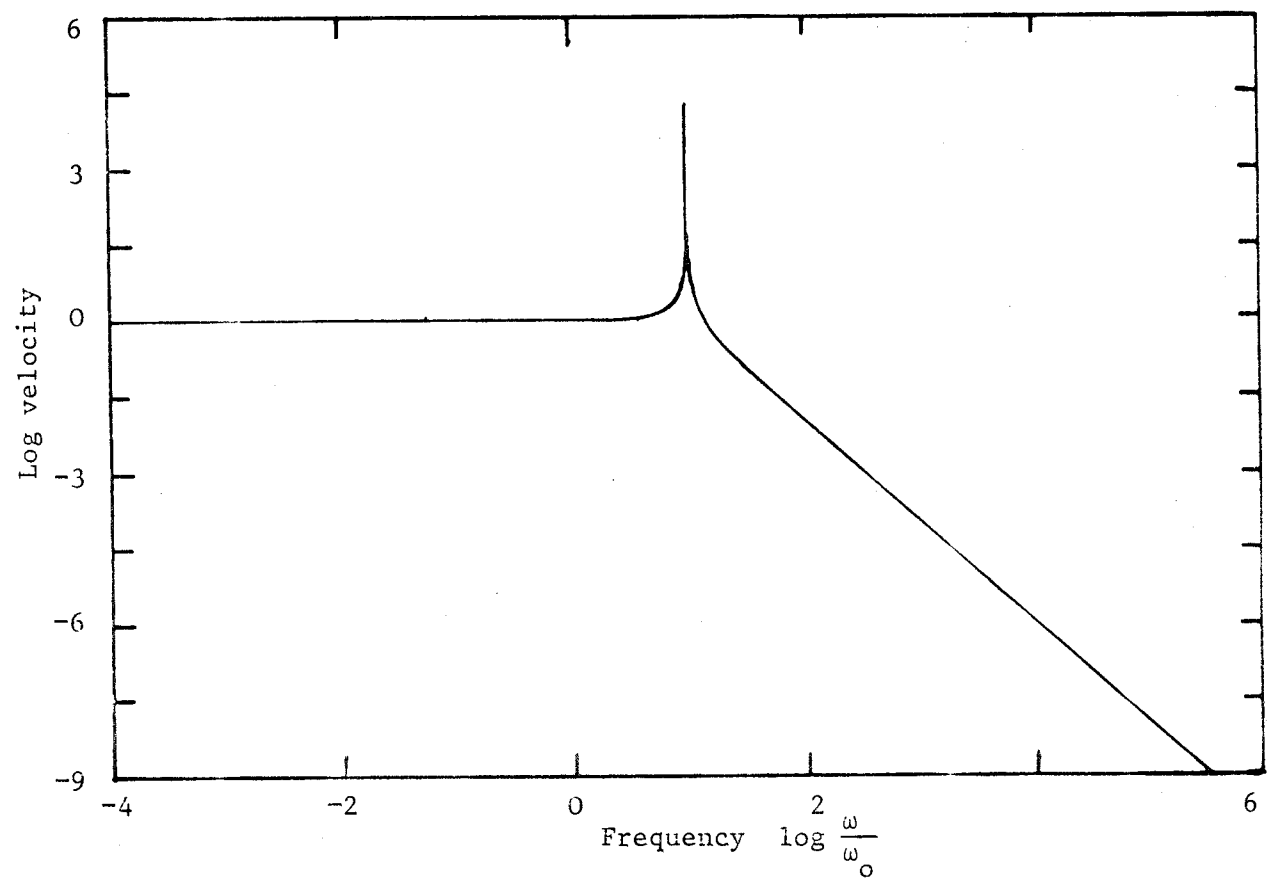

Figure 5.12 Velocity of blocking mass of two stage isolator with velocity source and beam-like foundation ($s = -\frac{1}{2}$; $\omega_1 = 10$; $\omega_o = 1$).

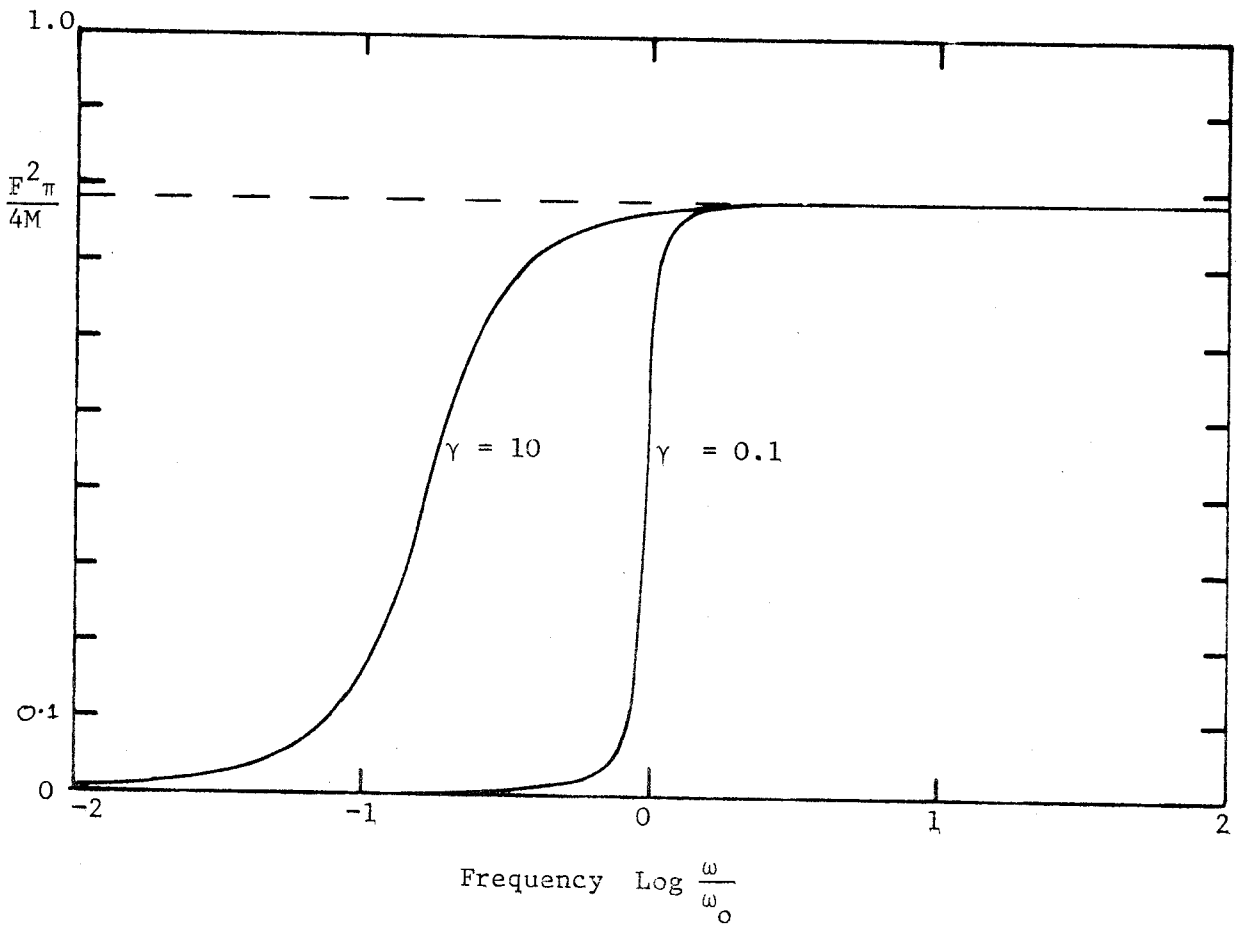

Figure 5.13 Running integral across power flow transmission spectra ($s = -\frac{1}{2}$; $M\omega_o = 1.0$; $F = 1$).

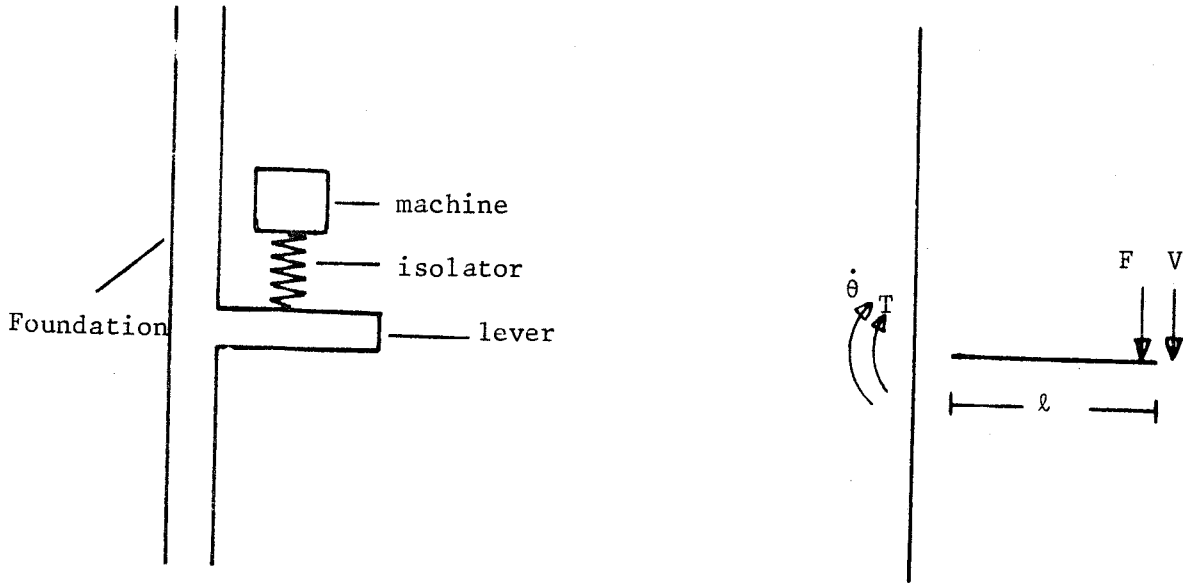

Figure 5.14 Method of mounting machinery which results in torque excitation of foundation.

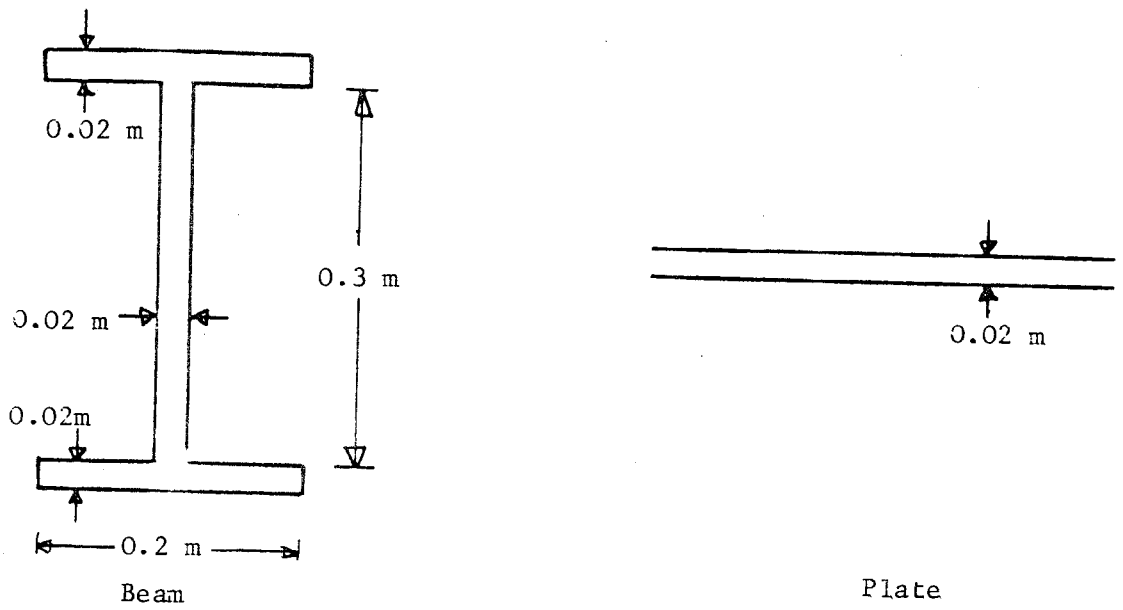

Figure 5.15 Dimensions of beam and plate used in Figure 5.16.

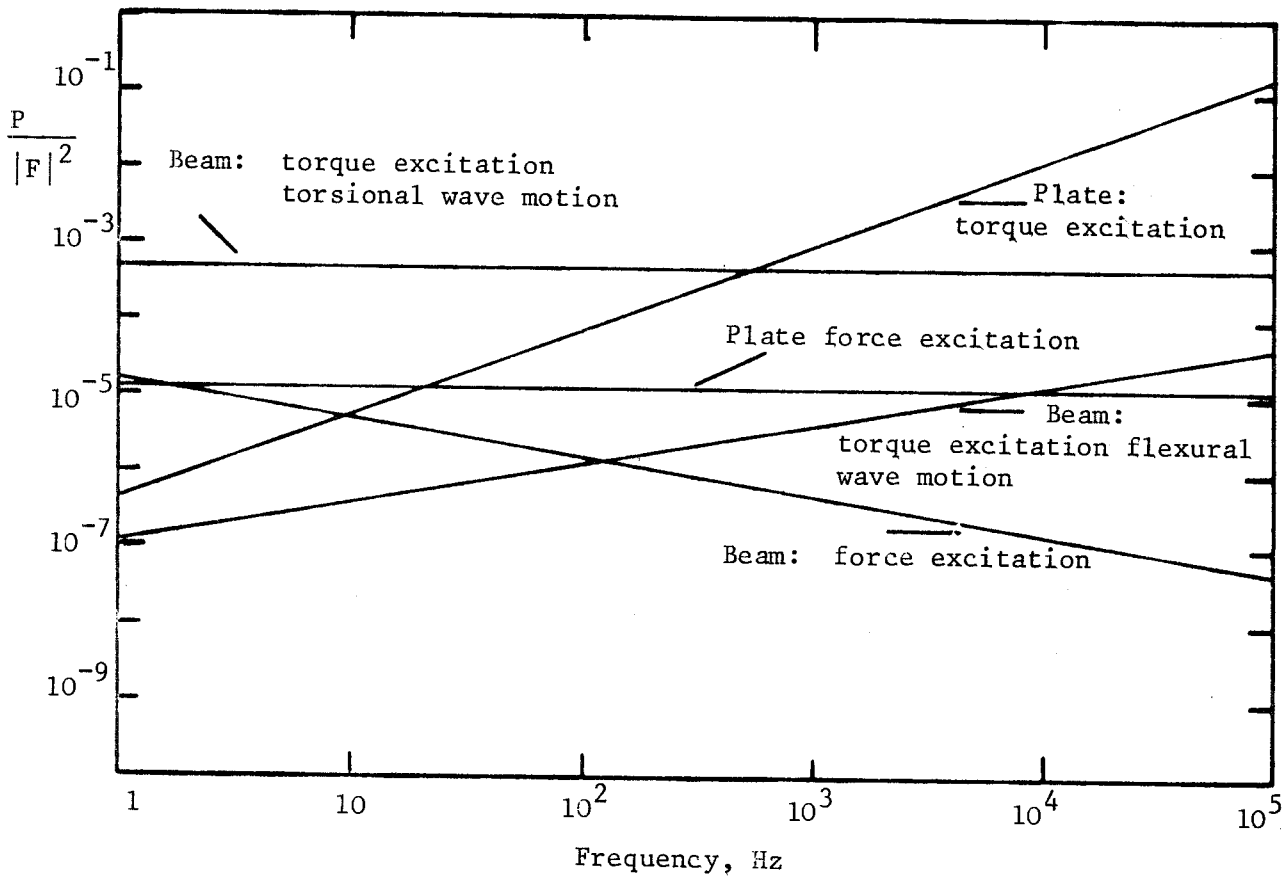

Figure 5.16 Power flow transmission spectra for a beam and plate (dimensions, figure 5.15) with a force source applied directly or as a torque by means of a lever of length 1.0m.

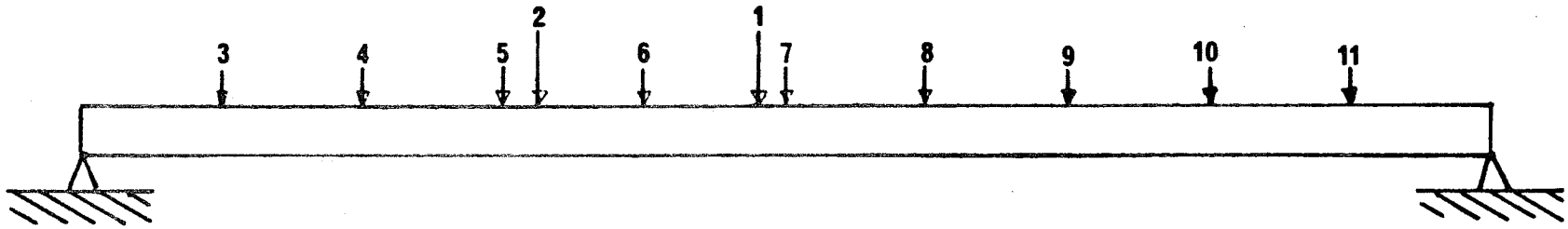

Stations 3-11 Equally Spaced Along Beam

Stations 1, 2 Excitation and Response

Stations 3-11 Response Only

Figure 6.1 Position of measurement stations

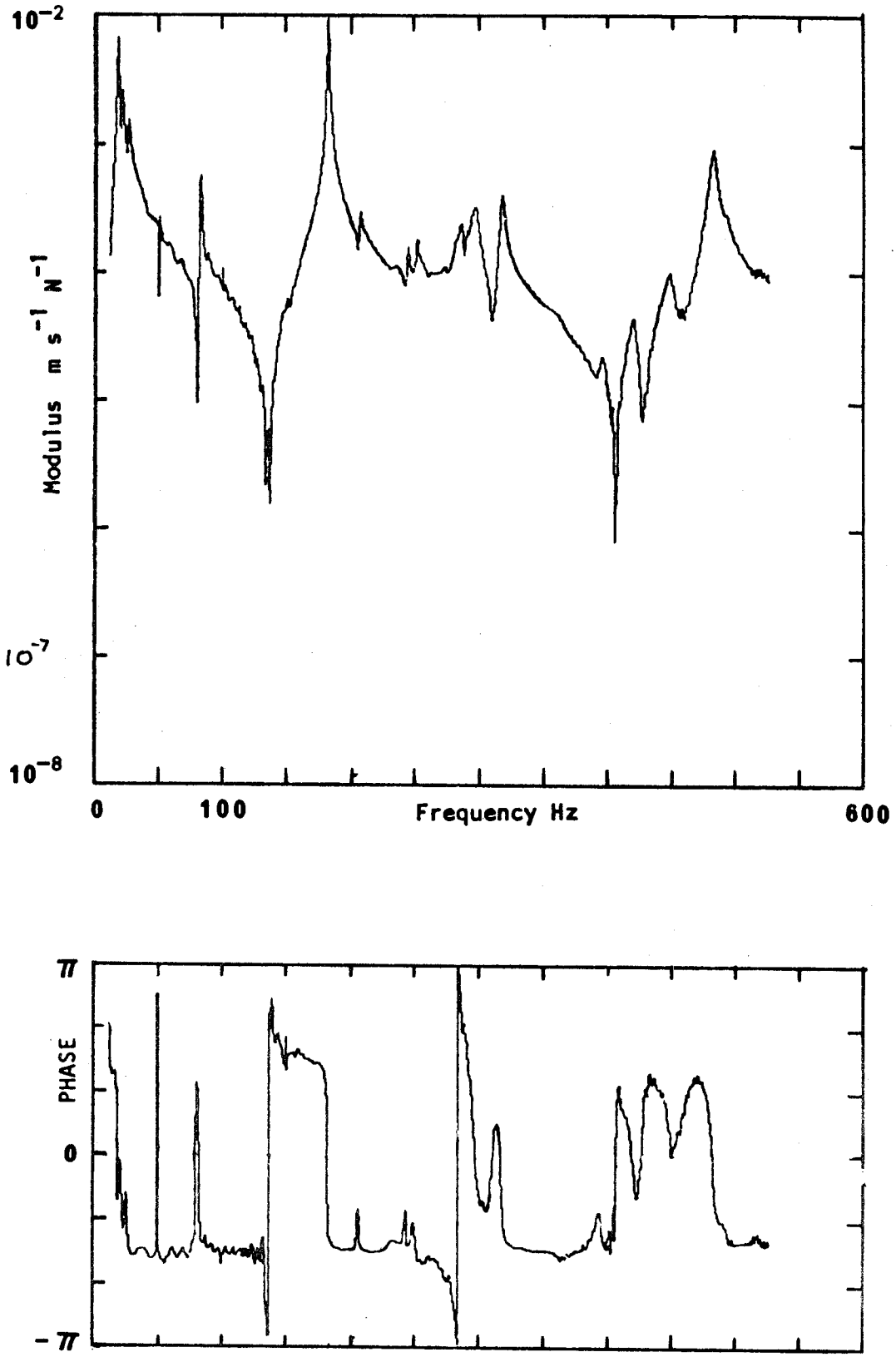

Figure 6.2 Point mobility - measured data

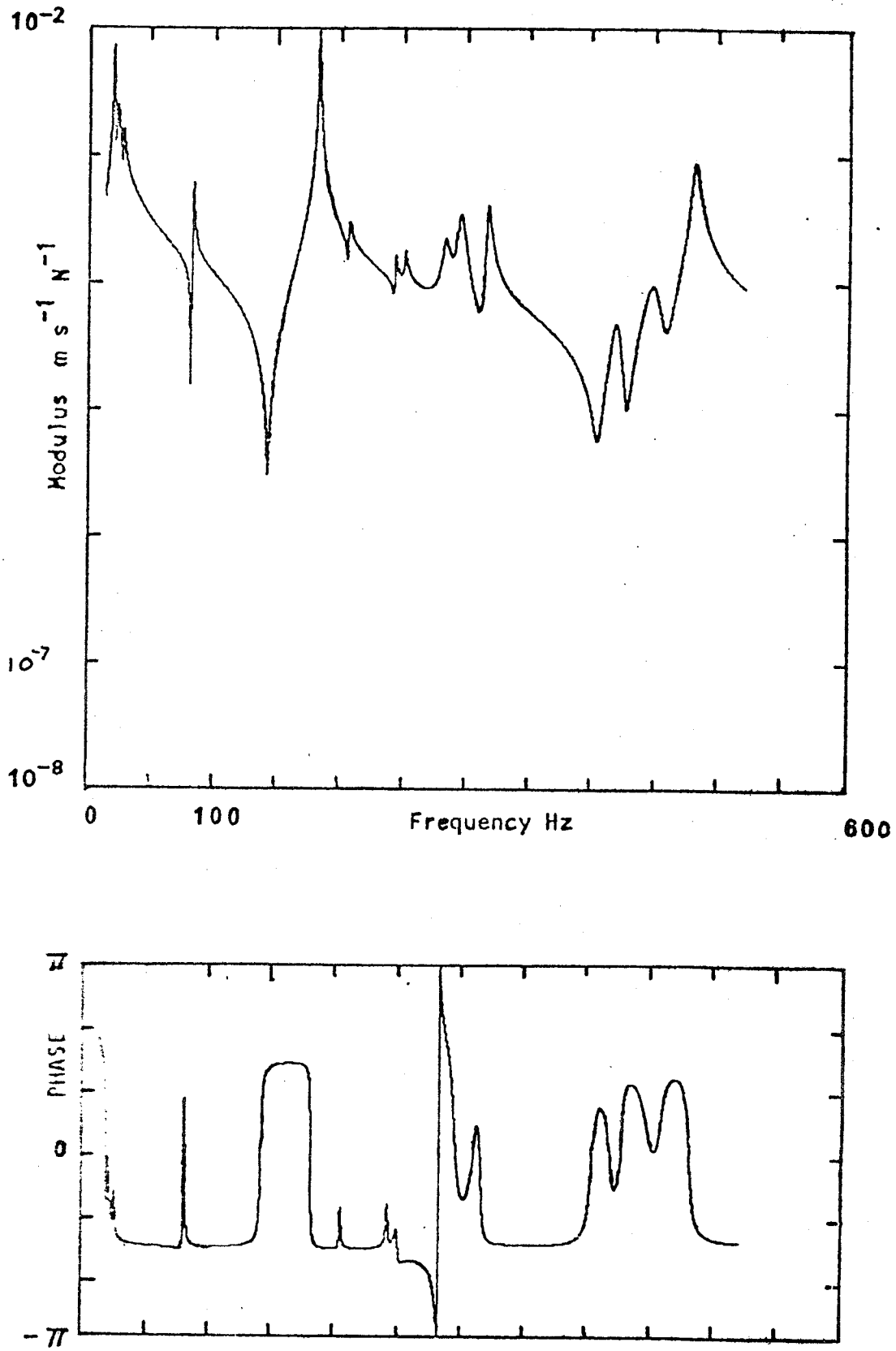

Figure 6.3 Point mobility - fitted data

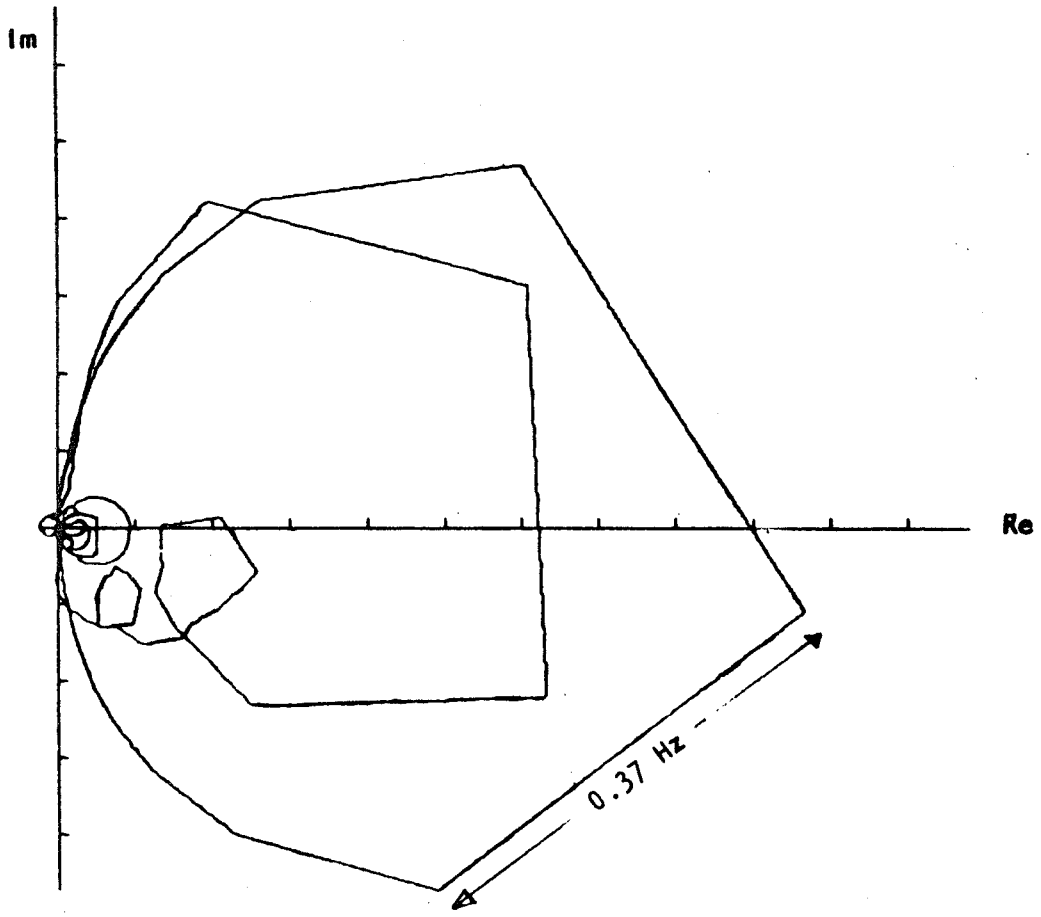

Figure 6.4 Argand diagram of point mobility - measured data

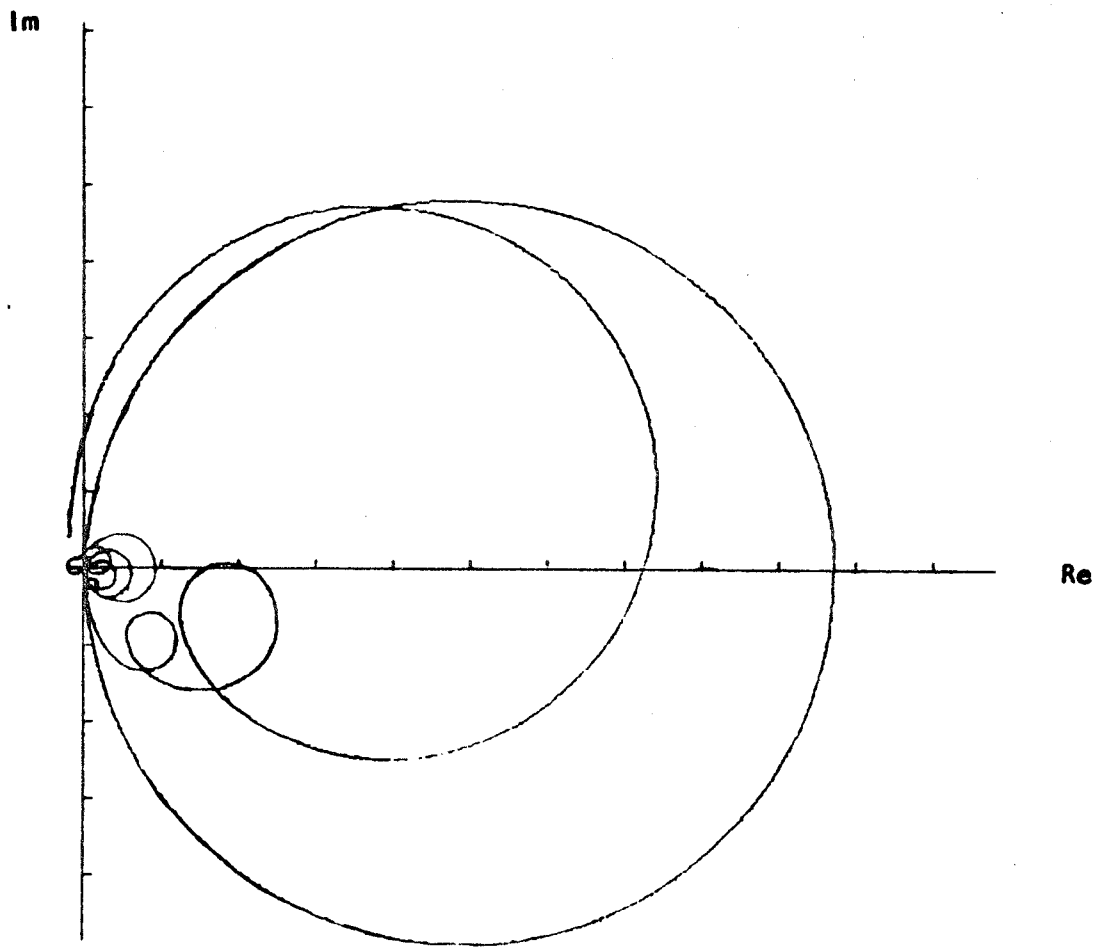

Figure 6.5 Argand diagram of point mobility - fitted data.

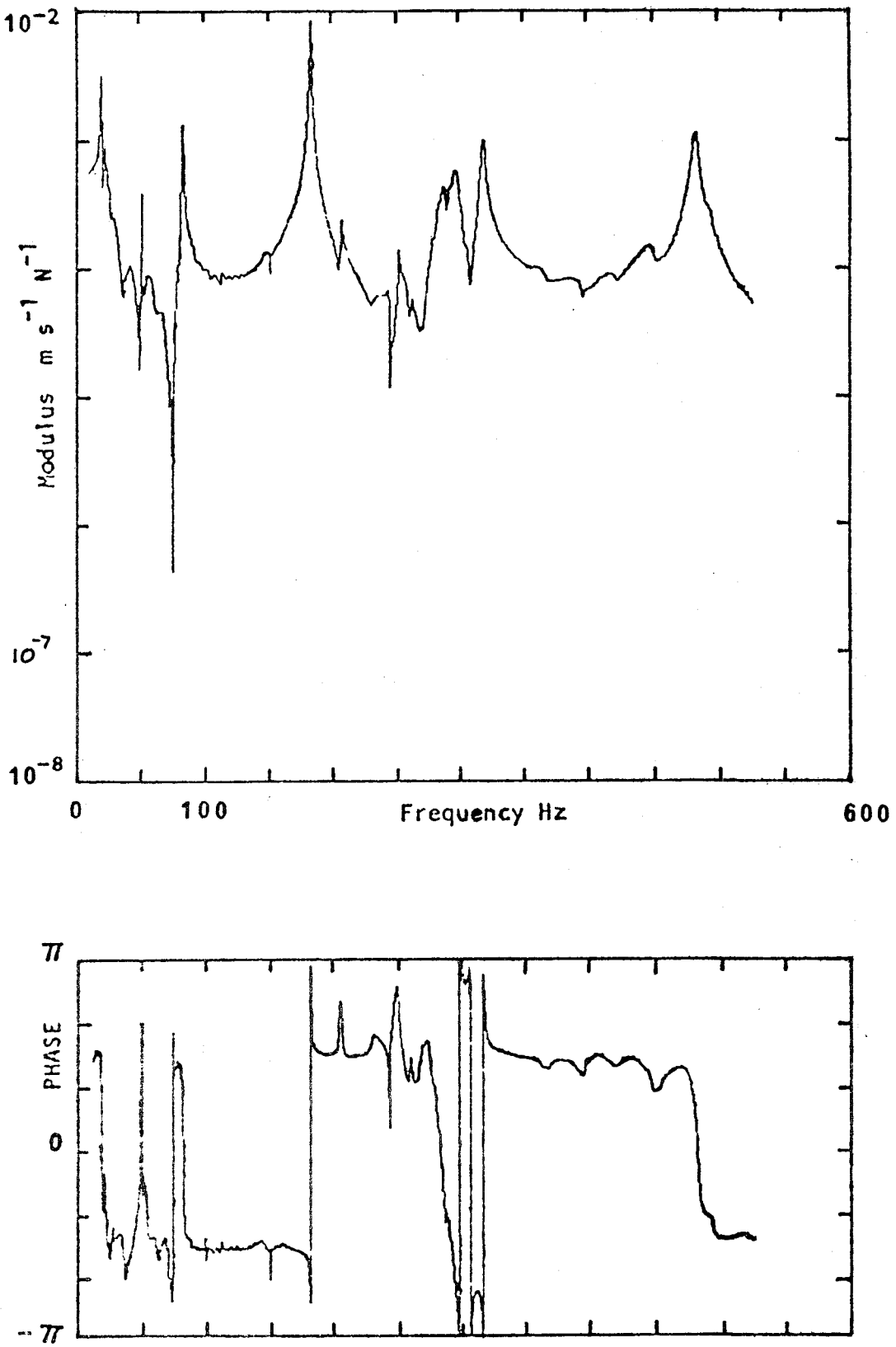

Figure 6.6 **Transfer mobility - measured data**

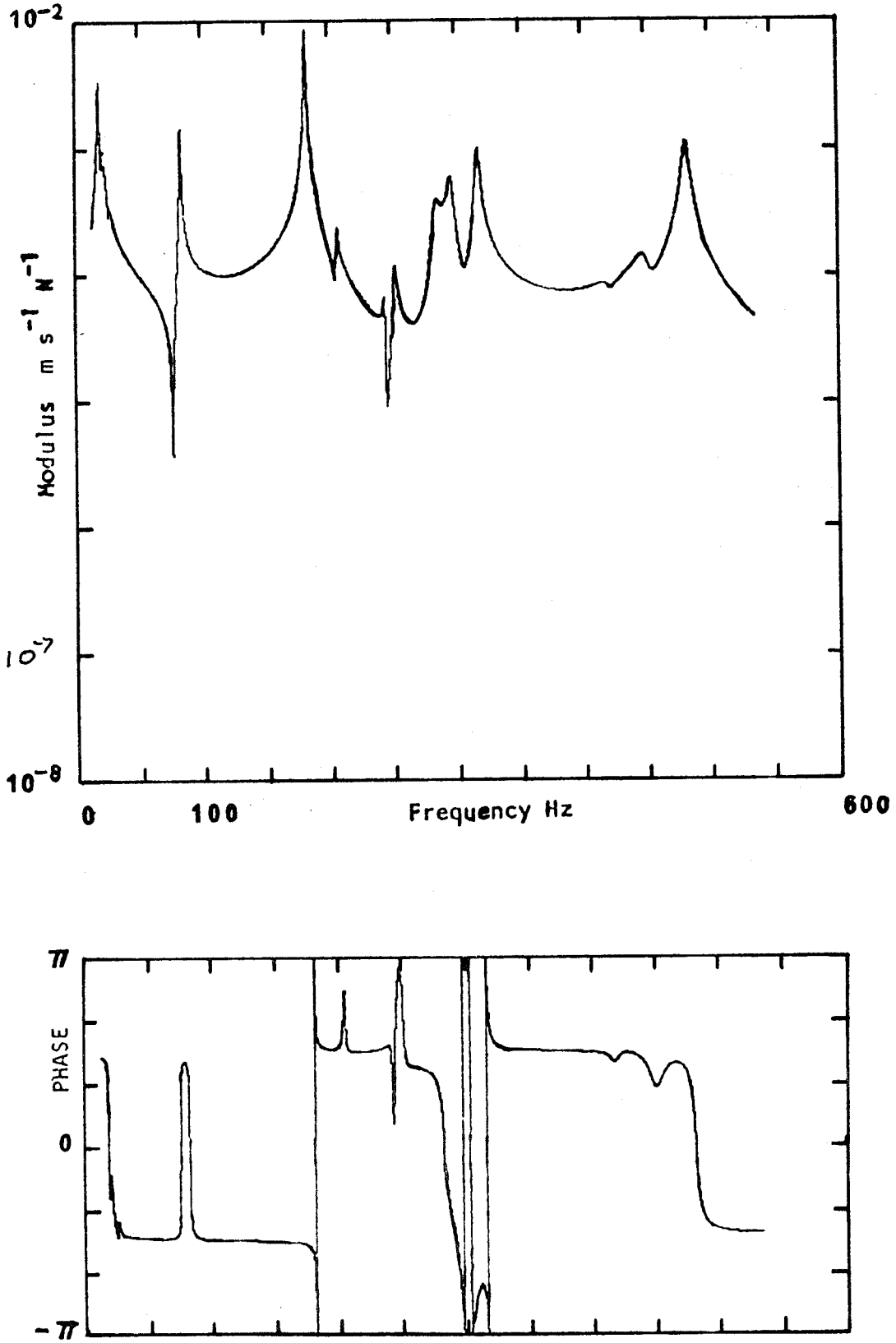

Figure 6.7 Transfer mobility - fitted data

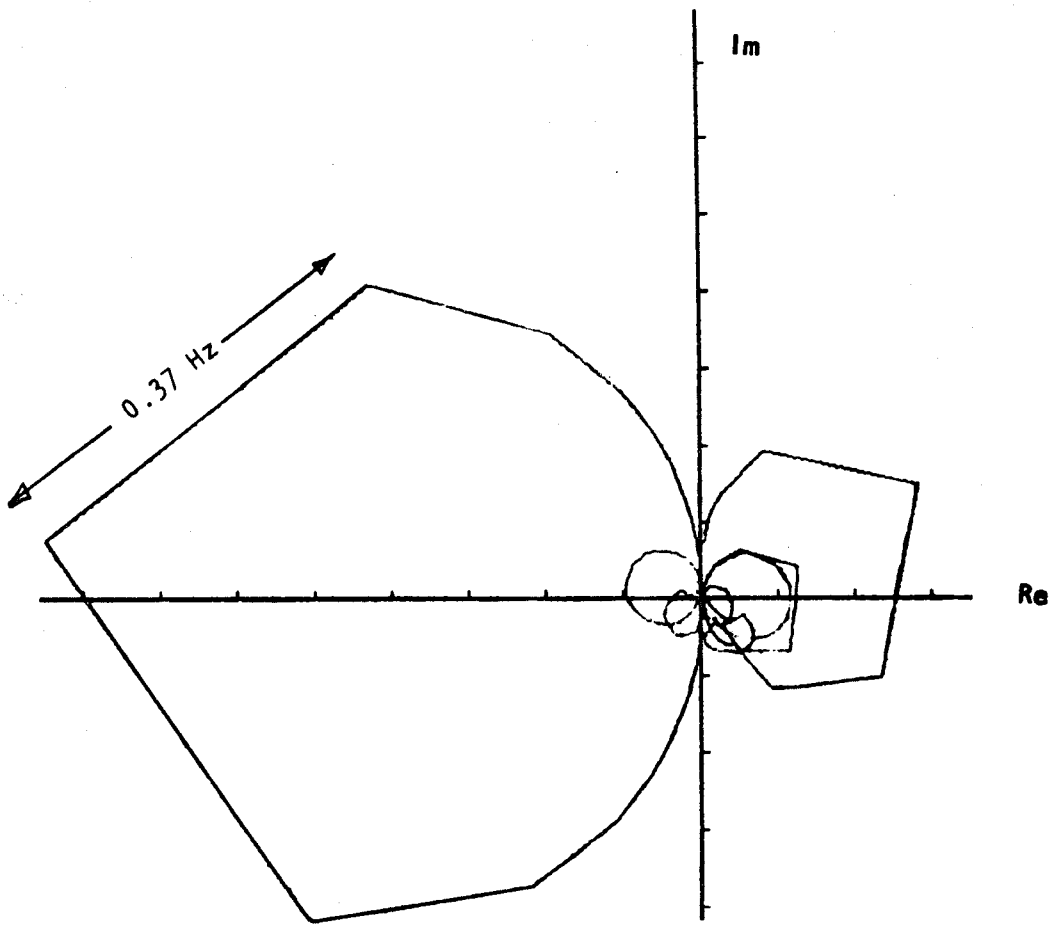

Figure 6.8 Argand diagram of transfer mobility - measured data

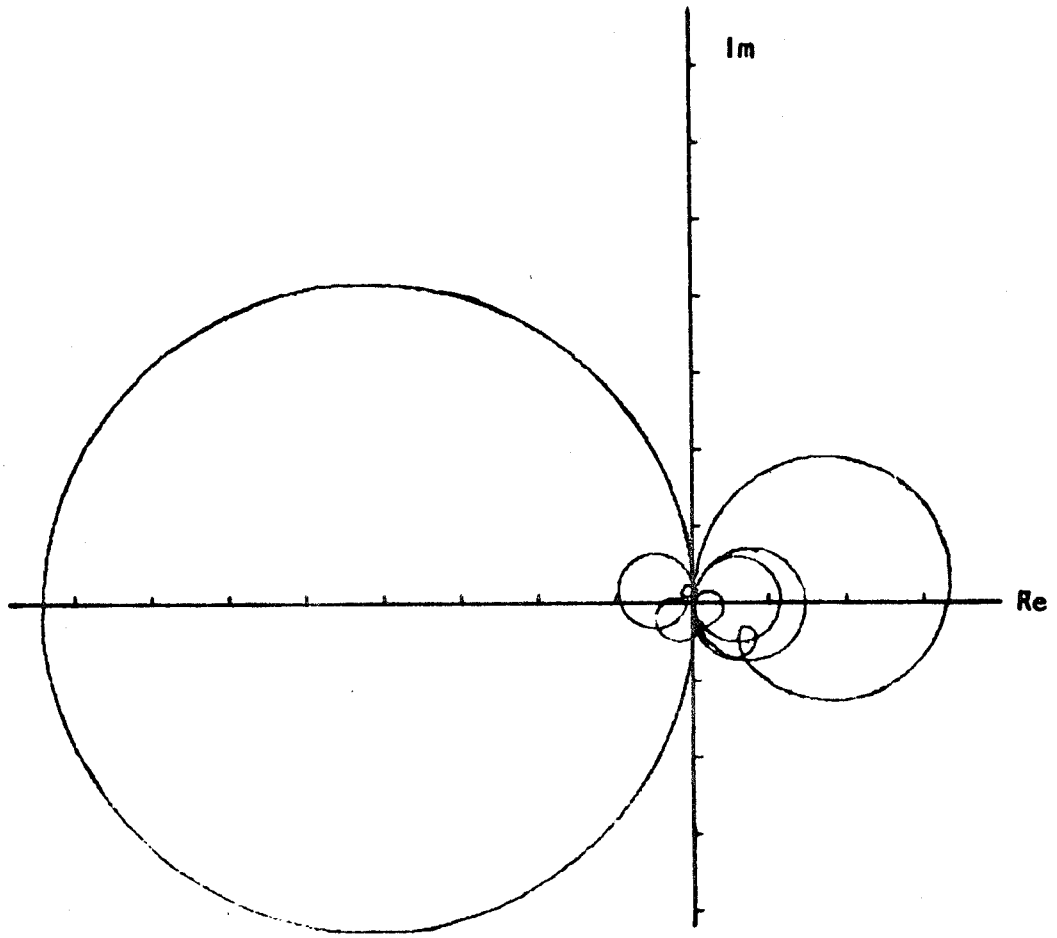

Figure 6.9 Argand diagram of transfer mobility - fitted data

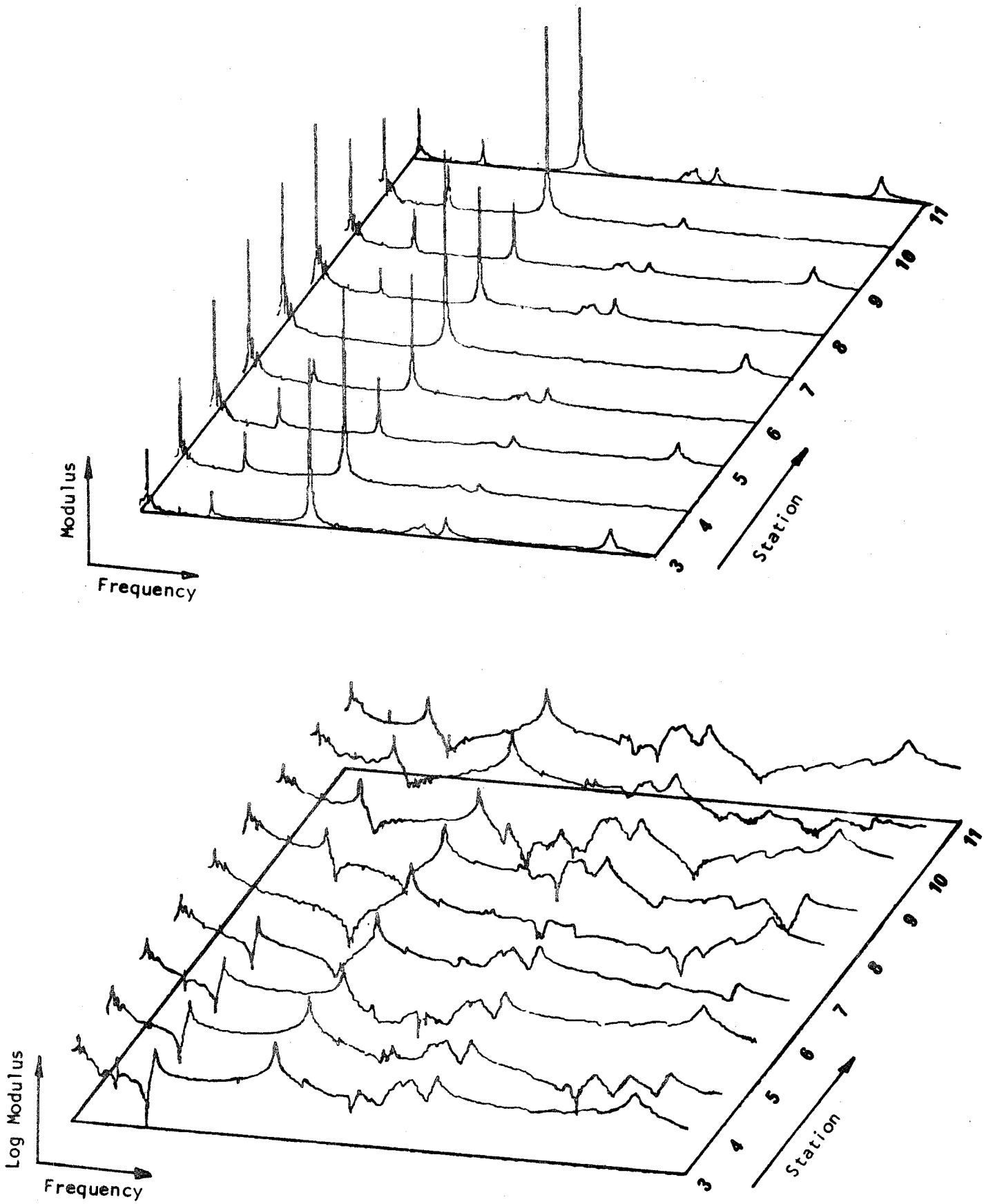

Figure 6.10 Measured mobility data

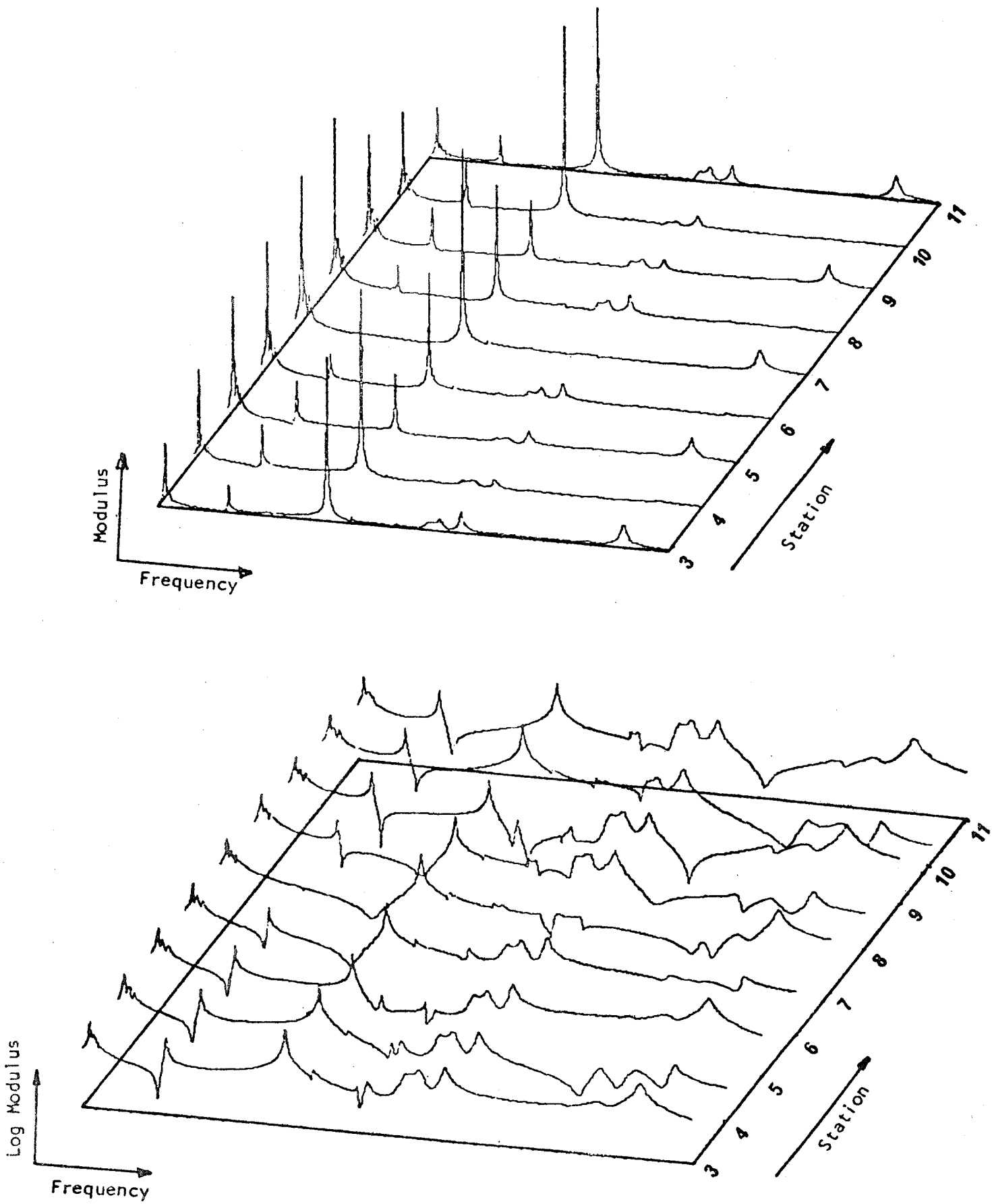

Figure 6.12 Fitted mobility data

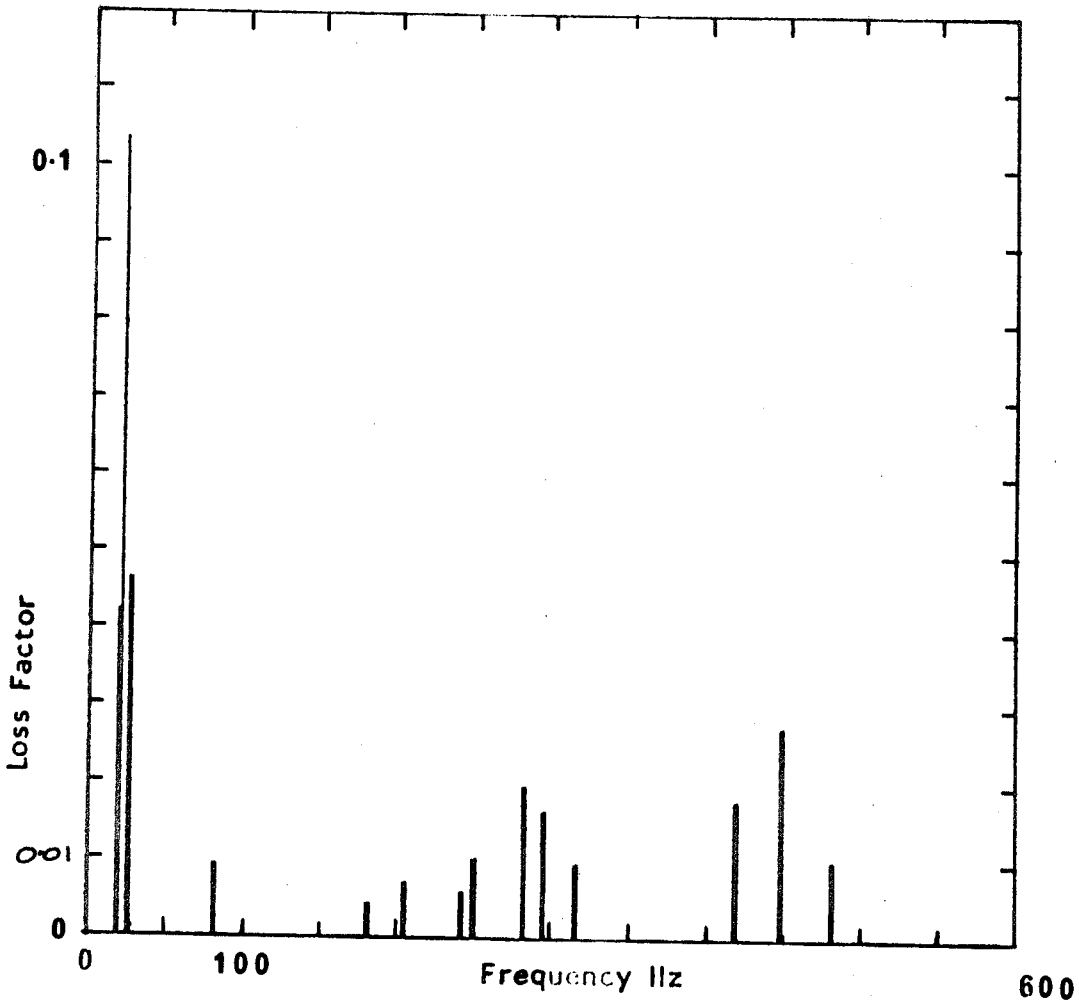

Figure 6.13 Resonsnace frequencies showing loss factor

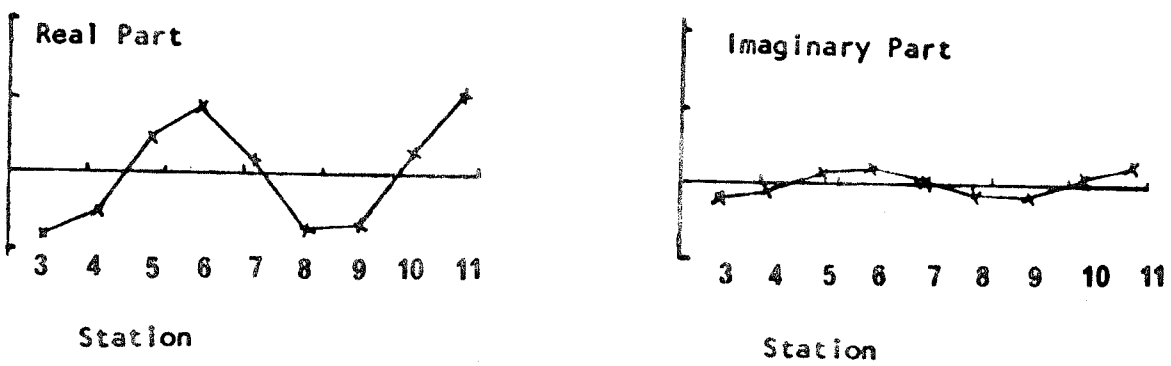

KEY TO COMPLEX MODE SHAPES

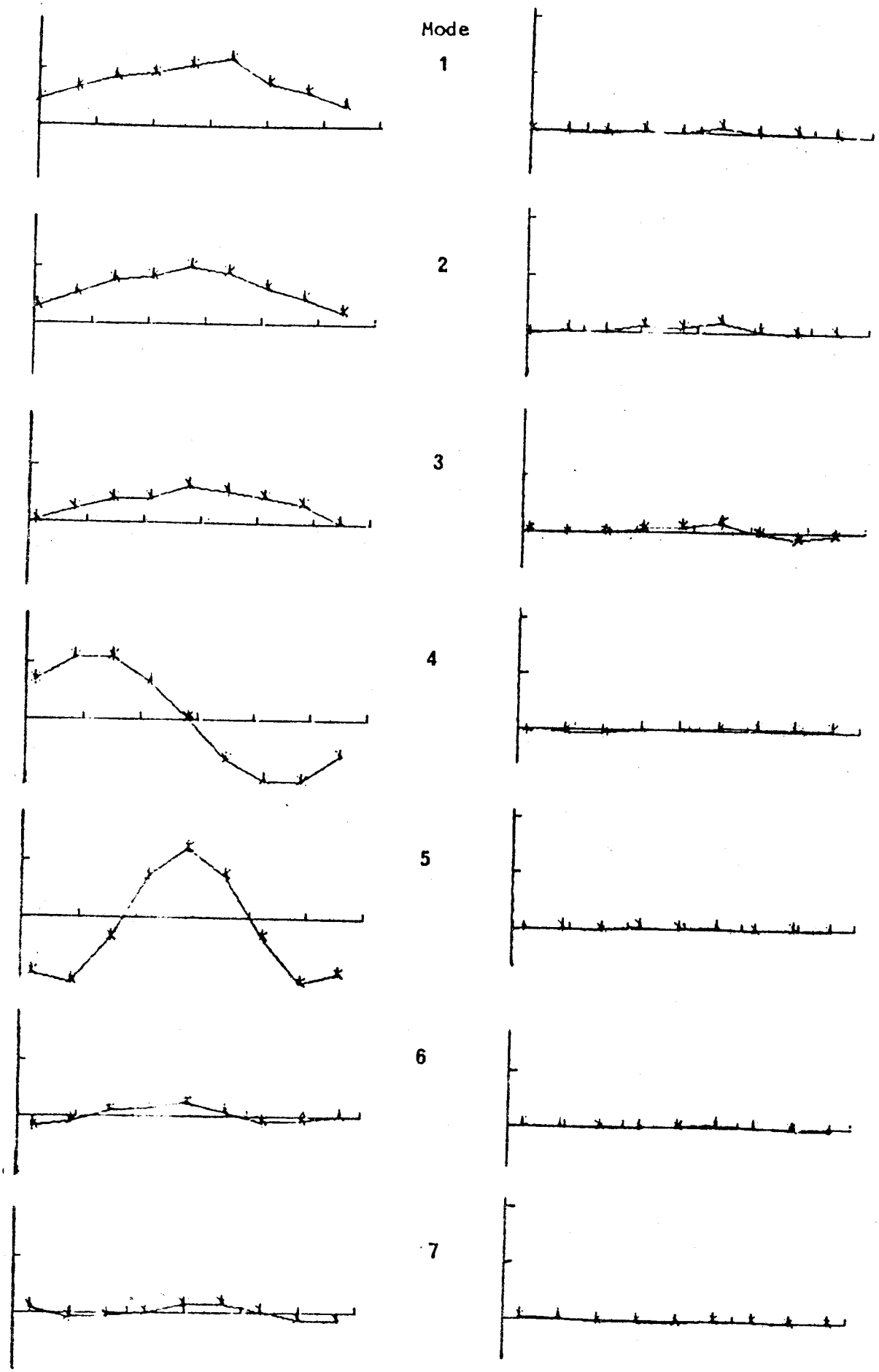

Figure 6.14(a) Complex mode shapes (for key see under Figure 6.13)

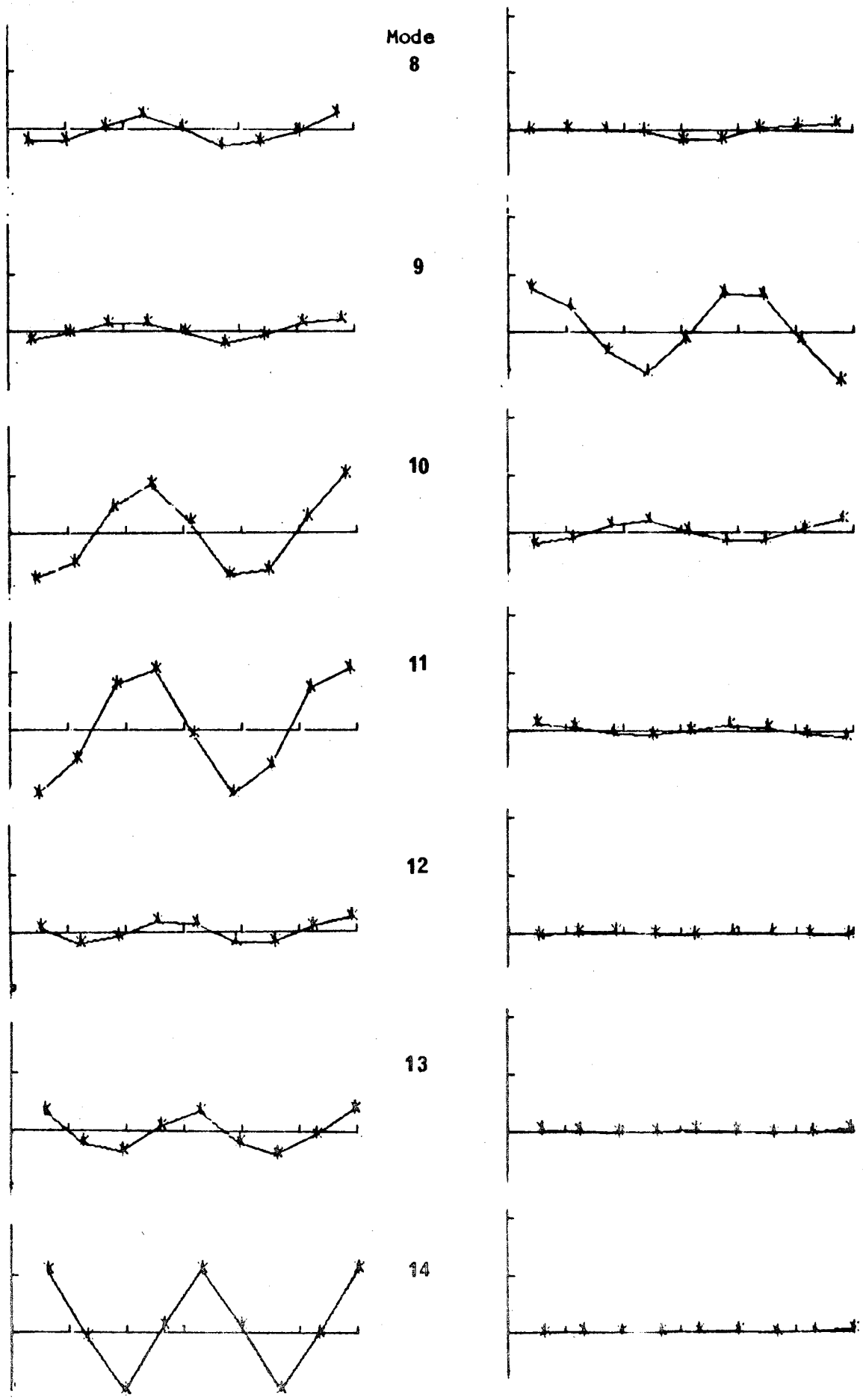

Figure 6.14(b) Complex mode shapes (for key see under Figure 6.13)

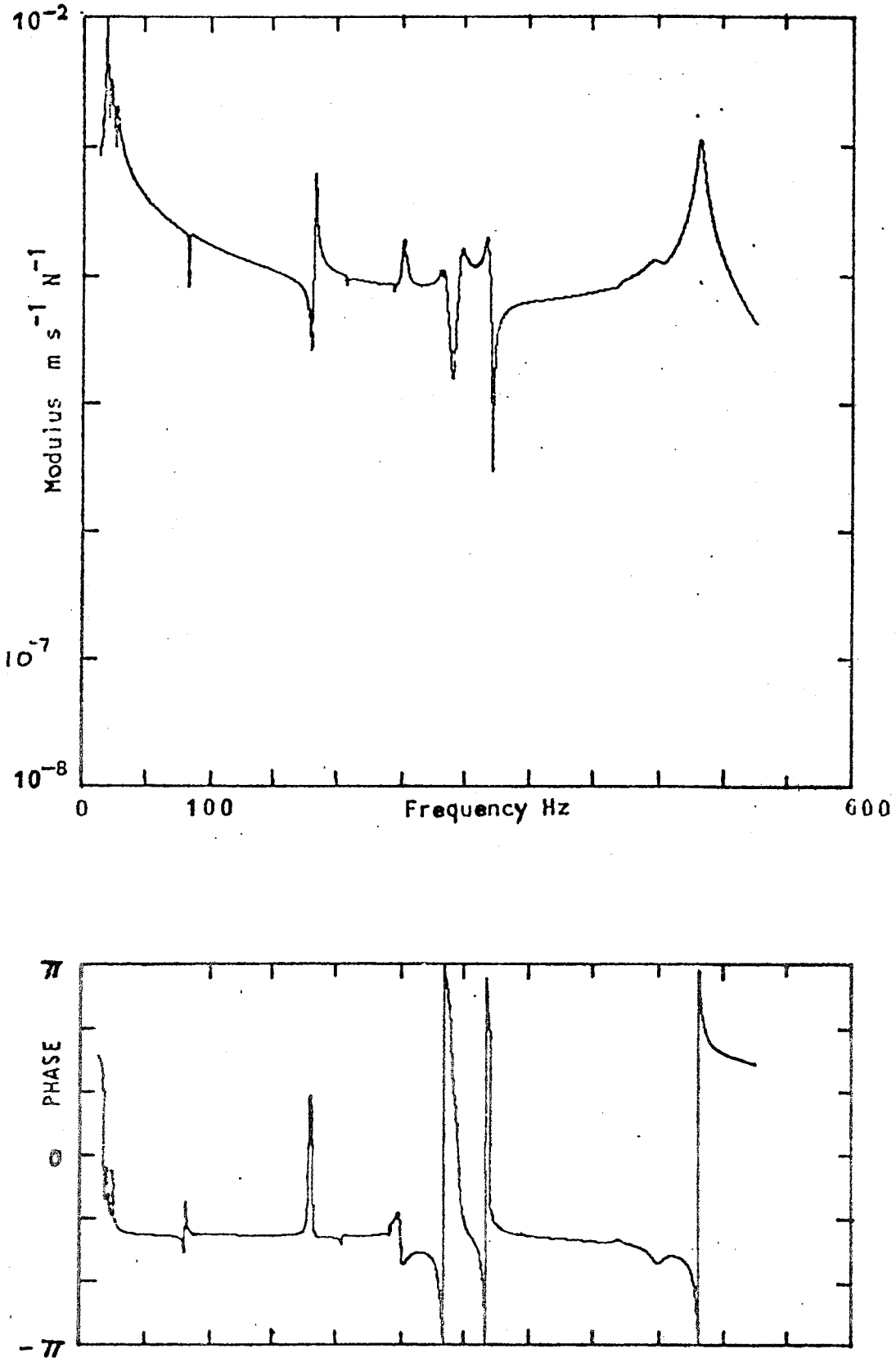

Figure 6.15 Mobility predicted from model.

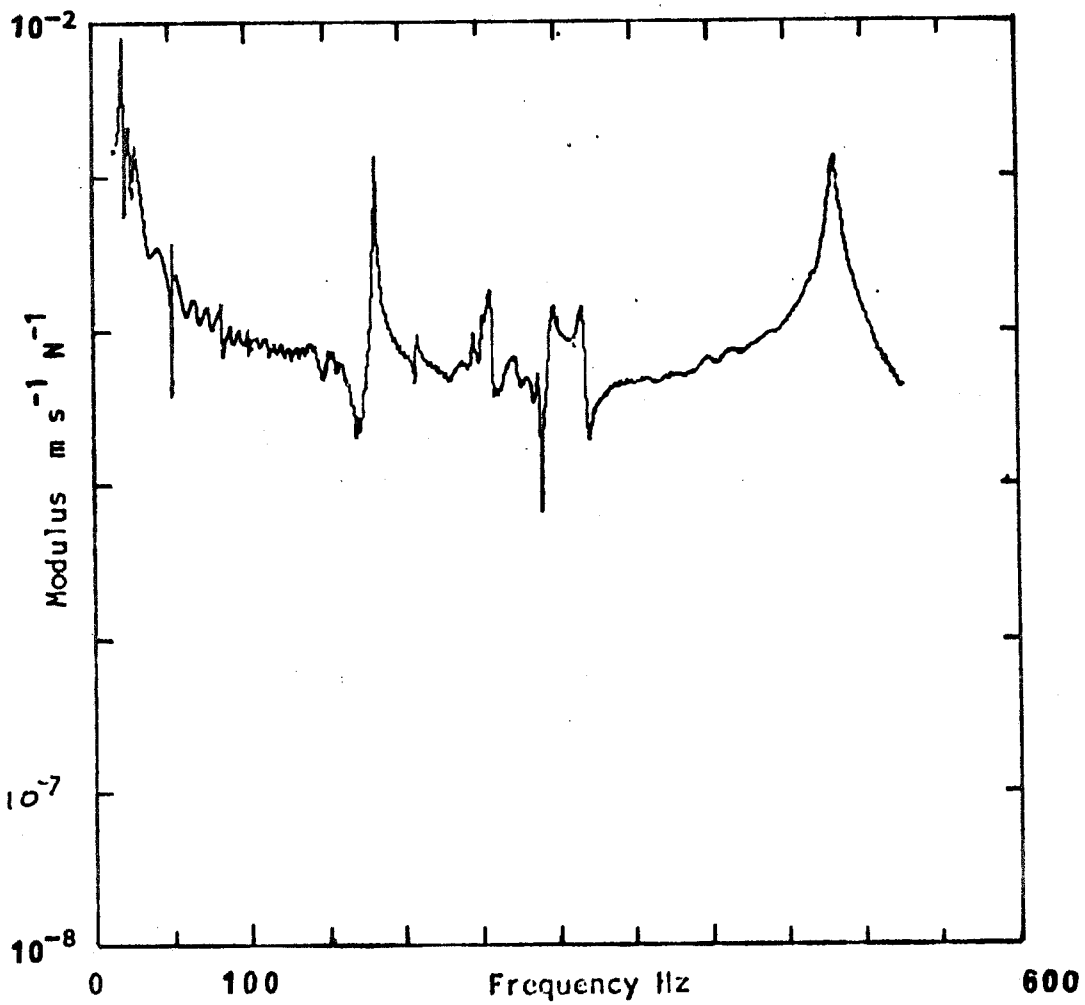

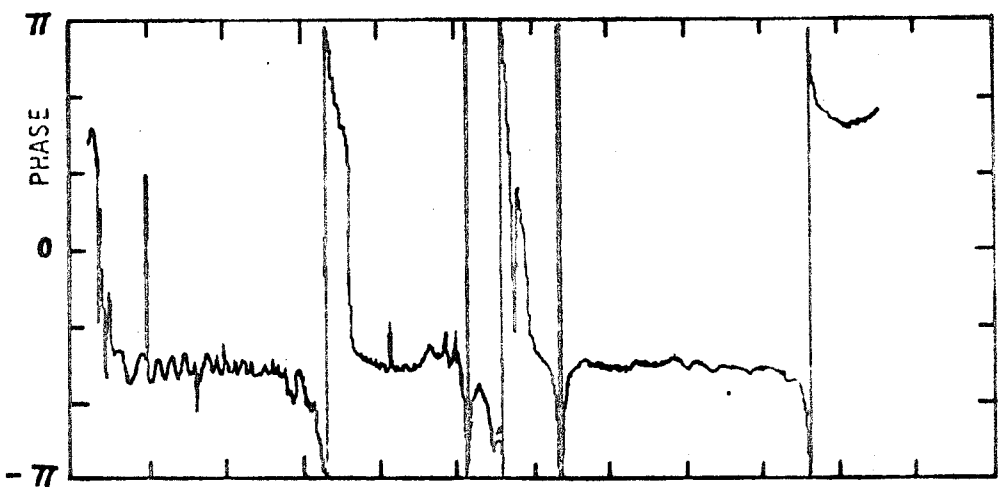

Figure 6.16 Measured mobility

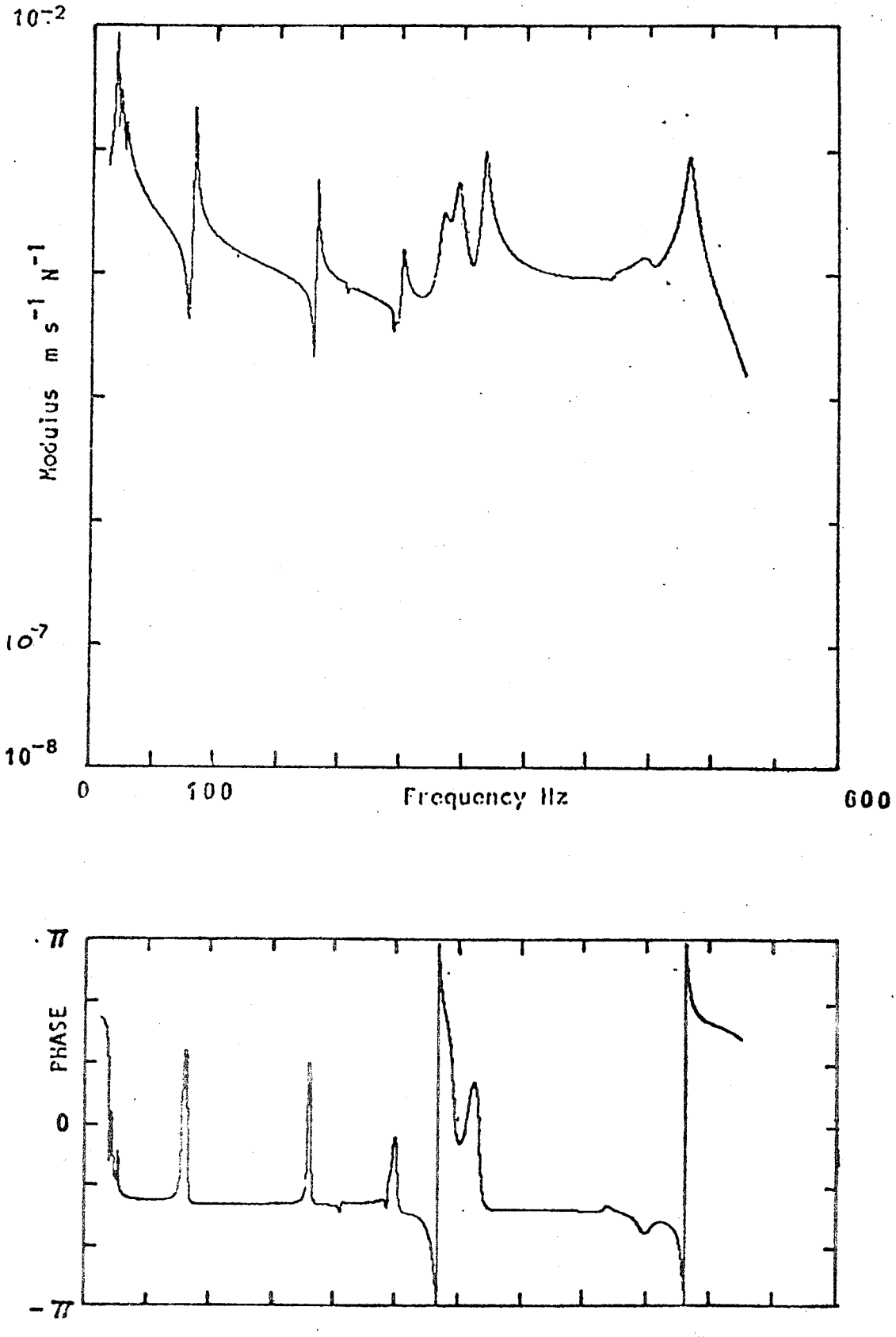

Figure 6.17 Mobility predicted from model.

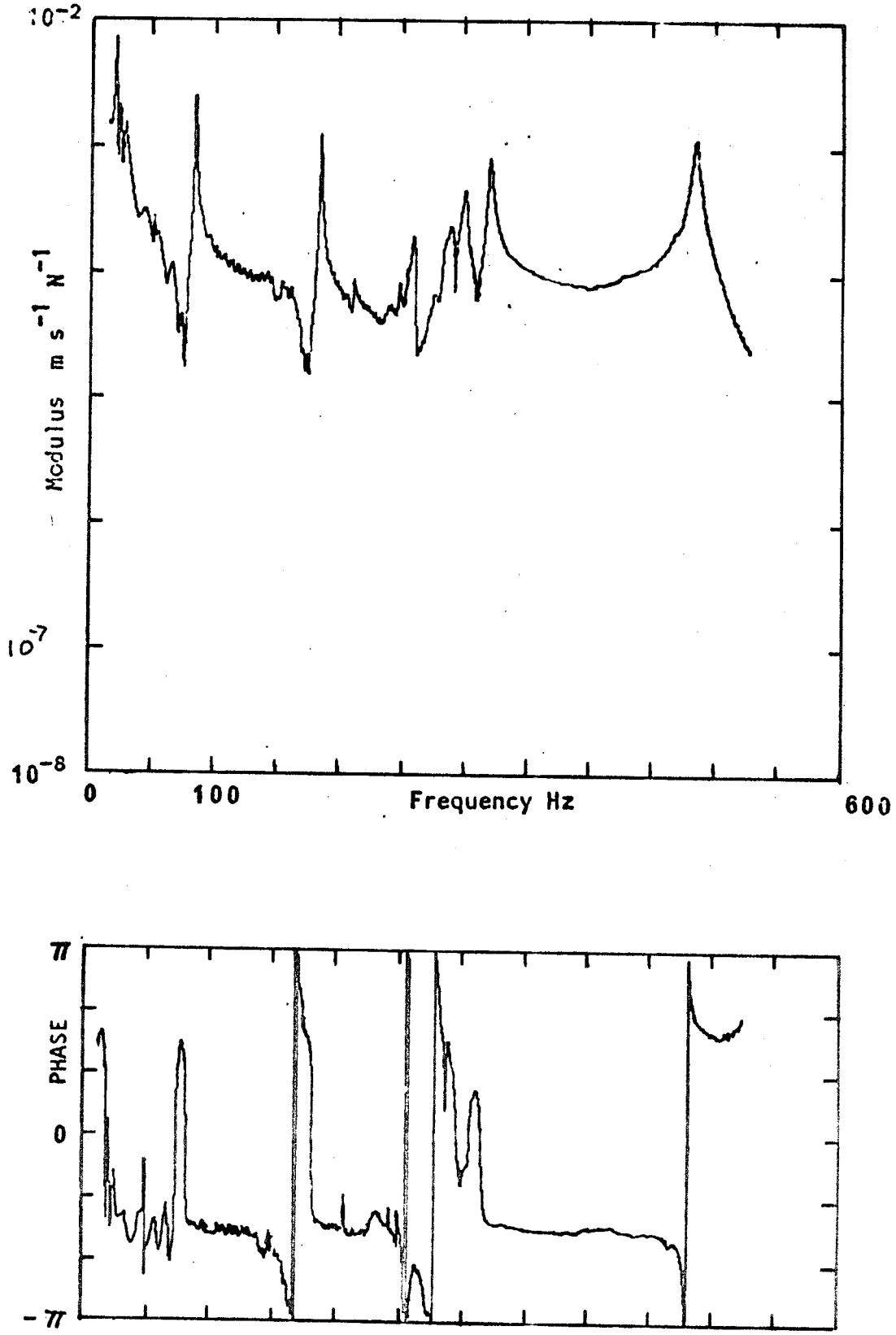

Figure 6.18 Measured mobility

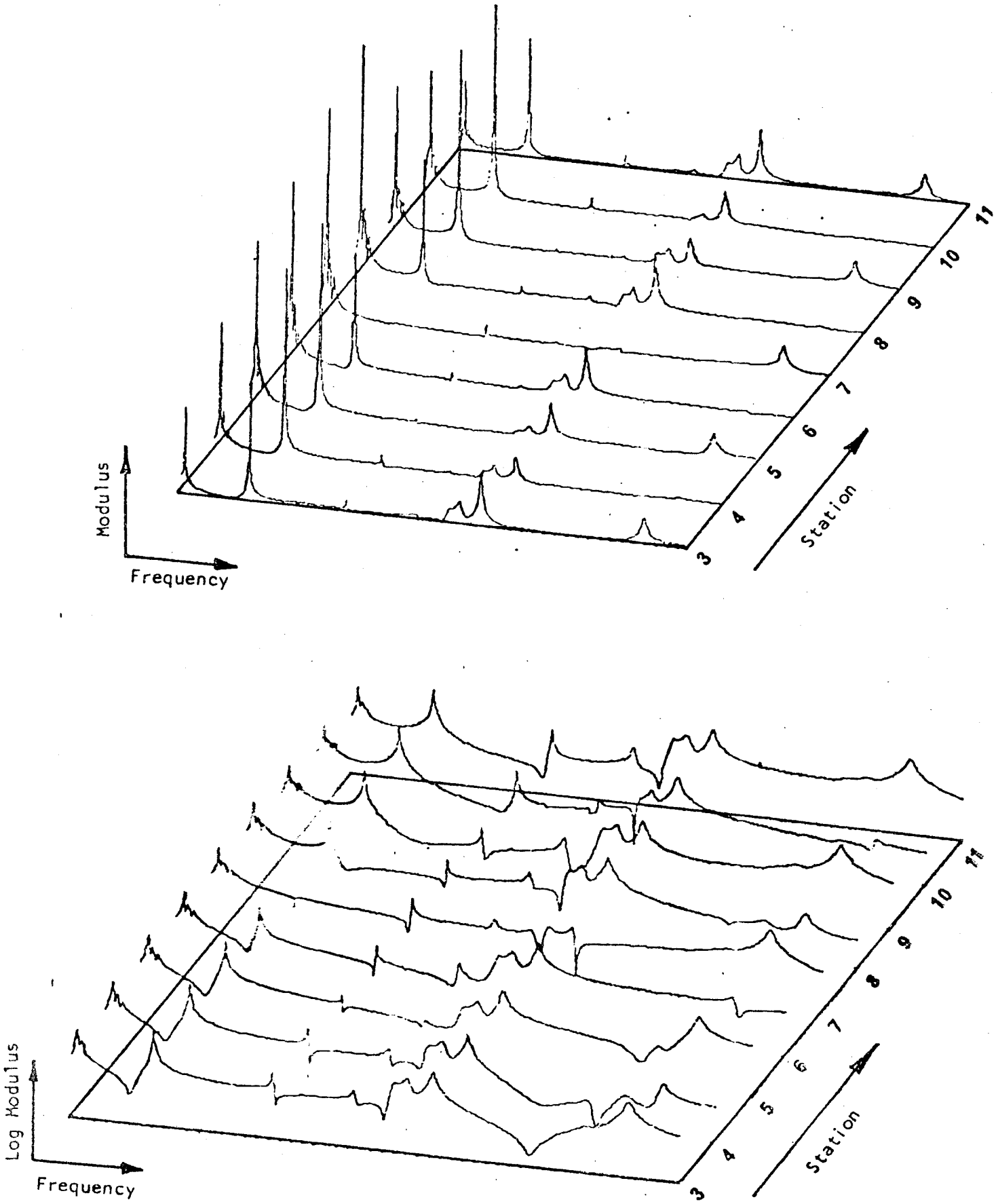

Figure 6.19 Mobility data predicted from model

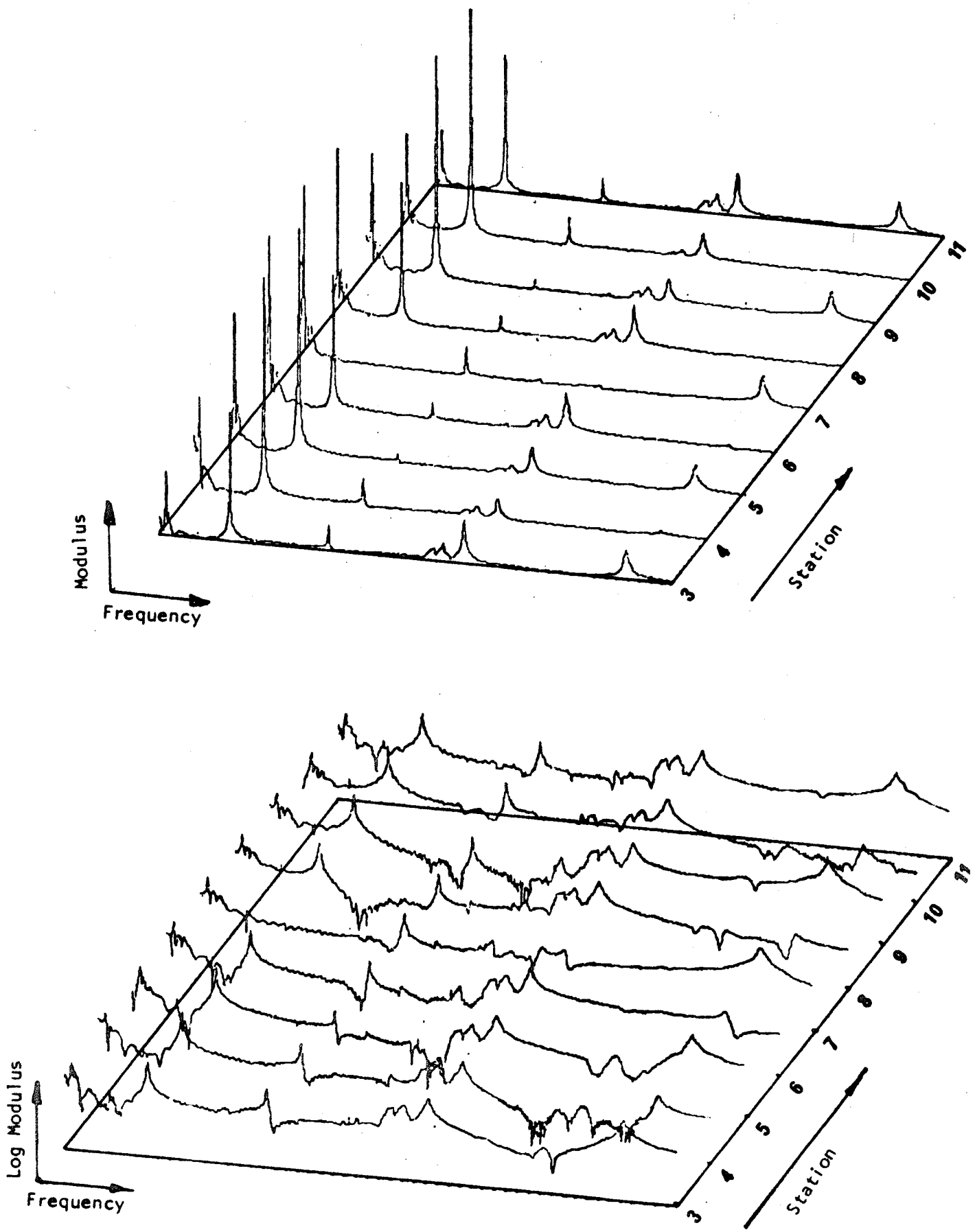

Figure 6.20 Measured mobility data

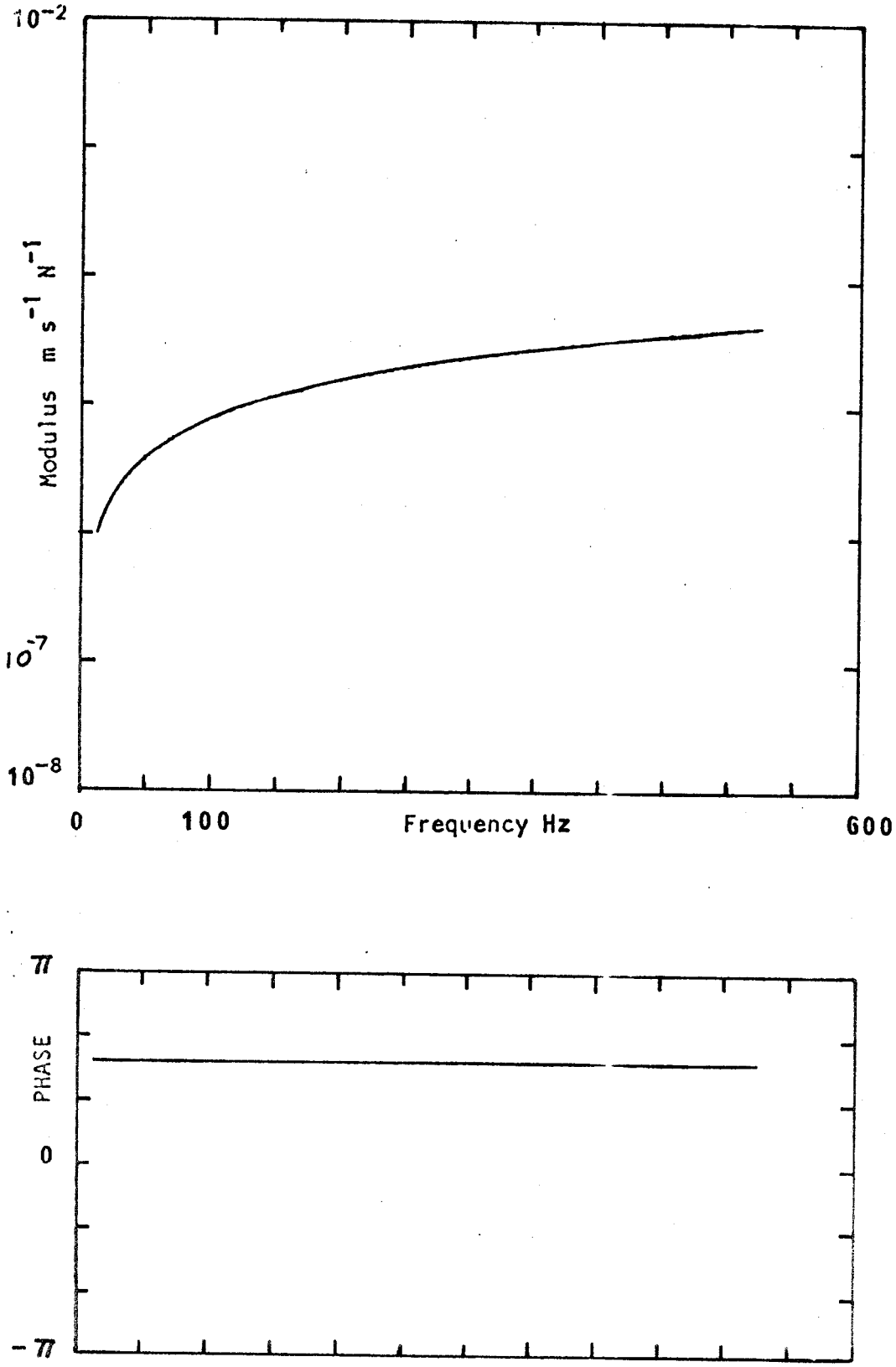

Figure 6.21 Contribution of stiffness remainder to point mobility.

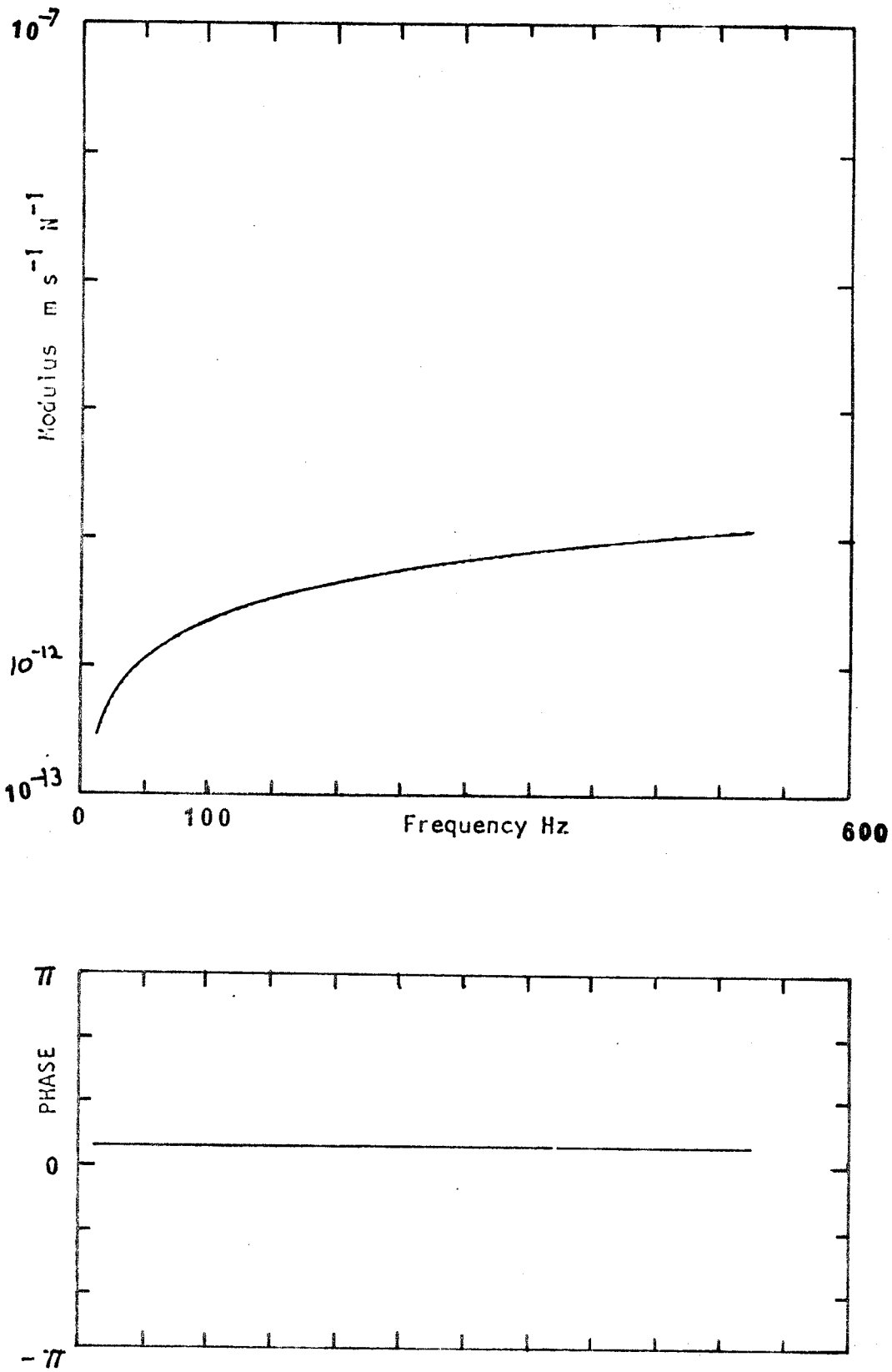

Figure 6.22 Contribution of stiffness remainder to transfer mobility

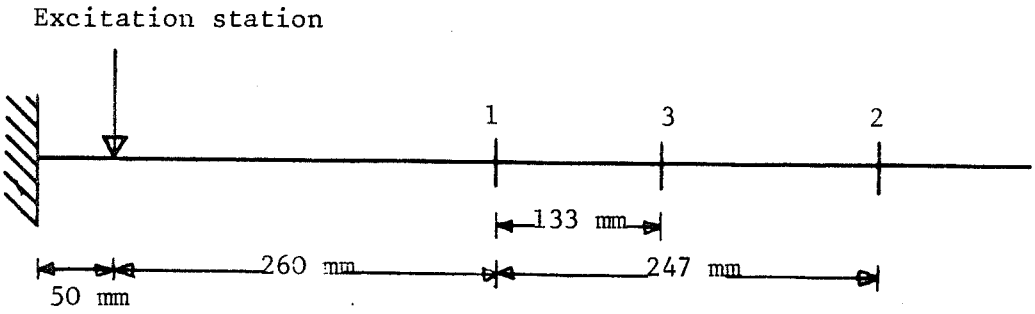

1,2 Measurement stations
3 Station for which response was predicted

Figure 6.23 Aluminium beam used to test the method given in section 6.7.

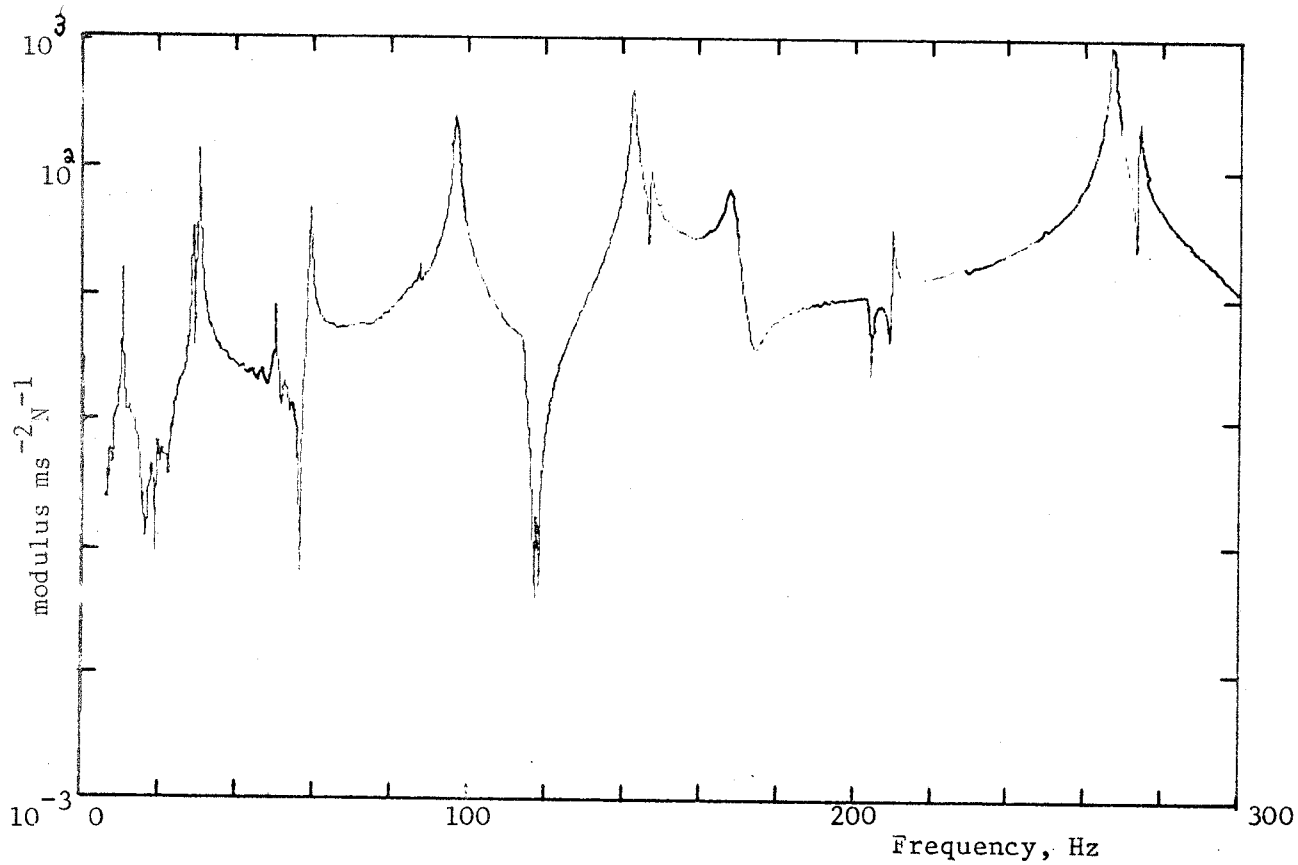

Figure 6.24 Measured transfer inertance at station 1.

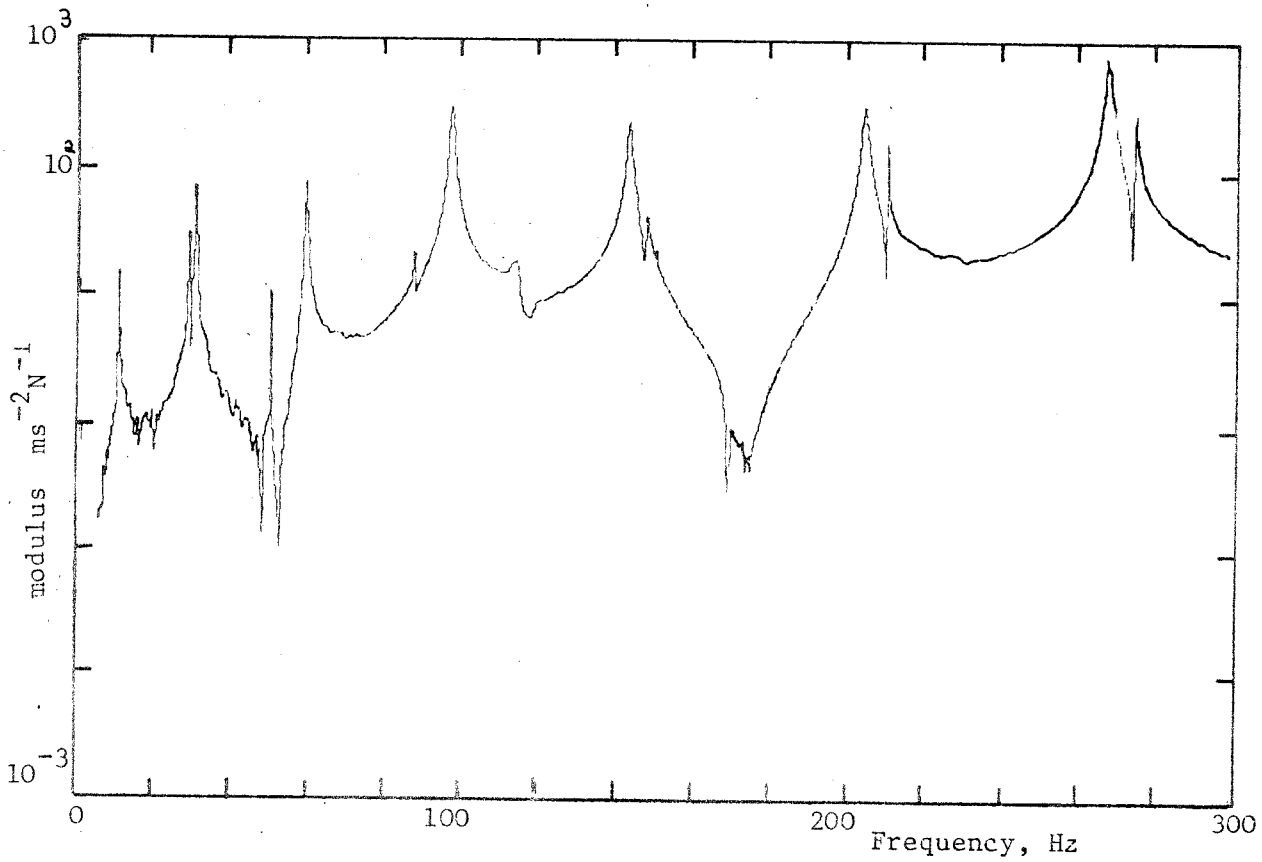

Figure 6.25 Measured transfer inertance at Station 2.

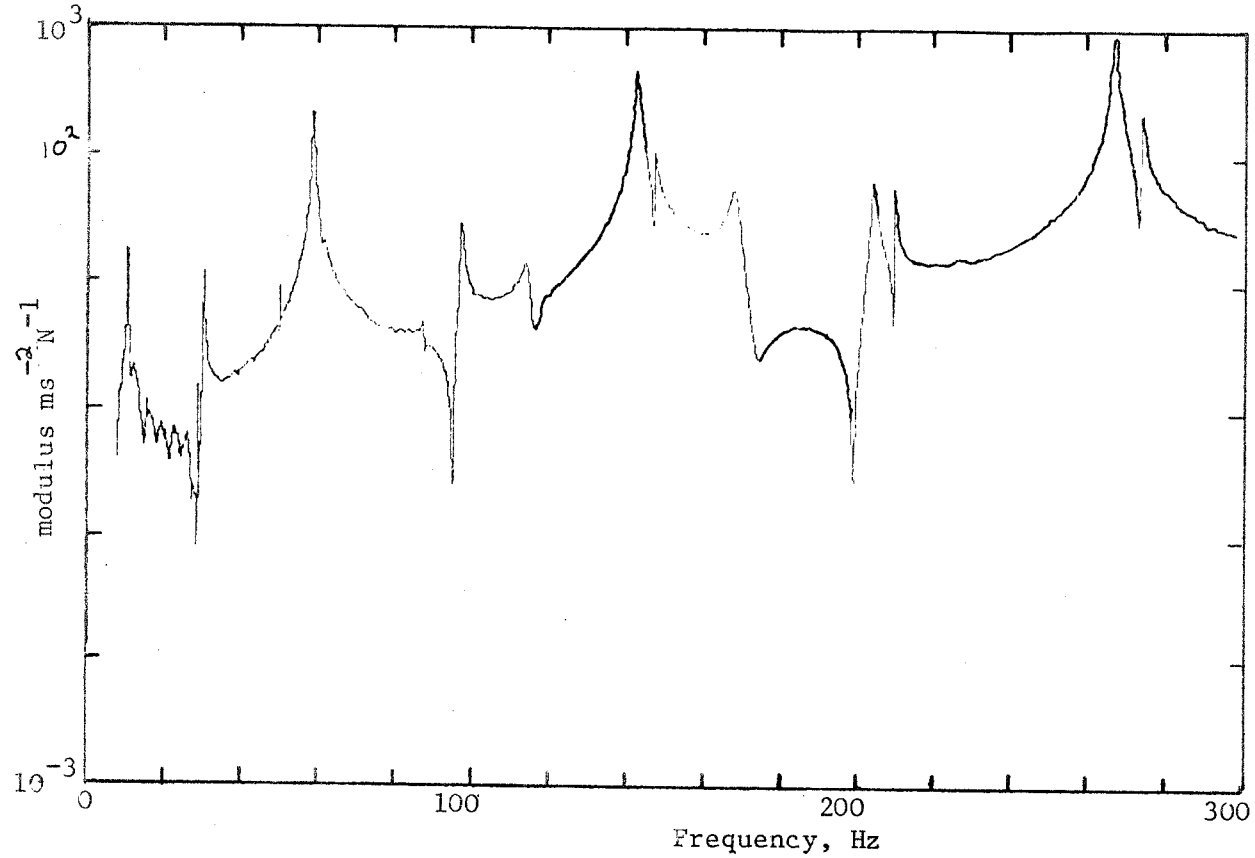

Figure 6.26 Predicted transfer inertance at station 3.

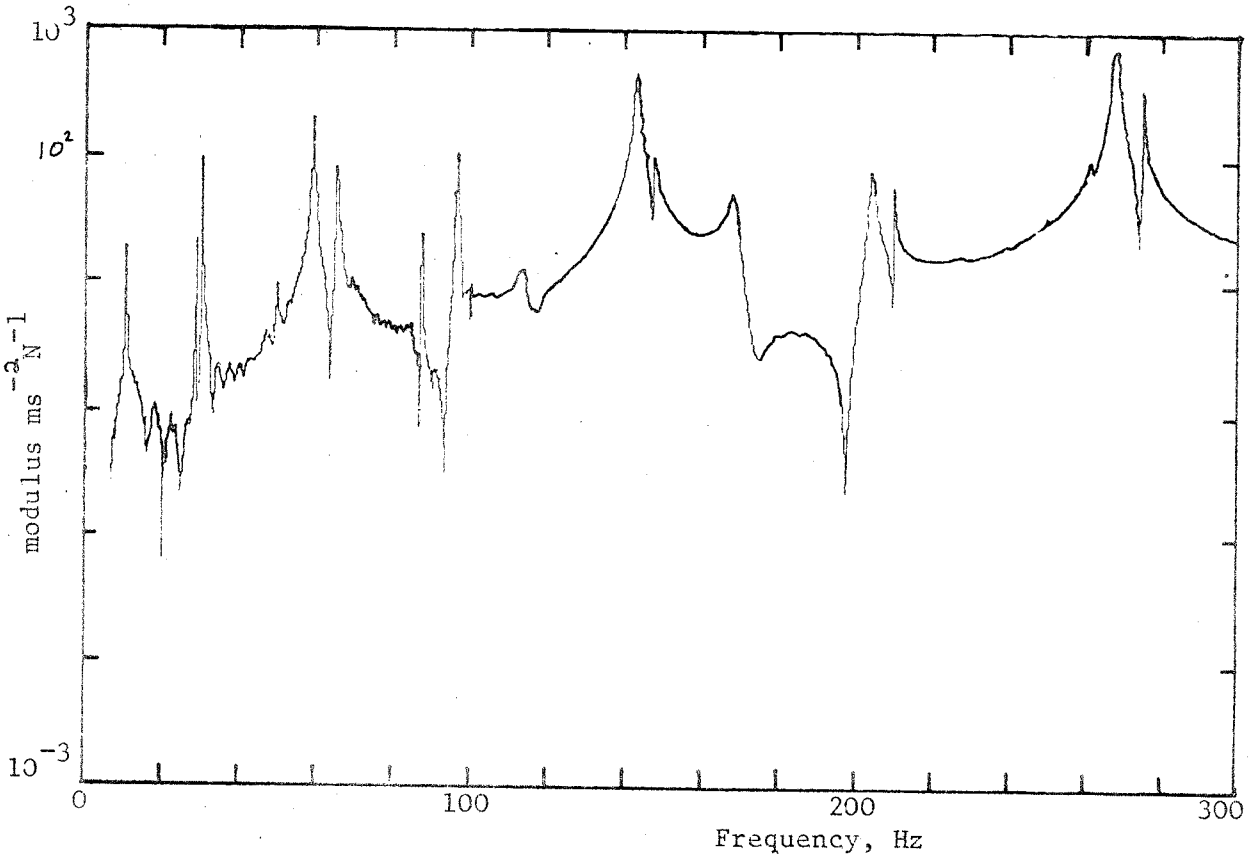

Figure 6.27 Measured transfer inertance at station 3.

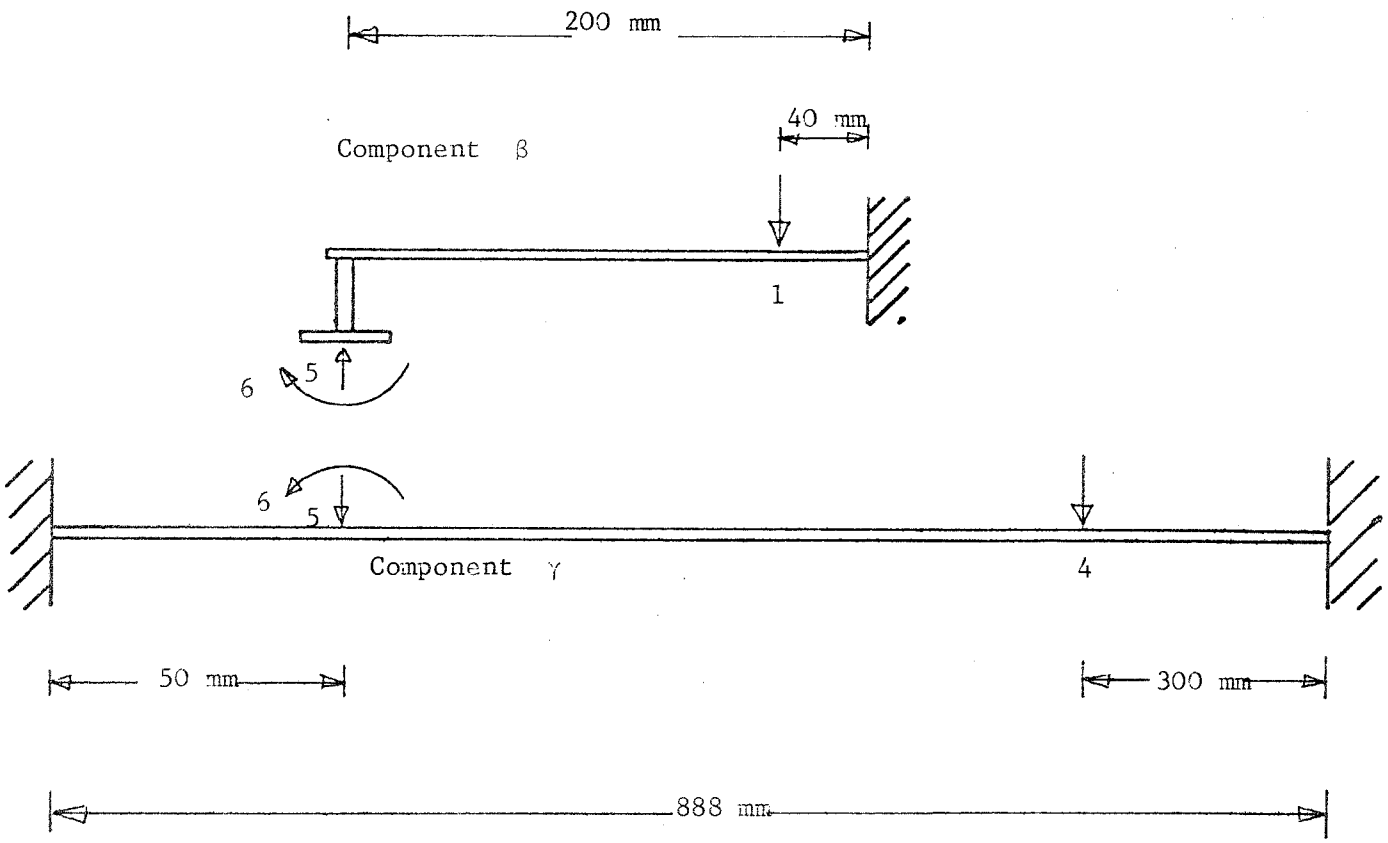

Figure 7.1 The structure, consisting of two components which are to be joined at coordinates 5 and 6, used to examine system coupling methods.

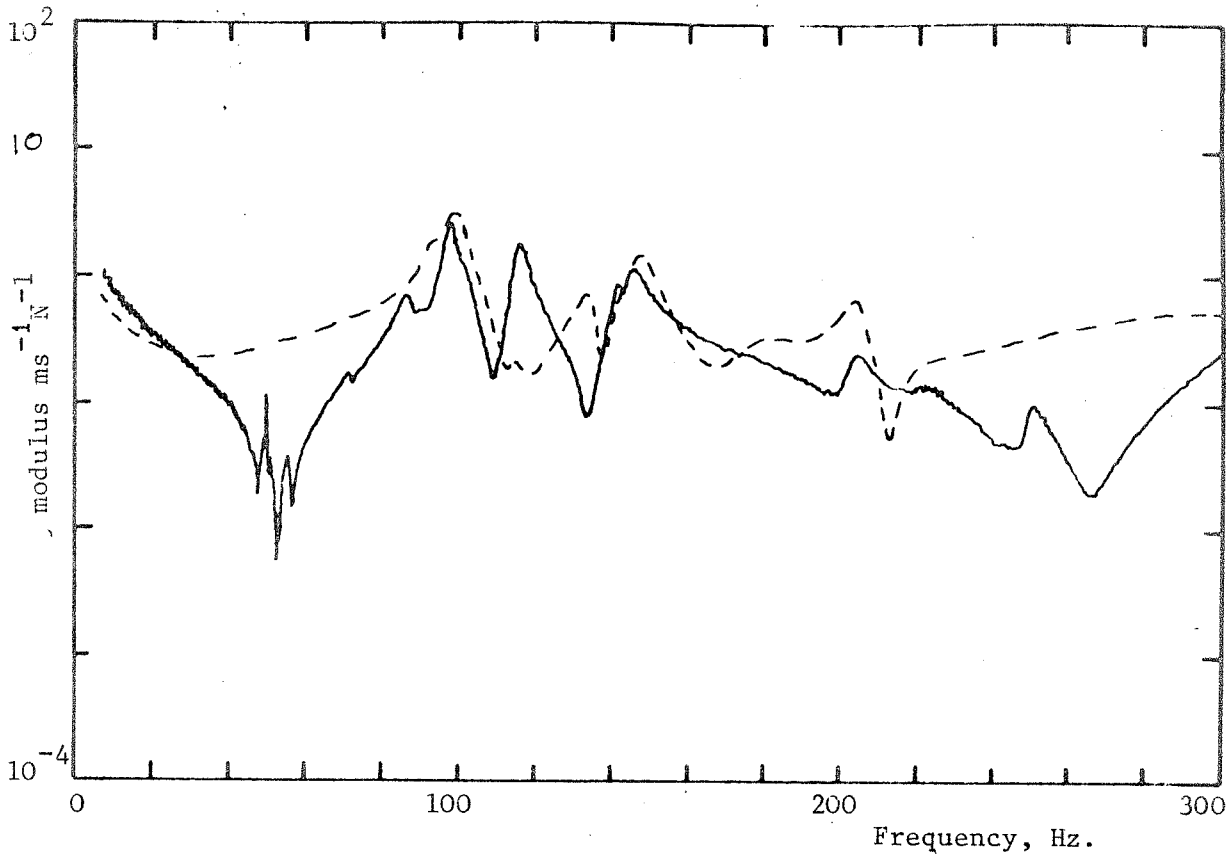

Figure 7.2 Predicted (-----) and measured (_____) point mobility of station 1.

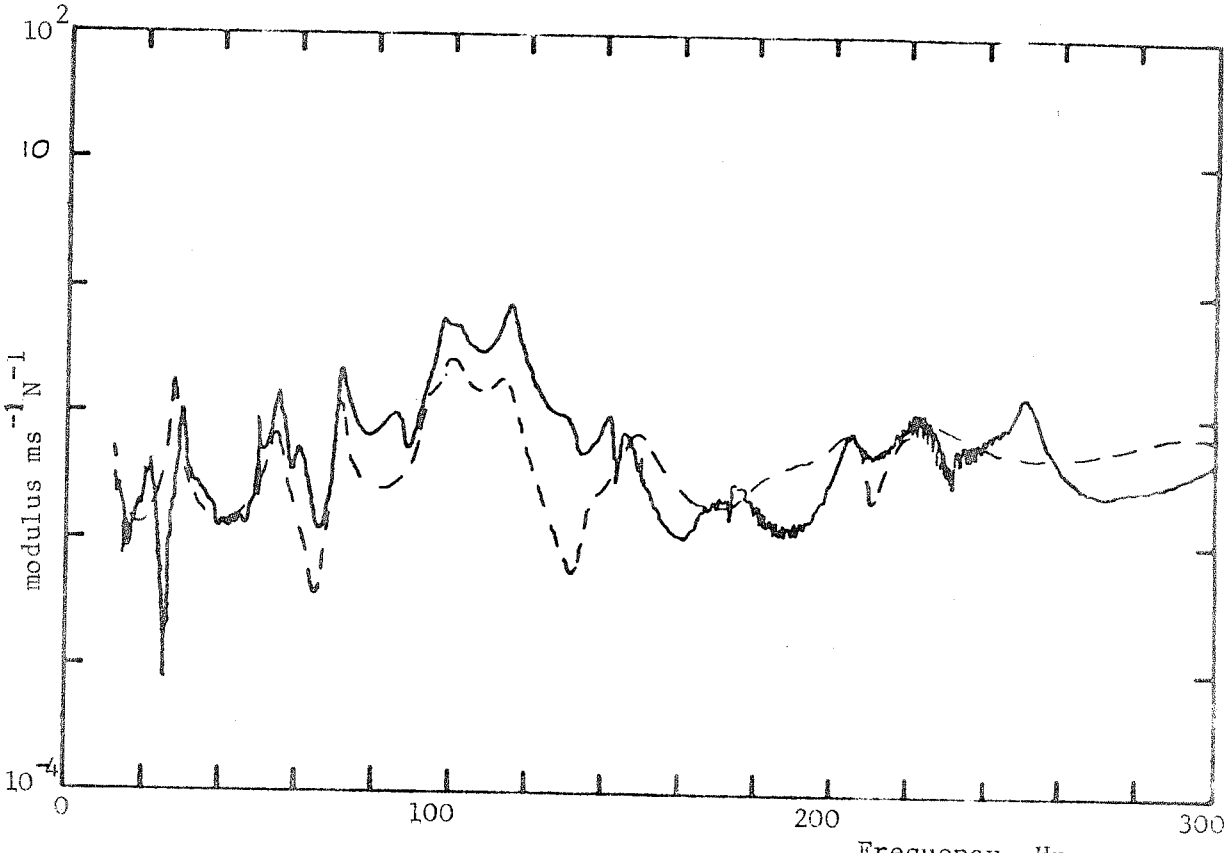

Figure 7.3 Predicted (----) and measured (_____) transfer mobility of station 4.

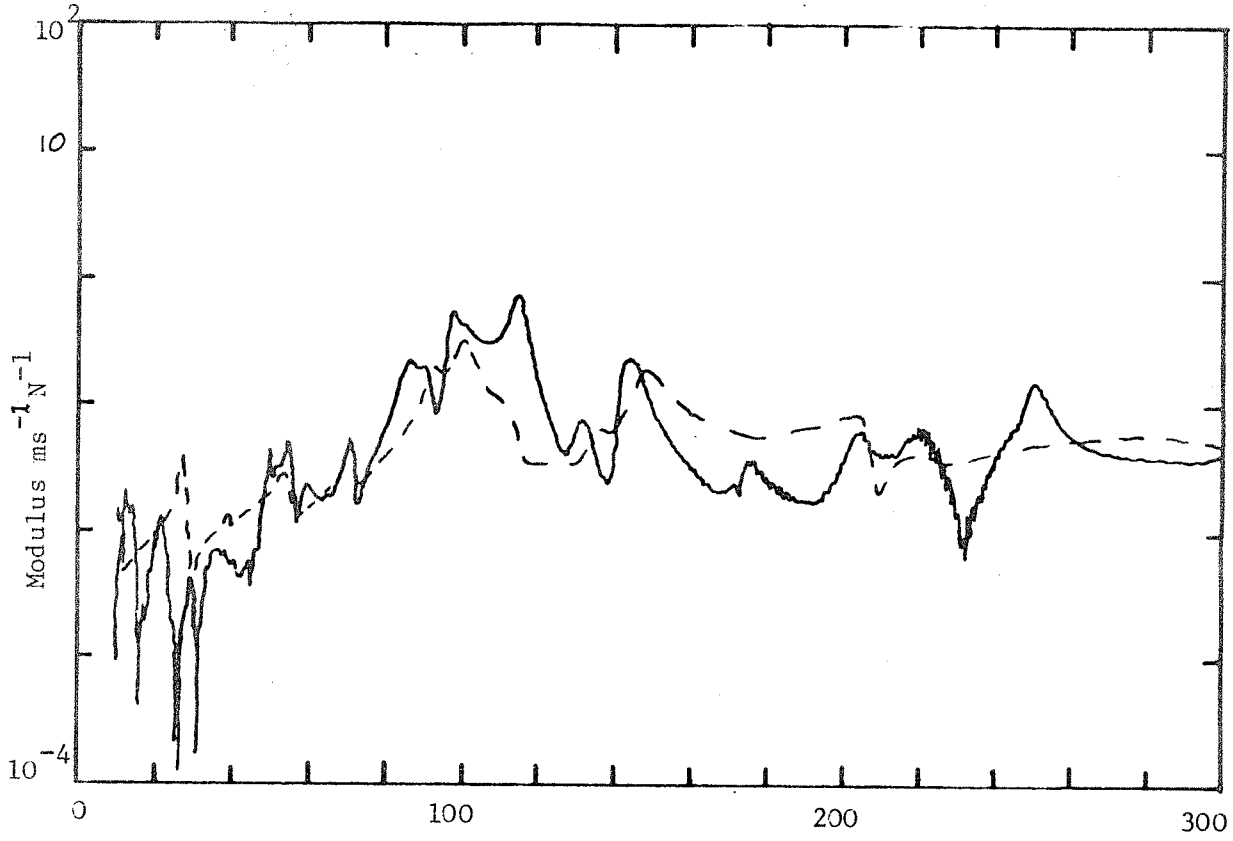

Figure 7.4 Predicted (----) and measured (_____) transfer mobility of station 5.

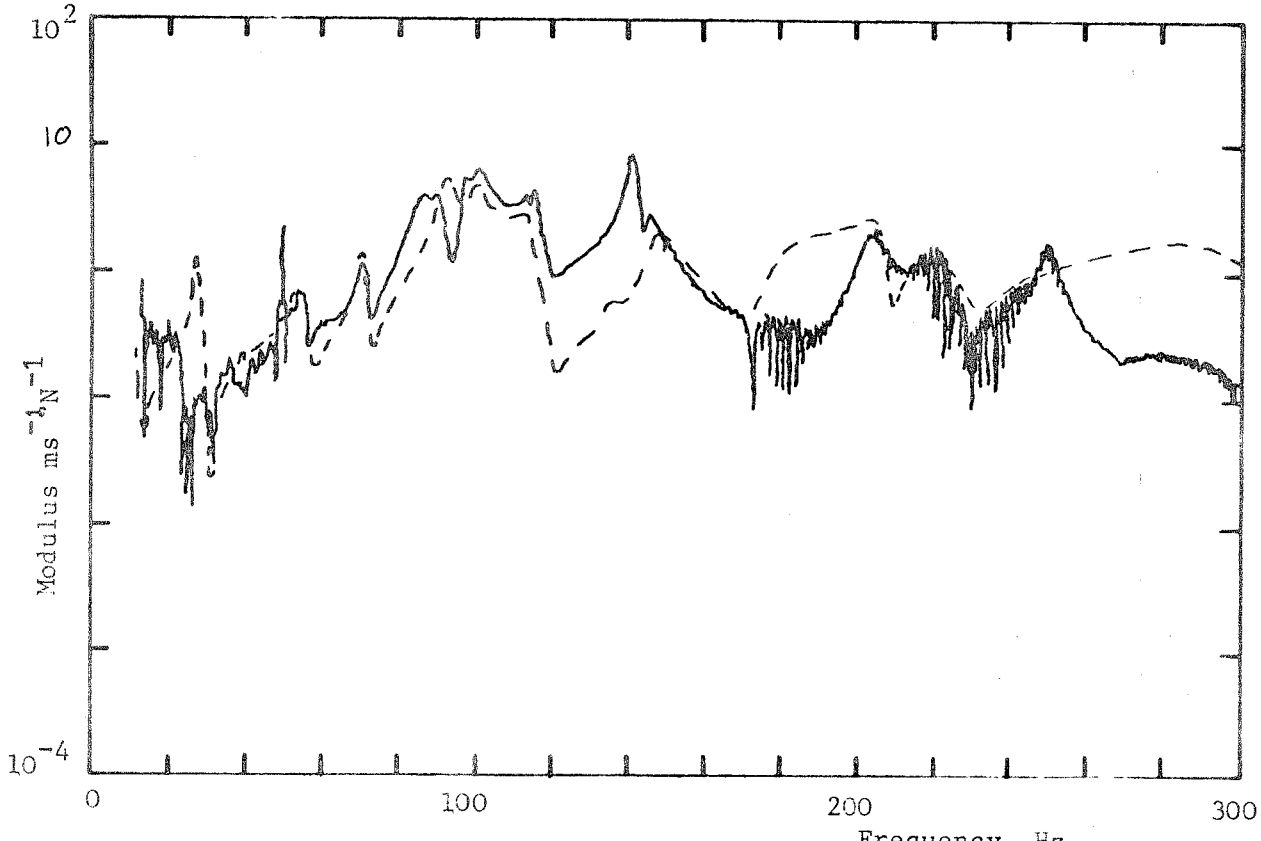

Figure 7.5 Predicted (---) and measured (_____) transfer mobility of station 6.

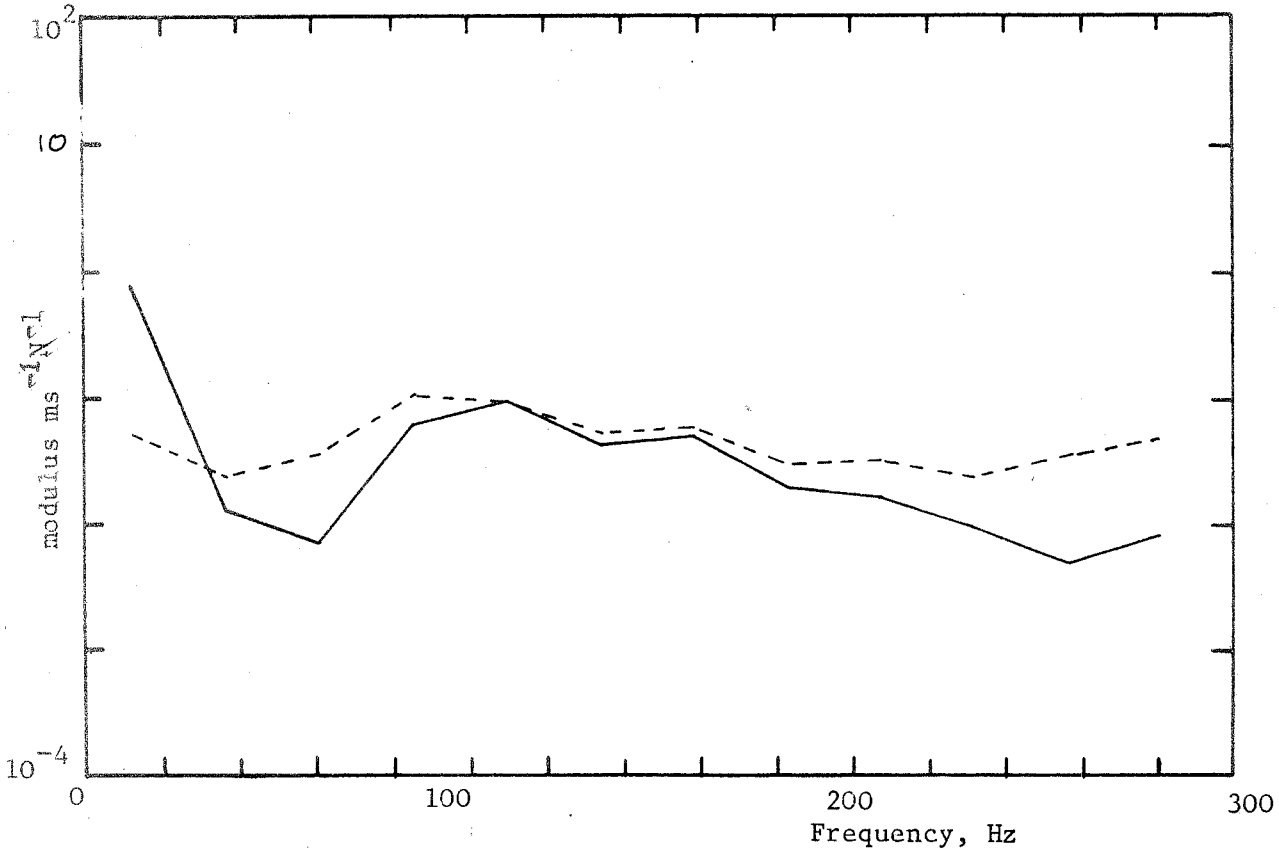

Figure 7.6 Predicted (----) and measured (_____) point mobility of station 1, with responses averaged.

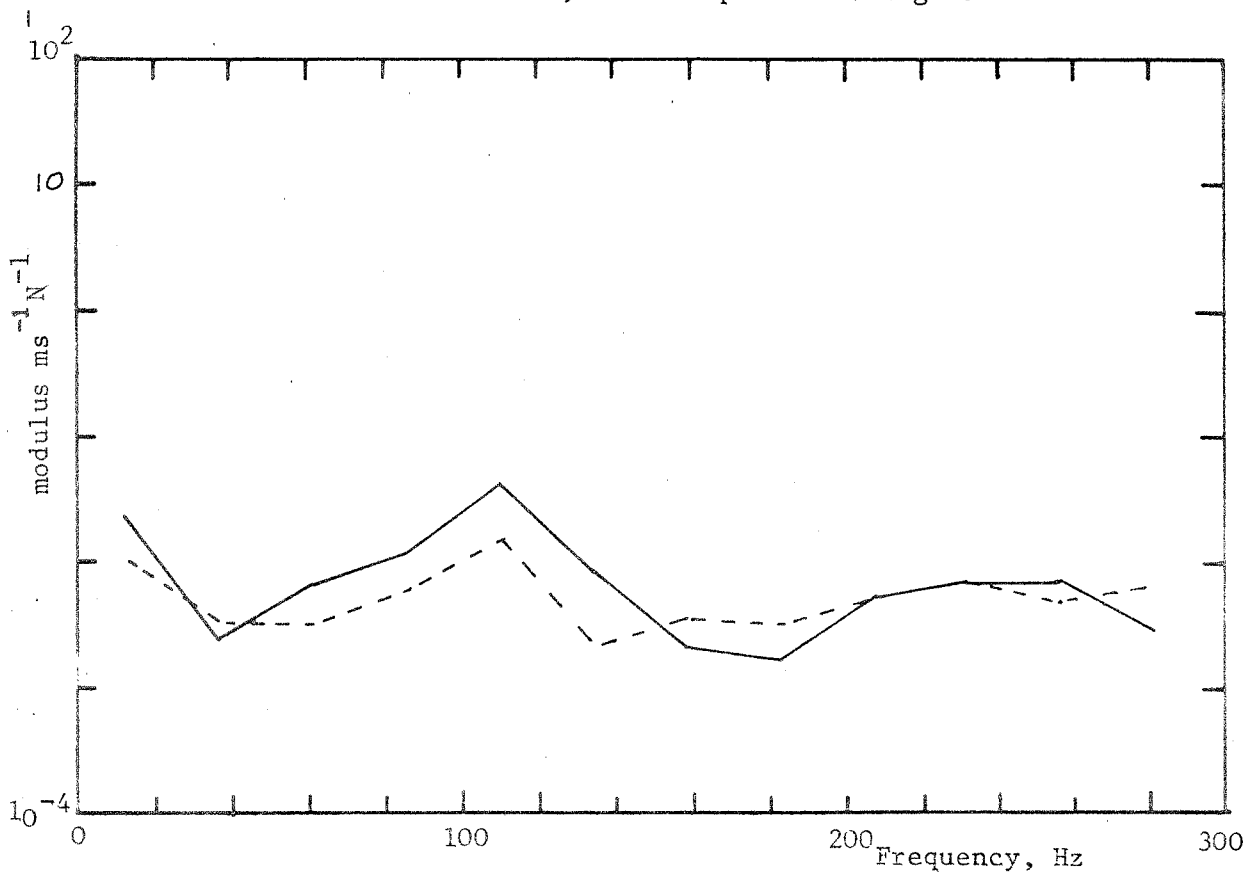

Figure 7.7 Predicted (---) and measured (_____) transfer mobility of station 4, with responses averaged.

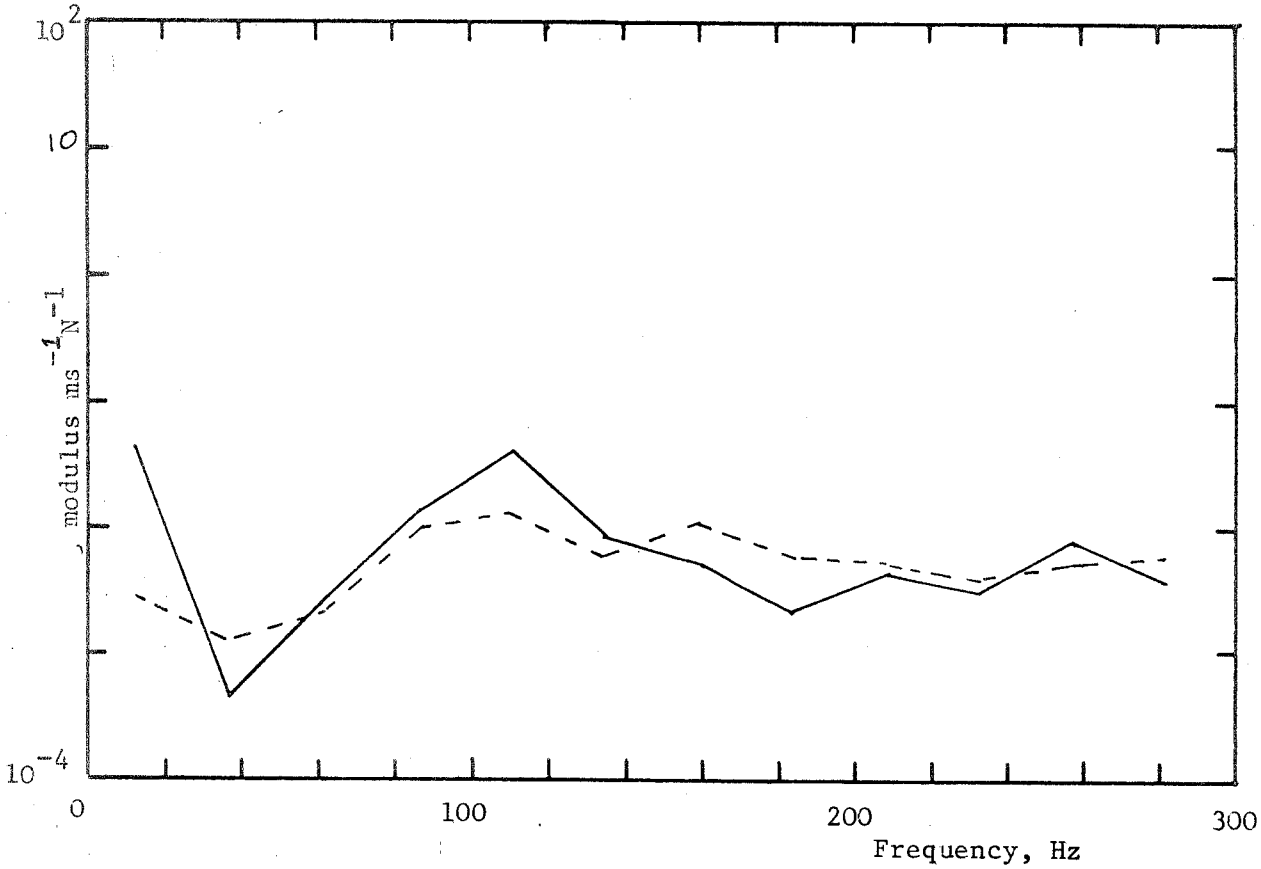

Figure 7.8 Predicted (---) and measured (_____) transfer mobility of station 5, with response averaged.

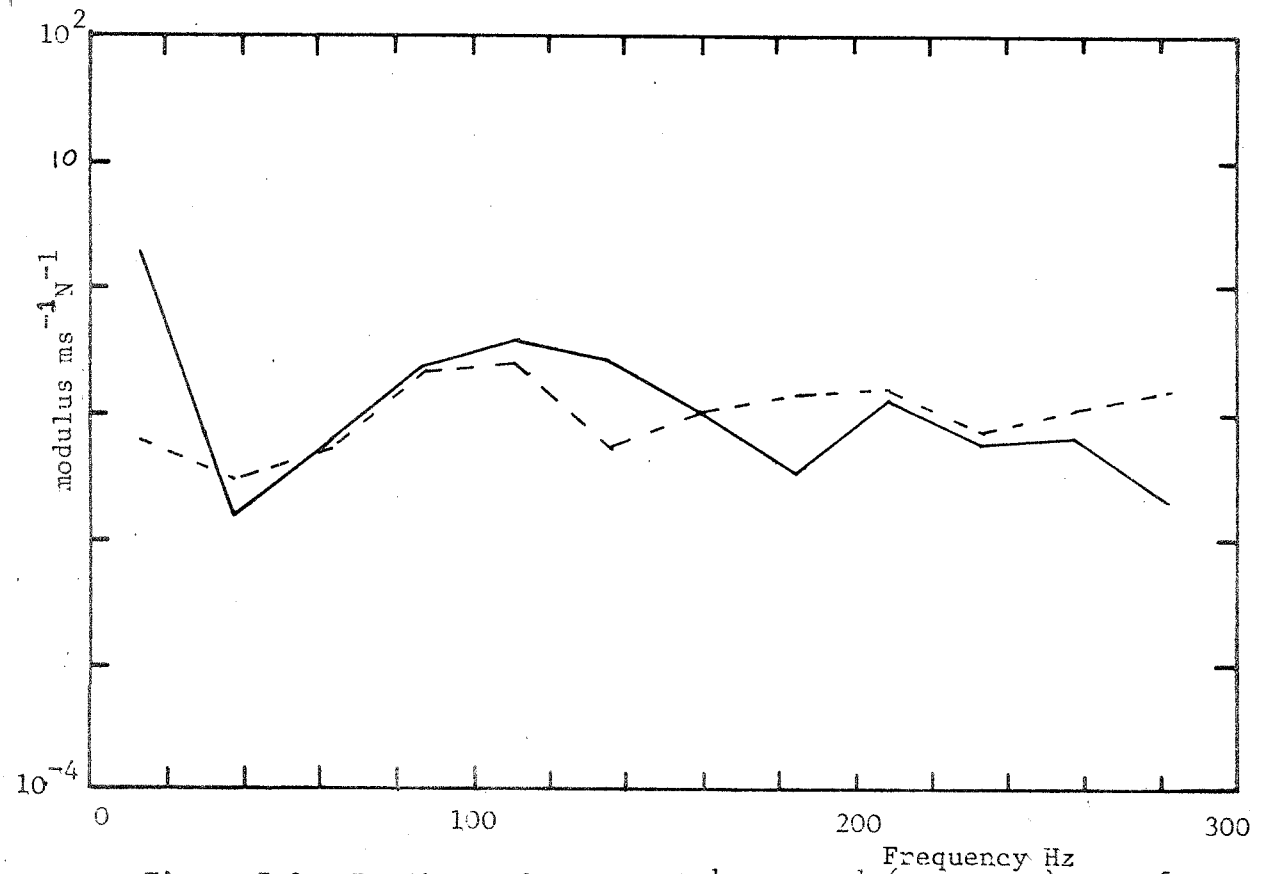

Figure 7.9 Predicted (———) and measured (_____) transfer mobility of station 6, with responses averaged.

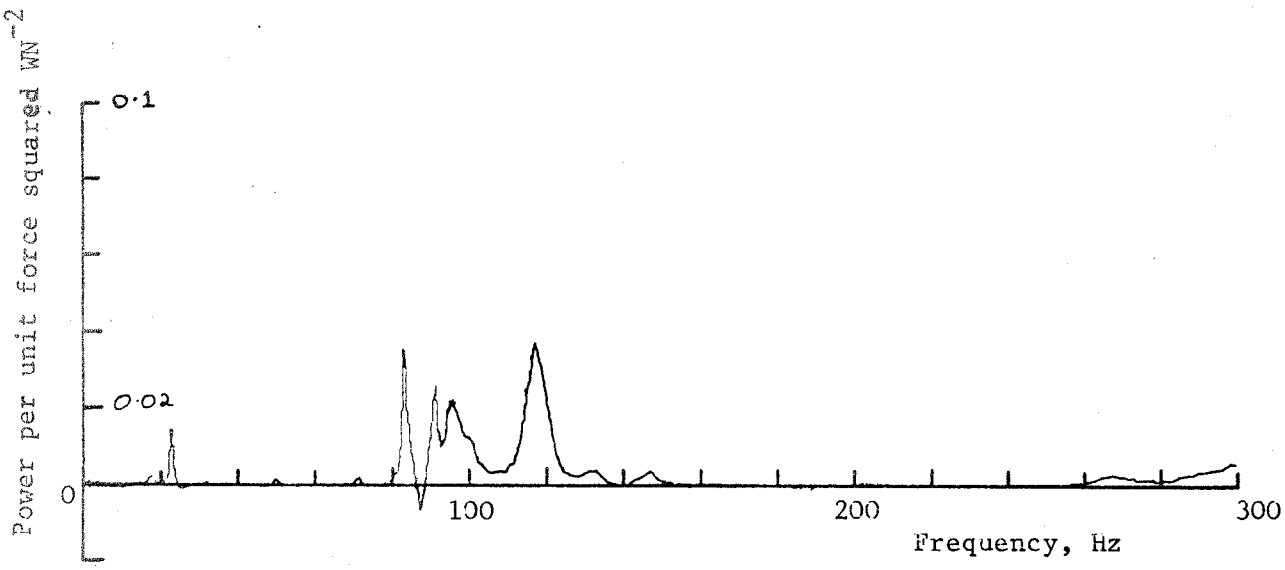

Figure 7.10 Power flow into component γ associated with force at connection point due to unit force at input to structure.

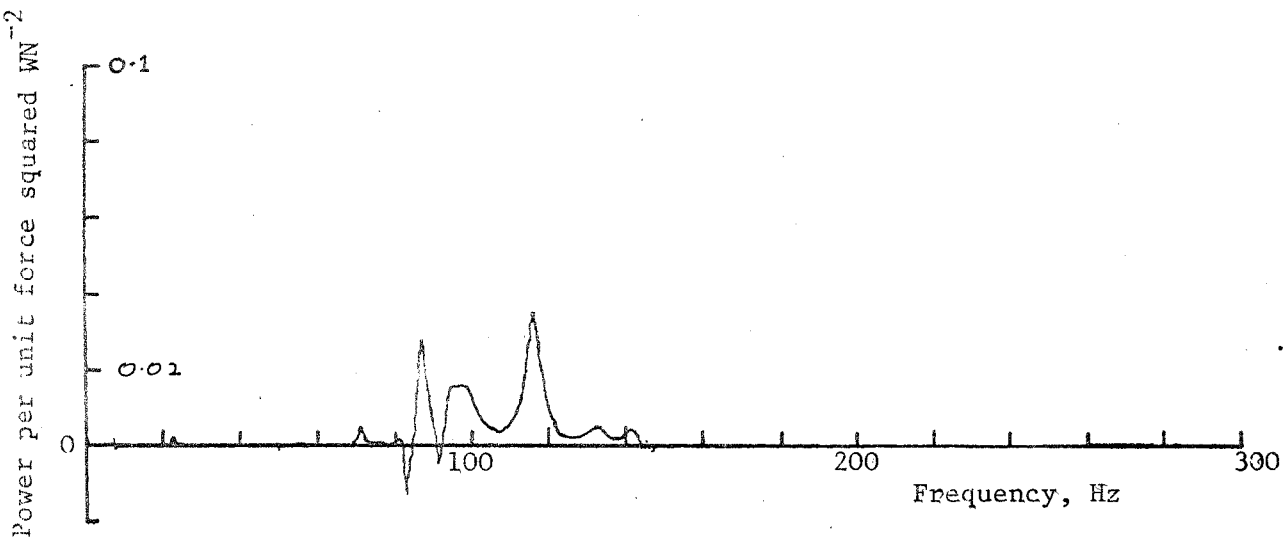

Figure 7.11 Power flow into component γ associated with torque at connection point due to unit force at input to structure.

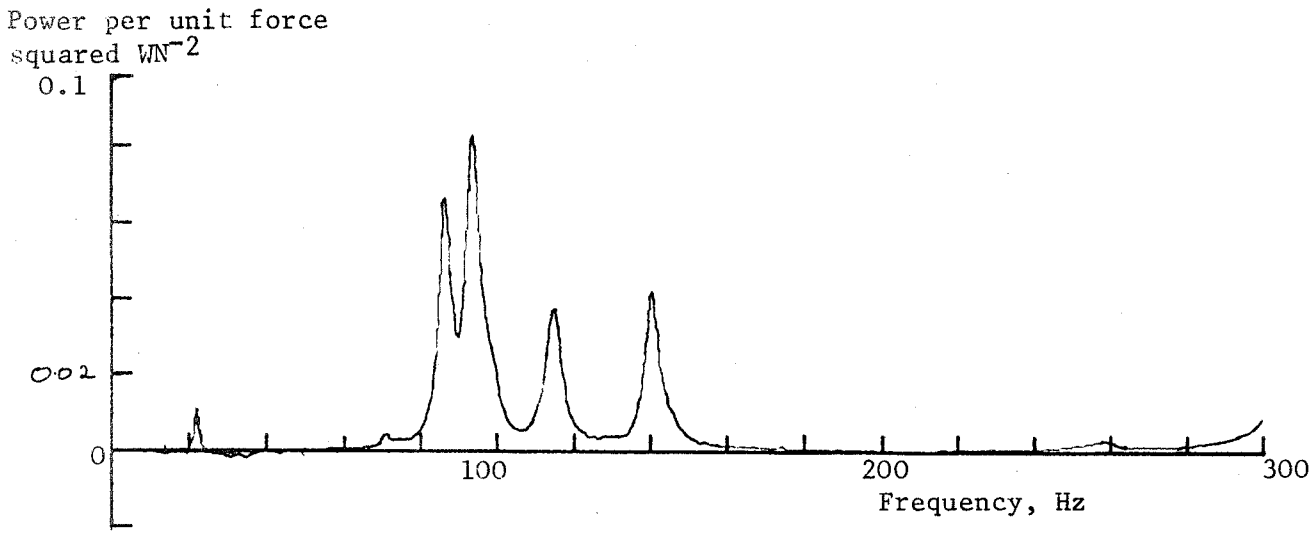

Figure 7.12 Total power at input to structure due to unit force.

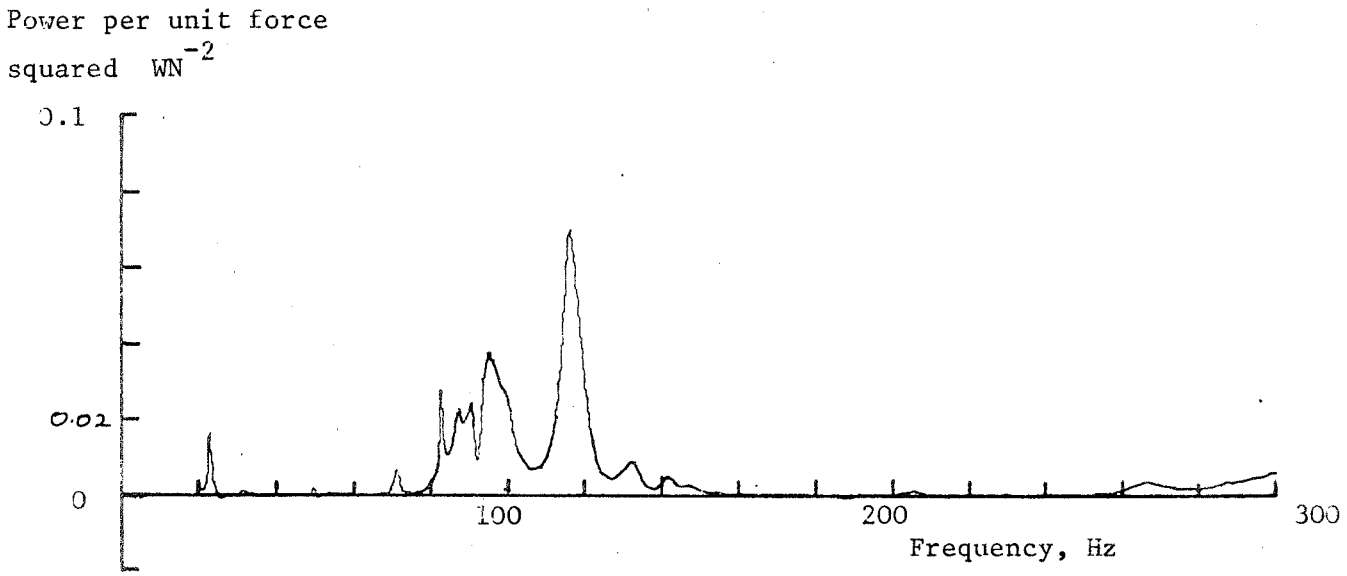

Figure 7.13 Total power flow into component γ due to unit force at input to structure.

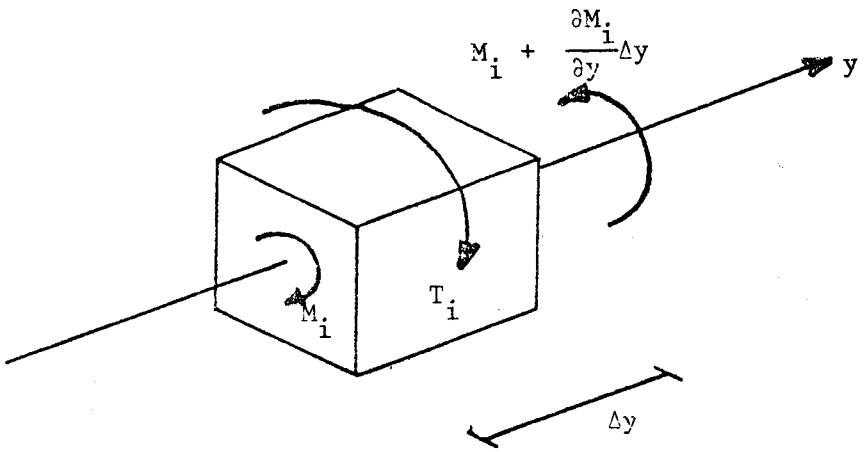

Figure A.1 Element of beam with torsional excitation.

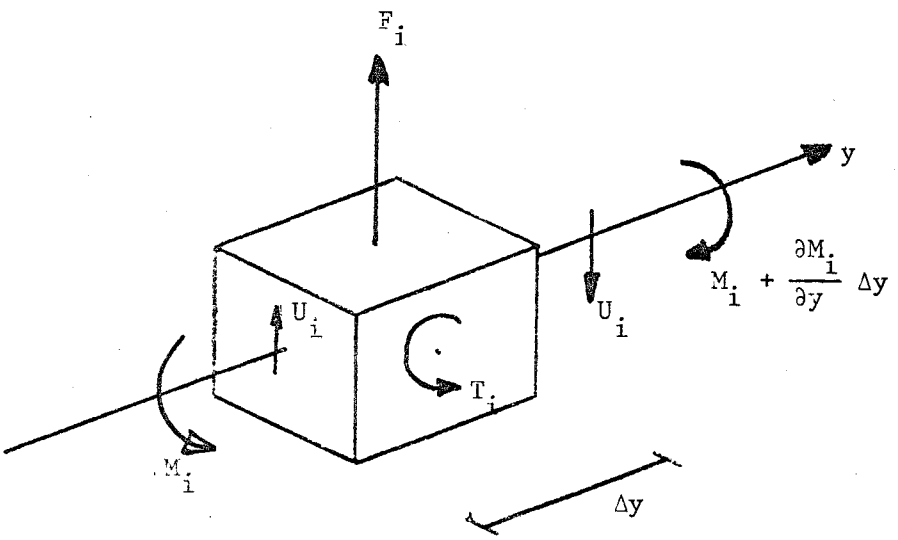

Figure A.2 Element of beam excited into flexural vibration by external forces and torques.

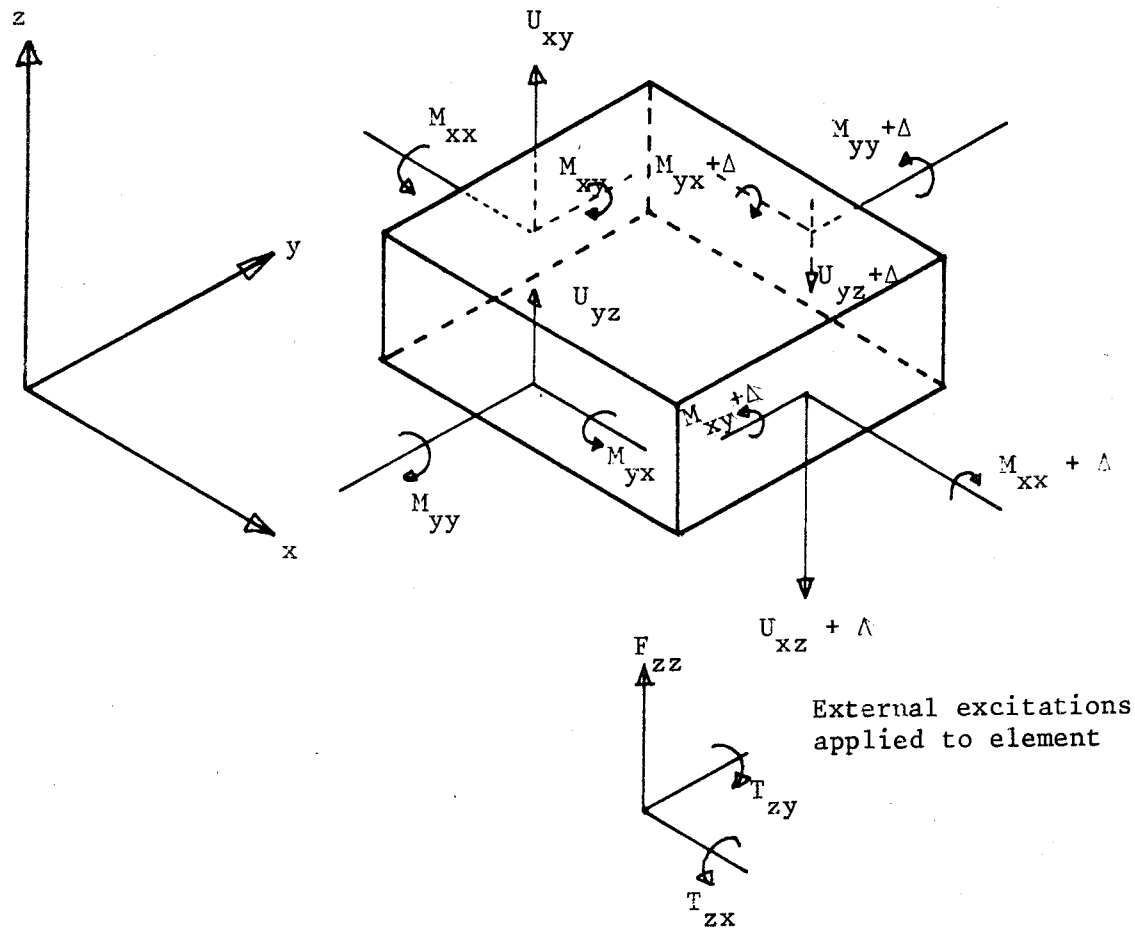

Figure A.3 Element of plate excited into flexural vibrations by external forces and torques.

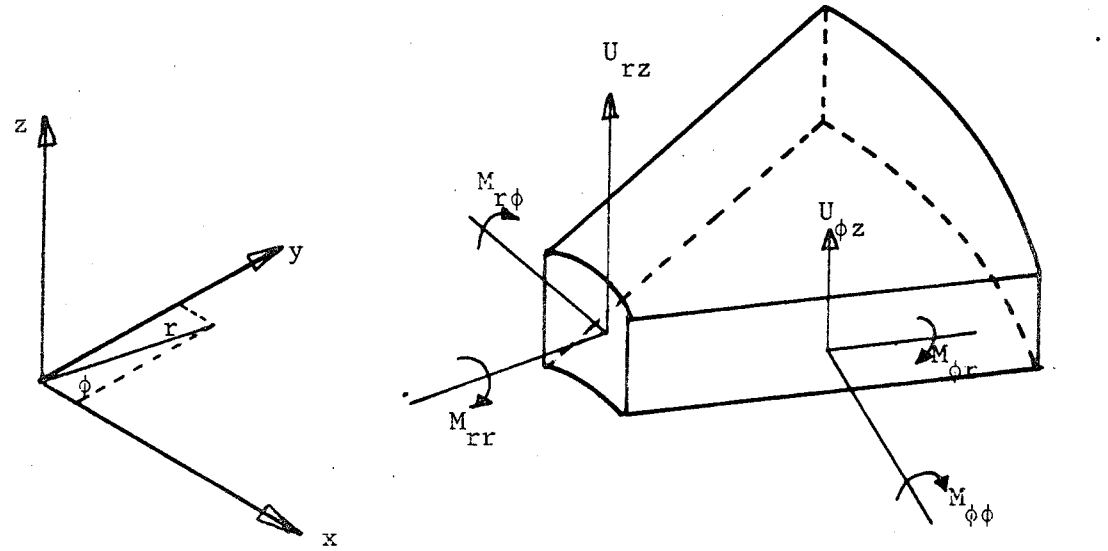

Figure A.4 Element of plate in polar coordinates.

APPENDIX I: The Equation of Motion for Torsional Waves Including an Excitation Function

Figure A.1 shows an element of a beam laying along the y axis with an applied torque of T_i per unit length. Writing J for the mass moment of inertia per unit length and M_i for the internal twisting moment, and applying Newton's law, gives:-

$$J \frac{\partial^2 \theta_i}{\partial t^2} = T_i - \frac{\partial M_i}{\partial y} \tag{A.1}$$

where θ is the angular displacement of the beam. From standard elasticity relationships [7]:-

$$M_i = -GQ \frac{\partial \theta_i}{\partial y} \tag{A.2}$$

where Q is the torsion constant.

Combining (A.1) and (A.2) gives:-

$$J \frac{\partial^2 \theta_i}{\partial t^2} = GQ \frac{\partial^2 \theta_i}{\partial y^2} + T_i \tag{A.3}$$

which is the required relationship.

APPENDIX II: The Equation of Motion of Flexural Waves in Beams Including Excitation Functions.

Figure A.2 shows an element of a beam laying along the y axis with an external excitation of F_i and T_i per unit length corresponding to a force and torque, respectively. The coordinate system is arranged so that the power associated with the internal force or torque is positive for power flow in the positive y direction. Applying Newton's law for the acceleration of the element gives:-

$$-\frac{\partial u_i}{\partial y} + F_i = \rho A_s \frac{\partial^2 \xi_i}{\partial t^2} \tag{A.4}$$

where u_i is the internal shear force, ρ the volume density, A_s the cross sectional area and ξ_i the displacement of the beam. Assuming the rotary inertia and shear deformation to be small gives an equilibrium of torques which may be written:-

$$-\frac{M_i}{\partial y} + T_i - F_i = 0 \tag{A.5}$$

where M_i is the internal bending moment. From standard equations in elasticity [7] the relation

$$M_i = -EI \frac{\partial^2 \xi_i}{\partial y^2} \tag{A.6}$$

may be written where I is the second moment of area of the cross section. Combining equations (A.4), (A.5) and (A.6) gives the required relationship:-

$$\frac{\partial^4 \xi_i}{\partial y^4} + \frac{\rho A_s}{EI} \frac{\partial^2 \xi_i}{\partial t^2} = \frac{F_i}{EI} - \frac{1}{EI} \frac{\partial T_i}{\partial y} \tag{A.7}$$

APPENDIX III: The Equation of Motion for Flexural Waves in a Plate Including Excitation Functions

Figure A.3 shows an element of a plate laying in the x-y plane. The plate is excited by an external pressure (force per unit area) acting in a direction normal to the plate and by two external torque distributions (torque per unit area) acting about axes parallel to the x and y axes, respectively. Two subscripts will be used for each force and torque; the first subscript is the direction of the normal to the surface on which the force or torque acts; the second is the direction of the action. A right handed coordinate system is used throughout.

The internal force and two internal bending moments acting on each edge of the plate element are also shown in figure A.3.

Applying Newton's law to the vertical motion results in:-

$$\rho h \frac{\partial^2 \xi_i}{\partial t^2} = F_{zz} - \frac{\partial u_{xz}}{\partial x} - \frac{\partial u_{yz}}{\partial y} \tag{A.8}$$

where h is the plate thickness, F_{zz} the external pressure and u the internal shear forces per unit length.

Moment equilibrium about the x and y axes results in two equations giving the shear force:-

$$-\frac{\partial M_{xx}}{\partial x} - \frac{\partial M_{yx}}{\partial y} + T_{zx} = u_{yz} \tag{A.9}$$

$$\frac{\partial M_{yy}}{\partial y} + \frac{\partial M_{xy}}{\partial x} - T_{zy} = u_{xz} \tag{A.10}$$

where M is the internal bending moment per unit length and T the externally applied torques.

From standard results in elasticity [7] the relationship between bending moments and displacement may be written:-

$$M_{yx} = -B\left[\frac{\partial^2}{\partial y^2} + \nu\frac{\partial^2}{\partial x^2}\right]\xi_i \tag{A.11}$$

$$M_{xy} = B\left[\frac{\partial^2}{\partial x^2} + \nu\frac{\partial^2}{\partial y^2}\right]\xi_i \tag{A.12}$$

$$M_{yy} = -M_{xx} = B(1 - \nu) \frac{\partial^2 \xi_i}{\partial x \partial y} \tag{A.13}$$

where B is the bending stiffness for a plate given by:-

$$B = \frac{Eh^3}{12(1 - \nu^2)}$$

Combining equations (A.8)-(A.13) gives the required plate equation:-

$$B\nabla^4 \xi_i + \rho h \frac{\partial^2 \xi_i}{\partial t^2} = F_{zz} + \frac{\partial T_{yy}}{\partial x} - \frac{\partial T_{xx}}{\partial y} \tag{A.15}$$

where $$\nabla^4 = \frac{\partial^4}{\partial x^4} + 2 \frac{\partial^4}{\partial x^2 \partial y^2} + \frac{\partial^4}{\partial y^4}$$

In order to calculate power flow intensities it is necessary to obtain the relationships between displacements and internal shear forces and bending moments. Figure A.4 shows the internal forces and torques acting on an element of a plate in polar coordinates. By assuming the polar and Cartesian elements to be equivalent according to the method of Timoshenko [36,p.259] the relationships may be written:-

$$u_{rz} = B \frac{\partial}{\partial r}(\nabla^2 \xi_i) \tag{A.16}$$

$$M_{r\phi} = B\left[\frac{\partial^2 \xi_i}{\partial r^2} + \nu\left(\frac{1}{r} \frac{\partial \xi_i}{\partial r} + \frac{1}{r^2} \frac{\partial^2 \xi_i}{\partial \phi^2}\right) \right] \tag{A.17}$$

$$M_{rr} = -B(1 - \nu)\left[\frac{1}{r} \frac{\partial^2 \xi_i}{\partial r \partial \phi} + \frac{1}{r^2} \frac{\partial \xi_i}{\partial \phi} \right] \tag{A.18}$$

$$u_{\phi z} = B \frac{1}{r} \frac{\partial}{\partial \phi} (\nabla^2 \xi_i) \tag{A.19}$$

$$M_{\phi r} = -B\left[\frac{1}{r} \frac{\partial \xi_i}{\partial r} + \frac{1}{r^2} \frac{\partial^2 \xi_i}{\partial \phi^2} + \mu \frac{\partial^2 \xi_i}{\partial r^2} \right] \tag{A.20}$$

$$M_{\phi\phi} = - M_{rr} \tag{A.21}$$

APPENDIX IV: DETAILS OF THE CONTOUR INTEGRATION OF EQUATION (4.34)

The values of the residues are found from:-

$$\text{Res}(p_1;\ p_2) \quad = \quad \left. \frac{\alpha_y^{\ 2}}{\frac{\partial}{\partial \alpha_y}\ (g)} \right|_{\alpha_y\ =\ p_1;\ p_2}$$

(equation (4.38)). Writing L for $\frac{B_b}{B_p}$ and α for α_y enables the denominator of the above expression to be evaluated as:-

$$\frac{\partial}{\partial \alpha}(g) = 4\alpha^3 - \frac{2i}{L}(-4\alpha^3)\ \{(k_p^{\ 2} - \alpha^2)^{-\frac{1}{2}} - i(k_p^{\ 2} + \alpha^2)^{-\frac{1}{2}}\}$$

$$- \frac{2i}{L}(k_p^{\ 4} - \alpha^4)\quad \{\frac{\alpha}{(k_p^{\ 2} - \alpha^2)^{3/2}} + \frac{i\alpha}{(k_p^{\ 2} + \alpha^2)^{3/2}}\}$$

For simplicity the two poles p_1 and p_2 (equations (4.22) and (4.23)) may be written as:-

$$p_1 = k_b\left[1 + \frac{iA}{2Lk_b s^3}\right]$$

and

$$p_2 = ik_b\left[1 + \frac{iB}{2Lk_b s^3}\right]$$

where A and B are expressions in s. The residue of the pole p_1 will first be evaluated. The value of the denominator to first order in Lk_b is:-

$$\text{Denom} = 4k_b^{\ 3}\left[1 + \frac{3iA}{2Lk_b s^3}\right],$$

$$+ \frac{8isk_b^{\ 3}}{Lk_b}\left[1 + \frac{3iA}{2Lk_b s^3}\right]\{\left[1 - (s^2 + \frac{iA}{Lk_b s})\right]^{-\frac{1}{2}} - i\left[1 + s^2 + \frac{iA}{Lk_b s}\right]^{-\frac{1}{2}}\}$$

$$- \frac{2ik_p k_b}{L\,k_p^{\ 3}}\left[1 - s^4 - \frac{2iAs}{Lk_b}\right]\left[1 + \frac{iA}{2Lk_b s^3}\right]\{\left[1 - s^2 - \frac{iA}{Lk_b s}\right]^{-3/2}$$

$$+ i\left[1 + s^2 + \frac{iA}{Lk_b s}\right]^{-3/2}\}$$

$$\text{or} \quad \text{Denom} = 4k_b^3 \{1 + \frac{3iA}{2Lk_b s^3} + \frac{2is}{Lk_b} \left[(1 - s^2)^{-\frac{1}{2}} - i(1 + r^2)^{-\frac{1}{2}}\right]$$

$$- \frac{i(1 - s^4)}{2Lk_b s} \left[(1 - s^2)^{-3/2} + i(1 + s^2)^{-3/2}\right]\}$$

$$\text{or} \quad \text{Denom} = 4k_b^3 \{1 + \frac{i}{2Lk_b s^3} \left[3(1 - s^4)^{\frac{1}{2}}\left[(1 + s^2)^{\frac{1}{2}} - i(1 - s^2)^{\frac{1}{2}}\right]\right.$$

$$+ 4s^4\left[(1 - s^2)^{-\frac{1}{2}} - i(1 + s^2)^{-\frac{1}{2}}\right] - s^2(1 - s^4)\left|(1 - s^2)^{-3/2}\right.$$

$$\left.\left. + i(1 + s^2)^{-3/2}\right]\right]\}$$

$$\text{or} \quad \text{Denom} = 4k_b^3 \{1 + \frac{i}{2Lk_b s^3} \left[\frac{3 - s^2}{(1 - s^2)^{\frac{1}{2}}} - i\frac{s^2 + 3}{(1 + s^2)^{\frac{1}{2}}}\right]\}$$

The residue is thus given by:-

$$\text{Res}\{p_1\} = k_b^2 \left[1 + \frac{i(1 - s^4)^{\frac{1}{2}}}{k_b L s^3} \{(1 + s^2)^{\frac{1}{2}} - i(1 - s^2)^{\frac{1}{2}}\}\right] \left[\frac{1}{4k_b^3}\{1 - \frac{i}{2Lk_b s^3}\right.$$

$$\times \left[\frac{3 - s^2}{(1 - s^2)^{\frac{1}{2}}} - i\frac{s^2 + 3}{(1 + s^2)^{\frac{1}{2}}}\right]\}\Big]$$

$$\text{or} \quad \text{Res}\{p_1\} = \frac{1}{4k_b}\{1 - \frac{i}{2Lk_b s^3} \left[\frac{2s^4 - s^2 + 1}{(1 - s^2)^{\frac{1}{2}}} - i\frac{2s^4 + s^2 + 1}{(1 + s^2)^{\frac{1}{2}}}\right]\}$$

which is the required result. The residue of the pole p_2 may be found in a similar manner. In this case the denominator may be written:-

$$i4k_b^3 \left[1 + \frac{i}{2Lk_b s^3}\left\{\frac{3 + s^2}{(1 + s^2)^{\frac{1}{2}}} - i\frac{3 - s^2}{(1 - s^2)^{\frac{1}{2}}}\right\}\right]$$

and eventually the residue is given by:-

$$\mathrm{Res}\{p_2\} = \frac{-i}{4k_b}\{1 - \frac{i}{2Lk_b s^3}\left[\frac{2s^4 + s^2 + 1}{(1+s^2)^{\frac{1}{2}}} - i\,\frac{2s^4 - s^2 + 1}{(1-s^2)^{\frac{1}{2}}}\right]\}$$

The integral (equation (4.35)) must be calculated along the two paths around the branch lines so that the branch points are excluded from the contour. The branch lines have been deliberately chosen to simplify the two integrations. Along both paths $|\alpha| > k_p$ and the integrand may be written as:-

$$\frac{\alpha^2}{\alpha^4(1 - \frac{k_b^4}{\alpha^4})\left[1 - \frac{2i(\frac{k_p^4}{\alpha^4} - 1)}{L\alpha(1 - \frac{k_b^4}{\alpha^4})}\{(\frac{k_p^2}{\alpha^2} - 1)^{-\frac{1}{2}} - i(\frac{k_p^2}{\alpha^2} + 1)^{-\frac{1}{2}}\}\right]}$$

or to first order

$$\frac{\alpha^2\{1 + \frac{2i(\frac{k_p^4}{\alpha^4} - 1)}{L\alpha(1 - \frac{k_b^4}{\alpha^4})}\{(\frac{k_p^2}{\alpha^2} - 1)^{-\frac{1}{2}} - i(\frac{k_p^2}{\alpha^2} + 1)^{-\frac{1}{2}}\}\}}{\alpha^4(1 - \frac{k_b^4}{\alpha^4})}$$

This may be rewritten as three terms:-

$$\frac{\alpha^2}{\alpha^4(1 - \frac{k_b^4}{\alpha^4})} + \frac{2i\alpha(\frac{k_p^4}{\alpha^4} - 1)}{L\alpha^4(1 - \frac{k_b^4}{\alpha^4})^2(\frac{k_p^2}{\alpha^2} - 1)^{\frac{1}{2}}} + \frac{2\alpha(\frac{k_p^4}{\alpha^4} - 1)}{L\alpha^4(1 - \frac{k_b^4}{\alpha^4})^2(\frac{k_p^2}{\alpha^2} + 1)^{\frac{1}{2}}}$$

This expression must be integrated around both branch lines. For the branch line Γ_1 (figure 4.3) the first and third terms are the same on both sides of the branch line and thus do not contribute. In the second term the expression $(\frac{k_p^2}{\alpha^2} - 1)^{\frac{1}{2}}$ has the value $+i(1 - \frac{k_p^2}{\alpha^2})^{\frac{1}{2}}$ along the lower portion

of the branch line and $-i(1 - \frac{k_p^2}{\alpha^2})^{\frac{1}{2}}$ along the upper portion. These values are chosen to be consistent with a wavemotion propagating away from the source. The integral around the branch line Γ_1 is thus given by:-

$$\int_{\Gamma_1} = \int_{\infty}^{k_p} \frac{2i\alpha(\frac{k_p^4}{\alpha^4} - 1)}{L\alpha^4(1 - \frac{k_b^4}{\alpha^4})^2 \left[+i(1 - \frac{k_p^2}{\alpha^2})^{\frac{1}{2}}\right]} d\alpha$$

$$+ \int_{k_p}^{\infty} \frac{2i\alpha(\frac{k_p^4}{\alpha^4} - 1)}{L\alpha^4(1 - \frac{k_b^4}{\alpha^4})^2 \left[-i(1 - \frac{k_p^2}{\alpha^2})^{\frac{1}{2}}\right]} d\alpha$$

or by letting $\alpha = k_p x$

$$\int_{\Gamma_2} = \frac{4}{Lk_p^2} \int_1^{\infty} \frac{(x^4 - 1)x^2}{(x^4 - s^4)^2(x^2 - 1)^{\frac{1}{2}}} dx$$

Around the second branch cut Γ_2 the first two terms of the integral do not contribute and in the third term the expression $((k_p^2/\alpha^2) + 1)^{\frac{1}{2}}$ takes the value $+(1 + \frac{k_p^2}{\alpha^2})^{\frac{1}{2}}$ on the right of the branch line and $-(1 + \frac{k_p^2}{\alpha^2})^{\frac{1}{2}}$ on the left of the branch line. The integral along the second branch line may thus be written:-

$$\int_{\Gamma_2} = \int_{\infty}^{ik_p} \frac{2\alpha(\frac{k_p^4}{\alpha^4} - 1)}{L\alpha^4(1 - \frac{k_b^4}{\alpha^4})^2 \left[+(1 + \frac{k_p^2}{\alpha^2})^{\frac{1}{2}}\right]} d\alpha$$

$$+ \int_{ik_p}^{\infty} \frac{2\alpha(\frac{k_p^4}{\alpha^4} - 1)}{L\alpha^4(1 - \frac{k_b^4}{\alpha^4})^2 \left[-(1 + \frac{k_p^2}{\alpha^2})^{\frac{1}{2}}\right]} d\alpha$$

or, by letting $\alpha = ik_p x$,

$$\int_{\Gamma_2} = \frac{-4}{Lk_p^2} \int_1^{\infty} \frac{(x^4 - 1)x^2}{(x^4 - s^4)^2 (x^2 - 1)^{\frac{1}{2}}} \, dx$$

Thus $$\int_{\Gamma_1} + \int_{\Gamma_2} = 0$$

and the branch line integrals do not contribute.

APPENDIX V: THE FREQUENCY RESPONSE OF A DAMPED STRUCTURE

The general equation of motion for steady harmonic vibration of a hysteretically damped structure with n degrees of freedom is:-

$$-\omega^2 M\xi + \left[K + iD\right]\xi = F \qquad (A.22)$$

where M, K and D are square $n \times n$ mass stiffness and damping matrices and ξ and F are $n \times 1$ displacement and force column vectors, respectively. This equation gives f in terms of ξ while the reverse — ξ in terms of F is required.

To construct the inverse relationship, the left hand side of equation (A.22) may be diagonalised by adopting a complex Eigenvalue procedure. The Eigenvalue problem is defined by

$$\left[-\omega^2 M + K + iD \right]\xi = 0 \qquad (A.23)$$

and the eigenvalues are found as the roots of the complex polynomial of degree n in ω^2 given by:

$$\left[-\omega^2 M + K + iD \right] = 0 \qquad (A.24)$$

(Only values of ω^2 are found in this equation as opposed to the viscously damped case where there are both ω and ω^2 terms.) In general, there will be n complex roots which may be written as:

$$\omega_1^2, \quad \omega_2^2, \quad \ldots, \quad \omega_n^2.$$

A set of column vectors (eigenvectors) may now be found by substituting each eigenvalue into equation (A.23) and solving the homogeneous set of equations. The column vectors so formed may not be determined uniquely but only to the extent of an arbitrary constant. In general, both the column vector and the constant will be complex. For convenience, the eigenvector may be normalised and a satisfactory basis for this is given later.

The set of eigenvectors may be written:

$$\psi^{(1)}; \quad \psi^{(2)}; \quad \psi^{(3)}; \quad \ldots \quad \psi^{(n)}$$

with each eigenvector satisfying the relation:

$$-\omega_n^2 M\psi^{(n)} = [K + iD]\psi^{(n)} \tag{A.25}$$

In particular it may be shown that

$$\psi^{(r)^T} M\psi^{(s)} = 0 \qquad r \neq s \tag{A.26}$$

$$\psi^{(r)^T} [K + iD]\psi^{(s)} = 0 \tag{A.27}$$

The matrix R may now be defined so that the columns of R are the eigenvectors. Employing relations (A.26) and (A.27) it is possible to write:

$$R^T M R = \begin{bmatrix} m_r \end{bmatrix} \tag{A.28}$$

$$R^T [K + iD] R = \begin{bmatrix} k_r + id_r \end{bmatrix} \tag{A.29}$$

where m_r and $k_r + id_r$ are defined according to:

$$\psi^{(r)^T} M\psi^{(r)} = m_r \tag{A.30}$$

$$\psi^{(r)^T} [k + iD]\psi^{(r)} = k_r + id_r \tag{A.31}$$

m_r will in general be complex. By multiplying equation (A.25) by $\psi^{(n)^T}$ it is seen that

$$\omega_n^2 = \frac{k_n + id_n}{m_n} \tag{A.32}$$

ω_n^2 may be identified as the complex resonance frequency and $\psi^{(n)}$ as the complex mode shape.

Equation (A.22) may now be diagonalised by premultiplying by R^T and inserting RR^{-1} so that:

$$R^T \left[-\omega^2 M + K + iD\right] R R^{-1} \xi = R^T f \tag{A.33}$$

Multiplying through the bracket and employing equations (A.28), (A.29) and (A.32) gives:

$$\left[(\omega_r^2 - \omega^2) m_r\right] \left[R^{-1}\right] \xi = \left[R^T\right] f \tag{A.34}$$

or

$$\xi = \left[R\right] \left[\frac{1}{(\omega_r^2 - \omega^2)\, m_r}\right] \left[R^T\right] f \tag{A.35}$$

To still further simplify the equation it is possible to arrange for the column vector $\psi^{(n)}$ to be normalised so that equation (A.28) appears as

$$R^T M R = I \tag{A.36}$$

where I is the unit matrix. Equation (A.35) may now be written as

$$\xi = R \left[\frac{1}{\omega_n^2 - \omega^2}\right] R^T F \tag{A.37}$$

which is the required relationship.

APPENDIX VI; CURVE FITTING TO DATA FROM MANY STATIONS

Let $\underline{H}(i\omega)^*$ be a column vector of frequency response data obtained from many stations but with the same excitation station employed throughout. Each element of $\underline{H}$ is therefore a complex frequency response function. The theoretical form of the frequency response is

$$\underline{H} = \sum_{r=1}^{n} \frac{i\omega \underline{X}(r)}{\omega_r^2 - \omega^2} \tag{A.38}$$

where $\underline{X}^{(r)}$ is a complex column vector corresponding to the r^{th} mode. $\underline{X}^{(r)}$ may be expressed in terms of the complex modes so that:-

$$\underline{X}^{(r)} = \underline{\psi}^{(r)} \psi_j^{(r)} \tag{A.39}$$

where j is the forcing station. The error equation for the k^{th} frequency may now be written as:

$$\underline{E}_K = \sum_{r=1}^{n} \frac{i\omega_K \underline{X}^{(r)}}{\omega_r^2 - \omega_K^2} - \underline{H}(i\omega_k) \tag{A.40}$$

where $\underline{E}_K$ is a column vector of complex errors.

To enable each term in equation (A.40) to be curve fitted individually, the substitution:

$$\underline{A}(i\omega_K) = \sum_{\substack{r=1 \\ r \neq m}}^{n} \frac{i\omega_K \underline{X}^{(r)}}{\omega_r^2 - \omega_K^2} - \underline{H}(i\omega_K) \tag{A.41}$$

may be made to give:

$$\underline{E}_K = \frac{i\omega_K \underline{X}^{(m)}}{\omega_m^2 - \omega_K^2} + \underline{A}(i\omega_K) \tag{A.42}$$

---

*In this section, column vectors will be indicated by a line drawn beneath the symbol.

which is the error equation for the m^{th} mode. The weighting function $W(i\omega_K)$ may be used to linearise the error equation so that

$$\underline{E}_K = \frac{1}{W(i\omega_K)} \left[i\omega_K \underline{X}^{(m)} + (\omega_m^2 - \omega_K^2)\underline{A}(i\omega_K) \right] \tag{A.43}$$

where

$$\frac{1}{W(i\omega_K)} = \frac{1}{(\omega_m^2 - \omega_K^2)}$$

ω_m^2 for the weighting function having been chosen as an initial estimate or from the previous iteration.

To obtain the total error as a scalar $\underline{E}_K$ may be premultiplied by its transposed conjugate to give the real scalar equation:

$$\begin{aligned} \bar{\underline{E}}_K^T E_K &= \varepsilon_k^2 \\ &= \frac{1}{|W_k|^2} \left| -i\omega_k \bar{\underline{X}}^{(m)T} + (\overline{\omega_m^2} - \omega_k^2)\bar{\underline{A}}^T(i\omega_k) \right] \\ &\quad \times \left[i\omega_k \underline{X}^{(m)} + (\omega_m^2 - \omega_k^2)\underline{A}(i\omega_k) \right] \end{aligned} \tag{A.44}$$

Thus the sum of errors over the frequency interval containing one resonance is:

$$\begin{aligned} \sum_k \varepsilon^2 = \; & ||X||^2 \sum_k \frac{\omega_k^2}{|W_k|^2} - i\omega_m^2 \bar{\underline{X}}^{(m)T} \sum_k \frac{\omega_k \underline{A}_k}{|W_k|^2} + i\bar{\underline{X}}^{(m)T} \sum_k \frac{\omega_k^3 \underline{A}_k}{|W_k|^2} \\ & + i\overline{\omega_m^2} \left[\sum_k \frac{\omega_k \bar{\underline{A}}_k^T}{|W_k|^2} \right] \underline{X}^{(m)} + |\omega_m^2|^2 \sum_k \frac{\bar{\underline{A}}_k^T \underline{A}_k}{|W_k|^2} - \overline{\omega_m^2} \sum_k \frac{\omega_k^2 \bar{\underline{A}}_k^T \underline{A}_k}{|W_k|^2} \\ & - i\left[\sum_k \frac{\omega_k^3 \bar{\underline{A}}_k^T}{|W_k|^2} \right] \underline{X}^{(m)} - \omega_m^2 \sum_k \frac{\omega_k^2 \bar{\underline{A}}_k^T \underline{A}_k}{|W_k|^2} + \sum_k \frac{\omega_k^4 \bar{\underline{A}}_k^T \underline{A}_k}{|W_k|^2} \end{aligned} \tag{A.45}$$

where $||X||^2 = \bar{\underline{X}}^T \underline{X}$.

The series terms may be evaluated conveniently by means of a digital computer. The expression may be simplified by making the following substitutions:-

$$\sum \frac{\omega_k^2}{|W_k|^2} = B; \qquad i\sum \frac{\omega_k \underline{A}_k}{|W_k|^2} = \underline{C};$$

$$i\sum \frac{\omega_k^3 \underline{A}_k}{|W_k|^2} = \underline{D}; \qquad \sum \frac{\bar{\underline{A}}_k^T \underline{A}}{|W_k|^2} = E;$$

$$\sum \frac{\omega_k^2 \bar{\underline{A}}^T \underline{A}}{|W_k|^2} = F; \qquad \sum \frac{\omega_k^4 \bar{\underline{A}}^T \underline{A}}{|W_k|^2} = G$$

Equation (A.45) may now be written as

$$\sum \varepsilon_k^2 = B\bar{\underline{X}}^T\underline{X} - \omega_m^2\bar{\underline{X}}^T\underline{C} + \bar{\underline{X}}^T\underline{D} - \overline{\omega_m^2}\,\bar{\underline{C}}^T\underline{X} + |\omega_m^2|^2 E - \overline{\omega_m^2}\,F$$

$$+ \bar{\underline{D}}^T\underline{X} - \omega_m^2 F + G \qquad (A.46)$$

The values for the unknowns are found by taking derivatives with respect to each unknown and equating to zero. Thus for ω_m^2 the derivatives with respect to the real and imaginary parts are:-

$$\frac{\partial}{\partial \omega_m^{2R}} \left(\sum_k \varepsilon_k^2\right) = -\bar{\underline{X}}^T\underline{C} - \bar{\underline{C}}^T\underline{X} + 2(\omega_m^2)^R E - F - F = 0 \qquad (A.47)$$

$$\frac{\partial}{\partial \omega_m^{2I}} \left(\sum_k \varepsilon_k^2\right) = -i\bar{\underline{X}}^T\underline{C} + i\bar{\underline{C}}^T\underline{X} + 2(\omega_m^2)^I E + iF - iF = 0 \qquad (A.48)$$

These may be combined to give

$$-\bar{\underline{C}}^T\underline{X} + \omega_m^2 E - F = 0 \qquad (A.49)$$

Clearly, each derivative with respect to an unknown element in the column vector $\underline{X}$ will be similar; therefore only one element (the t^{th}) will be considered. The derivatives with respect to the real and imaginary parts of the t^{th} element are:-

$$\frac{\partial}{\partial \underline{X}_t^{(m)R}} \left(\sum_k k^2\right) = 2BX_t^{(m)R} - \omega_m^2 C_t + D_t - \overline{\omega_m^2}\,\bar{C}_t + \bar{D}_t = 0 \qquad \text{(A.50)}$$

$$\frac{\partial}{\partial \underline{X}_t^{(m)I}} \left(\sum_k k^2\right) = 2BX_t^{(m)I} + i\omega_m^2 C_t - iD_t - i\,\overline{\omega_m^2}\,\bar{C}_t + i\bar{D}_t = 0 \qquad \text{(A.51)}$$

which may be combined to give:

$$BX_t^{(m)} - \omega_m^2 C_t + D_t = 0 \qquad \text{(A.52)}$$

Equations (A.44) and (A.52) may be solved to give ω_m^2 and $\underline{X}^{(m)}$ the required unknowns. The procedure may now be repeated for each remaining interval in turn to complete the iteration.

APPENDIX VII: DIAGRAM OF COMPUTER PROGRAM